Regulation of the Proteolytic Processing and Function of Amyloid Precursor Protein by Candidate Ligands

Dissertation Advisor: Dennis J. Selkoe, MD Heather Caroline Rice

Regulation of the proteolytic processing and function of Amyloid Precursor Protein by candidate ligands

ABSTRACT

Despite intense interest in the proteolysis of Amyloid Precursor Protein (APP) in Alzheimer's disease (AD), how the normal processing and function of this type I receptor-like glycoprotein is regulated remains ill-defined. APP is reported to function in neurodevelopment, including migration of neuronal precursor cells into the cortical plate. In recent years, several candidate ligands for APP, including F-spondin, Reelin, β1 Integrin, Contactins, and Lingo-1 have been reported. However, a cognate ligand for APP that regulates its function or processing has yet to be widely confirmed in multiple laboratories.

First, in an unbiased approach to reveal novel ligands, Pancortin was identified by a mass spectrometry-based screen for factors that bind to the APP ectodomain in rodent brain. Each of the Pancortin isoforms was confirmed to interact with APP. However, only specific Pancortin isoforms reduced β-secretase but not α-secretase cleavage of endogenous APP. Using in utero electroporation to overexpress or knockdown Pancortin isoforms in rodent cortex, a previously unidentified role for Pancortin in cortical cell migration with evidence for a functional interaction with APP was discovered.

Next, I developed new assays in an effort to confirm a role for one or more of the published candidate ligands in regulating APP ectodomain shedding in a biologically relevant

context. A comprehensive quantification of APPsα and APPsβ, the immediate products of secretase processing, in both non-neuronal cell lines and primary neuronal cultures expressing endogenous APP yielded no evidence that any of these published candidate ligands *stimulate* ectodomain shedding. Rather, Reelin, Lingo-1 and Pancortin emerged as the most consistent ligands for significantly *inhibiting* ectodomain shedding.

These studies clarify mechanisms regulating the function and processing of APP, which is needed to understand consequences of chronically altering APP proteolysis to treat AD and to develop new potential drug targets.

Dedicated to Mom, Dad, Amanda, and Fred

For they have inspired, challenged, and believed in me

every step of the way

“Do what you have to do, to do what you want to do.”

- D. Washington

TABLE OF CONTENTS

ABBREVIATIONS

AD	Alzheimer's disease
ADAM	a disintegrin and metalloproteinase family
AICD	APP intracellular domain
APLP1	amyloid precursor-like protein 1
APLP2	amyloid precursor-like protein 2
APOER2	Apolipoprotein E receptor 2
APP	ß-amyloid precursor protein
Aß	amyloid ß-protein
BACE	β-site APP cleaving enzyme-1
BSA	bovine serum albumin
CM	conditioned medium
CNTN	contactin
CP	cortical plate
CTF	C-terminal fragment
CuBD	copper-binding domain
DAB1	disabled-1
DISC1	disrupted in schizophrenia-1
ELISA	enzyme-linked immunosorbent assay
ER	endoplasmic reticulum
fAD	familial Alzheimer's disease
FBS	fetal bovine serum

GFLD	growth factor-like domain
HEK	human embryonic kidney cells
IP	immunoprecipitation
iPSCs	induced pluripotent stem cells
IZ	intermediate zone
KPI	Kunitz-type protease inhibitor domain
Lingo-1	leucine rich repeat and Ig domain containing Nogo receptor interacting protein-1
MDCK	Madin-Darby canine kidney cells
Pan-1/Pan-3	pancortin-1/3
PKC	protein kinase C
PM	plasma membrane
PMA	phorbol-12-myristate-13-acetate
SF	serum-free
SVZ	subventricular zone
Swe	Swedish
VLDLR	very-low-density-lipoprotein receptor
VZ	ventricular zone
WB	Western blot

ACKNOWLEDGEMENTS

For me, completing a PhD in Neurobiology at Harvard Medical School and performing my dissertation research in the laboratory of Dennis Selkoe is an attainment of a dream bigger than I once thought imaginable. It would have not been in the realm of possibility without so many people who opened doors for me and provided mentorship, friendship, and support.

First, I would like to thank my mentor, Dennis Selkoe. When he accepted me into his laboratory, I felt he had given me the opportunity of a lifetime, but now I know he has actually given me a lifetime of opportunities. I cannot thank him enough for his guidance and encouragement. I came away from each of our meetings, more excited, motivated, and inspired to continue on my research project and career path. I will continue to look to Dennis as a shining example of how to ask important, interesting questions and how to answer them with rigorous, solid research. I also thank Dennis for his gift of providing me with my co-mentor, Tracy Young-Pearse. I am fortunate that the research project I chose led to me also being mentored by Tracy. I am grateful to have received the most incredible training from her in the Selkoe lab and then also to be a part of her establishing her lab at the CND. I also thank Matt LaVoie for his scientific and career advice; he has made me a better scientist.

I also want to thank all of the members of these labs for making the CND the type of environment that I could love doing research. I especially thank Soyon Hong and Tim Bartels for being amazing baymates, Allen Chen for his never ending help, Eric Luth for his support throughout graduate school as a fellow labmate and classmate, Beth Ostaszewski and Andrew Newman for all they do to keep the Selkoe lab running smoothly, the TYPs of the PYT lab (Mei-Chen Liao, Christina Muratore, and Priya Srikanth) for being brilliant, supportive examples of

women in science. I also thank the students I've mentored for all their hardwork and dedication, including Andrew Snavely, Amelia Chang, Sophie (Ran) Wang, Taewan Shin, and Giaynel Cordero-Taveras. I hope they have learned as much from me as I have from them, and I wish them much success and happiness in their futures. Lastly, I thank my entire PiN 2007 incoming class for the fun times we have shared and the ups and downs we have endured together.

I also thank those people who were a part of earlier steps of my career. I am grateful to those involved with the Oklahoma Medical Research Sir Alexander Fleming Scholar Program for giving me my first experience in scientific research, including Ken Hensley, Shari Hawkins, and Ginger Coleman Kelso. I thank Randy Hewes for his mentorship and the invaluable experience I gained in his lab during my undergraduate thesis work at the University of Oklahoma. I also thank Kelly Damphousse and Jon and Cathryn Withrow who provided mentorship, encouragement, and support to me while at OU. There are so many people to thank in the community of Watonga, OK in which I was raised and will forever call home. Growing up in Watonga has made me the person I am today, and I continue to be overwhelmed by the support I receive from my community. I especially owe a big thanks to those teachers who have had the biggest impact on my life, including Mrs. Nelson, Mrs. Fisher, Mrs. Bordelon, Mrs. Alexander, Mrs. Curtin, Coach Grace, and Coach Butler.

Lastly, I owe the biggest thanks to my family, to whom I have dedicated my dissertation, including, Wade and Debbie; Amanda, Keith & Emily; Fred, Jennifer, Gizselle, & Manny; Grandma Spahn; Grandma Ward; 'Grandma' Lillie; Uncle Curt, Aunt Celia, & Cousin Kelsey; Uncle Darrell; Aunt Mandy; Aunt Becky. A special thank you to my mom and dad who have

taught me to dream big, to work hard to accomplish those dreams, and be open to new directions those dreams may take me. I cannot thank them enough for their never-ending belief in me, support in everything I do, and encouraging words. Also, a special thank you to my big sister Amanda and big brother Fred for always watching out for their little sister and being amazing role models. Lastly, I dedicate my future research to my niece Emily Paige who is the biggest inspiration and joy of all and has a bright future ahead of her.

Chapter 1:

Introduction

The Biology of Amyloid Precursor Protein

Importance of APP to human health

Alzheimer's disease

Amyloid Precursor Protein (APP) was identified just over 25 years ago (Goldgaber et al, 1987; Kang et al, 1987; Tanzi et al, 1987). Since then, a central role for APP in the pathogenesis of Alzheimer's disease (AD) has been established. APP is processed via regulated intramembrane proteolysis to generate, amount other fragments, the amyloid-beta peptide (Aβ) (reviewed in (De Strooper & Annaert, 2000). Aβ aggregates to form amyloid deposits in brain parenchyma and its microvasculature during aging and in AD(Glenner & Wong, 1984; Masters et al, 1985). These extracellular Aβ plaques along with neurofibrillarly tangles of hyperphosphorylated Tau are the pathological hallmarks found in post-mortem AD brain. A vast number of biochemical and *in vivo* animal studies provide solid evidence that Aβ at least in part initiates a cascade resulting in synaptic dysfunction, neurodegeneration, and ultimately memory impairment in AD (reviewed in (Hardy & Selkoe, 2002)). These neurotoxic effects of Aβ are often attributed to various oligomeric assembly forms of the peptide (Lesné et al, 2013; Shankar et al, 2007).

The strongest evidence implicating APP in AD comes from genetic studies of rare, early-onset, familial cases of the disease. Over 200 dominantly inherited missense mutations have been identified in either the APP gene or Presenilin-1 or 2 genes (subunits of the γ-secretase complex that cleaves APP to generate Aβ) (reviewed in(Tanzi, 2012)). Mutations within APP are known to lead to either increase Aβ production, Aβ aggregation, or $A\beta_{42}/AP_{40}$ ratios. For example, the 'Swedish' mutation (which will be briefly used in Chapter 3) resides near the β-secretase cleavage site of APP and elevates Aβ levels by enhancing β-secretase cleavage of APP

(Citron et al, 1992; Mullan et al, 1992). The 'London' V717I mutation (studied in Appendix 2) resides within the transmembrane domain of APP near the γ-secretase cleavage site and leads to increased Aβ42/40 ratio (Goate et al, 1991; Tamaoka et al, 1994).

As a result, intensive efforts are underway to enhance Aβ clearance or to chronically inhibit β- or γ-secretase cleavage of APP to prevent Aβ generation as rational approaches to the treatment and prevention of AD (reviewed in(Selkoe, 2011). In fact, such therapeutic strategies are currently in patient trials. Nevertheless, the fundamental biological function of APP has not been definitively established. Elucidating the physiological function of APP and the role proteolytic processing plays in these functions would help better understand potential side-effects of reducing APP processing to treat AD. Further, identifying the precise molecular mechanisms that regulate APP processing—for example, a ligand which triggers the initial cleavage event-- could yield novel, biologically relevant drug targets for AD.

The APP family

APP family members

Much of the difficulty in elucidating the precise function of APP has been attributed to functional redundancy and compensation by its conserved family members. In mammals, two homologues for APP, termed amyloid precursor-like protein 1 (APLP1) and APLP2 share 56% and 68% amino acid sequence homology to APP, respectively (Slunt et al, 1994; Wasco et al, 1993; Wasco et al, 1992). APP orthologs have also been identified in non-mammalian species including appa and appb in zebrafish with 70% homology (Musa et al, 2001), APP-like (APPL) in *Drosophila melanogaster* with 43% homology (Luo et al, 1990; Rosen et al, 1989), and APL-1 in Caenorhabditis elegans with 46% homology (Daigle & Li, 1993)(reviewed in(Walsh et al, 2007)).

Structure

APP is an integral type I transmembrane glycoprotein. With a large extracellular domain (accounting for at least 88% of the total protein mass (Gralle & Ferreria, 2007), a single transmembrane domain, and three lysine residues in a short cytoplasmic tail, APP has been predicted to be a cell-surface receptor since its initial discovery (Kang et al, 1987). While the crystal structure of entire full-length APP or its ectodomain have not been solved despite multiple attempts, individual domains of the protein have been structurally characterized (reviewed in (Gralle & Ferreria, 2007)). These structural studies predict the ectodomain has regions of flexibility enabling it to undergo multiple conformation changes, which may have interesting implications for a putative APP ligand (Botelho et al, 2003; Gralle et al, 2002; Gralle & Ferreria, 2007). The flexibility of the APP ectodomain may allow it to recognize multiple ligands with high specificity. Binding of such a ligands could induce a conformational changes to stabilize the ectodomain or expose the α- or β- secretase cleavage sites, thus promoting ectodomain shedding (reviewed in (Gralle & Ferreria, 2007)).

The APP ectodomain can be characterized in terms of three major regions: the E1, acidic, and carbohydrate regions (Figure 1.1.) (reviewed in (Reinhard et al, 2005)). The reported binding of candidate ligands are not confined to a specific region of the APP ectodomain, rather protein-protein interactions have been reported within each of these domains. The amino-terminal E1 region, to which Reelin (Hoe et al, 2009) and CNTN4 (Osterfield et al, 2008) (as well as Pancortin in studies presented in Chapter 2) are reported to interact, consists of the growth factor-like domain (GFLD) followed by the copper-binding domain (CuBD). The GFLD, enriched with cysteines, contains disulfide bonds, a heparin binding site, and a hydrophobic surface

patch. These types of hydrophobic regions are generally known to be important sites for protein-protein interactions (Rossjohn et al, 1999). While several candidate ligands (Reelin, CNTNs, Pancortins) have been reported to bind a region of APP that includes this patch (Hoe et al, 2009; Osterfield et al, 2008; Rice et al, 2012)), its importance for ligand binding is not clear but should be considered. Linking the E1 region to the carbohydrate region is an acidic region, which is one flexible region that does not participate in any secondary structure. This is followed by the Kunitz-type protease inhibitor (KPI) domain and OX2 domain, which is removed through alternative splicing in some isoforms (described in more detail in the next section). The KPI domain has been shown to inhibit multiple serine proteases in vitro (Sinha et al, 1990) and to be involved in the coagulation cascade in human plasma (Smith et al, 1990; van Nostrand et al, 1990). The carbohydrate region, which contains a heparin binding site and 2 glycosylation sites, consists of the E2/central APP domain (CAPPD) and an unstructured linker domain. The E2/CAPPD, to which the candidate ligand F-spondin (Ho & Sudhof, 2004) has been reported to interact, contains an RERMS sequence with proposed trophic functions(Li et al, 1997; Ninomiya et al, 1993). The Aβ region resides partly within the extracellular linker sequence and partly within the transmembrane domain. The transmembrane domain is followed by a small cytoplasmic tail known as the APP intracellular domain (AICD), which contains phosphorylation sites and an YENPTY sequence implicated in intracellular interactions (Kerr & Small, 2005).

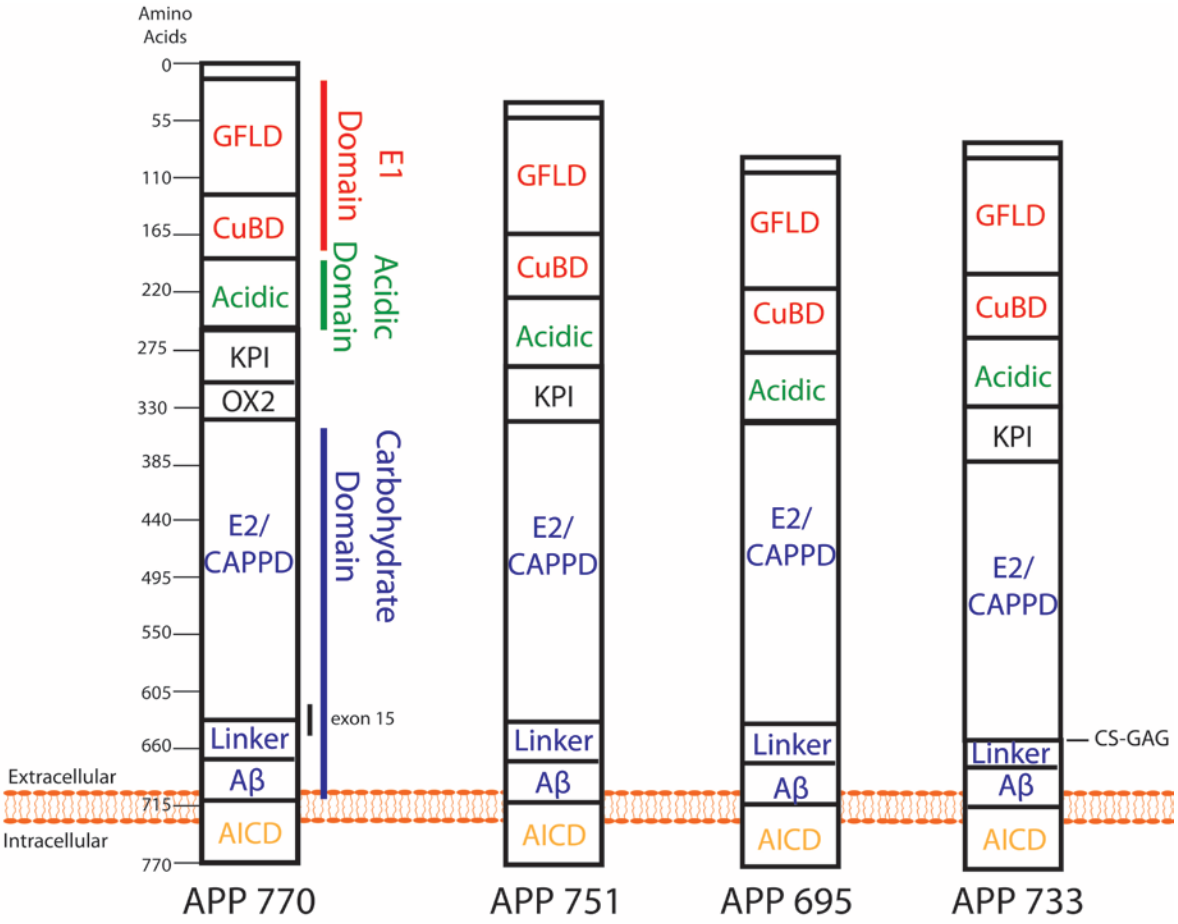

Figure 1.1 Structure and isoforms of APP.

The APP ectodomain is composed of the E1, Acidic, and Carbohydrate domains, each with multiple subdomains. Alternative splicing of APP leads to multiple isoforms, including APP770, APP751, APP695, and APP733 (also termed appican).

The structural similarities and differences of the APP family members may provide critical insights to both their redundant and separate functions. APP, APLP-1 and -2 have an almost entirely conserved intracellular domain, including the NPXY internalization motif (Walsh et al, 2007). Within the ectodomains of the APP family members, the E1 and E2 regions are also quite conserved; however, the juxtamembrane regions including the Aβ sequence are highly divergent (Walsh et al, 2007). Thus, the AD-relevant Aβ peptide is unique to APP. Recently, evidence has begun to suggest that these structural similarities enable the APP family members to form both homo- and heter-dimerization in cis and trans. Multiple sites of interaction have been described including a requirement of the E1 region for APP and APLP2 dimerization and the requirement of the E2 region for dimerization of APLP1 (Kaden et al, 2009; Soba et al, 2005). A GxxxG motif within the transmembrane domain has been reported to be a third site for stabilization of APP dimers (Munter et al, 2007).

Expression

In mammals, the APP gene, containing 19 exons, is expressed as multiple isoforms through alternative splicing (Figure 1.1) (Yoshikai et al, 1990). The APP700 isoform results from the non-spliced transcript; whereas, APP751 results from splicing of exon 8 containing the OX2 sequence, and APP695 results from splicing of both exons 7 and 8 which removes the KPI domain as well as the OX2 sequence. In addition to these three main isoforms, the APP733 isoform often termed 'appican' is generated by splicing of exon 15 to yield a consensus sequence for the attachment of chondroitin sulfate chains at the exon 14-16 fusion site just n-terminal to the Aβ sequence(Pangalos et al, 1995). APLP2, but not APLP1, undergoes alternative splicing to generate similar isoforms as APP (Lenkkeri et al, 1998).

While APP is enriched in neuronal tissues, it is also expressed ubiquitously throughout non-neural tissues. APP695 is the predominant isoform in neuronal tissue, and APP770 and APP751 are the predominant isoforms in non-neuronal tissues but are also expressed in the brain (Ohyagi et al, 1990; Sisodia et al, 1993). APP733 is expressed primarily in astrocytes. The Like APP, APLP2 is ubiquitously expressed but enriched in neurons; whereas, APLP1 is expressed almost exclusively by neurons (Lorent et al, 1995). Expression levels of each of the APP family members increase progressively over embryonic development (Lorent et al, 1995). Within the embryonic cortex, evidence suggests that APP family members may differ in their expression patterns. APP is reported to be expressed throughout the cortical plate (CP) and in a subset of cells in the intermediate (IZ) and ventricular (VZ) zones; whereas APLP1 expression is reported to be more confined to the VZ and subventricular zone (SVZ) and APLP1 to the CP (López-Sánchez et al, 2005; Young-Pearse et al, 2007). Within neurons, APP is localized in neurites to growth cones and at both presynaptic and postsynaptic terminals (Sabo et al, 2003; Yamazaki et al, 1997).

Trafficking and proteolytic processing of APP

Amyloidogenic and non-amyloidogenic processing pathways

APP undergoes sequential proteolytic processing during normal cell metabolism (Figure 1.2) (Haass et al, 1992). Two distinct processing pathways can lead to either the generation of Aβ (the amyloidogenic pathway) or preclude Aβ generation (the non-amyloidogenic pathway) (reviewed in(De Strooper & Annaert, 2000). In the amyloidogenic pathway, the initial cleavage event is performed by β-secretase primarily between Met596 and Asp597 (APP695 numbering)

but also to a lesser degree between Tyr606 and Glu607. This results in shedding of the large APP ectodomain, releasing a fragment termed APPsβ. The remaining C-terminal fragment (CTFβ) of 99 amino acids is then cleaved by γ-secretase. Cleavage of CTFβ by γ-secretase releases Aβ into the luminal/extracellular space and AICD into the cytoplasm. The non-amyloidogenic pathway is quite similar except the initial cleavage event is performed by α-secretase between Lys612 and Leuc613 within the Aβ sequence, thereby preventing Aβ generation. APPsα is shed into the extracellular space and CTFα of 83 amino acids is retained in the membrane. CTFα is cleaved by γ-secretase to release p3 into the luminal/extracellular space and AICD into the cytoplasm. APLP-1 and -2 undergo similar sequential proteolytic processing as APP, but it does not result in generation of an Aβ peptide due to sequence differences. Recently, an additional cleavage event has been proposed, in which a yet unknown protease further cleaves APPsβ to generate a 35kDa fragment termed N-APP (Nikolaev et al, 2009). However, this has yet to be further investigated and confirmed by multiple laboratories.

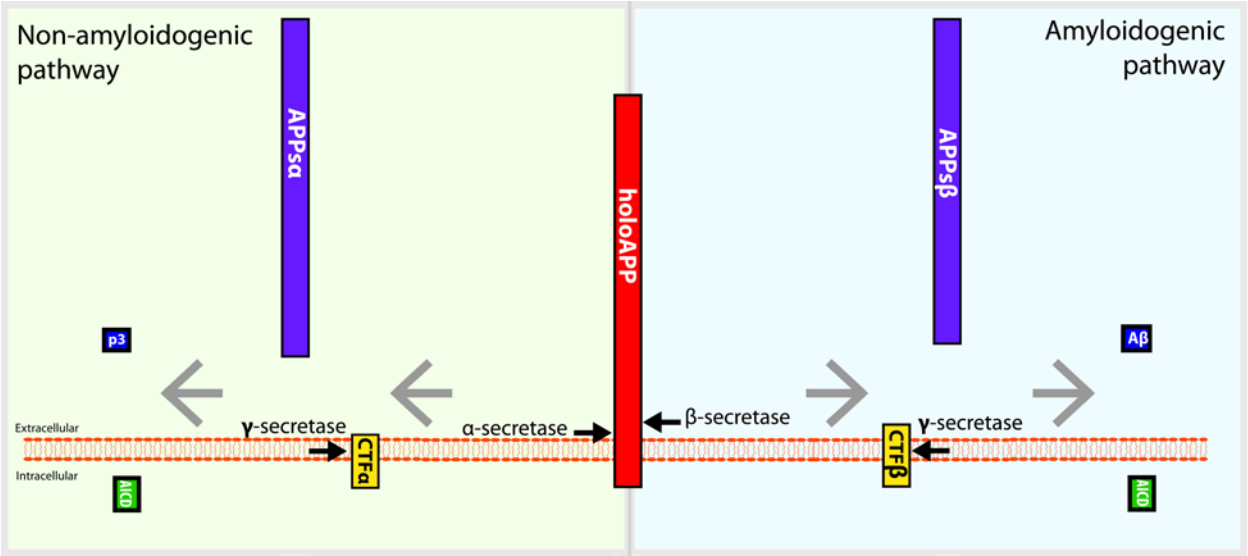

Figure 1.2 Proteolytic processing of APP

Sequential proteolytic processing APP occurs in either an amyloidogenic pathway, which produces Aβ or a non-amyloidogenic pathway which precludes Aβ production.

The secretases

Beta-site APP-cleaving enzyme-1 (BACE1) has been identified as the principal β-secretase (Hussain et al, 1999; Sinha et al, 1999; Vassar et al, 1999; Yan et al, 1999). BACE1 is a type I single-transmembrane aspartyl protease with two active sites in the lumen/extracellular space. BACE1 is ubiquitously expressed with highest expression in brain. BACE1 is most active in acidic environments, and evidence suggests that β-secretase cleavage of APP occurs within the Golgi apparatus and endosomes (Vassar et al, 1999). Many preclinical studies and clinical trials have aimed to inhibit BACE1 to prevent Aβ production. However, the identification of a range of BACE1 substrates (Hemming et al, 2009) involved in many important biological pathways have given rise to safety concerns regarding this strategy (Wang et al, 2013).

Several members of the ADAM (a disintegrin and metalloproteinase) family of enzymes, which are type I transmembrane proteins, have been implicated in α-secretase activity, including ADAM17 (TACE), ADAM10, and ADAM9 (Buxbaum et al, 1998; Koike et al, 1999; Lammich et al, 1999). APP undergoes constitutive cleavage by α-secretase, which is reported to release approximately 30% of cell surface APP as APPsα (Koo, 1997). However, cleavage also can be elevated above constitutive levels in a pathway known as 'regulated' cleavage. ADAM10 is thought to be the primary secretase involved in constitutive cleavage particularly in neurons (Kuhn et al, 2010). ADAM17/TACE is thought to participate only in regulated cleavage of APP (Buxbaum et al, 1998). The regulated α-secretase pathway involves activation of protein kinase C (PKC) (Zhu et al, 2001). Treatment with phorbol esters or stimulation of muscarinic acetylcholine receptors, which activate PKC, increases the secretion of APPsα and decreases secretion of APPsβ and Aβ in some cells (Caporaso et al, 1992; Farber et al, 1995; Nitsch et al,

1992). Some findings suggest that PKC-regulated α-secretase activity is largely localized to intracellular trans- or post-Golgi compartments (Skovronsky et al, 2000), whereas, constitutive α-secretase activity predominantly occurs at the cell surface (Parvathy et al, 1999) .

γ-secretase is a large complex consisting of presenilin (PS)-1 or 2, the catalytic component, as well as nicastrin, anterior pharynx defective (APH)-1, and PS enhancer (PEN)-2 (reviewed in (De Strooper et al, 2012)). Presenilin is an aspartyl intramembrane protease that cleaves at several sites within the transmembrane domain of APP to produce Aβ peptides of different lengths with different propensities for aggregation (Wolfe et al, 1999). Findings by multiple groups support a model of sequential processivity of APP by γ-secretase in which cleavage occurs every 3 amino acids and begins either after amino acid 48 (of the Aβ peptide) and leads predominantly to Aβ42 or after amino acid 49 leading predominantly to Aβ40 ((Sastre et al, 2001; Weidemann et al, 2002). γ-secretase has also been the target of AD therapeutics, but with its many substrates (Hemming et al, 2008), more recent focus has been on γ-secretase modulators with APP selectivity rather than non-selective inhibitors.

Relationship between the amyloidogenic and non-amyloidogenic pathways, and the secretases

In non-neuronal cells, the non-amyloidgenic pathway is clearly predominant. However, processing by the amyloidogenic pathway is greater in neurons than in other cell lines and often reported to be the predominant pathway (Colombo et al, 2012; Simons et al, 1996), most likely due to higher expression levels of BACE1 in neurons. Reported ratios of APPsα/APPsβ found in cerebral spinal fluid (CSF) of healthy human controls include approximately 3.5 or 5

(depending on the ELISA) (Brinkmalm et al, 2013), 2 (Rosén et al, 2012), .6 (Lewczuk et al, 2010), and .3 (Lewczuk et al, 2010).

It has long been assumed that α-secretase and β-secretase compete for cleavage of APP, and thus an increase in α-secretase cleavage will result in a decrease in β-secretase cleavage and vice versa. These studies were primarily conducted using pharmacological stimulation or overexpression of the secretases (Hung et al, 1993; Kuhn et al, 2010; Skovronsky et al, 2000), a more recent well designed study compared cleavage of endogenous APP in several cell lines as well as primary neuronal cultures with knock-down or pharmacological inhibition of the endogenous secretases rather than over-expression (Colombo et al, 2012). In this study, α- and β- secretase did not appear to compete for cleavage of APP in several cell lines tested. However, there was a unidirectional inverse coupling of α- and β- secretase of APP in primary neuronal cultures. Knock-down of BACE1 enhanced APP cleavage by ADAM10, but knock-down of ADAM10 had no effect on BACE1 cleavage (Colombo et al, 2012).

Lastly, each of the secretases have long been considered to be separated both spatially and temporally. However, new evidence suggests a model in which a multi-protease complex containing both α- and γ-secretases sequentially cleaves APP (Chen et al., unpublished). Both α- and β- secretase were found to co-immunoprecipitate with γ-secretase. γ-secretase was found to positiviely regulate ADAM10 maturation. Furthermore, pharmacological inhibition of γ-secretase increased α-secretase activity and reduced β-secretase activity (Chen et al., unpublished).

APP Trafficking

APP is trafficked according to the constitutive secretory pathway from the endoplasmic reticulum (ER) through the Golgi apparatus to the plasma membrane (PM). It is estimated that only 10% of overexpressed APP expressed in the cell reach the PM (Haass et al, 2012). The half-life of APP at the cell surface is estimated to be only 10 mins or less before it is either recycled into endocytic vesicles or undergoes ectodomain shedding (Koo et al, 1996; Koo, 1997). Approximately 30% of the APP at the PM undergoes ectodomain shedding (Koo et al, 1996). holoAPP then is internalized into endocytic vesicles and sorted to the golgi, lysosomes, or recycled back to the PM. The half-life of APP within the cell is reported to be only 30 mins (Koo et al, 1996).

In Madin-Darby canine kidney (MDCK) cells to model trafficking in a polarized cell, APP and ADAM10 are targeted to the basolateral membrane and BACE1 to the apical membrane (De Strooper et al, 1995; Haass et al, 1994; Wilde-Bode et al, 1997). In neurons, APP is transported to both axons and dendrites. The transport of APP in has been more characterized in axons and involves continuous unidirectional fast axonal transport by kinesin-1 (Kaether et al, 2000)

Parallels between APP and Notch proteolytic processing

Soon after Presenilin was discovered as the aspartyl protease responsible for the intramembrane proteolytic cleavage of APP to generate Aβ, Notch was discovered as another substrate of presenlin mediated cleavage. Notch, a single type I transmembrane receptor, is an essential protein for early development and functions in cell fate determination (Artavanis-

Tsakonas et al, 1999). After an initial cleavage within the Notch ectodomain by a Furin-like protease in the golgi, the cleaved fragments associate together and travel to the plasma membrane (PM) (Blaumueller et al, 1997). At the PM, binding of its ligands, Delta or Jagged, stimulates α-secretase cleavage by TACE followed by presenilin mediated cleavage to release the cytoplasmic domain (NICD)(Brou et al, 2000; Zeng et al, 1998). NICD translocates to the nucleus and activates the CSL (CBR/suppressor of hairless/Lag1) family of transcription factors which regulates expression of specific gene targets such as the HES (Hairy/Enhancer of Split) family (Kopan, 2002). While there are important differences between APP and Notch proteolytic processing, the striking similarities bolstered the idea that APP also may be a cell receptor with a ligand that stimulates its ectodomain shedding by α-secretase.

APP Function

APP/APLP knockout animals

The classic method to determine the function of a particular gene product is to delete that gene in model organisms to generate "knockouts". In the case of APP, apparent compensation by its family members (and perhaps other type I transmembrane proteins) as well as the presence of multiple cleaved fragments of APP have made understanding its function difficult and led to an array of complex findings. APP does not seem to be essential for life, as knockout of APP results in viable and fertile mice with relatively minor defects (Li et al, 1996; Müller et al, 1994; Zheng et al, 1995). APP knockouts have lower body and brain weight, the latter of which appears to be attributed to deficits in the size of forebrain commisures and the corpus callosum (Magara et al, 1999; Müller et al, 1994). The mice also exhibit locomotor

and grip strength impairment (Ring et al, 2007; Zheng et al, 1995), gliosis (Seabrook et al, 1999; Zheng et al, 1995), hypersensitivity to seizures (Steinbach et al, 1998), and altered exploratory and circadian activity (Müller et al, 1994; Ring et al, 2007). With aging, APP null mice show impairment in long-term potentiation and learning and spatial memory (Dawson et al, 1999; Ring et al, 2007; Seabrook et al, 1999). Many of these defects in APP null mice can largely be rescued by knock-in of APPsα, suggesting that the APP ectodomain is vital to APP function (Ring et al, 2007).

The relatively mild phenotype of APP knockout mice is attributed to the proposed functional redundancy between APP and APLPs. While no phenotypes have been characterized for APLP2 knockouts and APLP1 knockouts only exhibit a reduction in body weight, combined APP/APLP2, APLP1/APLP2, and APP/APLP1/APLP2 knockouts are early postnatal lethal (Heber et al, 2000; von Koch et al, 1997). APP/APLP2 null mice display defects at neuromuscular and other peripheral synapses, including misalignment of pre- and postsynaptic markers, excessive nerve terminal sprouting, and a reduction in synaptic vesicles density and active zone size (Wang et al, 2005; Yang et al, 2005). These effects of APP on synaptic development at the NMJ have been attributed to its regulation of endocystosis of the high-affinity choline transporter (Wang et al, 2007; Wang et al, 2009). Conditional knockouts with a loss of APP in either presynaptic motor neurons or postsynaptic muscle cells separately on a APLP2 null background led to similar defects at the neuromuscular synapse, indicative of a role for APP both pre- and post-synaptically perhaps through trans-dimerization (Wang et al, 2009). Knock-in of APPsβ was unable to rescue APP/APLP2 knock-out (Li et al, 2010); however, knock-in of APPsα rescues largely rescues postnatal lethality (Weyer et al, 2011). However, many defects in

neurotransmission and cognition remain in these mice, suggesting there are some functions of full-length APP/APLP2 that cannot be accounted for by APPsα (Weyer et al, 2011). APP/APLP1/APLP2 null mice exhibit cortical dysplasias in which focal regions of neuroblasts migrate beyond their appropriate cortical layer, a defect resembling human type II cobblestone lissencephaly (Herms et al, 2004). A partial loss of the Reelin expressing Cajal Retzius cells was also reported(Herms et al, 2004) (Herms et al., 2004).

Drosophila with deletion of APPL are also viable and fertile but have some behavioral (Luo et al, 1992) and synaptic (Ashley et al, 2005; Torroja et al, 1999) deficits. Phenotypes at the synapse include a reduced numbers of synaptic boutons, reduced amplitude of evoked excitatory junctional potentials, and enhanced amplitude and frequency miniature excitatory junction potentials (Ashley et al, 2005; Torroja et al, 1999). In Caenorhabditis elegans, loss of apl-1 causes defects in molting and morphogenesis, leading to lethality during the larval stage (Hornsten et al, 2007). Similar to mice, overexpression of the apl-1 ectodomain rescues lethality (Hornsten et al, 2007) further emphasizing the functional importance of the APPsα fragment.

In utero electroporation studies

Another method, besides combined APP/APLP knockouts, utilized to circumvent the problem of compensation by the APP family members is *in utero* electroporation. *In utero* electroporation has revealed roles for APP in cortical migration and APLP2 in neural differentiation within the rodent cortex (Shariati et al, 2013; Young-Pearse et al, 2007). With electroporation of APP shRNA, newly postmitotic cells in the ventricular zone largely failed to enter the cortical plate, and those in the lateral ventricle were able to migrate in the lateral

cortical stream but then later failed to enter the cortical plate (Young-Pearse et al, 2007). Electroporation of APP or the APLPs rescued this defect. However, the intracellular or extracellular domains of APP alone were unable to rescue (Young-Pearse et al, 2007). Taken together, these findings suggest that APP has a specific role in cortical plate entry, not just general motility of cortical neurons, and that the function of APP in cortical migration is redundant with the other APLP members and requires the full-length protein or perhaps its *regulated* cleavage. Further mechanistic studies demonstrated that interaction with two cytosolic signaling proteins, disabled 1 (DAB1) and disrupted in schizophrenia 1 (DISC1) mediated the effects of APP-dependent cell migration (Young-Pearse et al, 2010; Young-Pearse et al, 2007). In utero electroporation of APLP2 shRNA in APP/APLP1 knockout mice also resulted in abnormal positioning of cells in the cortical plate(Shariati et al, 2013). However, this was attributed to a decreased cell cycle exit and thus progenitors remaining longer within the ventricular zone in an undifferentiated state (Shariati et al, 2013). Further experiments should be performed to determine whether these represent distinct or overlapping functions of APP and APLP2 to produce effects on cell positioning within the cortical plate.

In vitro and cell culture studies

APP has been implicated as a cell adhesive factor, which is consistent with other demonstrated functions in neuronal cortical migration, synapse formation, and neurite outgrowth. APP colocalizes with markers of adhesion patches (Storey et al, 1996) and more specifically with Integrin β1 at these contact sites (Yamazaki et al, 1997). Integrin β1 interacts with APP and promotes cell adhesion through an RHDS motif located in the most C-terminal

portion of the APP ectodomain (Ghiso et al, 1992). The reported interactions of APP with extracellular matrix proteins, including heparin and collagen, further implicate APP as a cell adhesion factor (Beher et al, 1996; Multhaup, 1994). Lastly, multiple reports have implicating trans-acting dimerization of members of the APP family in promoting cell adhesion (Kaden et al, 2008; Soba et al, 2005).

A role in neurite outgrowth has long been attributed to holoAPP and APPs. However, there have been some conflicting data as to whether holoAPP and APPs enhance or inhibit neurite outgrowth. Studies which measured neurite outgrowth within 48 hrs reported an outgrowth promoting effect by holoAPP (Allinquant et al, 1995; Qiu et al, 1995), but studies which measured neurite outgrowth at longer time points reported a suppression in neurite outgrowth by holoAPP (Perez et al, 1997; Young-Pearse et al, 2008). Likewise, some studies suggest APPs stimulates neurite outgrowth (Araki et al, 1991; Milward et al, 1992; Ohsawa et al, 1995; Young-Pearse et al, 2008).

APP family members have been implicated in synapse formation and function primarily in peripheral synapses (i.e. the neuromuscular junction) (Wang et al, 2005; Wang et al, 2009; Weyer et al, 2011; Yang et al, 2005) and to a lesser extent in central synapses (Priller et al, 2006; Tyan et al, 2012; Wang et al, 2009). In primary hippocampal cultures from APP knockout mice, the amplitudes of evoked EPSCs, the size of the readily releasable synaptic vesicle pool, and the frequency of mEPSCS were each enhanced. However, the release probability of synaptic vesicles and the amplitude of mEPSCs were unaltered, suggesting that lack of APP leads to an increase in the number of synapses per neuron (Priller et al, 2006). In an

HEK293/primary neuron co-culture system a transynaptic interaction of APP family members promoted synaptogenesis (Wang et al, 2009).

Summary of APP function in the brain

In summary, through both ex vivo and in vivo studies, APP and its family members have been implicated in a number of diverse functions in the development of the nervous system, including synapse formation and function, cortical cell migration, neurite outgrowth, and cell adhesion. A number of studies have implicated APP at the synapse including 1) hypersensitivity to seizure and LTP defects in APP null mice, 2) defects at peripheral synapses in APP/APLP2 mice, 3) synaptic defects in hippocampal cultures from APP/APLP2 double knockout mice, and 4) synapse promoting effects of APP in a mixed culture assay. Evidence for a role of APP in neuronal cell migration includes 1) an overmigration phenotype displayed by focal cortical dysplasias in the combined triple knockout mice, and 2) a failure in cortical plate entry for cells with knockdown of APP by in utero electroporation . These seemingly opposite migratory effects, could be accounted for by such technical differences as chronic vs acute and global vs. local knockdown of APP using these two methods, but regardless it is strong evidence towards a roll of APP in cortical cell migration. A role for APP in neurite outgrowth is suggested by 1) deficits in the size of forebrain commisures and the corpus callosum and 2) effects of APP knockdown or APPsα treatment on neurite outgrowth (both promotion and inhibition) in a large number primary neuronal culture studies. This array of functions described for APP in cortical cell migration, synapse formation, and neurite outgrowth may indicate APP is more generally a cell adhesive factor.

APP as a receptor with a putative ligand

Since its initial cloning over 25 years ago, APP was predicted to be a cell surface receptor (Kang et al, 1987). Comparison of APP processing to that of Notch which is known to be regulated by ligand binding, promoted the idea of APP as a receptor with a physiological ligand to regulate its processing and function (Figure 1.3). For many functions of APP, such as cortical cell migration, the intracellular and extracellular domains are both required for proper functioning, which has led to the hypothesis that that specific extracellular factors bind the ectodomain of holoAPP on the cell surface and transmit a signal to intracellular signaling cascades. Important downstream factors described for APP include Dab1, DISC1, Tip60, and Fe65(Cao & Sudhof, 2004; Kimberly et al, 2001; Young-Pearse et al, 2010; Young-Pearse et al, 2007) (Figure 1.4). The intracellular domain of APP (AICD) has been reported to function as a transcription factor. However, this has been highly controversial, potential target genes typically have been reported by single labs and using overexpressed systems with artificial reporter constructs. Attempts to confirm such genes regulated by AICD has been largely unsuccessful (Chen & Selkoe, 2007; Hass & Yankner, 2005; Hebert et al, 2006). However, there is stronger evidence that the cleaved extracellular domain of APP itself has biological activities (Ring et al, 2007), suggesting a functional consequence of regulated cleavage of APP. In recent years, several candidate protein ligands for APP, including F-spondin (Ho & Sudhof, 2004; Hoe et al, 2005), Reelin (Hoe et al, 2009; Hoe et al, 2006), β1 Integrin (Hoe et al, 2009; Young-Pearse et al, 2008), Contactins (Bai et al, 2008; Ma et al, 2008; Osterfield et al, 2008), and Lingo-1 (Bai et al, 2008) have been reported to interact physically with the ectodomain of APP and

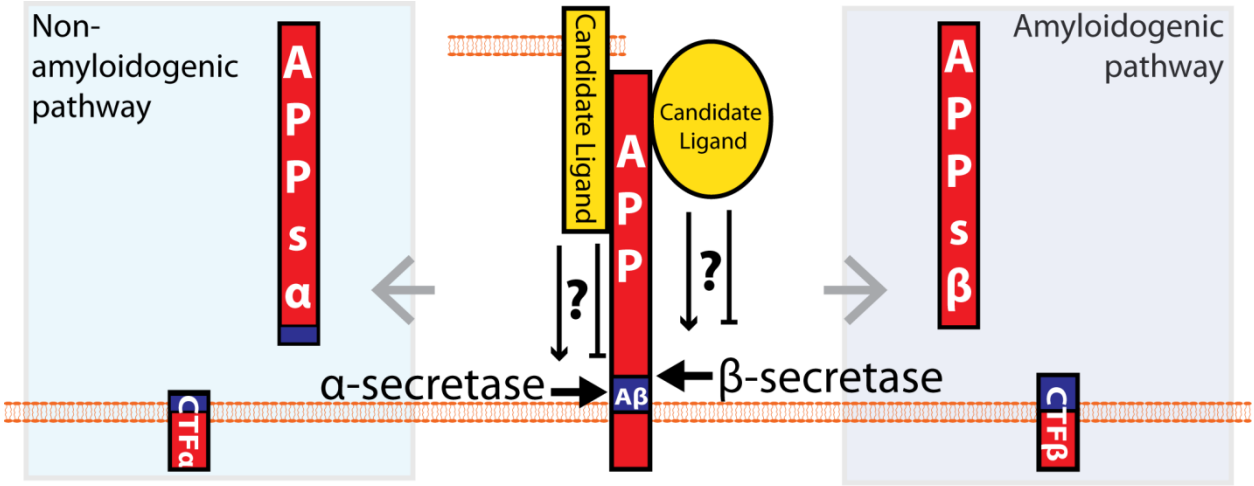

Figure 1.3 Hypothesis of APP as a receptor with a putative ligand

My central hypothesis is that one or more protein ligands for APP are present in the central nervous system that regulate the ectodomain shedding of APP, either be promoting or reducing α- and/or β- secretase cleavage of APP. A ligand for APP could be either a secreted or a membrane-bound protein that interacts with the APP ecotodomain.

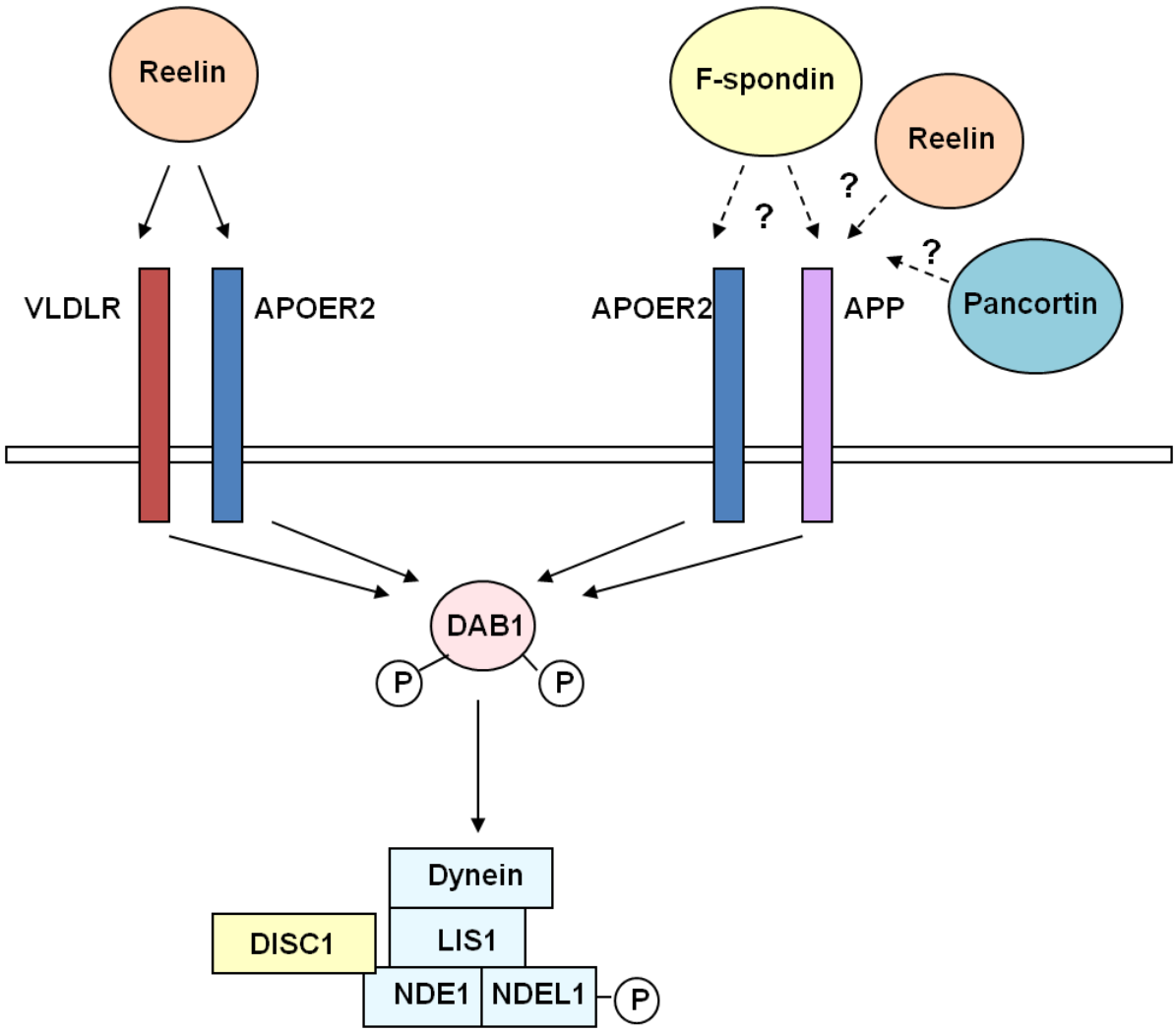

Figure 1.4 Schematic representation of factors involved in cortical cell migration.

The canonical Reelin-mediated effects of APOER2 and VLDLR on cortical migration are shown merged with the recently described effects of APP. Recently, our group found that DAB1 acts downstream of APP-mediated neuronal entry into the CP and that DISC1 acts downstream of holoAPP-DAB1. An important next question is whether binding of extracellular factors (e.g., Reelin, F-spondin, Pancortin and other candidates) is required for this developmental function of APP.

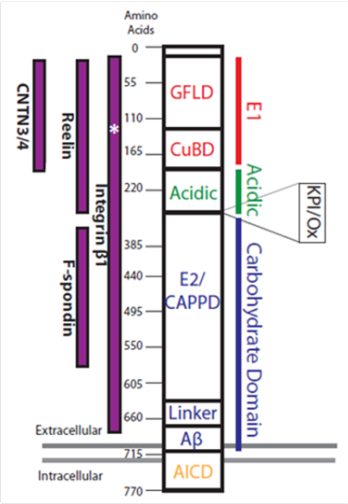

Candidate Ligands	APP Processing	APP Function	Reference
F-Spondin	↓CTFβ	n.d.	Ho & Südhof, 2004
	↑ APPsα, ↑CTFα, ↓CTFβ	n.d.	Hoe et al., 2005
Reelin	↑ APPsα, ↑CTFα	n.d.	Hoe et al., 2006
	↑ APPsα, ↑CTFα	Neurite Outgrowth	Hoe et al., 2009
β1 Integrin	n.d.	Neurite Outgrowth	Young-Pearse et al., 2008
	↑ APPsα, ↑CTFα	Neurite Outgrowth	Hoe et al., 2009
CNTN2	↑AICD	Neurogenesis	Ma et al., 2008
CNTN4	both ↑ and ↓ CTFα	Neurite Outgrowth	Osterfield et al., 2008
Lingo-1	↓CTFα, ↑ CTFβ	n.d.	Bai et al., 2008

Figure 1.5 Summary of published candidate APP ligands

A number of candidate ligands for APP have been described which interact with the APP ectodomain, modulate processing of APP by α- or β- secretase, and in some cases modulate APP function.

modulate APP processing and, in some cases, APP function in neurodevelopment (Figure 1.5). However, a cognate ligand for APP that regulates its function or processing has yet to be widely confirmed in multiple laboratories.

Published candidate APP ligands

F-spondin

F-spondin is composed of an amino-terminal reelin domain, a central F-spondin specific domain, and 6 thrombospondin type-1 repeats (TSRs) in its carboxy-terminus (Burstyn-Cohen et al, 1999). After secretion, F-spondin is cleaved by plasmin, a serine protease, at several sites (Tzarfaty-Majar et al, 2001). F-spondin is expressed at high levels in the floor plate (Klar et al, 1992), peripheral nerves (Burstyn-Cohen et al, 1998), and somatic regions avoided by migrating neural crest cells (Debby-Brafman et al, 1999) during embryonic development in rodents. Expression of F-spondin begins around E10 and diminishes by birth except after axonal injury (Burstyn-Cohen et al, 1998; Klar et al, 1992). F-spondin possesses dual activity by both promoting outgrowth of commissural axons (Burstyn-Cohen et al, 1999) and inhibiting outgrowth of neural crest cells (Debby-Brafman et al, 1999)and motor neurons (Tzarfati-Majar et al, 2001). F-spondin also has less characterized roles in neurogenesis(Schubert et al, 2006), angiogenesis (Terai et al, 2001), and axonal regeneration following injury (Burstyn-Cohen et al, 1998).

Three independent studies have demonstrated a physical interaction between F-spondin and APP (Ho & Sudhof, 2004; Hoe et al, 2005). F-spondin was first identified as an APP interacting protein through an affinity chromatography screen to identify solubilized proteins

from the membrane fraction of rat brains that bound the CAPPD domain of APP (Ho & Sudhof, 2004). The interaction between APP and F-spondin was validated by pull down of holoAPP by F-spondin (Ho & Sudhof, 2004). A subsequent study confirmed that full-length APP co-immunoprecipitates with F-spondin (Hoe et al, 2005). F-spondin was also later identified in an unbiased screen as one of several proteins that co-immunoprecipitated with APP from in vivo cross-linked mouse brains(Bai et al, 2008). Both the reelin and spondin domains of F-spondin as well as the CAPPD domain of APP were shown to be necessary for the binding of F-spondin to APP (Ho & Sudhof, 2004; Hoe et al, 2005). F-spondin also binds to ApoEr2, and full length F-spondin increases the co-immunoprecipitation of ApoEr2 with APP, suggesting that F-spondin, APP, and ApoEr2 cluster at the cell surface as a complex (Hoe et al, 2005).

Multiple groups have reported effects of F-spondin on APP processing. F-spondin was initially reported to decrease CTFβ levels in cells co-transfected with APP and BACE1, suggesting F-spondin inhibits β-secretase cleavage (Ho & Sudhof, 2004). While this study did not directly examine cleavage by α-secretase, F-spondin inhibited APP-dependent transactivation of Gal4-Tip60 mediated transcription, suggesting that α-secretase cleavage would also be inhibited by F-spondin (Ho & Sudhof, 2004). Contrary to this prediction, a subsequent study reported F-spondin (with co-transfection of APOER2) reduced CTFβ and enhanced both APPsα and CTFα levels (Hoe et al, 2005). Most recently, F-spondin gene transfer was shown to reduce Aβ levels in mouse brain (Hafez et al, 2012).No studies have yet to demonstrate a consequence of F-spondin interaction with APP on APP function in neurodevelopment.

Reelin

Reelin, a large secreted glycoprotein, consists of an N-terminal Reelin domain, eight Reelin repeats, each with an EGF-like repeat, and a C-terminal region rich in arginines. Reelin undergoes proteolytic cleavages at both its C-terminal and N-terminal ends to generate five fragments (Jossin et al, 2007; Jossin et al, 2004; Lambert de Rouvroit et al, 1999). Reelin is secreted from Cajal-Retzius cells in the embryonic cortex and regulates the migration of neuronal precursor cells (reviewed in (Honda et al, 2011)). In the adult cortex, Reelin is secreted by a subset of interneurons and plays a role in synaptic plasticity (reviewed in (Förster et al, 2010)). The Reelin signaling pathway includes activation of its canonical receptors APOER2 and VLDLR which leads to Disabled phosphorylation and other downstream (D'Arcangelo et al, 1999; Hiesberger et al, 1999).

Reelin has been associated with AD in multiple studies. In these studies, AD brains have increased Reelin expression, as do brains from transgenic APP mice (Botella-López et al, 2010). Reelin associated with fibrillary Aβ species (Knuesel et al, 2009) and co-localized with oligomeric Aβ (Doehner & Knuesel, 2010). Reelin could reduce the Aβ-induced suppression of LTP (Durakoglugil et al, 2009). In AD transgenic mice, Aβ and tau pathology is accelerated with reduced Reelin expression (Kocherhans et al, 2010). Reelin knockouts (Reeler) and APOER2/VLDLR double knockout mice show hyperphosphorylated Tau (Hiesberger et al, 1999).

Reelin has been shown to interact with APP in mouse brain, primary cortical neuronal cultures, and non-neuronal cell lines through co-immunoprecipitation studies (Hoe et al, 2009). The 3– 6 reelin repeats and the E1 domain of APP were essential for this interaction (Hoe et al, 2009). In cells COS7 cells overexpressing APP, treatment with Reelin conditioned media

enhanced APPsα and CTFα (Hoe et al, 2009; Hoe et al, 2006) . In both COS7 cells overexpressing APP and neurons from APP transgenic mice, Reelin CM reduced Aβ levels (Hoe et al, 2006). Reelin also increased cell surface levels of APP and enhanced to co-IP of APP with Dab1(Hoe et al, 2009; Hoe et al, 2006). Subsequently, another group showed that reduction of Reelin enhanced both CTFβ and Aβ in APP transgenic mice (Kocherhans et al, 2010).A functional interaction between Reelin and APP in neurite outgrowth has been described, in which Reelin enhanced neurite length in the presence of endogenous APP, but had no effect after APP knockdown (Hoe et al, 2009).

β*1 Integrin*

Integrins are type-1 transmembrane proteins that form heterodimers of α and β chains and link the extracellular matrix or other cells to intracellular signaling cascades. Integrins function in cell adhesion, cell migration, and neurite outgrowth (reviewed in (Schwartz, 2001)). β1 Integrin colocalizes and biochemically interact with APP (Ghiso et al, 1992; Yamazaki et al, 1997; Young-Pearse et al, 2007). Transfection of β1 Integrin in COS7 cells overexpressing APP enhanced APPsα and CTFα (Hoe et al, 2009). β1 Integrin has been reported to mediate the neurite outgrowth effects of APP, whereby a function-blocking antibody to β1 Integrin abolished the effects of APP knock-down, APP over-expression, or APPsα treatment (Hoe et al, 2009; Young-Pearse et al, 2008).

Contactins

The Contactins (CNTNs) are GPI-anchored neuronal-specific cell adhesion molecules characterized by six aminio-terminal immunoglobulin-like domains and four carboxyl-terminal

fibronectin type III-like domains (Karagogeos, 2003). The CNTNs can remain bound to the membrane through its GPI anchor or be released as a soluble protein by GPI-specific phospholipase (Durbec et al, 1992; Furley et al, 1990; Lierheimer et al, 1997). The individual CNTNs are expressed in both overlapping and distinctive patterns within the developing and adult nervous system (Yoshihara et al, 1995). Expression of the CNTNs is enriched in axonal processes and is most robust during developmental stages (Dodd et al, 1988; Gennarini et al, 1989; Karagogeos, 2003). The CNTNs have been primarily implicated in neurite outgrowth (Furley et al, 1990; Gennarini et al, 1991; Yoshihara et al, 1994).

CNTN1 and CNTN4 were identified in separate unbiased screens as APP binding partners, and CNTN2 and CNTN3 were identified as APP binding partners through candidate approaches (Bai et al, 2008; Ma et al, 2008; Osterfield et al, 2008). CNTN1 was discovered by mass spectrometry as one of several proteins that co-immunoprecipitated with APP from in vivo cross-linked mouse brains (Bai et al, 2008). CNTN4 was identified in a screen for extracellular APP binding partners in embryonic chick brain (Osterfield et al, 2008). The fibronectin domain of CNTN4 and the E1 domain of APP were sufficient for this interaction (Osterfield et al, 2008). CNTN2 was investigated as an APP ligand because it was previously identified as a ligand for Notch and was confirmed to co-IP with APP from mouse brain (Ma et al, 2008). Both the immunoglobulin and the fibronectin domains of CNTN2 were reported to interact with APP (Ma et al, 2008). One study directly compared each of the six CNTN members in binding to APP and the closely related APLP1 in vitro. Only CNTN3 and CNTN4 interacted strongly with APPsα, only CNTNs 3, 4, and 5 interacted strongly with APLP1 (Osterfield et al,

2008). Noticeably, CNTNs 1, 2, and 6 either failed to or only very weakly interacted with APPs or APLP1 (Osterfield et al, 2008), despite other reports of physical interactions with APP.

Both CNTN2 and CNTN4 have been implicated in APP processing. CNTN2 enhanced AICD release as measured by a luciferase assay and Western blot analysis in CHO cells over-expressing APP as well as mouse embryonic fibroblasts endogenously expressing APP (Ma et al, 2008). In addition to AICD, CTFα and CTFβ were enhanced by CNTN2, suggesting CNTN2 stimulates α- and β- secretase cleavages. CNTN4 modified CTFα levels as measured by Western blot analysis in cells over-expressing CNTN4 and APP (Osterfield et al, 2008). In the majority of experiments, CNTN4 mediated an increase in CTFα levels. Interestingly, CNTN4 also produced a decrease in CTFα levels in a smaller number of experiments. However, in these studies holoAPP expression increased or decreased with CTF levels (Osterfield et al, 2008).

CNTN2 and CNTN4 have also been implicated in APP function. CNTN4 was reported to be involved in APP-NgCAM dependent neurite outgrowth (Osterfield et al, 2008) [11]. Both treatment with CNTN4 recombinant protein, which may act as a dominant negative, and transfection of CNTN4 shRNA inhibited the enhanced neurite outgrowth seen with APPs/NgCAM stimulation (Osterfield et al, 2008). In one study, CNTN2 was reported to regulate neurogenesis through an AICD/Fe65 signaling pathway (Ma et al, 2008).

Lingo-1

Lingo-1 (leucine rich repeat and Ig domain-containing Nogo receptor interacting protein-1), is a single-transmembrane protein with 12 leucine rich repeats, an Ig domain, a trans-membrane domain, and a short cytoplasmic tail with an epidermal growth factor

receptor-like tyrosine phosphorylation site. Lingo-1 is expressed in neurons and oligodendrocytes with peak expression around postnatal day 1 and decreasing thereafter, except after injury. Lingo-1 is a member of the Nogo-66 receptor complex and negatively regulates axonal myelination and regeneration (reviewed in (Mi et al, 2008)).

Lingo-1 was among the proteins identified (along with F-spondin) in the APP interactome study of intact mouse brain (Bai et al, 2008). This study further confirmed a physical interaction between APP and Lingo-1 and showed that knockdown of Lingo-1 in HEK293 cells stably overexpressing APP bearing the "Swedish" AD mutation increased CTFα and lowered CTFβ, whereas overexpression of Lingo-1 increased CTFβ (Bai et al, 2008). A separate group confirmed a physical interaction in an overexpressed cell system and determined that the interaction occurs via the ectodomain of Lingo-1 (Stein & Walmsley, 2012).

Pancortin, a novel candidate ligand

Pancortin is a secreted glycoprotein present in the extracellular matrix as four different isoforms specified as BMZ, BMY, AMZ, and AMY (Danielson et al, 1994). Differential promoter utilization generates an amino-terminus composed of either an A or B domain. Each isoform contains a common central M domain. Alternative splicing produces a carboxyl-terminus composed of either a Y or Z domain (Danielson et al, 1994). AMZ and AMY Pancortin isoforms are reported to be more efficiently secreted than the BMZ and BMY isoforms (Moreno & Bronner-Fraser, 2001).

Pancortins are expressed in neurons of both the embryonic and mature cortex. AMZ and AMY are the predominant isoforms expressed in the rodent embryonic cortex (Danielson et al,

1994; Nagano et al, 2000). In situ hybridization of rodent embryonic cortical sections detected mRNA for the A and Z domains at E12.5 in the neuroepithelium and mRNA for the A, Z, and Y domains at E16.5 in the neuroepithelium, subplate, cortical plate but not intermediate zone (Nagano et al, 2000). Western blot analysis further demonstrated that AMZ is initially expressed at E12.5 followed by AMY at E14.5 and BMZ at E16.5 (Nagano et al, 2000). In the adult cortex, the protein expression is similar for all four Pancortin isoforms (Nagano et al, 2000). While slightly different expression profiles are detected in chick and Xenopus, both further suggest a role of Pancortin in neuronal development. In chick, mRNA for the Z domain is present during early embryonic stages, and BMZ is expressed in a gradient within the open neural plate (Barembaum et al, 2000). In Xenopus, BMZ and AMZ are first detected following neural tube closure, and all four isoforms are robustly expressed in the adult cortex (Moreno & Bronner-Fraser, 2001).

While the function of Pancortin in the mammalian nervous system has not been fully elucidated, the BMZ and AMY isoforms of Pancortin have been reported to play a role in neurodevelopment in Xenopus and chick (Barembaum et al, 2000; Moreno & Bronner-Fraser, 2001). Over-expression of BMZ in chick embryos revealed a role for BMZ in neural crest formation (Barembaum et al, 2000). Studies in Xenopus suggest that BMZ and AMY cooperate in regulating the timing of neuronal differentiation (Moreno & Bronner-Fraser, 2001). In addition to these functions in neuronal development, one study reported a role for Pancortin in the adult rodent brain. Through studies in mice that lacked Pancortin expression in the adult cortex, BMY was proposed to function in a complex that sequesters an anti-apoptotic factor and promotes cell death following ischemic injury (Cheng et al, 2007). However, it remains

unclear what the normal function of Pancortin may be during development, as the loss of Pancortin only protected adult but not embryonic neurons against ischemic death, and other putative developmental phenotypes were not presented.

References

Allinquant B, Hantraye P, Mailleux P, Moya K, Bouillot C, Prochiantz A (1995) Downregulation of amyloid precursor protein inhibits neurite outgrowth in vitro. *J Cell Biol* **128:** 919-927.

Araki W, Kitaguchi N, Tokushima Y, Ishii K, Aratake H, Shimohama S, Nakamura S, Kimura J (1991) Trophic effect of β-amyloid precursor ptotein on cerebral cortical neurons in culture. *Biochem Biophys Res Commun* **181:** 265-271

Artavanis-Tsakonas S, Rand M, Lake R (1999) Notch signaling: cell fate control and signal integration in development. *Science (New York, NY)* **284:** 770-776

Ashley J, Packard M, Ataman B, Budnik V (2005) Fasciclin II signals new synapse formation through amyloid precursor protein and the scaffolding protein dX11/Mint. *J Neurosci* **25:** 5943-5955

Bai Y, Markham K, Chen F, Weerasekera R, Watts J, Horne P, Wakutani Y, Bagshaw R, Mathews PM, Fraser PE, Westaway D, St George-Hyslop P, Schmitt-Ulms G (2008) The in vivo brain interactome of the amyloid precursor protein. *Mol Cell Proteomics* **7:** 15-34

Barembaum M, Moreno T, LaBonne C, Sechrist J, Bronner-Fraser M (2000) Noelin-1 is a secreted glycoprotein involved in generation of the neural crest. *Nature Cell Biology* **2:** 219-244

Beher D, Hesse L, Masters CL, Multhaup G (1996) Regulation of amyloid protein precursor (APP) binding to collagen and mapping of the binding sites on APP and collagen type I. *J Biol Chem* **271:** 1613-1620

Blaumueller C, Qi H, Zagouras P, Artavanis-Tsakonas S (1997) Intracellular cleavage of Notch leads to a heterodimeric receptor on the plasma membrane. *Cell* **90:** 281-291

Botelho MM, Gralle M, Oliveira CLP, Torriani I, Ferreira ST (2003) Folding and stability of the extracellular domain of the human amyloid precursor protein. *J Biol Chem* **278:** 34259-34267

Botella-López A, Cuchillo-Ibáñez I, Cotrufo T, Mok S, Li Q-X, Barquero M-S, Dierssen M, Soriano E, Sáez-Valero J (2010) Beta-amyloid controls altered Reelin expression and processing in Alzheimer's disease. *Neurobiology of disease* **37:** 682-691

Brinkmalm G, Brinkmalm A, Bourgeois P, Persson R, Hansson O, Portelius E, Mercken M, Andreasson U, Parent S, Lipari F, Ohrfelt A, Bjerke M, Minthon L, Zetterberg H, Blennow K, Nutu M (2013) Soluble Amyloid Precursor Protein α and β in CSF in Alzheimer's Disease. *Brain research*

Brou C, Logeat F, Gupta N, Bessia C, LeBail O, Doedens JR, Cumano A, Roux P, Black RA, Israel A (2000) A novel proteolytic cleavage involved in Notch signaling: the role of the disintegrin-metalloprotease TACE. *Mol Cell* **5:** 207-216.

Burstyn-Cohen T, Frumkin A, Xu YT, Scherer SS, Klar A. (1998) Accumulation of F-spondin in injured peripheral nerve promotes the outgrowth of sensory axons. *J Neurosci*, Vol. 18, pp. 8875-8885.

Burstyn-Cohen T, Tzarfaty V, Frumkin A, Feinstein Y, Stoeckli E, Klar A. (1999) F-Spondin is required for accurate pathfinding of commissural axons at the floor plate. *Neuron*, Vol. 23, pp. 233-246.

Buxbaum J, Liu K, Luo Y, Slack J, Stocking K, Peschon J, Johnson R, Castner B, Cerretti D, Black R (1998) Evidence that tumor necrosis factor alpha converting enzyme is involved in regulated alpha-secretase cleavage of the Alzheimer amyloid protein precursor. *J Biol Chem* **273:** 27765-27767

Cao X, Sudhof TC (2004) Dissection of amyloid-beta precursor protein-dependent transcriptional transactivation. *J Biol Chem* **279:** 24601-24611

Caporaso GL, Gandy SE, Buxbaum JD, Ramabhadran TV, Greengard P (1992) Protein phosphorylation regulates secretion of Alzheimer β/A4 amyloid precursor protein. *Proc Natl Acad Sci USA* **89:** 3055-3059

Chen AC, Selkoe DJ. (2007) Response to: Pardossi-Piquard et al., "Presenilin-Dependent Transcriptional Control of the Abeta-Degrading Enzyme Neprilysin by Intracellular Domains of betaAPP and APLP." Neuron 46, 541-554. *Neuron*, Vol. 53, pp. 479-483.

Cheng A, Arumugam T, Liu D, Khatri R, Mustafa K, Kwak S, Ling H-P, Gonzales C, Xin O, Jo D-G, Guo Z, Mark R, Mattson M (2007) Pancortin-2 interacts with WAVE1 and Bcl-xL in a mitochondria-associated protein complex that mediates ischemic neuronal death. *The Journal of neuroscience : the official journal of the Society for Neuroscience* **27:** 1519-1547

Citron M, Oltersdorf T, Haass C, McConlogue L, Hung AY, Seubert P, Vigo-Pelfrey C, Lieberburg I, Selkoe DJ (1992) Mutation of the β-amyloid precursor protein in familial Alzheimer's disease increases β-protein production. *Nature* **360:** 672-674

Colombo A, Wang H, Kuhn P-H, Page R, Kremmer E, Dempsey P, Crawford H, Lichtenthaler S (2012) Constitutive α- and β-secretase cleavages of the amyloid precursor protein are partially coupled in neurons, but not in frequently used cell lines. *Neurobiology of disease* **49C:** 137-147

D'Arcangelo G, Homayouni R, Keshvara L, Rice DS, Sheldon M, Curran T (1999) Reelin is a ligand for lipoprotein receptors. *Neuron* **24:** 471-479

Daigle I, Li C (1993) Apl-1, a *C. elegans* gene encoding a protein related to the human β-amyloid protein precursor. *Proc Natl Acad Sci USA* **90:** 12045-12049

Danielson PE, Forss-Petter S, Battenberg EL, deLecea L, Bloom FE, Sutcliffe JG (1994) Four structurally distinct neuron-specific olfactomedin-related glycoproteins produced by differential promoter utilization and alternative mRNA splicing from a single gene. *J Neurosci Res* **38:** 468-478

Dawson GR, Seabrook GR, Zheng H, Smith DW, Graham S, O'Dowd G, Bowery BJ, Boyce S, Trumbauer ME, Chen HY, Van der Ploeg LH, Sirinathsinghji DJ (1999) Age-related cognitive deficits, impaired long-term potentiation and reduction in synaptic marker density in mice lacking the beta-amyloid precursor protein. *Neuroscience* **90:** 1-13.

De Strooper B, Annaert W (2000) Proteolytic processing and cell biological functions of the amyloid precursor protein. *J Cell Sci* **113:** 1857-1870

De Strooper B, Dewachter I, Moechars D, Van Leuven F, Van Den Berghe H (1995) Basolateral secretion of amyloid precursor protein in Madin-Darby canine kidney cells is disturbed by alterations of intracellular pH and by introducing a mutation associated with familial Alzheimer's disease. *J Biol Chem* **270:** 4058-4065

De Strooper B, Iwatsubo T, Wolfe M (2012) Presenilins and γ-secretase: structure, function, and role in Alzheimer Disease. *Cold Spring Harbor perspectives in medicine* **2**

Debby-Brafman A, Burstyn-Cohen T, Klar A, Kalcheim C. (1999) F-Spondin, expressed in somite regions avoided by neural crest cells, mediates inhibition of distinct somite domains to neural crest migration. *Neuron*, Vol. 22, pp. 475-488.

Dodd J, Morton RA, Karagogeos D, Yamamoto T, Jessel T (1988) Spatial regulation of axonal glycoprotein expression on subsets of embryonic spinal neurons. *Neuron* **1:** 105-166

Doehner J, Knuesel I (2010) Reelin-mediated Signaling during Normal and Pathological Forms of Aging. *Aging and disease* **1:** 12-29

Durakoglugil M, Chen Y, White C, Kavalali E, Herz J (2009) Reelin signaling antagonizes beta-amyloid at the synapse. *Proceedings of the National Academy of Sciences of the United States of America* **106:** 15938-15981

Durbec P, Gennarini G, Goridis C, Rougon G (1992) A soluble form of the F3 neuronal cell adhesion molecule promotes neurite outgrowth. *J Cell Biol* **117**

Farber SA, Nitsch RM, Schulz JG, Wurtman RJ (1995) Regulated secretion of beta-amyloid precursor protein in rat brain. *J Neurosci* **15:** 7442-7451.

Förster E, Bock H, Herz J, Chai X, Frotscher M, Zhao S (2010) Emerging topics in Reelin function. *Eur J Neurosci* **31:** 1511-1519

Furley AJ, Morton SB, Manalo D, Karagogeos D, Dodd J, Jessell TM (1990) The axonal glycoprotein TAG-1 is an immunoglobulin

superfamily member with neurite outgrowth promoting activity. *Cell* **61**

Gennarini G, Cibelli G, Rougon G, Mattei M, Goridis C (1989) The mouse neuronal cell surface protein F3: a phosphatidylinositol- anchored member of the immunoglobulin superfamily related to chicken contactin. *J Cell Biol* **109**

Gennarini G, Durbec P, Boned A, Rougon G, Goridis C (1991) Transfected F3/F11 neuronal cell surface protein mediates intercellular adhesion and promotes neurite outgrowth. *Neuron* **6:** 595-606

Ghiso J, Rostagno A, Gardella JE, Liem L, Gorevic PD, Frangione B (1992) A 109-amino-acid C-terminal fragment of Alzheimer's-disease amyloid precursor protein contains a sequence, -RHDS-, that promotes cell adhesion. *Biochem J* **288:** 1053-1059

Glenner GG, Wong CW (1984) Alzheimer's disease and Down's syndrome: Sharing of a unique cerebrovascular amyloid fibril protein. *Biochem Biophys Res Commun* **122:** 1131-1135

Goate A, Chartier-Harlin M-C, Mullan M, Brown J, Crawford F, Fidani L, Giuffra L, Haynes A, Irving N, James L, Mant R, Newton P, Rooke K, Roques P, Talbot C, Pericak-Vance M, Roses A, Williamson R, Rossor M, Owen M, Hardy J (1991) Segregation of a missense mutation in the amyloid precursor protein gene with familial Alzheimer's disease. *Nature* **349:** 704-706

Goldgaber D, Lerman MI, McBridge OW, Saffiotti V, Gajdusek DC (1987) Characterization and chromosomal localization of a cDNA encoding brain amyloid of Alzheimer's disease. *Science* **235:** 877-880

Gralle M, Botelho MM, de Oliveria CLP, Torriani I, Ferreira ST (2002) Solution studies and structural model of the extracellular domain of the human amyloid precursor protein. *Biophysical Journal* **83:** 3513-3524

Gralle M, Ferreria ST (2007) Structure and functions of human amyloid precursor protein: The whole is more than the sum of its parts. *Progress in Neurobiology* **82:** 11-32

Haass C, Kaether C, Thinakaran G, Sisodia S (2012) Trafficking and Proteolytic Processing of APP. *Cold Spring Harbor Perspectives in Medicine* **2**

Haass C, Koo EH, Teplow DB, Selkoe DJ (1994) Polarized secretion of β-amyloid precursor protein and amyloid β-peptide in MDCK cells. *Proc Natl Acad Sci USA* **91:** 1564-1568

Haass C, Schlossmacher M, Hung AY, Vigo-Pelfrey C, Mellon A, Ostaszewski B, Lieberburg I, Koo EH, Schenk D, Teplow D, Selkoe D (1992) Amyloid β-peptide is produced by cultured cells during normal metabolism. *Nature* **359:** 322-325

Hafez D, Huang J, Richardson J, Masliah E, Peterson D, Marr R (2012) F-spondin gene transfer improves memory performance and reduces amyloid-β levels in mice. *Neuroscience* **223:** 465-472

Hardy J, Selkoe D (2002) The amyloid hypothesis of Alzheimer's disease: progress and problems on the road to therapeutics. *Science (New York, NY)* **297:** 353-359

Hass M, Yankner B (2005) A {gamma}-secretase-independent mechanism of signal transduction by the amyloid precursor protein. *J Biol Chem* **280:** 36895-37799

Heber S, Herms J, Gajic V, Hainfellner J, Aguzzi A, Rulicke T, von Kretzschmar H, von Koch C, Sisodia S, Tremml P, Lipp HP, Wolfer DP, Muller U (2000) Mice with combined gene knock-outs reveal essential and partially redundant functions of amyloid precursor protein family members. *J Neurosci* **20:** 7951-7963.

Hebert SS, Serneels L, Tolia A, Craessaerts K, Derks C, Filippov MA, Muller U, De Strooper B (2006) Regulated intramembrane proteolysis of amyloid precursor protein and regulation of expression of putative target genes. *EMBO Rep* **7:** 739-745

Hemming M, Elias J, Gygi S, Selkoe D (2008) Proteomic profiling of gamma-secretase substrates and mapping of substrate requirements. *PLoS biology* **6**

Hemming M, Elias J, Gygi S, Selkoe D (2009) Identification of beta-secretase (BACE1) substrates using quantitative proteomics. *PloS one* **4**

Herms J, Anliker B, Heber S, Ring S, Fuhrmann M, Kretzschmar H, Sisodia S, Muller U (2004) Cortical dysplasia resembling human type 2 lissencephaly in mice lacking all three APP family members. *Embo J* **23:** 4106-4115

Hiesberger T, Trommsdorff M, Howell B, Goffinet A, Mumby M, Cooper J, Herz J (1999) Direct binding of Reelin to VLDL receptor and ApoE receptor 2 induces tyrosine phosphorylation of disabled-1 and modulates tau phosphorylation. *Neuron* **24:** 481-489

Ho A, Sudhof TC (2004) Binding of F-spondin to amyloid-beta precursor protein: a candidate amyloid-beta precursor protein ligand that modulates amyloid-beta precursor protein cleavage. *Proc Natl Acad Sci* **101:** 2548-2553

Hoe H-S, Lee K, Carney R, Lee J, Markova A, Lee J-Y, Howell B, Hyman B, Pak D, Bu G, Rebeck G (2009) Interaction of reelin with amyloid precursor protein promotes neurite outgrowth. *J Neurosci* **29:** 7459-7532

Hoe HS, Tran TS, Matsuoka Y, Howell BW, Rebeck GW (2006) DAB1 and Reelin effects on amyloid precursor protein and ApoE receptor 2 trafficking and processing. *J Biol Chem* **281:** 35176-35185

Hoe HS, Wessner D, Beffert U, Becker AG, Matsuoka Y, Rebeck GW (2005) F-spondin interaction with the apolipoprotein E receptor ApoEr2 affects processing of amyloid precursor protein. *Mol Cell Biol* **25:** 9259-9268

Honda T, Kobayashi K, Mikoshiba K, Nakajima K (2011) Regulation of cortical neuron migration by the Reelin signaling pathway. *Neurochem Res* **36:** 1270-1279

Hornsten A, Lieberthal J, Fadia S, Malins R, Ha L, Xu X, Daigle I, Markowitz M, O'Connor G, Plasterk R, Li C (2007) APL-1, a Caenorhabditis elegans protein related to the human beta-amyloid precursor protein, is essential for viability. *Proceedings of the National Academy of Sciences of the United States of America* **104:** 1971-1976

Hung A, Munsat T, Selkoe D (1993) Regulation of β-amyloid precursor protein processing into non-amyloidogenic and amyloidogenic derivatives by protein kinase C. *Society for Neuroscience Abstract* **19:** in press

Hussain I, Powell D, Howlett DR, Tew DG, Meek TD, Chapman C, Gloger IS, Murphy KE, Southan CD, Ryan DM, Smith TS, Simmons DL, Walsh FS, Dingwall C, Christie G (1999) Identification of a novel aspartic protease (Asp 2) as beta-secretase [In Process Citation]. *Mol Cell Neurosci* **14:** 419-427

Jossin Y, Gui L, Goffinet A (2007) Processing of Reelin by embryonic neurons is important for function in tissue but not in dissociated cultured neurons. *J Neurosci* **27:** 4243-4295

Jossin Y, Ignatova N, Hiesberger T, Herz J, Lambert de Rouvroit C, Goffinet A (2004) The central fragment of Reelin, generated by proteolytic processing in vivo, is critical to its function during cortical plate development. *J Neurosci* **24:** 514-521

Kaden D, Munter L-M, Joshi M, Treiber C, Weise C, Bethge T, Voigt P, Schaefer M, Beyermann M, Reif B, Multhaup G (2008) Homophilic interactions of the amyloid precursor protein (APP) ectodomain are regulated by the loop region and affect beta-secretase cleavage of APP. *The Journal of biological chemistry* **283:** 7271-7280

Kaden D, Voigt P, Munter L-M, Bobowski K, Schaefer M, Multhaup G (2009) Subcellular localization and dimerization of APLP1 are strikingly different from APP and APLP2. *Journal of Cell Science* **122:** 368-377

Kaether C, Skehel P, Dotti C (2000) Axonal membrane proteins are transported in distinct carriers: a two-color video microscopy study in cultured hippocampal neurons. *Molecular biology of the cell* **11:** 1213-1224

Kang J, Lemaire H-G, Unterbeck A, Salbaum JM, Masters CL, Grzeschik K-H, Multhaup G, Beyreuther K, Muller-Hill B (1987) The precursor of Alzheimer's disease amyloid A4 protein resembles a cell-surface receptor. *Nature* **325:** 733-736

Karagogeos D (2003) Neural GPI-anchored cell adhesion molecules. *Frontiers in Bioscience* **8**

Kerr ML, Small DH (2005) Cytoplasmic domain of the b-amyloid protein precursor of Alzheimer's disase: Function, regulation and proteolysis, and implications for drug development. *Journal of Neuroscience Research* **80:** 151-159

Kimberly WT, Zheng JB, Guenette SY, Selkoe DJ (2001) The intracellular domain of the beta-amyloid precursor protein is stabilized by Fe65 and translocates to the nucleus in a notch-like manner. *J Biol Chem* **276:** 40288-40292

Klar A, Baldassare M, Jessel T (1992) F-Spondin: A gene expressed at high levels int he floor plate encodes a secreted protein that promotes neural cell adhesion and neurite extension. *Cell* **69:** 95-110

Knuesel I, Nyffeler M, Mormède C, Muhia M, Meyer U, Pietropaolo S, Yee B, Pryce C, LaFerla F, Marighetto A, Feldon J (2009) Age-related accumulation of Reelin in amyloid-like deposits. *Neurobiology of aging* **30:** 697-716

Kocherhans S, Madhusudan A, Doehner J, Breu K, Nitsch R, Fritschy J-M, Knuesel I (2010) Reduced Reelin expression accelerates amyloid-beta plaque formation and tau pathology in transgenic Alzheimer's disease mice. *J Neurosci* **30:** 9228-9268

Koike H, Tomioka S, Sorimachi H, Saido T, Maruyama K, Okuyama A, Fujisawa-Sehara A, Ohno S, Suzuki K, Ishiura S (1999) Membrane-anchored metalloprotease MDC9 has an alpha-secretase activity responsible for processing the amyloid precursor protein. *The Biochemical journal* **343 Pt 2:** 371-375

Koo E, Squazzo S, Selkoe DJ, Koo CH (1996) Trafficking of cell-surface amyloid β-protein precursor. I. Secretion, endocytosis, and recycling as detected by labeled monoclonal antibody. *J Cell Sci* **109:** 991-998

Koo EH (1997) Phorbol esters affect multiple steps in beta-amyloid precursor protein trafficking and amyloid beta-protein production. *Molecular Mediciene* **3:** 204-211

Kopan R (2002) Notch: a membrane-bound transcription factor. *Journal of Cell Science* **115:** 1095-1097

Kuhn P-H, Wang H, Dislich B, Colombo A, Zeitschel U, Ellwart J, Kremmer E, Rossner S, Lichtenthaler S (2010) ADAM10 is the physiologically relevant, constitutive alpha-secretase of the amyloid precursor protein in primary neurons. *The EMBO journal* **29:** 3020-3032

Lambert de Rouvroit C, de Bergeyck V, Cortvrindt C, Bar I, Eeckhout Y, Goffinet A (1999) Reelin, the extracellular matrix protein deficient in reeler mutant mice, is processed by a metalloproteinase. *Exp Neurol* **156:** 214-217

Lammich S, Kojro E, Postina R, Gilbert S, Pfeiffer R, Jasionowski M, Haass C, Fahrenholz F (1999) Constitutive and regulated alpha-secretase cleavage of Alzheimer's amyloid precursor protein by a disintegrin metalloprotease. *PNAS* **96:** 3922-3927

Lenkkeri U, Kestilä M, Lamerdin J, McCready P, Adamson A, Olsen A, Tryggvason K (1998) Structure of the human amyloid-precursor-like protein gene APLP1 at 19q13.1. *Human genetics* **102:** 192-196

Lesné S, Sherman M, Grant M, Kuskowski M, Schneider J, Bennett D, Ashe K (2013) Brain amyloid-β oligomers in ageing and Alzheimer's disease. *Brain : a journal of neurology*

Lewczuk P, Kamrowski-Kruck H, Peters O, Heuser I, Jessen F, Popp J, Bürger K, Hampel H, Frölich L, Wolf S, Prinz B, Jahn H, Luckhaus C, Perneczky R, Hüll M, Schröder J, Kessler H, Pantel J, Gertz HJ, Klafki HW, Kölsch H, Reulbach U, Esselmann H, Maler J, Bibl M, Kornhuber J, Wiltfang J (2010) Soluble amyloid precursor proteins in the cerebrospinal fluid as novel potential biomarkers of Alzheimer's disease: a multicenter study. *Molecular psychiatry* **15:** 138-145

Li H, Wang B, Wang Z, Guo Q, Tabuchi K, Hammer R, Südhof T, Zheng H (2010) Soluble amyloid precursor protein (APP) regulates transthyretin and Klotho gene expression without rescuing the essential function of APP. *Proceedings of the National Academy of Sciences of the United States of America* **107:** 17362-17369

Li HL, Roch JM, Sundsmo M, Otero D, Sisodia S, Thomas R, Saitoh T (1997) Defective neurite extension is caused by a mutation in amyloid beta/A4 (A beta) protein precursor found in familial Alzheimer's disease. *J Neurobiol* **32:** 469-480

Li Z, Stark G, Götz J, Rülicke T, Gschwind M, Huber G, Müller U, Weissmann C (1996) Generation of mice with a 200-kb amyloid precursor protein gene deletion by Cre recombinase-mediated site-specific recombination in embryonic stem cells. *Proceedings of the National Academy of Sciences of the United States of America* **93:** 6158-6162

Lierheimer R, Kunz B, Vogt L, Savoca R, Brodbeck U, Sonderegger P (1997) The neuronal cell-adhesion molecule axonin- 1 is specifically released

by an endogenous glycosylphosphatidylinositol-specific phospholipase. *Eur J Biochem* **243:** 502-510

López-Sánchez N, Müller U, Frade J (2005) Lengthening of G2/mitosis in cortical precursors from mice lacking beta-amyloid precursor protein. *Neuroscience* **130:** 51-60

Lorent K, Overbergh L, Moechars D, De Strooper B, Van Leuven F, Van den Berghe H (1995) Expression in mouse embryos and in adult mouse brain of three members of the amyloid precursor protein family, of the alpha-2-macroglobulin receptor/low density lipoprotein receptor-related protein and of its ligands apolipoprotein E, lipoprotein lipase, alpha-2-macroglobulin and the 40,000 molecular weight receptor-associated protein. *Neuroscience* **65:** 1009-1025

Luo L, Martin-Morris LE, White K (1990) Identification, secretion and neural expression of APPL, a Drosophila protein similar to human amyloid protein precursor. *J Neurosci Res* **10:** 3849-3861

Luo L, Tully T, White K (1992) Human amyloid precursor protein ameliorates behavioral deficit of flies deleted for Appl gene. *Neuron* **9:** 595-605.

Ma QH, Futagawa T, Yang WL, Jiang XD, Zeng L, Takeda Y, Xu RX, Bagnard D, Schachner M, Furley AJ, Karagogeos D, Watanabe K, Dawe GS, Xiao ZC (2008) A TAG1-APP signalling pathway through Fe65 negatively modulates neurogenesis. *Nat Cell Biol* **10:** 283-294

Magara F, Müller U, Li Z, Lipp H, Weissmann C, Stagljar M, Wolfer D (1999) Genetic background changes the pattern of forebrain commissure defects in transgenic mice underexpressing the beta-amyloid-precursor protein. *Proceedings of the National Academy of Sciences of the United States of America* **96:** 4656-4661

Masters CL, Multhaup G, Simms G, Pottigiesser J, Martins RN, Beyreuther K (1985) Neuronal origin of a cerebral amyloid: neurofibrillary tangles of Alzheimer's disease contain the same protein as the amyloid of plaque cores and blood vessels. *EMBO J* **4:** 2757-2763

Mi S, Sandrock A, Miller R (2008) LINGO-1 and its role in CNS repair. *Int J Biochem Cell Biol* **40:** 1971-1978

Milward EA, Papadopoulos R, Fuller SJ, Moir RD, Small D, Beyreuther K, Masters CL (1992) The amyloid protein precursor of Alzheimer's disease is a mediator of the effects of nerve growth factor on neurite outgrowth. *Neuron* **9:** 129-137

Moreno T, Bronner-Fraser M (2001) The secreted glycoprotein Noelin-1 promotes neurogenesis in Xenopus. *Developmental biology* **240:** 340-400

Mullan M, Crawford F, Houlden H, Axelman K, Lilius L, Winblad B, Lannfelt L (1992) A pathogenic mutation for probable Alzheimer's disease in the APP gene at the N-terminus of β-amyloid. *Nature Genet* **1:** 345-347

Müller U, Cristina N, Li Z, Wolfer D, Lipp H, Rülicke T, Brandner S, Aguzzi A, Weissmann C (1994) Behavioral and anatomical deficits in mice homozygous for a modified beta-amyloid precursor protein gene. *Cell* **79:** 755-765

Multhaup G (1994) Identification and regulation of the high affinity binding site of the Alzheimer's disease amyloid protein precursor to glycosaminoglycans. *Biochimie* **76:** 304-311

Munter L-M, Voigt P, Harmeier A, Kaden D, Gottschalk K, Weise C, Pipkorn R, Schaefer M, Langosch D, Multhaup G (2007) GxxxG motifs within the amyloid precursor protein transmembrane sequence are critical for the etiology of Abeta42. *The EMBO journal* **26:** 1702-1712

Musa A, Lehrach H, Russo V (2001) Distinct expression patterns of two zebrafish homologues of the human APP gene during embryonic development. *Development genes and evolution* **211:** 563-567

Nagano T, Nakamura A, Konno D, Kurata M, Yagi H, Sato M (2000) A2-Pancortins (Pancortin-3 and Pancortin-4) are the dominant Pancortins during neocortical development. *J Neurochem* **75**

Nikolaev A, McLaughlin T, O'Leary D, Tessier-Lavigne M (2009) APP binds DR6 to trigger axon pruning and neuron death via distinct caspases. *Nature* **457:** 981-989

Ninomiya H, Roch J, Sundsmo MP, Otero DAC, Saitoh T (1993) Amino acid sequence RERMS represents the active domain of amyloid β/A4 protein precursor that promotes fibroblast growth. *J Cell Biol* **121:** 879-886

Nitsch RM, Slack BE, Wurtman RJ, Growdon JH (1992) Release of Alzheimer amyloid precursor derivatives stimulated by activation of muscarinic acetylcholine receptors. *Science* **258:** 304-307

Ohsawa I, Hirose Y, Ishiguro M, Imai Y, Ishiura S, Kohsaka S (1995) Expression, purification, and neurotrophic activity of amyloid precursor protein-secreted forms produced by yeast. *Biochem Biophys Res Commun* **213:** 52-58

Ohyagi Y, Takahashi K, Kamegai M, Tabira T (1990) Developmental and differential expression of beta amyloid protein precursor mRNAs in mouse brain. *Biochem Biophys Res Commun* **18:** 54-60

Osterfield M, Egelund R, Young LM, Flanagan JG (2008) Interaction of amyloid precursor protein with contactins and NgCAM in the retinotectal system. *Development* **135:** 1189-1199

Pangalos M, Shioi J, Robakis N (1995) Expression of the chondroitin sulfate proteoglycans of amyloid precursor (appican) and amyloid precursor-like protein 2. *Journal of Neurochemistry* **65:** 762-771

Parvathy S, Hussain I, Karran EH, Turner AJ, Hooper N (1999) Cleavage of Alzheimer's amyloid precursor protein by a-secretase occurs at the surface of neuronal cells. *Biochemistry* **38:** 9728-9734

Perez RG, Zheng H, Van der Ploeg LH, Koo EH (1997) The beta-amyloid precursor protein of Alzheimer's disease enhances neuron viability and modulates neuronal polarity. *J Neurosci* **17:** 9407-9414

Priller C, Bauer T, Mitteregger G, Krebs B, Kretzschmar HA, Herms J (2006) Synapse formation and function is modulated by the amyloid precursor protein. *J Neurosci* **26:** 7212-7221

Qiu WQ, Ferreira A, Miller C, Koo EH, Selkoe DJ (1995) Cell-surface β-amyloid precursor protein stimulates neurite outgrowth of hippocampal neurons in an isoform-dependent manner. *J Neurosci* **15:** 2157-2167

Reinhard C, Hebert SS, De Strooper B (2005) The amyloid-beta precursor protein: integrating structure with biological function. *Embo J* **24:** 3996-4006

Rice H, Townsend M, Bai J, Suth S, Cavanaugh W, Selkoe D, Young-Pearse T (2012) Pancortins interact with amyloid precursor protein and modulate cortical cell migration. *Development* **139:** 3986-3996

Ring S, Weyer S, Kilian S, Waldron E, Pietrzik C, Filippov M, Herms J, Buchholz C, Eckman C, Korte M, Wolfer D, Müller U (2007) The secreted beta-amyloid precursor protein ectodomain APPs alpha is sufficient to rescue the anatomical, behavioral, and electrophysiological abnormalities of APP-deficient mice. *The Journal of neuroscience : the official journal of the Society for Neuroscience* **27:** 7817-7843

Rosén C, Andreasson U, Mattsson N, Marcusson J, Minthon L, Andreasen N, Blennow K, Zetterberg H (2012) Cerebrospinal fluid profiles of amyloid β-related biomarkers in Alzheimer's disease. *Neuromolecular medicine* **14:** 65-73

Rosen DR, Martin-Morris L, Luo L, White K (1989) A *Drosophila* gene encoding a protein resembling the human β-amyloid precursor protein. *Proc Natl Acad Sci USA* **86:** 2478-2482

Rossjohn J, Cappai R, Feil SC, Henry A, McKinstry WJ, Galatis D, Hesse L, Multhaup G, Beyreuther K, Masters CL, Parker MW (1999) Crystal structure of the N-terminal, growth factor-like domain of Alzheimer amyloid precursor protein. *Nat Struct Biol* **6:** 327-331.

Sabo SL, Ikin AF, Buxbaum JD, Greengard P (2003) The amyloid precursor protein and its regulatory protein, FE65, in growth cones and synapses in vitro and in vivo. *J Neurosci* **23:** 5407-5415

Sastre M, Steiner H, Fuchs K, Capell A, Multhaup G, Condron MM, Teplow DB, Haass C (2001) Presenilin-dependent gamma-secretase processing of beta-amyloid precursor protein at a site corresponding to the S3 cleavage of Notch. *EMBO Rep* **2:** 835-841

Schubert D, Klar A, Park M, Dargusch R, Fischer WH (2006) F-spondin promotes nerve precursor differentiation. *J Neurochem* **96:** 444-453

Schwartz M (2001) Integrin signaling revisited. *Trends in cell biology* **11:** 466-470

Seabrook GR, Smith DW, Bowery BJ, Easter A, Reynolds T, Fitzjohn SM, Morton RA, Zheng H, Dawson GR, Sirinathsinghji DJ, Davies CH, Collingridge GL, Hill RG (1999) Mechanisms contributing to the deficits in

hippocampal synaptic plasticity in mice lacking amyloid precursor protein. *Neuropharmacology* **38:** 349-359

Selkoe D (2011) Resolving controversies on the path to Alzheimer's therapeutics. *Nature medicine* **17:** 1060-1065

Shankar GM, Bloodgood BL, Townsend M, Walsh DM, Selkoe DJ, Sabatini BL (2007) Natural oligomers of the Alzheimer amyloid-beta protein induce reversible synapse loss by modulating an NMDA-type glutamate receptor-dependent signaling pathway. *J Neurosci* **27:** 2866-2875

Shariati S, Lau P, Hassan B, Müller U, Dotti C, De Strooper B, Gärtner A (2013) APLP2 regulates neuronal stem cell differentiation during cortical development. *Journal of Cell Science*

Simons M, de Strooper B, Multhaup G, Tienari PJ, Dotti CG, Beyreuther K (1996) Amyloidogenic processing of the human amyloid precursor protein in primary cultures of rat hippocampal neurons. *J Neurosci* **16:** 899-908

Sinha S, Anderson JP, Barbour R, Basi GS, Caccavello R, Davis D, Doan M, Dovey HF, Frigon N, Hong J, Jacobson-Croak K, Jewett N, Keim P, Knops J, Lieberburg I, Power M, Tan H, Tatsuno G, Tung J, Schenk D, Seubert P, Suomensaari SM, Wang S, Walker D, John V (1999) Purification and cloning of amyloid precursor protein beta-secretase from human brain. *Nature* **402:** 537-540

Sinha S, Dovey HF, Seubert P, Ward PJ, Blacher RW, Blaber M, Bradshaw RA, Arici M, Mobley WC, Lieberburg I (1990) The protease inhibitory properties of the Alzheimer's β-amyloid precursor protein. *J Biol Chem* **265:** 8983-8985

Sisodia S, Koo E, Hoffman P, Perry G, Price D (1993) Identification and transport of full-length amyloid precursor proteins in rat peripheral nervous system. *The Journal of neuroscience : the official journal of the Society for Neuroscience* **13:** 3136-3142

Skovronsky DM, Moore BM, Milla ME, Doms RW, Lee VMY (2000) Protein kinase C-dependent a-secretase competes with b-secretase for cleavage of amyloid-b precursor protein in the trans-golgi network. *Journal of Biological Chemistry* **275:** 2568-2575

Slunt HH, Thinakaran G, Von Koch C, Lo ACY, Tanzi RE, Sisodia SS (1994) Expression of a ubiquitous, cross-reactive homologue of the mouse β-amyloid precursor protein (APP). *J Biol Chem* **269:** 2637-2644

Smith RP, Higuchi DA, Broze Jr. GJ (1990) Platelet coagulation factor XIa-inhibitor, a form of Alzheimer amyloid precursor protein. *Science* **248:** 1126-1128

Soba P, Eggert S, Wagner K, Zentgraf H, Siehl K, Kreger S, Lower A, Langer A, Merdes G, Paro R, Masters CL, Muller U, Kins S, Beyreuther K (2005) Homo- and heterodimerization of APP family members promotes intercellular adhesion. *EMBO J* **24:** 3624-3634

Stein T, Walmsley A (2012) The leucine-rich repeats of LINGO-1 are not required for self-interaction or interaction with the amyloid precursor protein. *Neuroscience Letters* **509:** 9-12

Steinbach J, Müller U, Leist M, Li Z, Nicotera P, Aguzzi A (1998) Hypersensitivity to seizures in beta-amyloid precursor protein deficient mice. *Cell death and differentiation* **5:** 858-866

Storey E, Beyreuther K, Masters CL (1996) Alzheimer's disease amyloid precursor protein on the surface of cortical neurons in primary culture co-localizes with adhesion patch components. *Brain Res* **735:** 217-231

Tamaoka A, Odaka A, Ishibashi Y, Usami M, Sahara N, Suzuki N, Nukima N, Mizusawa H, Shoji S, Kanazawa I, Mori H (1994) APP717 missense mutation affects the ratio of amyloid ß protein species (Aß1-42/43 and Aß1-40) in familial Alzheimer's disease brain. *J Biol Chem* **269:** 32721-32724

Tanzi R (2012) The genetics of Alzheimer disease. *Cold Spring Harbor perspectives in medicine* **2**

Tanzi RE, Gusella JF, Watkins PC, Bruns GAB, St. George-Hyslop PH, Van Keuren ML, Patterson D, Pagan S, Kurnit DM, Neve RL (1987) Amyloid β-protein gene: cDNA, mRNA distribution, and genetic linkage near the Alzheimer locus. *Science* **235:** 880-884

Terai Y, Abe M, Miyamoto K, Koike M, Yamasaki M, Ueda M, Ueki M, Sato Y. (2001) Vascular smooth muscle cell growth-promoting factor/F-spondin inhibits angiogenesis via the blockade of integrin alphavbeta3 on vascular endothelial cells. *J Cell Physiol*, Vol. 188, pp. 394-402.

Torroja L, Packard M, Gorczyca M, White K, Budnik V (1999) The Drosophila beta-amyloid precursor protein homolog promotes synapse differentiation at the neuromuscular junction. *J Neurosci* **19:** 7793-7803

Tyan S-H, Shih A, Walsh J, Maruyama H, Sarsoza F, Ku L, Eggert S, Hof P, Koo E, Dickstein D (2012) Amyloid precursor protein (APP) regulates synaptic structure and function. *Molecular and cellular neurosciences* **51:** 43-52

Tzarfati-Majar V, Burstyn-Cohen T, Klar A. (2001) F-spondin is a contact-repellent molecule for embryonic motor neurons. *Proc Natl Acad Sci USA*, Vol. 98, pp. 4722-4727.

Tzarfaty-Majar V, López-Alemany R, Feinstein Y, Gombau L, Goldshmidt O, Soriano E, Muñoz-Cánoves P, Klar A. (2001) Plasmin-mediated release of the guidance molecule F-spondin from the extracellular matrix. *J Biol Chem*, Vol. 276, pp. 28233-28241.

van Nostrand WE, Schmaier AH, Farrow JS, Cunningham DD (1990) Protease nexin-II (amyloid β-protein precursor): A platelet α-granule protein. *Science* **248:** 745-748

Vassar R, Bennett BD, Babu-Khan S, Kahn S, Mendiaz EA, Denis P, Teplow DB, Ross S, Amarante P, Loeloff R, Luo Y, Fisher S, Fuller J, Edenson S, Lile J, Jarosinski MA, Biere AL, Curran E, Burgess T, Louis JC, Collins F, Treanor J, Rogers G, Citron M (1999) Beta-secretase cleavage of Alzheimer's amyloid precursor protein by the transmembrane aspartic protease BACE. *Science* **286:** 735-741

von Koch CS, Zheng H, Chen H, Trumbauer M, Thinakaran G, van der Ploeg LH, Price DL, Sisodia SS (1997) Generation of APLP2 KO mice and early postnatal lethality in APLP2/APP double KO mice. *Neurobiol Aging* **18:** 661-669

Walsh DM, Minogue AM, Frigerio CS, Fadeeva JV, Wasco W, Selkoe DJ (2007) The APP family of proteins: similarities and differences. *Biochemical Society Transactions* **35:** 416-420

Wang B, Yang L, Wang Z, Zheng H (2007) Amyolid precursor protein mediates presynaptic localization and activity of the high-affinity choline transporter. *Proceedings of the National Academy of Sciences of the United States of America* **104:** 14140-14145

Wang H, Li R, Shen Y (2013) β-Secretase: its biology as a therapeutic target in diseases. *Trends in pharmacological sciences*

Wang P, Yang G, Mosier D, Chang P, Zaidi T, Gong Y-D, Zhao N-M, Dominguez B, Lee K-F, Gan W-B, Zheng H (2005) Defective neuromuscular synapses in mice lacking amyloid precursor protein (APP) and APP-Like protein 2. *The Journal of neuroscience* **25:** 1219-1244

Wang Z, Wang B, Yang L, Guo Q, Aithmitti N, Songyang Z, Zheng H (2009) Presynaptic and postsynaptic interaction of the amyloid precursor protein promotes peripheral and central synaptogenesis. *The Journal of neuroscience* **29:** 10788-11589

Wasco W, Brook DJ, Tanzi RE (1993) The amyloid precursor-like protein (APLP) gene maps to the long arm of chromosome 19. *Genomics* **15:** 237-239

Wasco W, Bupp K, Magendantz M, Gusella J, Tanzi RE, Solomon F (1992) Identification of a mouse brain cDNA that encodes a protein related to the Alzheimer disease-associated amyloid β-protein precursor. *Proc Natl Acad Sci USA* **89:** 10758-10762

Weidemann A, Eggert S, Reinhard FB, Vogel M, Paliga K, Baier G, Masters CL, Beyreuther K, Evin G (2002) A novel epsilon-cleavage within the transmembrane domain of the Alzheimer amyloid precursor protein demonstrates homology with Notch processing. *Biochemistry* **41:** 2825-2835

Weyer S, Klevanski M, Delekate A, Voikar V, Aydin D, Hick M, Filippov M, Drost N, Schaller K, Saar M, Vogt M, Gass P, Samanta A, Jäschke A, Korte M, Wolfer D, Caldwell J, Müller U (2011) APP and APLP2 are essential at PNS and CNS synapses for transmission, spatial learning and LTP. *The EMBO journal* **30:** 2266-2346

Wilde-Bode C, Yamazaki T, Capell A, Leimer U, Steiner H, Ihara Y, Haass C (1997) Intracellular generation and accumulation of amyloid β-peptide terminating at amino acid 42. *J Biol Chem* **272:** 16085-16088

Wolfe MS, Xia W, Ostaszewski BL, Diehl TS, Kimberly WT, Selkoe DJ (1999) Two transmembrane aspartates in presenilin-1 required for presenilin endoproteolysis and γ-secretase activity. *Nature* **398:** 513-517

Yamazaki T, Koo EH, Selkoe DJ (1997) Cell surface amyloid beta-protein precursor colocalizes with beta 1 integrins at substrate contact sites in neural cells. *J Neurosci* **17:** 1004-1010

Yan R, Bienkowski MJ, Shuck ME, Miao H, Tory MC, Pauley AM, Brashier JR, Stratman NC, Mathews WR, Buhl AE, Carter DB, Tomasselli AG, Parodi LA, Heinrikson RL, Gurney ME (1999) Membrane-anchored aspartyl protease with Alzheimer's disease beta- secretase activity. *Nature* **402:** 533-537

Yang G, Gong Y-D, Gong K, Jiang W-L, Kwon E, Wang P, Zheng H, Zhang X-F, Gan W-B, Zhao N-M (2005) Reduced synaptic vesicle density and active zone size in mice lacking amyloid precursor protein and APP-like protein 2. *Neurosci Lett* **384:** 66-71

Yoshihara Y, Kawasaki M, Tamada A, Nagata S, Kagamiyama H, Mori K (1995) Overlapping and differential expression of BIG-2, BIG-1, TAG-1, and F3: Four members of an axon-associated cell adhesion molecule subgroup of the immunoglobulin superfamily. *J of Neurobiology* **28:** 51-69

Yoshihara Y, Kawasaki M, Tani A, Tamada A, Nagata S, Kagamiyama H, Mori K (1994) BIG-1: a new TAG-1/F 3-related member of the immunoglobulin superfamily with neurite outgrowth-promoting activity. *Neruon* **13:** 415

Yoshikai S, Sasaki H, Doh-ura K, Furuya H, Sakaki Y (1990) Genomic organization of the human amyloid beta-protein precursor gene. *Gene* **87:** 257-263

Young-Pearse T, Suth S, Luth E, Sawa A, Selkoe D (2010) Biochemical and functional interaction of disrupted-in-schizophrenia 1 and amyloid precursor protein regulates neuronal migration during mammalian cortical development. *The Journal of neuroscience : the official journal of the Society for Neuroscience* **30:** 10431-10471

Young-Pearse TL, Bai J, Chang R, Zheng JB, Loturco JJ, Selkoe DJ (2007) A Critical Function for beta-Amyloid Precursor Protein in Neuronal Migration Revealed by In Utero RNA Interference. *J Neurosci* **27:** 14459-14469

Young-Pearse TL, Chen A, Chang R, Marquez C, Selkoe DJ (2008) Secreted APP regulates the function of full-length APP in neurite outgrowth through interaction with integrin beta1. *Neural Development* **3**

Zeng C, Younger-Shepherd S, Jan L, Jan Y (1998) Delta and Serrate are redundant Notch ligands required for asymmetric cell divisions within the Drosophila sensory organ lineage. *Genes & development* **12:** 1086-1091

Zheng H, Jiang M, Trumbauer ME, Sirinathsinghji DJS, Hopkins R, Smith DW, Heavesn RP, Dawson GR, Boyce S, Conner MW, Stevens KA, Slunt HH, Sisodia SS, Chen HY, Van der Ploeg LHT (1995) β-amyloid precursor protein-deficient mice show reactive gliosis and decreased locomotor activity. *Cell* **81:** 525-531

Zhu G, Wang D, Lin Y-H, McMahon T, Koo EH, Messing RO (2001) Protein Kinase C e suppresses Abeta production and promotes activation of alpha-secretase. *Biochemical and Biophysical Research Communications* **285:** 997-1006

Chapter 2:

Pancortins interact with Amyloid Precursor Protein and modulate cortical cell migration

Heather C. Rice, Matthew Townsend, Jilin Bai, Seiyam Suth,William Cavanaugh,

Dennis J. Selkoe and Tracy L. Young-Pearse

Experimental contributions to this chapter: HCR performed all co-IPs, APP shedding assays, Western Blots, and ELISAs with the exception of Fig 2.3 E , F performed by SS; MT performed APP binding screen; JB and TYP performed in utero electroporations; WC and HCR performed brain slicing and immunohistochemistry,

This chapter was modified from a manuscript published in Development 139, 3986-3996, November 2012

Abstract

Neuronal precursor cell migration in the developing mammalian brain is a complex process requiring the coordinated interaction of numerous proteins. We have recently shown that Amyloid Precursor Protein (APP) plays a role in migration into the cortical plate through its interaction with two cytosolic signaling proteins, Disabled-1 (DAB1) and Disrupted in Schizophrenia-1 (DISC1). In order to identify extracellular factors that may signal through APP to regulate migration, we performed an unbiased mass spectrometry-based screen for factors that bind to the extracellular domain of APP in the rodent brain. Through this screen, we identified an interaction between APP and Pancortins, proteins expressed throughout the developing and mature cerebral cortex. Via co-immunoprecipitation, we show that APP interacts with all four of the mammalian Pancortin isoforms (AMY, AMZ, BMY, BMZ). We demonstrate that the BMZ and BMY isoforms of Pancortin can specifically reduce β-secretase but not α-secretase cleavage of endogenous APP in cell culture, suggesting a biochemical consequence of the association between Pancortins and APP. Using in utero electroporation to overexpress and knock down specific Pancortin isoforms, we reveal a novel role for Pancortins in migration into the cortical plate. Interestingly, we observe opposing roles for alternate Pancortin isoforms, with AMY overexpression and BMZ knock down both preventing proper migration of neuronal precursor cells. Finally, we show that BMZ can partially rescue a loss of APP expression and that APP can rescue effects of AMY overexpression, suggesting that Pancortins act in conjunction with APP to regulate entry into the cortical plate. Taken together, these results suggest a biochemical and functional interaction between APP and Pancortins and reveal a previously unidentified role for Pancortins in mammalian cortical development.

Introduction

Migration of neuronal precursor cells in the developing cerebral cortex is a complex process that requires the coordinated interaction of many factors. Extracellular cues are relayed to intracellular signaling pathways via transmembrane receptors to mediate migration of formative neurons from the ventricular and subventricular zones through the intermediate zone and to the proper layer of the cortical plate. While dozens of genes have been identified that play important roles in this process, large gaps remain in our understanding of the molecular mechanisms involved.

We have recently shown that Amyloid Precursor Protein (APP) plays a role in migration of neuronal precursor cells into the cortical plate. APP is a type I single transmembrane glycoprotein centrally involved in the pathogenesis of Alzheimer's disease (AD) [reviewed in (Hardy & Selkoe, 2002)]. APP undergoes sequential proteolytic processing by β- and γ-secretase to generate the amyloid β-peptide (Aβ) [reviewed in (De Strooper & Annaert, 2000)]. Several therapeutic strategies for AD, some of which have already entered clinical trials, aim to chronically inhibit β- or γ-secretase to prevent Aβ generation [reviewed in (Selkoe, 2011)]. To understand the potential effects of chronically reducing APP processing to treat AD, it is important to decipher the normal functions of APP and understand the molecular pathways through which APP executes these functions.

Recent studies from several labs have begun to clarify an essential role for APP in the development of the nervous system. APP is now believed to function in neurite outgrowth (Araki et al, 1991; Perez et al, 1997; Young-Pearse et al, 2008), cell adhesion (Ghiso et al, 1992;

Soba et al, 2005), synapse formation (Priller et al, 2006; Wang et al, 2009) and migration of neuronal precursors (Pramatarova et al, 2006; Young-Pearse et al, 2007). The precise mechanisms regulating the proteolytic processing and function of APP are only partially understood. While the cleaved extracellular domain of APP itself has biological activities in vivo (Ring et al, 2007), we found that both the ectodomain and intracellular domain of APP are required to be expressed as a holoprotein in order to mediate proper neuronal precursor cell migration during cortical development (Young-Pearse et al, 2007), and that the cytoplasmic factors Disabled-1 (DAB1) and Disrupted in Schizophrenia-1 (DISC1) biochemically and functionally interact with APP in this function (Pramatarova et al, 2008; Pramatarova et al, 2006; Young-Pearse et al, 2010). On the basis of these findings, we hypothesize that certain extracellular factors bind the ectodomain of holoAPP on the cell surface and transmit a signal to intracellular signaling cascades during development. Accordingly, identifying extracellular binding partners for APP will help reveal the molecular pathways that regulate APP processing and function.

Several candidate ligands for APP, including F-Spondin (Ho & Sudhof, 2004; Hoe et al, 2005), Contactins (Ma et al, 2008; Osterfield et al, 2008), and Reelin (Hoe et al, 2009; Hoe et al, 2006), have been reported to interact with the ectodomain of APP and modulate APP processing and/or APP function in neurodevelopment. However, despite these initial reports, an endogenous functional ligand for APP has yet to be widely confirmed in multiple laboratories. We initiated a search for additional factors that could interact with the APP ectodomain and modulate APP processing and/or function in vivo. Here, we identified

Pancortin in an unbiased screen for proteins that interact with the ectodomain of APP in the mouse cerebral cortex.

Pancortin, also known as Noelin (chicken and *Xenopus*), Olfactomedin-related glycoprotein (rats), and hOlfA (humans), is a secreted glycoprotein highly expressed in the developing and mature cortex (Danielson et al, 1994; Nagano et al, 2000). In the rodent, four isoforms of Pancortin are expressed; these variants are named based upon the domains incorporated and are designated BMZ, BMY, AMZ, and AMY (Danielson et al, 1994). Each isoform contains the common central M domain. Differential promoter utilization generates an amino-terminus composed of either the A or B domain, and alternative splicing produces a carboxyl-terminus composed of either the Y or Z domain (Danielson et al, 1994) (Fig. 2.1A). While the function of Pancortin in the developing mammalian nervous system has not been elucidated, the BMZ and AMY isoforms have reported functions in neurodevelopment in *Xenopus* and chick. The BMZ isoform functions in the migration of neural crest cells in chick embryos (Barembaum et al, 2000), and BMZ and AMY isoforms have opposing roles in regulating the timing of neuronal differentiation in *Xenopus* (Moreno & Bronner-Fraser, 2001; Moreno & Bronner-Fraser, 2005).

Here, we report the biochemical and functional interaction of APP and Pancortins and identify a novel function of Pancortins in mammalian cortical development. We identify Pancortin as an APP binding partner and show that specific Pancortin isoforms inhibit β-secretase cleavage of APP. We reveal that, similar to APP, Pancortins play a role in migration of neuronal precursor cells into the cortical plate, with different variants of Pancortin having opposing roles in this process. Together, our studies identify a novel function of Pancortins in

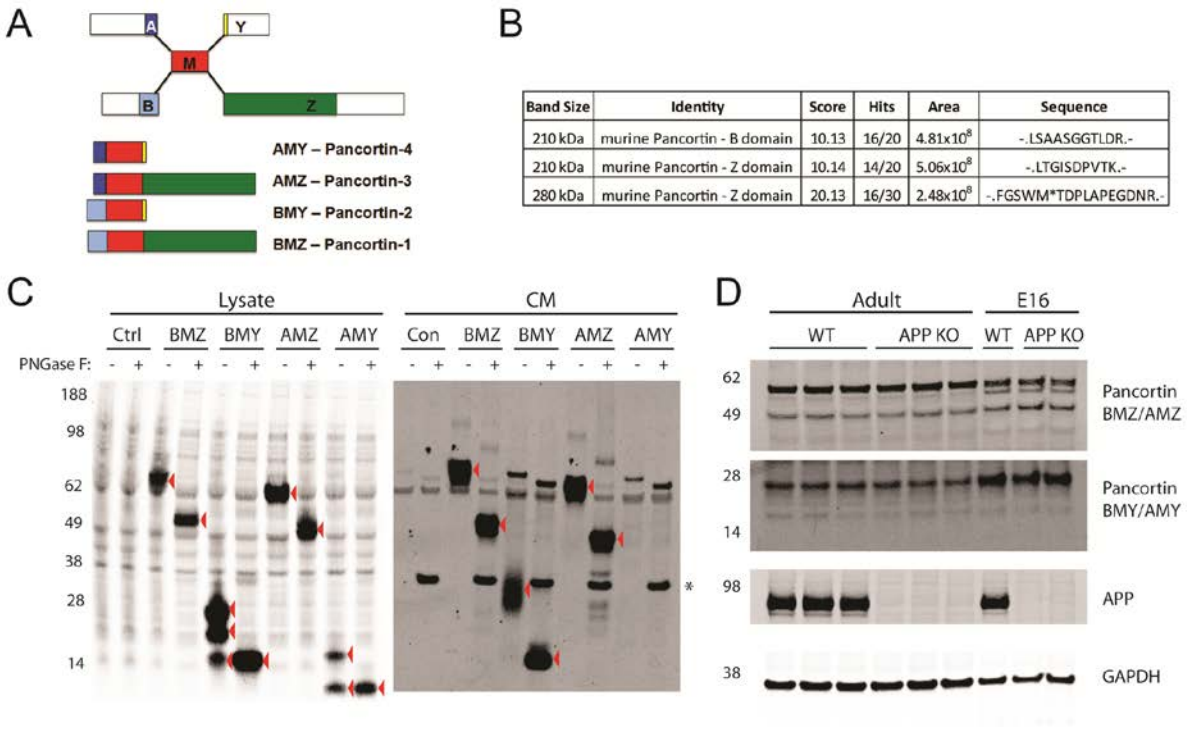

Band Size	Identity	Score	Hits	Area	Sequence
210 kDa	murine Pancortin - B domain	10.13	16/20	4.81×10^8	-.LSAASGGTLDR.-
210 kDa	murine Pancortin - Z domain	10.14	14/20	5.06×10^8	-.LTGISDPVTK.-
280 kDa	murine Pancortin - Z domain	20.13	16/30	2.48×10^8	-.FGSWM*TDPLAPEGDNR.-

Figure 2.1. **Identification of Pancortin as an APP binding partner. (A)** Schematic of Pancortin isoforms and their domains. **(B)** Pancortin peptides identified by mass spectrometry in an unbiased screen for extracellular factors within murine cortical slices that interact with the APP ectodomain. **(C)** Western blot (WB) for Pancortin (anti-FLAG) of the lysate and conditioned media (CM) from HEK293 cells transiently transfected with each of the Pancortins or control vector both with and without PNGase F treatment. Red arrowheads highlight specific bands. **(D)** WB for Pancortin isoforms ("BMZ/AMZ", Abcam; "BMY/AMY", Neuromab), APP, and GAPDH in E16 and adult brain homogenates from WT or APP KO mice.

cortical cell migration and give further mechanistic insight into the physiological function of APP, a protein central to the pathogenesis of AD.

Experimental Procedures

Screen for identification of APP binding partners

C57/BL6 mouse brains were vibratome sectioned (350 micron) and slices were aerated in artificial cerebrospinal fluid (aCSF), incubated with APPsα for 1 hr, followed by incubation in 250 uM DSS (Thermo Fisher, Rockford, IL) for 30 min. DTT (1 mM) was added to terminate the reaction. Slices were then homogenized in TEVP buffer (10 mM Tris-HCl, pH 7.4, 1mM EDTA, 1 mM EGTA, protease inhibitors, 320 mM sucrose), and lysates spun at 1000 g to pellet nuclei. Membranes were then pelleted at 100,000 g for 1 hr and the pellet resuspended in 1% NP40 STEN buffer (150 mM NaCl, 50 mM Tris, 2 mM EDTA, and 1.0% (v/v) NP-40). Following lysis, APP was immunoprecipitated with 8E5 (gift of Elan Pharmaceuticals) crosslinked to protein G agarose beads. Beads were washed in STEN buffer followed by 1% SDS-STEN buffer, and proteins eluted from the beads with ammonium hydroxide at pH 12 followed by neutralization. Eluted proteins were electrophoresed on a 10-20% Tricine gel, stained with colloidal blue, and bands excised and subjected to MALDI-TOF mass spectrometry.

Plasmids

Generation of APP and control shRNA constructs were described previously (Young-Pearse et al, 2007). Pancortin shRNA constructs were generated by cloning of oligonucleotides encoding the shRNA sequence into the pENTR-U6 plasmid (Invitrogen, Carlsbad, CA). Pancortin shRNAs target the following sequences: shRNA 3 (targeting AMY)

GGAGAAGATGGAGAACCAAAT; shRNA 4 (targeting BMZ) GCAACATTGTCATCAGCAAGC. Murine Pancortin cDNAs were cloned by PCR into the pCAGGs expression vector for mammalian expression, and the cDNAs confirmed to have the sequences corresponding to the following Genbank entries: NM_019498 (BMZ or transcript variant 1), NM_001038612 (BMY or transcript variant 2), NM_001038613 (AMZ or transcript variant 3), and NM_001038614 (AMY or transcript variant 4). In order to rescue shRNA 4 with a non-targetable BMZ construct ("BMZ4m"), four synonymous mutations (bold, underlined) were introduced at the shRNA 4 target site: GCAA**T**AT**C**GT**G**AT**A**AGCAAGC.

Protein expression, immunoprecipitation, and Western blotting

HEK293 cells were transiently transfected using Lipofectamine 2000 (Invitrogen, Carlsbad, CA) or Fugene HD (Promega, Madison, WI). 48 hrs after transfection, conditioned media (CM) was collected and cells lysed in 1% NP40 STEN buffer. E18 rat cortical neurons were nucleofected with the Amaxa 4D-Nucleofector Device using the P3 primary cell kit according to manufacturer's protocol (Lonza, Basel, Switzerland). For deglycosylation of Pancortin, lysates and CM from transfected HEK293 cells were treated with PNGase F (New England Bioloabs, Ipswich, MA) according to manufacturer's protocol. For IP, HEK293 cells were transfected with each of the FLAG-tagged Pancortin isoforms or domains plus either empty vector alone, human APP (695 residue splice variant), the C-terminal 99 amino acid fragment of APP (C99), or the APP ectodomain E1 or E2 deletion constructs, APPΔ1 and APPΔ2, respectively (kindly provided by T. Sudhof, Stanford University). Lysates were immunoprecipitated with M2-agarose (Sigma, St. Louis, MO) or the APP antiserum C9 with protein A and G agarose resin (Sigma, St. Louis,

MO) overnight and washed 3X with 1% NP40 STEN buffer. Lysates, CM, and immunoprecipitations were electrophoresed on 10–20% Tricine or 4-12% Bis-Tris gels (Invitrogen, Carlsbad, CA) and transferred to nitrocellulose. Western blotting was performed with primary antibodies anti-APP (C9, 1:1,000; Selkoe Lab), anti-APPsα (1736, 1:2,000; Selkoe Lab), anti-rodent APP/APPsα (597,1:200; Immuno-biological Laboratories, Minneapolis, MN), mouse anti-Pancortin (K96/7, 1:1000, UC Davis/NIH NeuroMab Facility, Davis, CA), rabbit anti-Pancortin (ab3512, 1:1000, abcam, Cambridge, MA) anti-GAPDH (1:2,000; Millipore, Billerica, MA), anti-FLAG (M2; 1:1,000; Sigma, St. Louis, MO), anti-BACE1 (1:500, Millipore, Billerica, MA), anti-ADAM 10 (1:1,000, Millipore, Billerica, MA), anti-ADAM17 (1:500, abcam, Cambridge, MA), anti-Nicastrin (1:1,000, BD Biosciences, San Jose, California), and anti-Presenilin-1 (1:1,000, Millipore, Billerica, MA) followed by IRDye800- or IRDye680-conjugated secondary antibodies (1:10,000; Rockland Immunochemicals, Gilbertsville, PA) and detection with the LICOR Odyssey detection system.

APP processing assay

HEK293 cells were plated in 6 well plates at 1x10^6 cells/well and transiently transfected with Pancortin isoforms or domains or empty vector (as control) using Fugene HD (Promega, Madison, WI). 24 hrs post-transfection, media (DMEM + 10% FBS) was replaced, and at 48 hrs post-transfection media were collected and centrifuged at 200 g for 5 min and cells were lysed in 1% NP-40 STEN buffer. APPsα, APPsβ, and Aβ levels in the CM was quantified by ELISA (Meso Scale Discovery, Gaithersburg, Maryland) and normalized to total intracellular protein. For each isoform, 2-4 independent experiments performed in triplicate were analyzed.

For the individual domains, a representative experiment performed in triplicate is shown. One-way ANOVA tests were performed with the Bonferroni correction for multiple comparisons.

In utero electroporation

Sprague Dawley rats (Charles River Laboratories, Wilmington, MA) were housed and cared for under the guidelines established by Harvard University's Institutional Animal Care and Use Committees in compliance with federal standards. Timed pregnant rats embryonic day 15.5 (E15.5) were anesthetized with ketamine/xylazine (100/10 mixture, 0.1 mg/g body weight, i.p.). The uterine horns were exposed, and a lateral ventricle of each embryo injected with DNA constructs and Fast Green (2 mg/ml; Sigma, St. Louis, MO) via a microinjector (Picospritzer III; General Valve, Fairfield, NJ) and pulled glass capillaries. For characterization of shRNA phenotypes, 1.0 –1.5 mg/ml of shRNA was co-electroporated with 0.5 mg/ml pCAG-green fluorescent protein (GFP). For cDNA expression, 0.5 mg/ml pCAG-GFP was co-electroporated with 3.0 mg/ml cDNA constructs. For rescue experiments, 0.5 mg/ml shRNA was co-electroporated with 0.5 mg/ml pCAG-GFP and 3.0 mg/ml rescue constructs. All rescue constructs were expressed in the pCAGGs vector. Electroporation was accomplished by discharging a 500 mF capacitor charged to 50–100 V with a sequencing power supply or with a BTX square wave electroporator, at 50–75 V, for 50 ms on followed my 950 ms off for 5 pulses. The voltage was discharged across copper alloy oval plates placed on the uterine wall across the head of the embryo. Brains from rat embryos were harvested 3 or 6 days following electroporation in 4% paraformaldehyde by immersion. For each plasmid combination, at least

three independent brains were analyzed. Ex vivo culture of electroporated cells were performed as described previously (Rice et al, 2010).

Quantitative analyses of cortical plate entry

For quantitative analyses of migration, all electroporations were performed targeting the same region of the developing rat cortex. This resulted in a reliable electroporation of the dorsal-lateral region of the neocortex adjacent to the lateral ventricle. After harvest, brains were vibratome-sectioned (150 µm) in the coronal plane and immunostained for microtubule-associated protein 2 (MAP2) to delineate the cortical plate. For each electroporation condition (i.e., each set of electroporated DNAs), greater than a total of 500 cells were counted and assessed for their location in either the MAP2+ cortical plate or the intermediate zone. To determine significant changes relative to control electroporations, at least three independent brains were electroporated and analyzed for each DNA condition. For each brain, the percentage of GFP-positive cells in the intermediate zone (IZ) and cortical plate (CP) were calculated. These values were then compared between electroporation conditions using GraphPad InStat (San Diego, CA). Using this program, one-way ANOVA tests were performed with the Bonferroni multiple comparisons test. This analysis was used to determine whether the percentage of cells in the CP in the specified electroporation condition was significantly different from the percentage cells in the CP of control electroporations, or in the case of rescue experiments, of shRNA-receiving electroporations (similarly, these same conditions were assessed for statistical significance when comparing the percentage cells in the IZ for each condition). Data presented in Figures 2.4 and 2.5 were generated in concomitant experiments

and are presented separately for clarity. Therefore, the combined data from the control electroporation condition with GFP alone for 3 and 6 days post-electroporation are presented twice in both figures for comparison to other conditions.

Immunofluorescent staining and confocal microscopy

Coronal sections of electroporated brains were incubated in blocking buffer (2% donkey or goat serum; 0.1% Triton X-100 in PBS) for >1 h. Sections were then incubated in primary antibody (anti-MAP2, 1:10,000 (Abcam, Cambridge, MA), anti-Tbr1, 1:200 (Abcam, Cambridge, MA) between 6 h and overnight at 4°C, followed by three washes in PBS. Sections were then incubated with Cy3 - and Cy5-conjugated secondary antibodies (1:500 –1:1000; Jackson Immunoresearch, West Grove, PA) for >2 h followed by four PBS washes. Sections were mounted on glass slides using GelMount (Biomeda, Foster City, CA). Images were acquired using a Zeiss (Oberkochen, Germany) LSM 510 confocal microscope with Axiovert 100M system.

Results

Identification of Pancortin as an APP binding partner

In an unbiased screen for extracellular proteins that interact with the APP ectodomain, murine cortical slices were treated with human APPs-α, cross-linked and homogenized. APP was immunoprecipitated (IPed) with a monoclonal antibody to the APP ectodomain and eluted. The eluted proteins were run on SDS-PAGE, and mass spectrometry was performed on horizontal slices excised from the gel that contained any co-immunoprecipitated (co-IPed) proteins. This method identified three dozen proteins, including APP. Of the published APP binding partners, only NCAM1 (Bai et al, 2008) was identified. Among the novel putative APP

interacting proteins identified, one of the top hits was Pancortin, with recovery of 2 peptides within the Z domain and 1 within the B domain (Fig. 2.1B).

To examine the potential biochemical interactions between APP and Pancortin, HEK293 cells were transiently transfected with empty vector (as control) or the four individually FLAG-tagged Pancortin isoforms (Fig. 2.1C). Each of the Pancortin isoforms was present in the HEK293 lysate with BMY and AMY detected as multiple specific bands. In the conditioned media (CM), all of the isoforms with the exception of AMY (which often was not secreted at detectable levels) were detected as a band migrating at a slightly higher molecular weight than in the lysate. The immunoreactive bands in the lysate and the higher migration of Pancortins in the CM appear to be due to N-linked glycosylation, as digestion of the respective lysates with Peptide: N-Glycosidase F (PNGase F) resulted in a single lower band now running at the same size in both the CM and lysate for each of the four isoforms.

Developmental expression of Pancortin isoforms

Previous studies have shown that multiple Pancortin isoforms are expressed in both the embryonic and mature cortex (Danielson et al, 1994; Nagano et al, 2000). Here, multiple antibodies for Pancortins were tested by Western blot analysis of purified, baculovirus-expressed Pancortin isoforms. We found that a rabbit polyclonal antibody (Abcam) preferentially recognizes the Z-domain-containing isoforms AMZ and BMZ and a monoclonal antibody (NeuroMab) that preferentially recognizes the Y-domain-containing isoforms AMY and BMY (Fig. 2.2A**)**. Using these antibodies, AMY/BMY and AMZ/BMZ expression were observed in

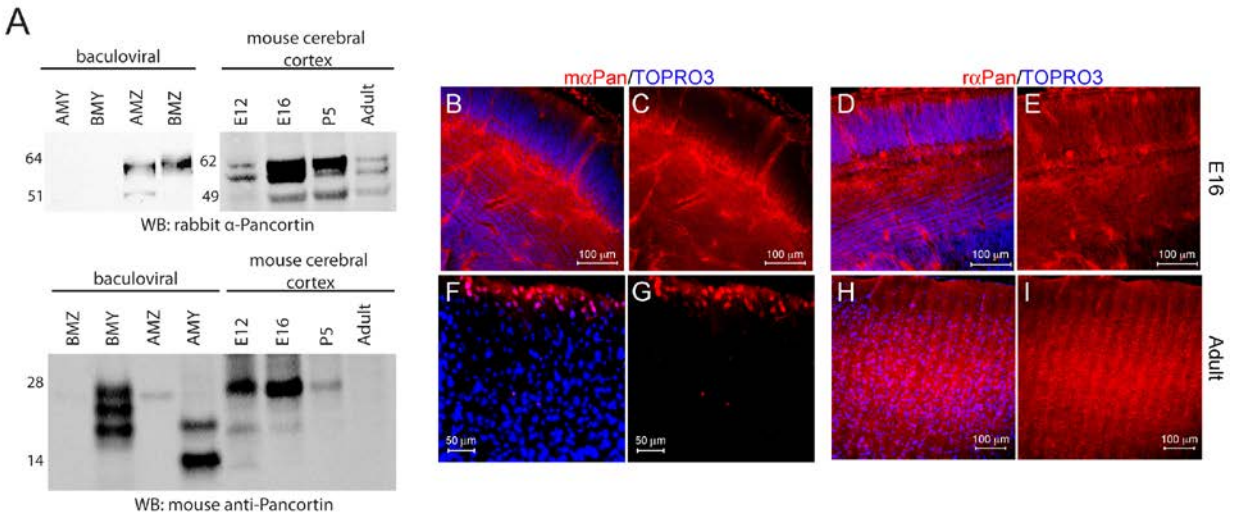

Figure 2.2. Pancortins are expressed in the developing and adult rodent cerebral cortex

(A) Western blots of lysates from mouse cerebral cortices at different developmental time points and of baculovirus produced Pancortin isoforms. Lysates were blotted with two different Pancortin antibodies. Rabbit anti-Pancortin (Abcam) appears to preferentially recognize AMZ and BMZ while a monoclonal antibody (NeuroMab) preferentially recognizes AMY and BMY. **(B-I)** Coronal sections of E16 and Adult wild type mouse brains immunostained with both Pancortin antibodies and counterstained with TOPRO3.

rodent cortex at both E16 (during active cortical migration) and adult ages (Fig. 2.1, 2.2). Levels of expression of the Pancortins were not affected by genomic disruption (knock out) of APP (Fig. 2.1D). Immunostaining of wild type E16 and adult mouse brain sections showed significant signal throughout the cerebral cortex with the Pancortin polyclonal antibody (favoring the Z-domain) (Fig. 2.2D,E,H,I). Immunostaining with the Pancortin monoclonal antibody (favoring the Y-domain) also showed extensive signal in the E16 brain, but signal was strongly diminished in the cortical plate (Fig. 2.2B,C).

Biochemical characterization of the interaction between APP and Pancortins

In order to confirm a biochemical interaction between APP and Pancortin, stable HEK293-APP695 cells were transiently transfected with the four individual FLAG-tagged Pancortin isoforms or vector alone. Cell lysates were IPed with M2 (anti-FLAG)-agarose beads and probed for both Pancortin (M2) and APP (C-terminal APP antiserum, C9). APP was able to co-IP with each of the Pancortin isoforms (Fig. 2.3A). Because each of the Pancortin isoforms co-IPs with APP, we predicted that the M domain common to each isoform was sufficient for an interaction with APP. FLAG-tagged B, M, and Z domains of Pancortin were expressed in stable HEK293-APP695 cells, and lysates were IPed with C9 (APP). The Y and A domains were not examined as they are only 1 and 22 amino acids in length, respectively. As predicted, the M domain was sufficient to co-IP with APP while the B domain was not (Fig 2.3B). Surprisingly, the Z domain also was capable of interacting with APP, however, this interaction was inconsistent between replicates (Fig. 2.3B).

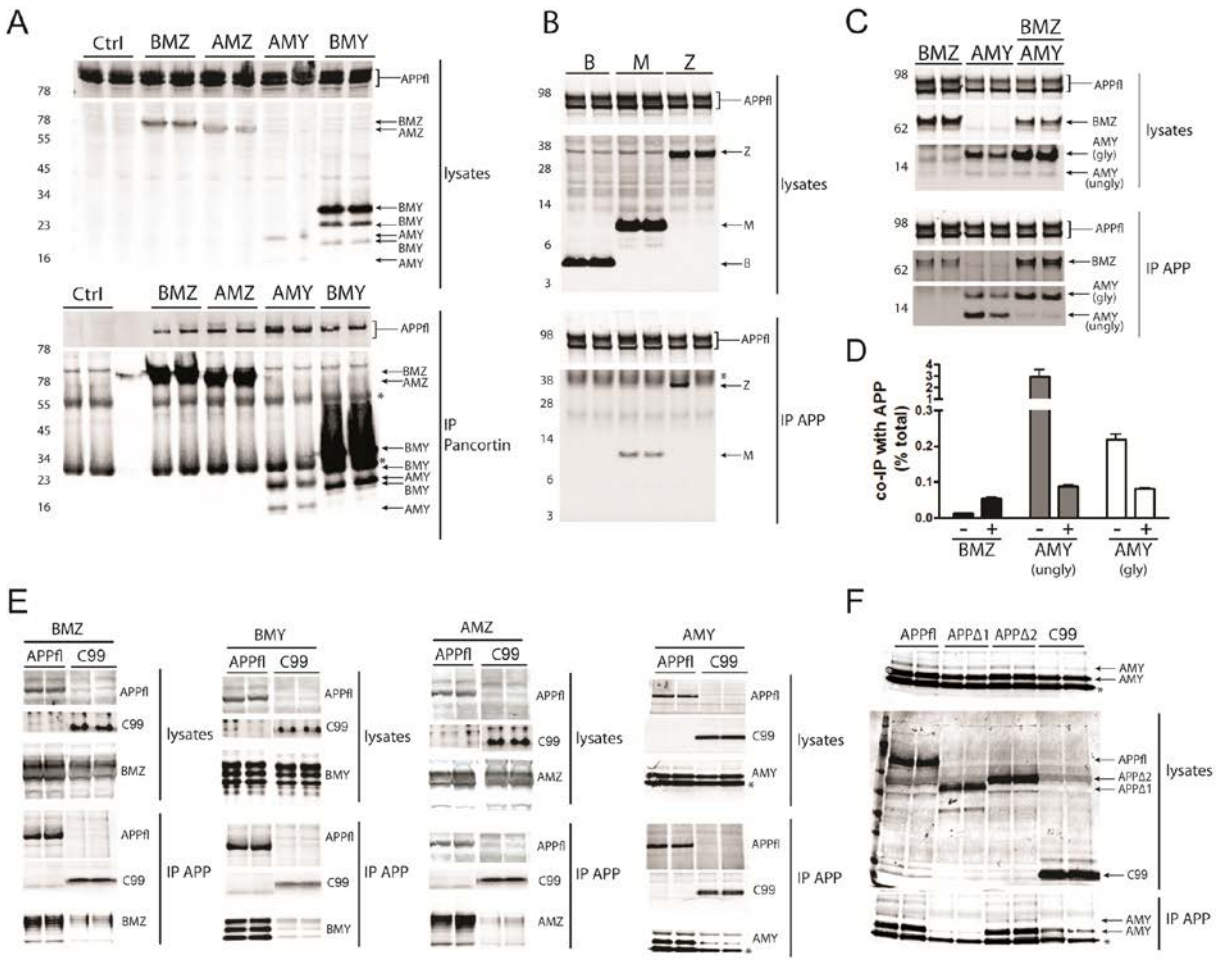

Figure 2.3. APP and Pancortins biochemically interact.

Figure 2.3. APP and Pancortins biochemically interact (continued). Western blots (WBs) for APP (anti-APP, C9) and FLAG-tagged Pancortin (anti-FLAG, M2) are shown for both the input (lysates) and the immunoprecipitated (IPed) products. Immunoprecipitations (IPs) of lysates for FLAG (M2) shown in A and for APP (C9) in B-F. Asterisks represent non-specific or cross-reactive IgG bands. **(A)** WBs of lysates of HEK293-APP695 cells transiently transfected with FLAG-tagged Pancortin isoforms or vector alone (ctrl). **(B)** WBs of lysates of HEK293-APP695 cells transiently transfected with FLAG-tagged Pancortin domains, B, M, and Z. **(C)** WBs of lysates of HEK293-APP695 cells transiently transfected with BMZ and AMY isoforms alone or together. **(D)** Quantification of the percent of BMZ and AMY co-IPed with APP relative to the total amount of each isoform in the lysate for BMZ and both the unglycosylated (lower band, "ungly") and glycosylated (upper band, "gly") forms of AMY when BMZ and AMY were expressed separately (-) or together (+). **(E)** WBs of lysates of HEK293 cells transiently transfected with each of the Pancortins and either full-length APP (APPfl) or a C-terminal fragment of APP (C99). **(F)** WBs of lysates of HEK293 cells transiently transfected with the AMY isoform of Pancortin and either full-length APP, APPΔ1 (lacking residues 36-289), APPΔ2

To investigate whether APP shows preferential interaction with specific isoforms of Pancortin, BMZ and AMY were expressed alone or together in HEK293 cells and the percentage of BMZ and AMY that co-IPed with APP relative to the total amount of each isoform in the lysate was quantified. AMY (both glycosylated and unglycosylated forms) had a higher co-IP efficiency than BMZ when each were expressed alone, but when expressed together the co-IP efficiency of AMY decreased and BMZ increased to reach a similar IP efficiency for each (Figs. 2.3C,D). Interestingly, the unglycosylated form of AMY (lower band) had a much greater binding efficiency than the glycosylated form (upper band) when expressed alone but not when co-expressed with BMZ (Figs 2.3C,D). Further, expression of BMZ stabilized the glycosylated form of AMY in the lysate of HEK293 cells (Fig. 2.3C).

To determine whether Pancortin interacts with the intracellular or extracellular region of APP, each of the Pancortins plus either full-length APP or the □-secretase cleaved, membrane-tethered C-terminal fragment of APP (C99) were expressed in HEK293 cells. Each of the Pancortins co-IPed strongly with full-length APP but weakly or not at all with C99, suggesting a requirement of the APP ectodomain for interaction with Pancortin (Fig. 2.3E). In order to narrow down this region of interaction, the AMY isoform of Pancortin and either full-length APP, APPΔ1 (lacking residues 36-289), APPΔ2 (lacking residues 288-493) or C99 were expressed in HEK293 cells. Deletion of the E1 domain of APP led to failure to co-IP AMY, whereas deletion of the E2 domain did not disrupt the interaction with AMY (Fig. 2.3F). Taken together, these studies demonstrate that APP interacts with each of the Pancortin isoforms and that the E1 domain of APP and both the M and Z domains of Pancortin are important for the interaction.

Effects of Pancortin isoforms on APP proteolytic processing

Pancortin may interact functionally with APP by altering the proteolytic processing of holoAPP, thus regulating potential downstream signaling activities of APP. Furthermore, cleavage of APP to generate Aβ is a process central to Alzheimer's disease pathogenesis, and understanding what factors trigger or inhibit this process may provide valuable insights into disease progression. The APP ectodomain is first shed by either α-secretase or β-secretase to release APPsα or APPsβ, respectively. When APP is cleaved by β-secretase followed by γ-secretase, Aβ is generated. To determine if Pancortins can modulate the processing of endogenous APP, HEK293 cells were transiently transfected with the Pancortin isoforms or empty vector (as control). Endogenous APPsα, APPsβ, and Aβ levels were measured in the conditioned media by ELISA.

Expression of the B domain containing isoforms resulted in a dramatic reduction in the generation of β-secretase cleavage products (APPsβ and Aβ), but had no significant effect on the α-secretase cleavage product (APPsα). BMZ and BMY reduced APPsβ levels by 51.8% ± 2.0% and 51.4% ± .8%, respectively (Fig. 2.4A) and reduced Aβ levels by 57.5% ± 3.4% and 65.6% ± 6.1%, respectively (Fig. 2.4B). The inhibition of β-secretase cleavage of APP by BMZ and BMY was a robust effect seen consistently in each individual experiment. While in these experiments slight changes in APPsα levels were seen in some experiments, overall there was no statistically significant effect of Pancortins on APPsα levels (Fig. 2.4A). Expression of AMZ did not significantly modulate α-secretase or β-secretase cleavage of APP, and expression of AMY resulted in smaller reductions in β-secretase cleavage of APP as compared to BMZ and BMY (Figs. 2.4A,B).

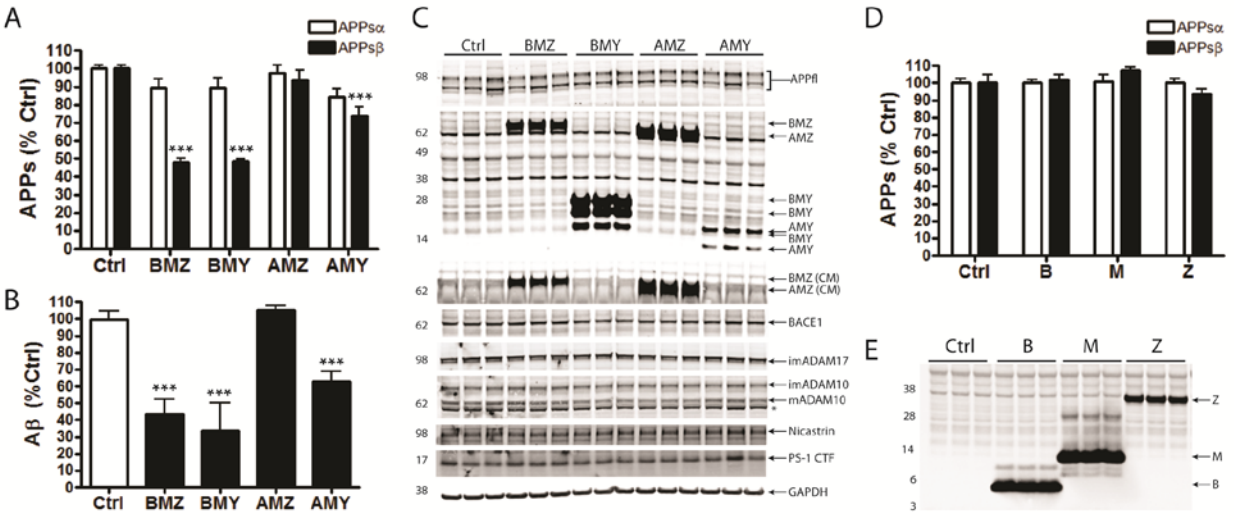

Figure 2.4. Specific Pancortin isoforms reduce β-secretase but not α-secretase cleavage of APP

HEK293 cells were transiently transfected with Pancortin isoforms and individual domains or empty vector (ctrl). 24 hours post-transfection, media was replaced, and after 24 additional hours media was collected and cells lysed. (**A,D**) Quantification of endogenous APPsα and APPsβ in the conditioned media (CM) via a multiplex ELISA, which allows for the simultaneous detection of each. (**B**) Quantification of Aβ40 in the CM by a separate ELISA. **(C,E)** Western blots of lysates (and conditioned media where noted by "CM") showing expression of endogenous full length APP, transfected Pancortins, and each of the secretases. Asterisk denotes a non-specific band. Each bar represents data from 2-4 independent experiments performed in triplicate for (**A)** and (**B)** and a single representative experiment performed in triplicate for (**D)**. Error bars represent s.e.m. ***p<0.001.

We next investigated the mechanism by which Pancortin isoforms regulate β-secretase cleavage of APP. The effects of the Pancortins on APP processing were not due to alterations in the expression of APP or its secretases, as transfection of the Pancortins did not alter endogenous holoAPP or the principal secretases responsible for cleavage at the β-site, BACE-1 (β-site APP cleaving enzyme-1), or α-site, ADAM17 and ADAM 10 (members of the disintegrin and metalloproteinase domain-containing family of proteins) (Fig 2.4C). Expression levels of Nicastrin and Presenilin-1, members of the γ-secretase complex, also were unchanged (Fig 2.4C). Because B domain-containing isoforms of Pancortin showed the most robust effects on APP processing but the B domain alone was not sufficient for binding APP, we tested whether a physical interaction with APP was necessary for the effects of BMZ and BMY on APP processing. As predicted, expression of the M and Z domains alone had no effect on APPsα or APPsβ (Figs. 2.4D,E) despite their ability to physically interact with APP (Fig 2.3D). However, the B domain alone also was not sufficient to reduce β-secretase cleavage of APP (Figs. 2.4D,E), suggesting that BMZ and BMY require a physical interaction with APP via the M and/or Z domains to modulate APP processing.

Role of Pancortin and APP in cortical cell migration

Since APP was previously shown to play an important role in cortical precursor cell migration (Young-Pearse et al, 2007; Young-Pearse et al, 2010), we asked whether Pancortins also function in this capacity. To address this question, E15.5 rat embryos were electroporated with a cDNA construct encoding GFP alone or co-electroporated with constructs encoding GFP and each of the Pancortin splice variants. Three days following electroporation, brains were

harvested, sectioned coronally, and immunostained for MAP2, which is expressed in differentiated neurons in the cortical plate, and for Tbr1, which is strongly expressed in cortical layer VI and in remnant subplate cells (and at lower levels in upper layers) at this developmental stage (Bulfone et al, 1995). At this time point (E18.5), electroporated cells are actively migrating from the ventricular zone through the intermediate zone and into the cortical plate. Using this experimental paradigm, cells electroporated with GFP alone were observed in both the cortical plate and below the cortical plate in the intermediate zone (Figs. 2.5A,B), as expected for day E18.5. Expression of each of the Pancortin isoforms had differential effects on location of the respective electroporated cells. While expression of BMZ resulted in a distribution of GFP-positive (i.e., BMZ-expressing) cells qualitatively similar to that observed with the control GFP-only electroporation, expression of AMY had a consistent effect of preventing electroporated cells from entering the cortical plate (Figs. 2.5A,B). Expression of AMZ and BMY had intermediate effects on cell location (Figs. 2.5A, B).

Given the consistent qualitative effects of AMY overexpression on cell location, we aimed to evaluate these effects by quantifying migration into the cortical plate of the electroporated cells at two time points: three days after electroporation, when control (GFP-only) electroporated cells are actively migrating, and six days after electroporation when the control cells have completed migration. At least three brains per condition were analyzed, and the summary results of these analyses are shown in Fig. 2.5A,D. AMY expression had a significant retarding effect on cell migration into the cortical plate at both 3 and 6 days post electroporation. At 6 days, almost all of the cells of control- and BMZ-electroporated brains entered the cortical plate, whereas AMY expressing brains show a major and significant

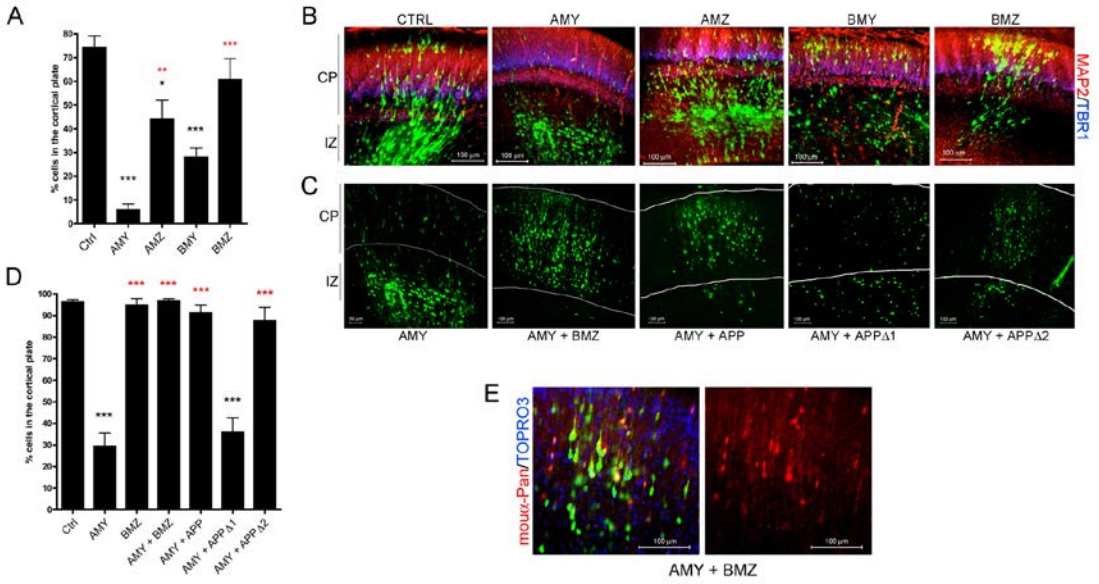

Figure 2.5. Expression of different Pancortin isoforms has opposing effects in migration of neural precursor cells into the cortical plate.

E15.5 rat embryos were co-electroporated with GFP and constructs encoding Pancortin cDNAs. Quantification of the percent of GFP-positive cells that migrated into the cortical plate after 3 (**A**) and 6 **(D)** days post electroporation. Each bar represents the average of data acquired from at least three independent embryos electroporated with constructs listed. Error bars represent s.e.m. *p<0.05, ***p<0.005. **(B)** Representative images from control brains or those expressing the listed Pancortin isoforms at 3 days post electroporation. MAP2 immunostaining is shown in red and TBR1 in blue. CP=cortical plate, IZ=intermediate zone **(C)** Representative images showing the 6 days post electroporation time point following electroporation of AMY with and without BMZ or APP co-electroporation. White lines mark boundaries of the cortical plate. **(E)** Two panels of a representative image showing GFP, Pancortin immunostaining (red) and TOPRO-3 staining (blue), or else Pancortin immunostaining alone of sections electroporated with AMY and BMZ.

impairment of cell movement past the IZ/CP boundary (Figs. 2.5C,D). Interestingly, co-expression of either BMZ or APP rescued this effect of AMY expression (Figs. 2.5C,D). To address whether expression of BMZ or APP prevented the overexpression of AMY, immunostaining for AMY was performed, and strong immunostaining for AMY was observed in sections from brains co-electroporated with AMY plus either BMZ or APP, at a level qualitatively similar to expression of AMY alone (Fig 2.5and data not shown).

To address whether a physical interaction between APP and Pancortin is necessary for proper rescue of the AMY defect by APP, we examined whether deletion of the AMY binding site within APP (APPΔ1) affected its ability to rescue. Indeed, co-expression of APPΔ1 with AMY failed to rescue the migration defect of AMY, while no effect was observed upon deletion of a neighboring domain in the APP ectodomain (APPΔ2) that does not affect binding to AMY (Figs. 2.5C,D). These data support the hypothesis that a biochemical interaction between APP and AMY is required for APP to rescue the failure of neuronal precursor to enter the cortical plate with AMY overexpression.

It has been reported that the AMZ and AMY Pancortin isoforms are more efficiently secreted than the BMZ and BMY isoforms (Barembaum et al, 2000; Moreno & Bronner-Fraser, 2005; Nagano et al, 2000). However, it also has been reported in multiple studies that the BMZ isoform is robustly secreted (Barembaum et al, 2000; Moreno & Bronner-Fraser, 2001). In order to examine whether Pancortin splice variants are secreted and/or retained intracellularly when expressed in cells of the developing cerebral cortex, brains electroporated with each of the FLAG-tagged splice variants were sectioned coronally and immunostained with an anti-FLAG antibody. With AMY or AMZ electroporation, immunostaining for FLAG showed a primarily

diffuse staining pattern in the cortical plate (Fig. 2.6A). In contrast, electroporation of BMY or BMZ resulted in an immunostaining pattern that was more strongly cell-associated and co-localized with cellular GFP fluorescence in the cortical plate, suggesting that these proteins are either primarily present intracellularly, or they are associated with the cell membrane of the cells in which they are expressed (Fig. 2.6B). In order to confirm and extend these observations, we performed ex-vivo cultures of the cells electroporated with the individual Pancortin isoforms (Appendix 1). Total Pancortin in the lysate and CM was determined by IP with M2 (anti-Flag)-agarose beads. Both BMZ and AMY were strongly detected in the CM, suggesting that both BMZ and AMY are secreted from electroporated neural cells. However, the level of secreted AMY was greater than BMZ relative to total expression in both the CM and the lysate (Fig. 2.6C). The levels of AMY in the lysate were below detection levels; therefore, to obtain higher expression levels and more accurately quantify the relative secretion of BMZ and AMY in neurons, we transfected E18 rat primary cortical neurons ex vivo using the Amaxa Nucleofector system. While both BMZ and AMY were again highly secreted, the percentage of AMY in the CM relative to total AMY in both the lysate and CM was greater than that of BMZ (Figs 2.6D,E). Co-expression of both BMZ and AMY had no effect on the secretion of either isoform (Figs 2.6D,E). Thus, we conclude that all isoforms are secreted, but the A-domain isoforms are secreted more robustly than the B-domain isoforms in developing neurons.

Next, we asked whether endogenous Pancortin expression is necessary for proper cortical migration. shRNA constructs were generated to target different Pancortin isoforms. The Pancortin shRNAs were first tested via transient transfection of HEK cells with each FLAG-tagged Pancortin isoform. Two days following this co-transfection, cells were lysed and Western

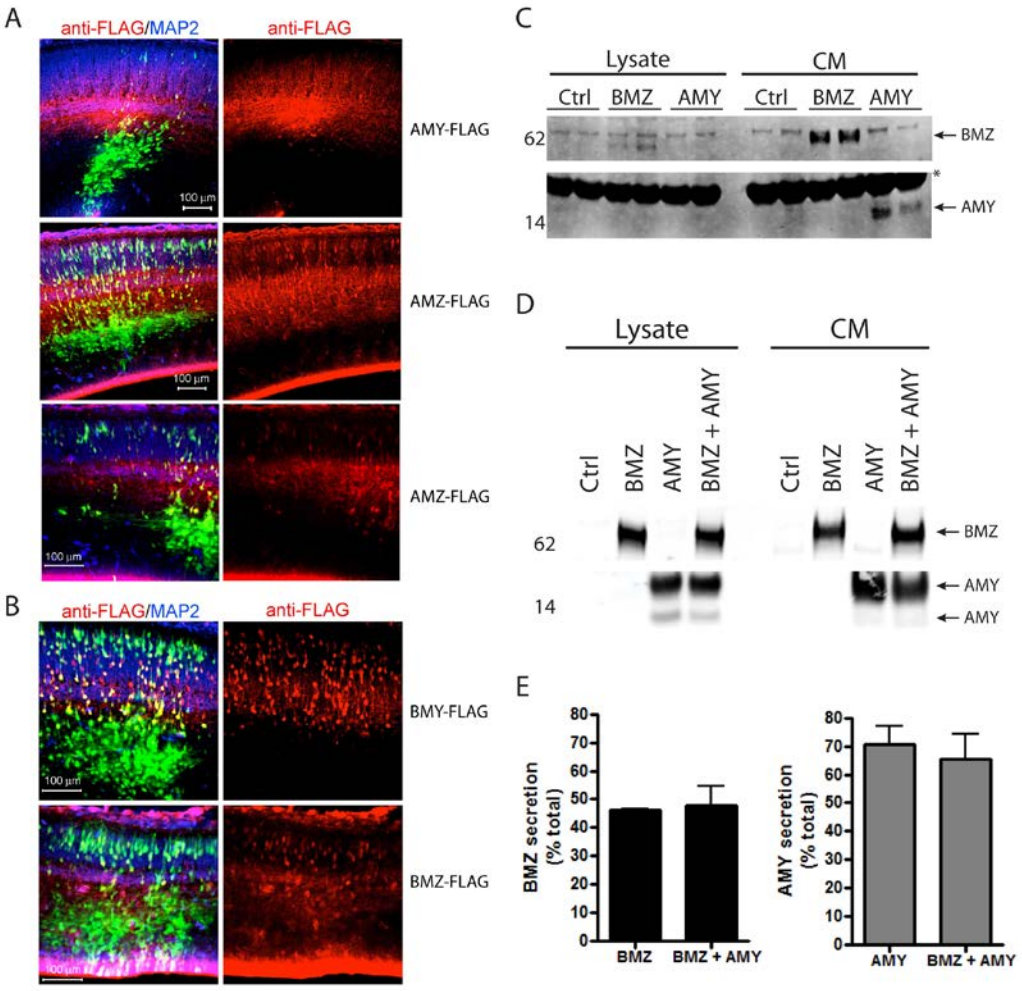

Figure 2.6. Differential secretion of the Pancortin isoforms from neuronal cells

(A-B) E15.5 rat embryos were co-electroporated in utero with GFP and constructs listed, and harvested 3 days later. Brains were sectioned and immunostained for FLAG and MAP2. Shown are representative images of GFP (green), anti-FLAG (red) and anti-MAP2 (blue). **(C-E)** Lysates and CM from ex-vivo cultures of cortical neurons electroporated in utero **(C)** or transfected in vitro **(D)** BMZ or AMY were IPed with M2 (anti-Flag)-agarose and WBs performed to detect FLAG-tagged Pancortin (anti-FLAG) **(C-D)**. **(E)** Quantification of the percent of BMZ and AMY detected in the CM relative to total (CM + lysate) following in vitro transfection of BMZ and AMY both together and separately.

blots performed. Pancortin shRNA 3 targets the “M” domain and was expected to target each of the Pancortin isoforms. Interestingly, although all splice variants contain the target site for shRNA 3, it was only effective in knocking down expression of AMY (Fig. 2.7A). Pancortin shRNA 4 targets domain “Z”, and it effectively knocked down BMZ but not other Pancortin isoforms (Fig. 2.7A).

With harvesting at 3 days post-electroporation, Pancortin shRNA 3 (targeting AMY) had no qualitative effect on cell location, whereas Pancortin shRNA 4 (targeting BMZ) resulted in a failure of electroporated cells to enter the cortical plate (Fig. 2.7B). The effects of knock down of BMZ with shRNA 4 persisted at 6 days post-electroporation, producing a phenotype strikingly similar to that observed with APP knock down or AMY overexpression (Fig. 2.7C & (Young-Pearse et al, 2007)). Quantification of these effects was performed at both 3 and 6 days, with analysis of at least three brains per condition (Figs. 2.7D,E). Knock down of AMY (by shRNA 3) only modestly decreased migration into the cortical plate at 3 days, and by 6 days, no significant effect on entry into the cortical plate was observed. However, those cells that entered the cortical plate were not localized to a single layer but rather were found in a “wavy” pattern throughout the cortical plate, which could be rescued by either APP or BMZ overexpression (Fig. 2.7F).

As expected, electroporation of shRNA 3, which knocks down AMY, rescued the AMY overexpression phenotype (Fig. 2.7D,E). In contrast, knock down of BMZ (with shRNA 4) did not rescue the AMY overexpression phenotype at 3 or 6 days (Fig. 2.7D,E). Similarly, knock down of APP had no additional effect on AMY overexpression. Overexpression of a mutated BMZ cDNA construct, which contains 4 synonymous mutations in the shRNA target site (“BMZ4m”),

rescued the knock down phenotype of Pancortin shRNA 4 (BMZ) at 3 and 6 days, suggesting that the effects observed with this shRNA are specifically due to a loss of Pancortin expression (Fig. 2.7E). Interestingly, overexpression of BMZ partially rescued the APP knock down phenotype at 6 days (Fig. 2.7E). Taken together, these data demonstrate a role of the Pancortins in proper migration of neuronal precursor cells into the cortical plate. Furthermore, our data suggest that APP and Pancortin may act in concert to regulate cortical precursor cell migration, as APP overexpression rescues both the defect in cortical plate entry of AMY overexpression and the “wavy” phenotype of AMY knock down.

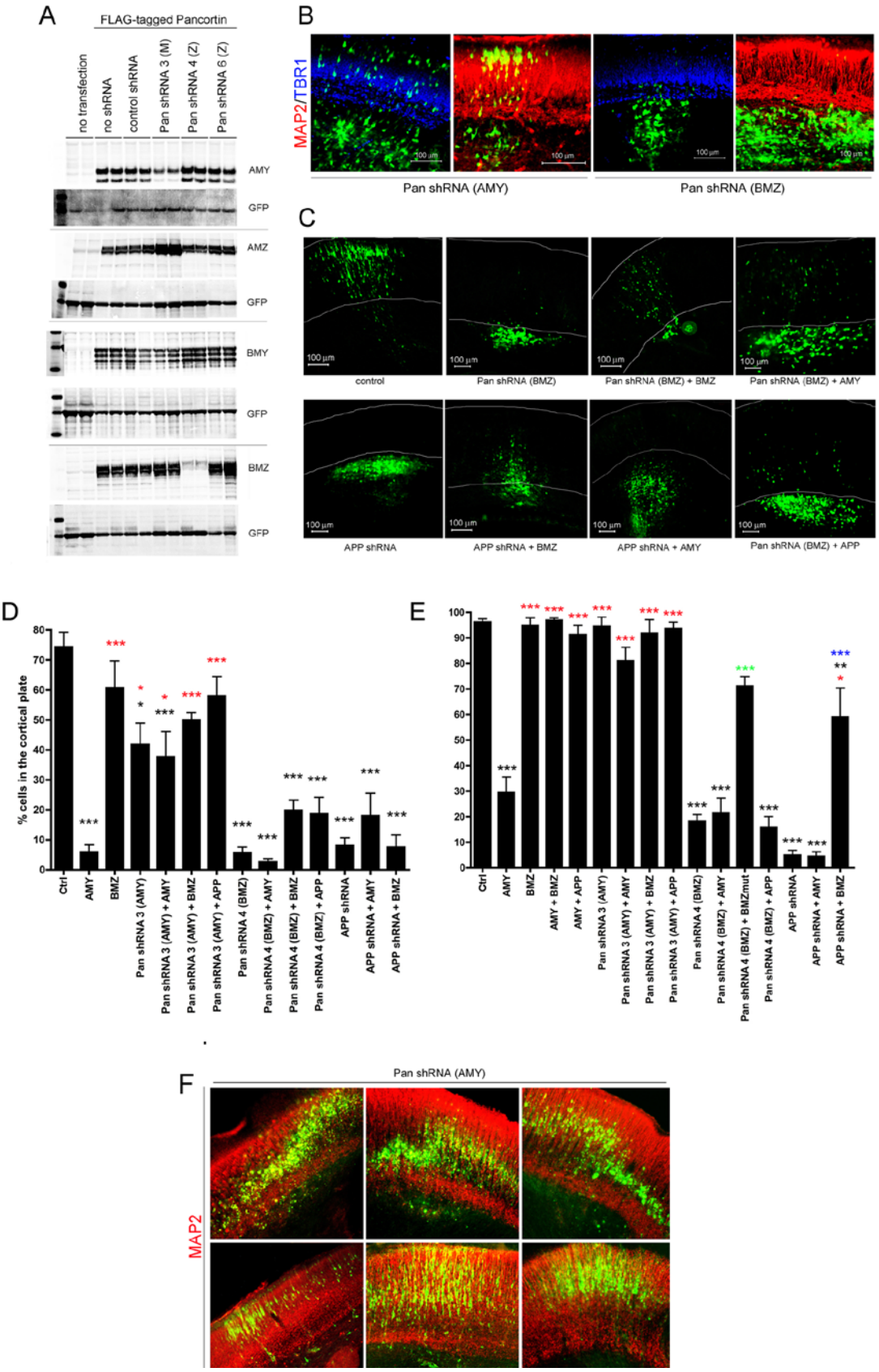

Figure 2.7. Pancortins are required for proper migration in the developing cerebral cortex.

Figure 2.7. Pancortins are required for proper migration in the developing cerebral cortex (continued).

(A) ShRNA constructs targeting Pancortin isoforms were generated and tested for their ability to knock down each of the FLAG-tagged Pancortin isoforms. HEK293 cells were transfected with construct combinations as labeled. GFP was co-transfected in all cases to monitor transfection efficiency. 48 hours following transfection, cells were lysed and Western blots performed to examine GFP and Pancortin levels, using M2 (α-FLAG). **(B-F)** E15.5 rat embryos were electroporated *in utero* with GFP and constructs listed, and harvested 3 or 6 days later. Brains were dissected, fixed, sectioned coronally, and immunostained for MAP2 and TBR1. **(B)** Representative images of a 3 day harvest following introduction of shRNA 3 (which knocks down AMY) and shRNA 4 (which knocks down BMZ). MAP2 immunostaining is shown in red and TBR1 in blue. **(C)** Representative images of brains electroporated with constructs listed and harvested 6 days later. White lines delineate the boundaries of the cortical plate as determined by MAP2 and TBR1 immunostaining. **(D,E)** Quantification of the percent of GFP positive cells present in the cortical plate after 3 **(D)** and 6 **(E)** days post electroporation. Each bar presents data from the average of at least three independent embryos electroporated with constructs listed. Error bars represent s.e.m. * $p<0.05$, ** $p<0.01$, *** $p<0.005$. Black asterisks represent significance relative to GFP vector control, red asterisks to AMY, green asterisk to Pancortin shRNA 4 (BMZ), and blue asterisk to APP shRNA. Quantifications from Fig. **3A,D** for GFP, AMY, BMZ, AMY+BMZ, and AMY+APP are re-shown here for direct comparison to knock down data. **(F)** Representative images of brains electroporated with shRNA targeting AMY with and without co-electroporation of AMY, APP, or BMZ and harvested at 6 days post

Discussion

A Role for Pancortins in Mammalian Cortical Development

Pancortin, originally named for its high expression in the cerebral cortex (Nagano et al, 1998), has been implicated in migration of neural crest cells and neuronal differentiation in chick embryos and *Xenopus*, respectively (Barembaum et al, 2000; Moreno & Bronner-Fraser, 2001; Moreno & Bronner-Fraser, 2005). However, no studies have yet identified a role for Pancortin in the development of the mammalian brain. In a single report of a Pancortin knockout mouse, it was proposed that Pancortins are mediators of ischemia-induced neuronal cell death in the adult brain (Cheng et al, 2007). However, it remains unclear what the normal function of Pancortin may be during development, as the loss of Pancortin only protected adult but not embryonic neurons against ischemic death, and other putative developmental phenotypes were not presented. Here, utilizing the technique of in utero electroporation to both overexpress Pancortin and knock down endogenous Pancortin in a subset of neural cells, we reveal a novel function of Pancortin in the migration of neuronal precursors into the cortical plate of the rat cortex. AMY knock down produces a phenotype in which neuronal precursors enter the cortical plate but exhibit abnormal positioning, a unique phenotype that we have not observed with in utero electroporation of over a dozen different genes thought to have roles in neuronal development. Overexpression of the AMY isoform or knock down of the BMZ isoform results in failure of neuronal precursors to enter the cortical plate. Phenotypes of abnormal cell positioning can result from a number of different types of primary insult including a decline in cell survival, defects in the cytoskeletal network critical for the mechanics of cell movement, and disruptions of signaling pathways that instruct cells when to migrate and when to stop and

differentiate. Here, we believe that the primary defect is not in cell survival, as there is no dramatic loss in electroporated cells between 3 and 6 days post electroporation. Further, electroporated cells are able to migrate away out of the ventricular zone and through the intermediate zone with AMY overexpression and BMZ knock down, suggesting that these cells have the necessary machinery for cell movement. Rather, cells stop just below the cortical plate boundary, similar to the defect observed with knock down of APP. We hypothesize that this is due to a defect in signaling within the cells that either fails to direct the cells to continue migrating or else directs the cells to prematurely halt migration.

Our data support an opposing role for BMZ and AMY in regulating developmental processes. While BMZ promotes migration into the cortical plate, AMY appears to inhibit normal cortical plate entry. Further, overexpression of BMZ rescues the phenotype observed with AMY overexpression. Interestingly, the observation of functional antagonism between the BMZ and AMY isoforms in neurodevelopment is consistent with previous studies in Xenopus in which BMZ promoted neuronal differentiation and AMY rescued this effect (Moreno & Bronner-Fraser, 2001; Moreno & Bronner-Fraser, 2005), perhaps through direct interaction of the BMZ and AMY isoforms (Moreno & Bronner-Fraser, 2005). In addition, our observation that both isoforms are able to bind to APP but differ in their co-IP efficiency with APP when each are expressed separately but reach similar co-IP efficiencies with APP when expressed together lend support to an additional model of competition between these isoforms for binding to putative receptors.

Biochemical and Functional Interaction of Pancortin and APP

Here, we report a novel biochemical and functional interaction between Pancortins and APP. In an unbiased screen, we identified Pancortins as extracellular binding partners for APP, and confirmed that each of the Pancortin isoforms binds either directly or indirectly to the APP ectodomain. The E1 region of the APP ectodomain and the M and Z domains of Pancortin were critical for a physical interaction. Further, expression of the B domain containing isoforms strongly inhibits β-secretase cleavage of APP, suggesting a biochemical consequence of the association between Pancortins and APP. However, the B domain, which confers activity but cannot physically interact with APP, has no effect on β-secretase processing when expressed alone, suggesting that a physical interaction between APP and Pancortin is required to modulate APP processing.

Knock down of BMZ or overexpression of AMY phenocopies a loss of APP expression in the developing rodent brain, each showing a specific defect in migration of neural precursor cells into the cortical plate. We hypothesize that for this function in cortical development, Pancortins act in part through binding to APP, but also though APP-independent mechanisms. Based upon the data presented herein (summarized in Fig. 2.8), we propose that BMZ binding to the extracellular domain of APP promotes proper migration into the cortical plate while binding of AMY to APP inhibits proper migration. Thus, loss of APP or BMZ, or else overexpression of AMY inhibits cortical plate entry (Fig. 2.5, 2.7). We posited that if AMY overexpression inhibits the functions of BMZ and APP in normal migration, then overexpression of either BMZ or APP should rescue the AMY defect, which was the effect that was observed (Fig. 2.5). Further, we found that APP rescues the AMY defect through a physical interaction, as

blockade of the interaction through deletion of the E1 domain of APP prevents rescue of the AMY defect (Fig. 2.5D). In HEK293 cells, co-expression of BMZ and AMY reduces binding of AMY to APP, suggesting that BMZ may rescue the AMY defect by preventing AMY from binding APP (Figs. 2.3C,D). Interestingly, overexpression of APP does not rescue the loss of BMZ (Fig. 2.5D,E), indicating that the migration-promoting effect of APP is dependent upon expression of BMZ.

Taken together, the data presented suggest that Pancortins functionally and biochemically interact with APP in cortical development. However, our data showing that BMZ overexpression can partially rescue the phenotype observed with knock down of APP suggest that Pancortins also may act through APP-independent mechanisms, perhaps through interaction with the highly homologous APP family members (APLP1 and 2) or possibly through other type I-transmembrane domain proteins. Future studies are warranted to examine how Pancortins interact with other known signaling pathways to regulate proper migration and differentiation of neuronal precursor cells in the mammalian cerebral cortex.

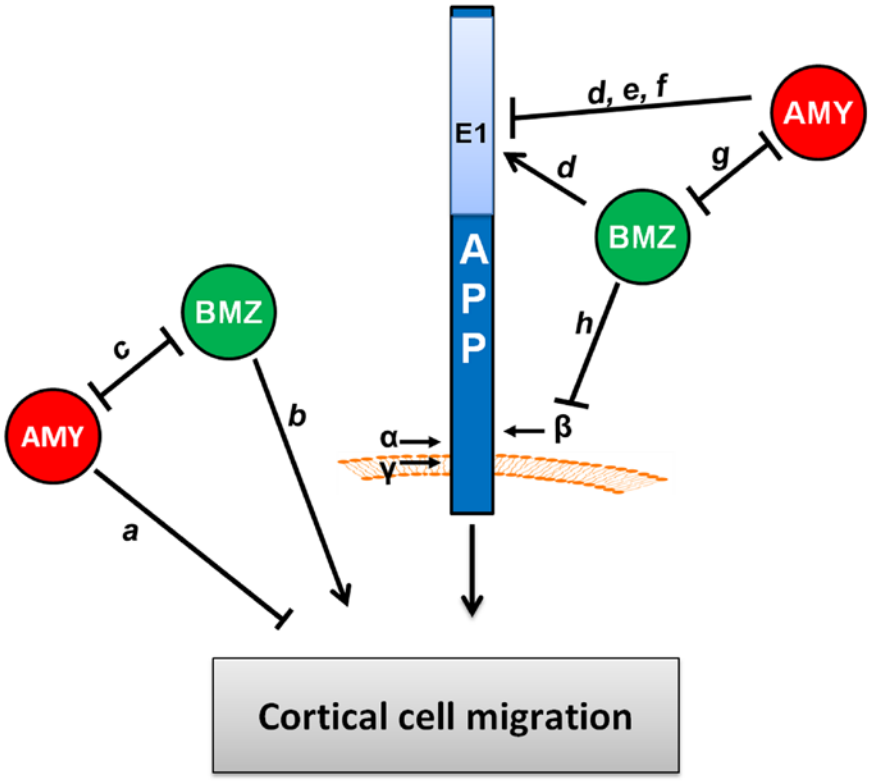

Figure 2.8. Summary of the effects observed of Pancortins and APP on migration in the developing cerebral cortex.

Figure 2.8. Summary of the effects observed of Pancortins and APP on migration in the developing cerebral cortex (continued).

In utero electroporation of Pancortin constructs in the developing rat brain revealed novel and opposing roles of the AMY and BMZ isoforms in cortical cell migration. (***a)*** Cells overexpressing AMY fail to enter the cortical plate suggesting that AMY inhibits cortical plate entry. (***b)*** Knock down of BMZ results in failure to enter the cortical plate, suggesting that endogenous BMZ promotes cortical plate entry. (***c)*** BMZ overexpression rescues the defect observed with AMY overexpression. Taken together with previous studies of neuronal differentiation in Xenopus (Moreno and Bronner-Fraser, 2005), the data support a model where AMY and BMZ mutually inhibit the activity of the other. In support of an APP-dependent mechanism , ***d)*** peptides to the B and Z domain of Pancortin were identified in an unbiased mass spectrometry screen for APP interacting proteins and both BMZ and AMY co-IP with APP, an interaction disrupted by deletion of the E1 region of the APP ectodomain. ***e)*** Overexpression of APP rescues AMY overexpression, but ***f)*** blockade of the interaction through deletion of the AMY binding site within APP (the E1 domain) prevents rescue of the AMY defect by APP, supporting a model whereby AMY inhibits the function of APP in cortical cell migration through a physical interaction. ***g)*** Expression of BMZ can decrease the co-IP efficiency of AMY with APP, which suggest that BMZ may rescue the AMY defect by preventing AMY from binding to APP. ***h)*** BMZ inhibits β-secretase cleavage of APP; however, whether this activity is mechanistically involved in regulating migration has yet to be determined.

References

Araki W, Kitaguchi N, Tokushima Y, Ishii K, Aratake H, Shimohama S, Nakamura S, Kimura J (1991) Trophic effect of β-amyloid precursor ptotein on cerebral cortical neurons in culture. *Biochem Biophys Res Commun* **181:** 265-271

Bai Y, Markham K, Chen F, Weerasekera R, Watts J, Horne P, Wakutani Y, Bagshaw R, Mathews PM, Fraser PE, Westaway D, St George-Hyslop P, Schmitt-Ulms G (2008) The in vivo brain interactome of the amyloid precursor protein. *Mol Cell Proteomics* **7:** 15-34

Barembaum M, Moreno TA, LaBonne C, Sechrist J, Bronner-Fraser M (2000) Noelin-1 is a secreted glycoprotein involved in generation of the neural crest. *Nat Cell Biol* **2:** 219-225

Bulfone A, Smiga SM, Shimamura K, Peterson A, Puelles L, Rubenstein JL (1995) T-brain-1: a homolog of Brachyury whose expression defines molecularly distinct domains within the cerebral cortex. *Neuron* **15:** 63-78

Cheng A, Arumugam TV, Liu D, Khatri RG, Mustafa K, Kwak S, Ling HP, Gonzales C, Xin O, Jo DG, Guo Z, Mark RJ, Mattson MP (2007) Pancortin-2 interacts with WAVE1 and Bcl-xL in a mitochondria-associated protein complex that mediates ischemic neuronal death. *J Neurosci* **27:** 1519-1528

Danielson PE, Forss-Petter S, Battenberg EL, deLecea L, Bloom FE, Sutcliffe JG (1994) Four structurally distinct neuron-specific olfactomedin-related glycoproteins produced by differential promoter utilization and alternative mRNA splicing from a single gene. *J Neurosci Res* **38:** 468-478

De Strooper B, Annaert W (2000) Proteolytic processing and cell biological functions of the amyloid precursor protein. *J Cell Sci* **113:** 1857-1870

Ghiso J, Rostagno A, Gardella JE, Liem L, Gorevic PD, Frangione B (1992) A 109-amino-acid C-terminal fragment of Alzheimer's-disease amyloid precursor protein contains a sequence, -RHDS-, that promotes cell adhesion. *Biochem J* **288:** 1053-1059

Hardy J, Selkoe DJ (2002) The amyloid hypothesis of Alzheimer's disease: progress and problems on the road to therapeutics. *Science* **297:** 353-356

Ho A, Sudhof TC (2004) Binding of F-spondin to amyloid-beta precursor protein: a candidate amyloid-beta precursor protein ligand that modulates amyloid-beta precursor protein cleavage. *Proc Natl Acad Sci* **101:** 2548-2553

Hoe HS, Lee KJ, Carney RS, Lee J, Markova A, Lee JY, Howell BW, Hyman BT, Pak DT, Bu G, Rebeck GW (2009) Interaction of reelin with amyloid precursor protein promotes neurite outgrowth. *J Neurosci* **29:** 7459-7473

Hoe HS, Tran TS, Matsuoka Y, Howell BW, Rebeck GW (2006) DAB1 and Reelin effects on amyloid precursor protein and ApoE receptor 2 trafficking and processing. *J Biol Chem* **281:** 35176-35185

Hoe HS, Wessner D, Beffert U, Becker AG, Matsuoka Y, Rebeck GW (2005) F-spondin interaction with the apolipoprotein E receptor ApoEr2 affects processing of amyloid precursor protein. *Mol Cell Biol* **25:** 9259-9268

Ma QH, Futagawa T, Yang WL, Jiang XD, Zeng L, Takeda Y, Xu RX, Bagnard D, Schachner M, Furley AJ, Karagogeos D, Watanabe K, Dawe GS, Xiao ZC (2008) A TAG1-APP signalling pathway through Fe65 negatively modulates neurogenesis. *Nat Cell Biol* **10:** 283-294

Moreno T, Bronner-Fraser M (2001) The secreted glycoprotein Noelin-1 promotes neurogenesis in Xenopus. *Developmental biology* **240:** 340-400

Moreno TA, Bronner-Fraser M (2005) Noelins modulate the timing of neuronal differentiation during development. *Dev Biol* **288:** 434-447

Nagano T, Nakamura A, Konno D, Kurata M, Yagi H, Sato M (2000) A2-Pancortins (Pancortin-3 and -4) are the dominant pancortins during neocortical development. *J Neurochem* **75:** 1-9

Nagano T, Nakamura A, Mori Y, Maeda M, Takami T, Shiosaka S, Takagi H, Sato M (1998) Differentially expressed olfactomedin-related glycoproteins (Pancortins) in the brain. *Brain Res Mol Brain Res* **53:** 13-23

Osterfield M, Egelund R, Young LM, Flanagan JG (2008) Interaction of amyloid precursor protein with contactins and NgCAM in the retinotectal system. *Development* **135:** 1189-1199

Perez RG, Zheng H, Van der Ploeg LH, Koo EH (1997) The beta-amyloid precursor protein of Alzheimer's disease enhances neuron viability and modulates neuronal polarity. *J Neurosci* **17:** 9407-9414

Pramatarova A, Chen K, Howell BW (2008) A genetic interaction between the APP and Dab1 genes influences brain development. *Mol Cell Neurosci* **37:** 178-186

Pramatarova A, Ochalski PG, Lee CH, Howell BW (2006) Mouse disabled 1 regulates the nuclear position of neurons in a Drosophila eye model. *Mol Cell Biol* **26:** 1510-1517

Priller C, Bauer T, Mitteregger G, Krebs B, Kretzschmar HA, Herms J (2006) Synapse formation and function is modulated by the amyloid precursor protein. *J Neurosci* **26:** 7212-7221

Rice H, Suth S, Cavanaugh W, Bai J, Young-Pearse T (2010) In utero electroporation followed by primary neuronal culture for studying gene function in subset of cortical neurons. *J Vis Exp* **44**

Ring S, Weyer SW, Kilian SB, Waldron E, Pietrzik CU, Filippov MA, Herms J, Buchholz C, Eckman CB, Korte M, Wolfer DP, Muller UC (2007) The secreted beta-amyloid precursor protein ectodomain APPs alpha is sufficient to rescue the anatomical, behavioral, and electrophysiological abnormalities of APP-deficient mice. *J Neurosci* **27:** 7817-7826

Selkoe D (2011) Resolving controversies on the path to Alzheimer's therapeutics. *Nature medicine* **17:** 1060-1065

Soba P, Eggert S, Wagner K, Zentgraf H, Siehl K, Kreger S, Lower A, Langer A, Merdes G, Paro R, Masters CL, Muller U, Kins S, Beyreuther K (2005) Homo- and heterodimerization of APP family members promotes intercellular adhesion. *EMBO J* **24:** 3624-3634

Wang Z, Wang B, Yang L, Guo Q, Aithmitti N, Songyang Z, Zheng H (2009) Presynaptic and postsynaptic interaction of the amyloid precursor protein promotes peripheral and central synaptogenesis. *J Neurosci* **29:** 10788-10801

Young-Pearse TL, Bai J, Chang R, Zheng JB, Loturco JJ, Selkoe DJ (2007) A Critical Function for beta-Amyloid Precursor Protein in Neuronal Migration Revealed by In Utero RNA Interference. *J Neurosci* **27:** 14459-14469

Young-Pearse TL, Chen A, Chang R, Marquez C, Selkoe DJ (2008) Secreted APP regulates the function of full-length APP in neurite outgrowth through interaction with integrin beta1. *Neural Development* **3**

Young-Pearse TL, Suth S, Luth ES, Sawa A, Selkoe DJ (2010) Biochemical and functional interaction of disrupted-in-schizophrenia 1 and amyloid precursor protein regulates neuronal migration during mammalian cortical development. *J Neurosci* **30:** 10431-10440

Chapter 3:

Systematic evaluation of candidate ligands regulating ectodomain shedding of Amyloid Precursor Protein

Heather C. Rice, Tracy L. Young-Pearse, and Dennis J. Selkoe

Experimental contributions to this chapter:HCR performed all experiments

This chapter was modified from a manuscript published in Biochemistry 2013 May 2. [Epub ahead of print].

Abstract

Despite intense interest in the proteolysis of the ß-Amyloid Precursor Protein (APP) in Alzheimer's disease (AD), how the normal processing of this type I receptor-like glycoprotein is physiologically regulated remains ill-defined. In recent years, several candidate protein ligands for APP, including F-spondin, Reelin, β1 Integrin, Contactins, Lingo-1 and Pancortin, have been reported. However, a cognate ligand for APP that regulates its processing by α- or β-secretase has yet to be widely confirmed in multiple laboratories. Here, we developed new assays in an effort to confirm a role for one or more of these candidate ligands in regulating APP ectodomain shedding in a biologically relevant context. A comprehensive quantification of APPsα and APPsβ, the immediate products of secretase processing, in both non-neuronal cell lines and primary neuronal cultures expressing endogenous APP yielded no evidence that any of these published candidate ligands *stimulate* ectodomain shedding. Rather, Reelin, Lingo-1 and Pancortin-1 emerged as the most consistent ligands for significantly *inhibiting* ectodomain shedding. These findings led us to conduct further detailed analyses of the interactions of Reelin and Lingo-1 with APP.

Introduction

Although the stepwise proteolysis of the ß-Amyloid Precursor Protein (APP) to release amyloid ß-protein (Aß) has been central to the study of Alzheimer's disease (AD), how the normal processing of this conserved type I membrane glycoprotein is physiologically regulated remains poorly defined. In AD, amyloid (neuritic) plaques are principally composed of the potentially neurotoxic Aβ peptides, which are generated by the sequential proteolytic processing of APP (reviewed in (Haass et al, 2012)). Cleavage of APP by either α- or β- secretase results in the shedding of large extracellular portions of APP termed APPsα or APPsβ, respectively. The remaining C-terminal fragments (CTFα and CTFβ) are then cleaved intramembranously by γ-secretase. Cleavage of CTFβ by γ-secretase releases Aβ into the luminal/extracellular space and AICD into the cytoplasm. Cleavage of CTFα by γ-secretase releases the smaller p3 fragment into the lumen/extracellular space and AICD into the cytoplasm. The latter pathway, which begins with APP ectodomain shedding by α-secretase, predominates in almost all cell types and precludes Aβ production.

Experimental studies suggest several roles for APP in brain development, including migration of neuronal precursor cells (Pramatarova et al, 2008; Young-Pearse et al, 2007), neurite outgrowth (Araki et al, 1991; Perez et al, 1997; Rama et al, 2012; Young-Pearse et al, 2008), cell adhesion (Ghiso et al, 1992; Soba et al, 2005) and synapse formation (Priller et al, 2006; Wang et al, 2009). Since its initial discovery, APP has been hypothesized to be a cell surface receptor (Kang et al, 1987). In recent years, several candidate protein ligands for APP, including F-spondin (Ho & Sudhof, 2004; Hoe et al, 2005), Reelin (Hoe et al, 2009; Hoe et al,

2006), β1 Integrin (Hoe et al, 2009; Young-Pearse et al, 2008), Contactins (Bai et al, 2008; Ma et al, 2008; Osterfield et al, 2008), Lingo-1 (Bai et al, 2008) and Pancortin (Rice et al, 2012), have been reported to interact physically with the ectodomain of APP and modulate APP processing and, in some cases, APP function in neurodevelopment.

F-spondin, a secreted extracellular matrix glycoprotein, was identified in unbiased screens for APP interactors (Bai et al, 2008; Ho & Sudhof, 2004). Transfection of F-spondin was initially found to inhibit β-secretase cleavage of APP as measured by CTFβ levels in human embryonic kidney (HEK) 293 cells also over-expressing APP and BACE1 (Ho & Sudhof, 2004). F-spondin inhibited AICD-dependent gene transactivation, suggesting that α-secretase cleavage was also inhibited by F-spondin (Ho & Sudhof, 2004). However, a subsequent study reported that F-spondin enhanced APPsα and CTFα in addition to reducing APPsβ in COS7 cells overexpressing APP (Hoe et al, 2005).

β1 Integrin is a type I single transmembrane protein important for cell adhesion. We have found β1 Integrin to physically interact with APP and to be involved in APP-dependent neurite outgrowth (Young-Pearse et al, 2008). These findings were confirmed in a study by another group in which they also reported that β1 Integrin enhanced APPsα and CTFα levels in COS7 cells overexpressing APP (Hoe et al, 2009).

The Contactins (CNTNs) are GPI-anchored neuronal-specific cell adhesion molecules (reviewed in (Shimoda, 2009)). CNTN4 was identified in a screen for extracellular APP binding partners in embryonic chick brain, and only CNTN3 and CNTN4 but not the remaining CNTN family members were found to directly bind APP *in vitro* (Osterfield et al, 2008). However, other

groups reported evidence of a physical interaction of CNTN2 (Ma et al, 2008) and CNTN1(Bai et al, 2008) with APP. Expression of CNTN4 in HEK cells overexpressing APP led to an increase of CTFα levels in some experiments and a decrease in others (Osterfield et al, 2008). CNTN2 was reported to enhance AICD, CTFα and CTFβ in both overexpressed and endogenous assays (Ma et al, 2008). Functional interactions between CNTN4 and APP in neurite outgrowth (Osterfield et al, 2008) and CNTN2 and APP in neurogenesis (Ma et al, 2008) have been reported.

Lingo-1 (leucine rich repeat and Ig domain-containing Nogo receptor interacting protein-1), a single-transmembrane protein, is a member of the Nogo-66 receptor complex and negatively regulates axonal myelination and regeneration (reviewed in (Mi et al, 2008)). Lingo-1 was among the proteins identified (along with F-spondin) in the APP interactome study of intact mouse brain (Bai et al, 2008). This study reported a physical interaction between APP and Lingo-1 and showed that knockdown of Lingo-1 in HEK293 cells stably overexpressing APP bearing the "Swedish" AD mutation increased CTFα and lowered CTFβ, whereas overexpression of Lingo-1 increased CTFβ (Bai et al, 2008). A separate group confirmed a physical interaction in an overexpressed cell system and determined that the interaction occurs via the ectodomain of Lingo-1 (Stein & Walmsley, 2012).

Reelin, a large glycoprotein, is secreted from Cajal-Retzius cells in the embryonic cortex and regulates the migration of neuronal precursor cells (reviewed in (Honda et al, 2011)). In the adult cortex, Reelin is secreted by a subset of interneurons and plays a role in synaptic plasticity (reviewed in (Förster et al, 2010)). In two studies, Reelin was shown to physically interact with APP and enhance APPsα and CTFα levels in COS7 cells overexpressing APP (Hoe et al, 2009; Hoe

et al, 2006) . Subsequently, another group showed that reduction of Reelin enhanced both CTFβ and Aβ in APP transgenic mice (Kocherhans et al, 2010). A functional interaction between Reelin and APP in neurite outgrowth has been described (Hoe et al, 2009).

We recently reported Pancortin, a secreted glycoprotein with multiple isoforms, as a candidate ligand for APP (Rice et al, 2012). Pancortin was identified in an unbiased screen of endogenous proteins from murine cortical slices that interacted with the APP ectodomain (Rice et al, 2012). Pancortin-1 and Pancortin-2 were found to specifically reduce β-secretase but not α-secretase cleavage of endogenous APP in HEK293 cells, while Pancortin-3 had no effect (Rice et al, 2012). We also uncovered a functional interaction of Pancortin isoforms with APP in regulating the entry of neuronal precursor cells into the cortical plate (Rice et al, 2012).

In the context of these numerous reports of candidate ligands with often variable individual results, a cognate ligand for APP that regulates its processing by α- or β- secretase has yet to be widely confirmed by multiple laboratories in biologically relevant systems. Here, in an effort to confirm a role for one or more reported candidate ligands in regulating α- or β-secretase cleavage of APP, we describe a systematic comparison of candidate ligands by directly quantifying APPsα and APPsβ, the immediate products of secretase processing, across multiple assays. First, we compare candidate APP ligands in a non-neuronal mammalian cell line with overexpression of APP, in keeping with virtually all of the above initial reports on these candidate ligands. Then, we compare the candidates in novel assays we have developed to measure proteolytic processing of *endogenous* APP in both non-neuronal and neuronal cell lines. From these studies, we do not confirm any candidates as triggering ectodomain shedding

of APP. However, Reelin, Lingo-1 and Pancortin-1 emerge as the most consistent ligands that reduce α- and/or β- secretase cleavage of APP. Accordingly, we report further detailed analyses of the interactions of Reelin and Lingo-1 with APP.

Experimental Procedures

Plasmids

Plasmids utilized for transient and stable transfections include, pCAX-APP751(human) as described (Young-Pearse et al, 2007), pcDNA-APP695-swedish (human), as described (Citron et al, 1992), pCAX-β1 Integrin (mouse) as described (Young-Pearse et al, 2008), PCAX –Pancortin-1 and -4 (mouse) as described (Rice et al, 2012). pcDNA4-His/Myc-F-spondin(human) was kindly provided by T. Südhof (Ho & Sudhof, 2004). Lingo-1 (human) was obtained from DF/HCC DNA Resource Core deposited by the Mammalian Gene Collection consortium and cloned into the pCDH vector. CNTN2-Fc(human) was kindly provided by J. Flanagan (Osterfield et al, 2008) and cloned into the pcDNA vector. pcDNA-Reelin (mouse) was kindly provided by T. Curran (D'Arcangelo et al, 1997). Constructs for the Reelin fragments (N-R6, R3-8, 3-6, N-R2, and R7-8) (mouse) were provided by A. Goffinet (Jossin et al, 2004). pcDNA-APOER2 were kindly provided by J. Herz. VLDLR-myc (mouse) was kindly provided by H-S Hoe (Hoe et al, 2005). HEK293 cell lines stably expressing Reelin or vector control, CER or CEP4 respectively, were kindly provided by T. Curran (Benhayon et al, 2003).

Immunoprecipitation (IP) and Western blotting (WB)

For IP studies, HEK293 cells were transfected with the specified combinations of Reelin, APOER2, VLDLR, and APP. Cells were lysed in 1% NP40 STEN buffer (150 mM NaCl, 50 mM Tris,

2 mM EDTA, and 1.0% (v/v) NP-40). Lysates were IPed with either anti-Reelin (G10, Millipore), anti-APOER2 (Abcam, Cambridge, MA) anti-VLDLR (R&D Systems, Minneapolis, MN), or anti-APP (C9) and protein A and G agarose resin (Sigma, St. Louis, MO) overnight and washed 3X with 1% NP40 STEN buffer. Lysates, CM, and immunoprecipitations were electrophoresed on 10–20% Tricine or 4-12% Bis-Tris gels (Invitrogen, Carlsbad, CA) and transferred to nitrocellulose. Western blotting (WB) was performed with primary antibodies anti-APP (C9, 1:1,000; Selkoe lab), anti-APPsα (1736, 1:2,000; Selkoe lab), anti-rodent APP/APPsα (597,1:200; Immuno-biological Laboratories, Minneapolis, MN), anti-GAPDH (1:2,000; Millipore, Billerica, MA), anti-FLAG (M2; 1:1,000; Sigma, St. Louis, MO), anti-Lingo-1(1:1,000; Millipore, Billerica, MA), anti-β1 Integrin (1:1,000; Abcam, Cambrdige, MA), anti-F-spondin (1:1,000 ; Abcam, Cambrdige, MA), anti-Reelin (N-terminal, G10) (1:500, Millipore, Billerica, MA), anti-Reelin (mid-region, R4B) (1:1000, Developmental Studies Hybridoma Bank, Iowa City, IA) anti-Reelin (C-terminal) (1:1000, E5, Santa Cruz Biotechnology, Santa Cruz, CA), anti-Tau (1:2,000, Dako, Carpinteria, CA), anti-BACE1 (1:500, Millipore, Billerica, MA), anti-ADAM17 (1:500, Abcam, Cambridge, MA), each followed by IRDye800- or IRDye680-conjugated secondary antibodies (1:10,000; Rockland Immunochemicals, Gilbertsville, PA) and detection with the LICOR Odyssey detection system. For quantitative Western blots, Pancortin-3 (Rice et al., 2012), Reelin and F-spondin (R&D systems, Minneapolis, MN) recombinant proteins were utilized as standards.

APP processing assays in HEK293 cells

HEK293 cells were plated in 6 well plates at 1x10^6 cells/well and transiently transfected with cDNA of each candidate ligand or empty vector (as control) using Fugene HD

(Promega, Madison, WI). In the assay to examine effects on overexpressed APP, APP751 was co-transfected with the candidate ligand or empty vector. At 24 hr post-transfection, media (DMEM + 10% FBS) were replaced, and at 48 hr post-transfection, media were collected and centrifuged at 200 g for 5 min, and cells were lysed in 1% NP-40 STEN buffer. Human APPsα, APPsβ, Aβ40, and Aβ42 levels in the CM was quantified by multiplex ELISA kits (Meso Scale Discovery, Gaithersburg, MD) and normalized to holoAPP in the lysate (for the overexpressed APP assay) or normalized to total intracellular protein (for the endogenous APP assay) . For DAPT treatment of Lingo-1 transfected HEK293 cells, cells were treated for 24 hrs with 5 μM DAPT in DMSO. One-way ANOVA tests were performed with the Bonferroni correction for multiple comparisons.

APP processing assays in rat primary cortical cultures

Cortical neurons from E18 Sprague Dawley rats were plated in 6-well poly-D-lysine coated plates at 7.5 x 10^5 cells/well typically for 4 DIV (but but some experiments ranged for 2-12 DIV with similar effects). In our co-culture assay, The HEK293 stable cell lines expressing the ligand of interest were pelleted by centrifugation and then resuspended in neuronal medium. The HEK293 cells are then plated at 7.5 x 10^5 cells/well overlying the neurons for 18-24 hr. Medium is then changed 4 hrs later to remove any unattached HEK293 cells. In our CM assay, neurons were treated for 18-24 hr with CM from the HEK293 cell lines stably expressing the ligand of interest. CM was obtained from stable cell lines conditioned for 24 hr in serum-free optiMEM concentrated 10x with Amicon Ultra 10K MWCO centrifugal filters (Millipore) and diluted to a 1X solution in Neurobasal media. After the 18-24 hr period of CM treatment or co-

culture, CM was collected and centrifuged at 2000 rpm for 5 min. Cells were lysed in 1% NP-40 STEN. Endogenous rat neuronal APPsα was quantified by a rodent-specific ELISA kit (Immuno-biological Laboratories). APPsα was normalized to a neuronal-specific protein, Tau, by WB analysis in the co-culture assay and to total intracellular protein by BCA assay (Fisher) in the CM assay. One-way ANOVA tests were performed with the Bonferroni correction for multiple comparisons.

Results

Effects of candidate ligands on APPsα and APPsβ levels in HEK293 cells

Candidate APP ligands were first examined in a non-neuronal mammalian cell line overexpressing APP, because this had been done in nearly all of the initial reports of these particular candidate ligands (reviewed in Introduction). In this assay, HEK 293 cells were transiently co-transfected with one of the putative ligands and human APP751, and the medium (DMEM with 10% FBS) was changed 24 hr after transfection. At 48 hr, the conditioned media (CM) were collected, and cells were lysed. APPsα and APPsβ levels in the CM were measured by a sensitive and highly reproducible MSD multiplex ELISA. APPsα and APPsβ levels were normalized to holoAPP, which was measured by WB of the respective cell lysates. Using this assay, F-spondin and CNTN2-Fc did not significantly modulate APPsα or APPsβ levels (Fig 3.1A-C). Expression of Reelin resulted in the greatest change of APPsα and APPsβ levels, with a decrease of 54.9 ± 3.5% ($p<0.001$) and 25.4 ± 4.2% ($p<0.001$), respectively (Fig 3.1A-C). Expression of Lingo-1 also significantly reduced levels of APPsα by 34.1 ± 4.2% ($p<0.001$) and

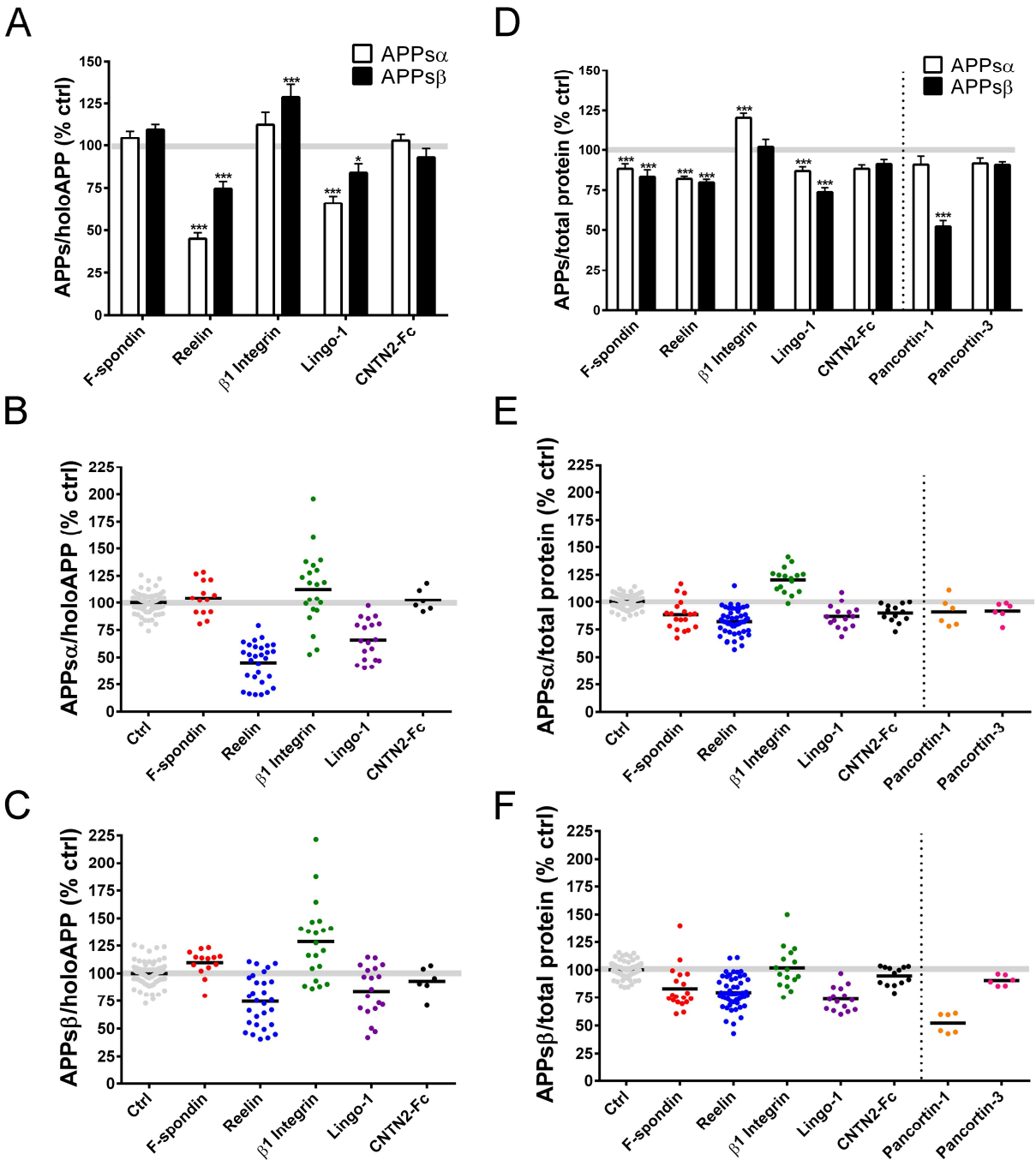

Figure 3.1: Effects of candidate ligands on APPsα and APPsβ levels in HEK293 cells

Figure 3.1: Effects of candidate ligands on APPsα and APPsβ levels in HEK293 cells (continued)

(A-C) HEK293 cells were co-transfected with APP751 (human, wild-type) and candidate ligands or empty vector (as control) . APPsα and APPsβ levels were quantified by ELISA and normalized to holoAPP by Western blot and shown as a percentage of control. **(D-F)** HEK293 cells (expressing only endogenous human APP) were transfected with candidate ligands or empty vector (as control) and APPsα and APPsβ levels were quantified by ELISA and normalized to total intracellular protein and shown as a percentage of control. **(A,D)** Bar graph showing average APPsα and APPsβ levels of all experiments. Scatter plots showing APPsα **(B,E)** and APPsβ **(C,F)** levels for each replicate of each experiment. Error bars represent

APPsβ by 16.1 ± 5.3% ($p<0.05$) (Fig 3.1A-C). β1 Integrin increased APPsβ levels by 28.6% ± 7.5 ($p<0.001$) and did not significantly modulate APPsα levels (Fig 3.1A-C).

Of note, these mean changes in soluble APP shedding were all determined by ELISAs on numerous individual samples performed over multiple experimental days (Fig. 3.1B, C). Reelin produced the most robust and consistent effect in this assay (see scatterplots in Fig. 3.1B-C). Across all replicates, Reelin overexpression resulted in a 25% or greater decrease in APPsα (Fig 3.1B). Transfection of β1 Integrin resulted in the highest variability across experiments, as APPsα and APPsβ levels were enhanced in some experiments but reduced in others (Figs 3.1B-C). These variable effects of β1 Integrin on APPsα and APPsβ shedding appeared to be due to differences in holoAPP expression levels. In this overexpression assay system, co-transfection of β1 Integrin with APP751 led to much greater percent changes in holoAPP levels than did co-transfection of the other 4 candidates (Fig 3.2). Even after normalization of the APPsα and APPsβ levels to holoAPP levels in each experiment, the effects of β1 Integrin on APPsα secretion were significantly correlated ($R^2 = .44$, $p<0.01$) with differences in holoAPP expression (Fig 3.2). For example, when holoAPP levels were relatively high in the β1 Integrin co-transfectants compared to vector transfected controls, then relative APPsα/holoAPP levels were also high. In contrast, we observed no significant correlations between APPsα/holoAPP and changes in holoAPP expression levels for F-spondin, Reelin and Lingo-1 (Fig. 3.2).

Proteolytic processing of overexpressed APP can be quite different than that of endogenous APP. For example, we observed that the APPsα/APPsβ ratio in CM was 6.6 ± 0.7 in HEK293 cells expressing just endogenous human APP but was a remarkable 78.4 ± 8.8 in

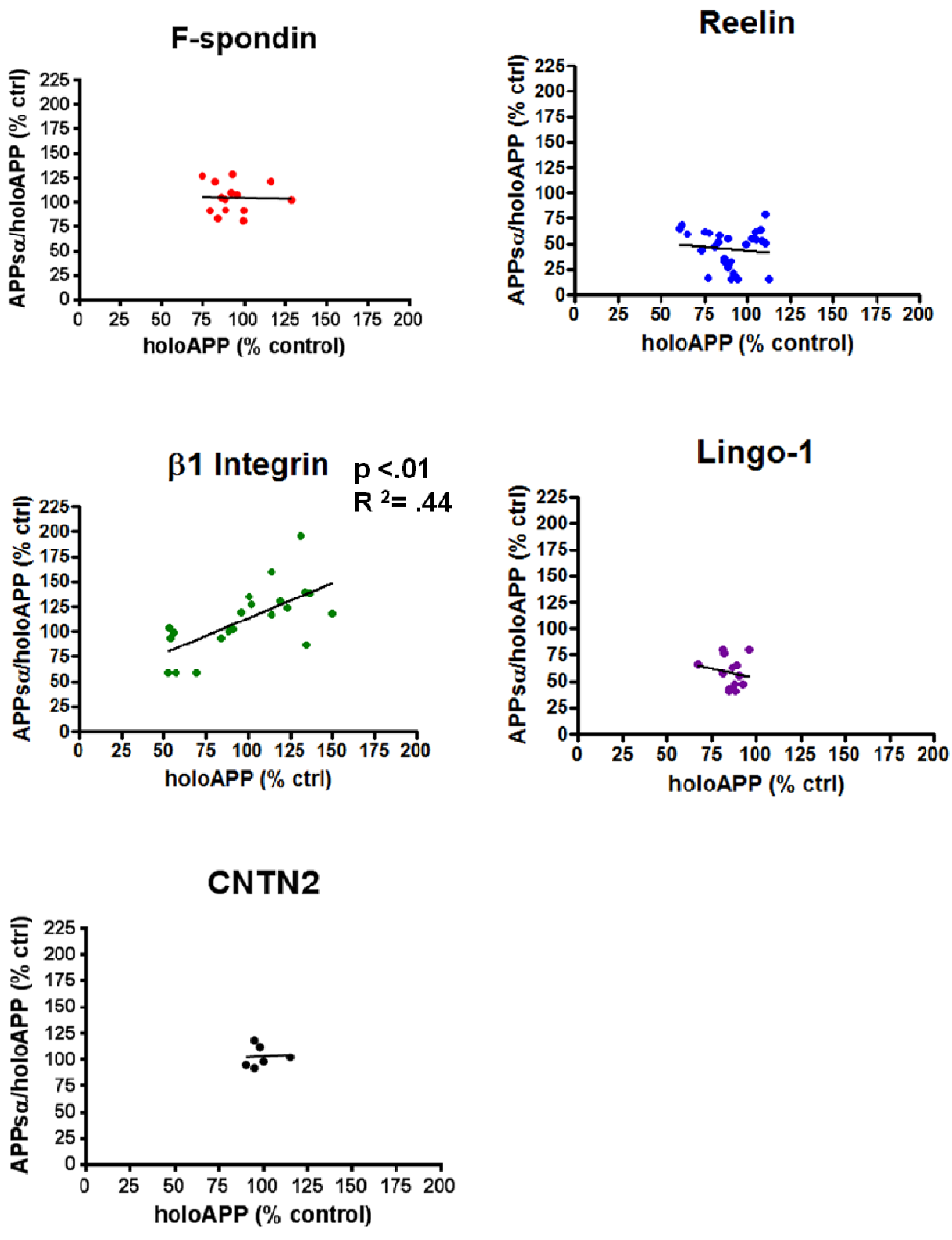

Figure 3.2: Only β1 Integrin shows a correlation between holoAPP and APPsα/holoAPP

Figure 3.2: Only β1 Integrin shows a correlation between holoAPP and APPsα/holoAPP (continued)

For co-transfection of candidate ligands with APP751 (human, wild-type) with HEK293 cells,the levels of percent change in APPsα/holoAPP was graphed as a function of holoAPP for each replicate. A regression correlation was performed, and p values represent statistical significanceof the slope deviating from 0.

HEK293 cells overexpressing human APP (Fig 3.3). This striking many-fold difference highlights the non-physiological nature of the procesing of overexpressed APP, and we therefore developed assays to investigate the effects of candidate ligands on proteolytic processing of endogenous APP, something that has not typically been reported for potential APP ligands. These experiments were initially performed in HEK293 cells using the same methods as in the above assay with the exception that no co-transfection of APP occurred. WBs of cellular lysates confirmed that the transfection of the candidate ligands did not alter endogenous holoAPP levels (Fig 3.4); therefore, endogenous APPsα and APPsβ levels in the CM were normalized to the more quantitative measure of total intracellular protein concentration in the lysate. Using this assay, we found that the expression of each candidate ligand resulted in a small but significant change in APPs level. APPsα and APPsβ levels were significantly reduced by the expression of F-spondin (APPsα: 11.7 ± 3.1%; $p<0.001$; APPsβ: 16.7 ± 4.3%; $p<0.001$), Reelin (APPsα: 18.0 ± 1.6%; $p<0.001$; APPsβ: 20.2 ± 2.0%; $p<0.001$), and Lingo-1 (APPsα: 13.1 ± 2.7%; $p<0.001$; APPsβ: 26.2 ± 2.8%; $p<0.001$) (Fig 3.1D-F). Expression of β1 Integrin significantly increased APPsα by 20.4 ± 2.9% ($p<0.001$) but did not significantly change APPsβ levels (Fig 3.1D). CNTN2 did not significantly affect APPsα or APPsβ levels. Thus, while Reelin and Lingo-1 strongly inhibited α- and β- secretase cleavage of overexpressed APP in HEK293 cells (Fig. 3.1A), cleavage of endogenous APP was more weakly – but still significantly -- inhibited by Reelin and Lingo-1 (Fig. 3.1D). As a comparative control in this same assay, we repeated experiments on the proteins Pancortin-1 and Pancortin-3 that we recently described as APP ectodomain ligands (Rice et al, 2012). In agreement with our previous report, Pancortin-1 significantly reduced β-secretase cleavage (47.9 ± 3.6%; $p<0.001$) without affecting α-secretase cleavage of

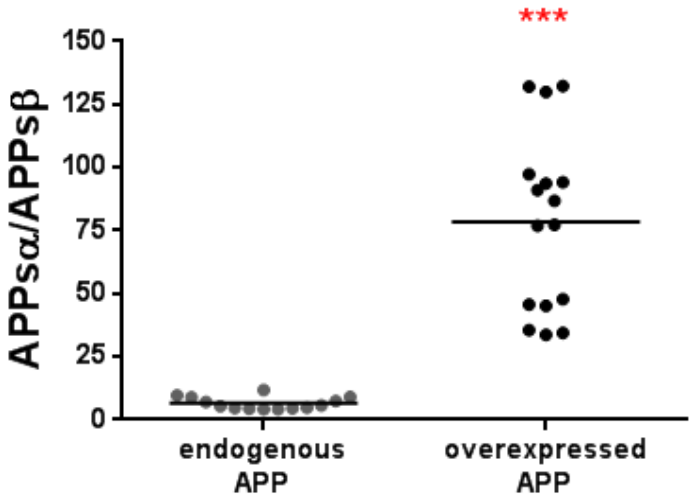

Figure 3.3 APPsα/APPsβ is dramatically higher and more variable with overexpressed relative to endogenous APP.

The ratio of APPsα to APPsβ is shown for HEK293 cells with endogenous APP (human) or HEK293 cells transiently transfected with APP751 (human, wild-type).

endogenous APP, whereas the isoform Pancortin-3 had no significant effects on either α- or β-secretase cleavage. The effect of Pancortin-1 on APPsβ was more robust and less variable than any of the other candidate ligands we tested in this endogenous APP cleavage assay in 293 cells (Fig 3.1E-F).

Western blots (WB) from representative experiments are shown for the HEK293 cell assays in which APP was either overexpressed (Fig 3.4A) or endogenous (Fig 3.4B), demonstrating the expression levels of both holoAPP and the candidate ligands. Expression levels were similar among the various candidate ligands, with an estimate of 5-10 μg/mg of cell lysate or 5-10 mg/mL secreted into the CM for those tested by quantitative Western blot (Fig 3.5). In the initial experiments where APP was overexpressed, CTFs and APPsα could be readily detected by WB, and these paralleled the changes in APPs by ELISA (Fig 3.4A, see e.g., Reelin and Lingo-1). Levels of ADAM17 (an α-secretase for APP) and BACE-1 (β-site APP cleaving enzyme-1, or β-secretase) were not changed by the expression of the candidate ligands (Fig 3.4B), suggesting that any effects on APP processing we observed were not due to changes in the levels of the secretases that cleave APP.

In both of these HEK293 cell assays (Fig. 3.1), we utilized DMEM media with 10% fetal bovine serum (FBS). Previous reports of these and other candidate APP ligands have used a variety of medium conditions, including medium with serum, serum-free (SF) medium, and SF medium supplemented with bovine serum albumin (BSA) as a carrier protein. This technical variability could help explain some of the different results obtained by different labs. We found that medium supplemented with either FBS or BSA enhanced the recovery and subsequent

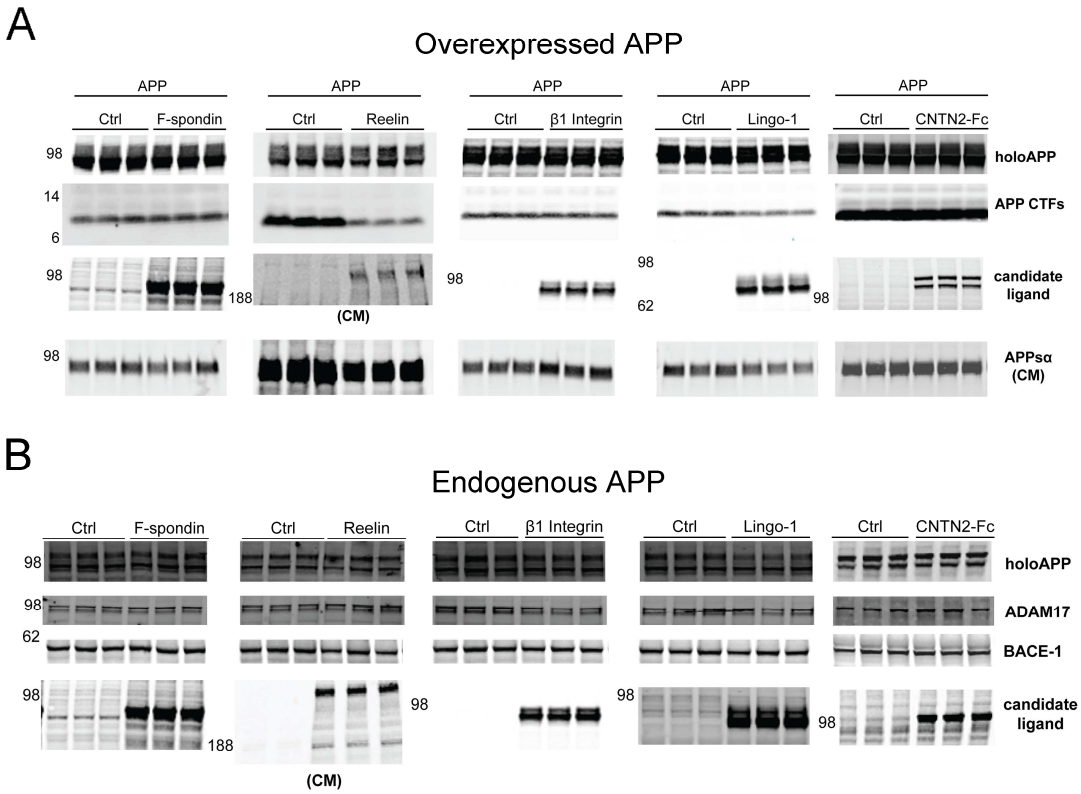

Figure 3.4 Representative Western blots of APP shedding assays with HEK293 cells

(A) Western blot of lysates (and CM where noted) showing expression levels of holoAPP, APP CTF, candidate ligands, and APPsα in a representative experiment with co-transfection of candidate ligands and APP751 into HEK293 cells. **(B)** Western blot of lysates (and CM where noted) showing expression levels of holoAPP, secretases, and candidate ligands from a representative experiment with transfection of candidate ligands into HEK293 cells with endogenous APP.

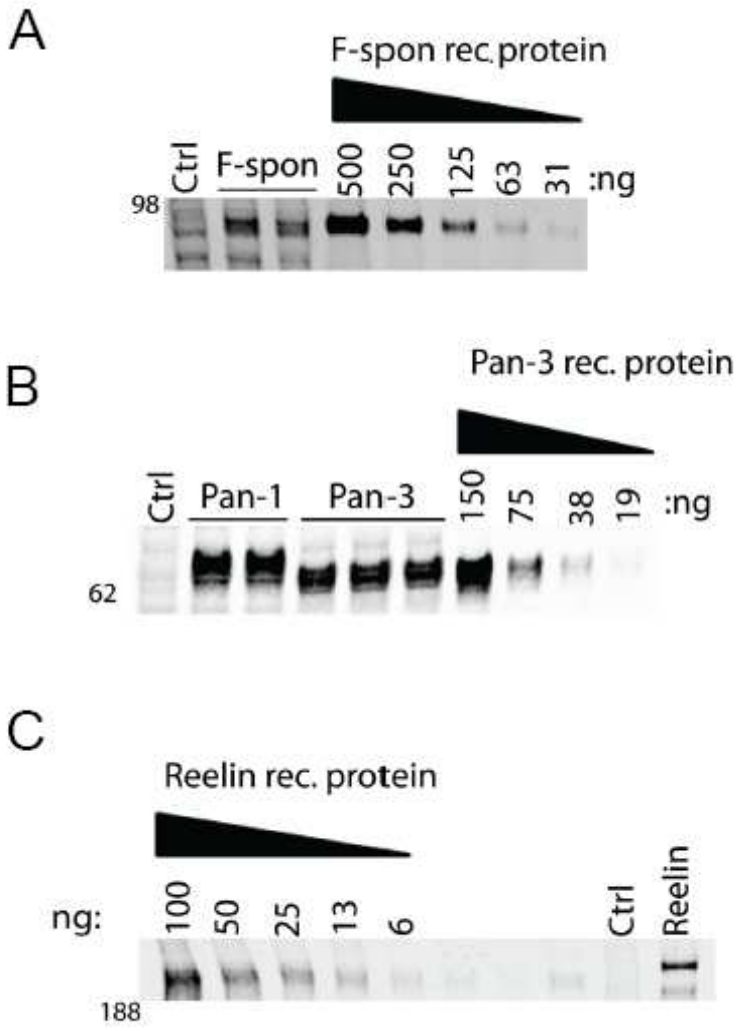

Figure 3.5 Quantitative Western blot analysis of candidate ligand expression levels

Relative levels of (A) F-spondin and (B) Pancortins expressed in the lysates and (C) Reelin secreted in the CM of HEK293 cells were determined by quantitative Western blot with recombinant proteins for each used as standards. 20 µg of cell lysates (A,B) or 10 uL of CM (C)were loaded for quantification.

detection of APPsα in the CM by over 3-fold (Fig 3.6A). Moreover, transfected cells conditioned in media with serum were healthier than those with only BSA. Therefore, we chose to condition our cells in DMEM+10% FBS for all of the studies reported above, as this allows the best health of the transfected cells and the best recovery of APPsα. Importantly, we showed that the effect of Reelin on endogenous APPsα levels was similar across these three media conditions (Fig 3.6B).

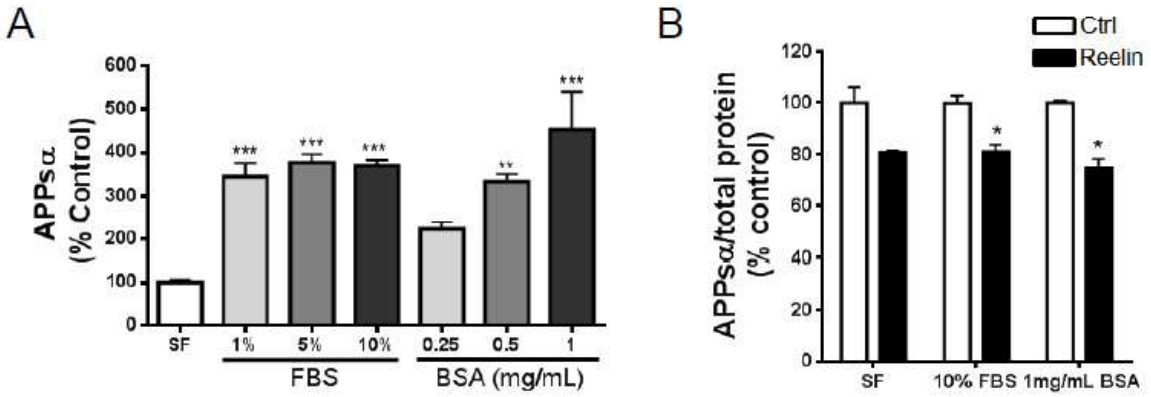

Figure 3.6 FBS and BSA increase the detection of APPsα

(A) HEK293-APP695 stable cell lines were cultured in serum-free media (SF), media supplemented with 1%, 5%, or 10% fetal bovine serum (FBS) or 0.25,0 .5 or 1.0 mg/mL bovine serum albumin (BSA). (B) HEK293 cells with endogenous APP were transfected with Reelin and cultured in SF media, media with 10% FBS, or SF media supplemented with 1mg/mL BSA.

Effects of candidate APP ligands on APPsα levels in primary cortical neuronal cultures

The most physiologically relevant culture system for analyzing putative ligands that regulate processing of APP in the central nervous system would assay the effects on endogenous APP in primary neurons with the ligands presented in trans. To this end, we developed both co-culture and conditioned medium (CM) assays in untransfected primary neuronal cultures (Fig. 3.7A). In both assays, E18 rat primary cortical neurons were utilized as the reporter cell. In our co-culture assay, stable HEK293 cells expressing the ligands of interest were co-cultured overlying the neurons for 18-24 hr (Fig. 3.7A). Alternatively, in our CM assay, neurons were treated with the CM of stably transfected HEK293 cells expressing the ligand of interest (Fig 3.7A). Endogenous APPsα produced from the neurons (but not from the human HEK293 cells) was detected by a rodent-specific APPsα ELISA. APPsα was normalized to a neuron-specific marker (Tau) in the lysate of our co-culture assay (in order to normalize to only the neuronal reporter cells but not the HEK293 ligand source) or to total intracellular protein in our CM assay. As an important negative control, we observed no significant difference in APPsα levels secreted from neurons cultured alone compared to those co-cultured with control (untransfected) HEK293 cells at the optimized densities of both cell types employed here (Fig 3.7B, first two bars). In both assays, an expected increase in neuronal APPsα could be detected in the CM upon treatment with PMA (phorbol-12-myristate-13-acetate) as a positive control (Fig 3.7B-C) (Buxbaum et al, 1998; Lammich et al, 1999). Further, human APPsα from the HEK293 cells represents a negligible percentage of the total APPsα detected in both the co-culture and CM assays, confirming the specificity of our rodent-specific ELISA (Figs 3.7B-C).

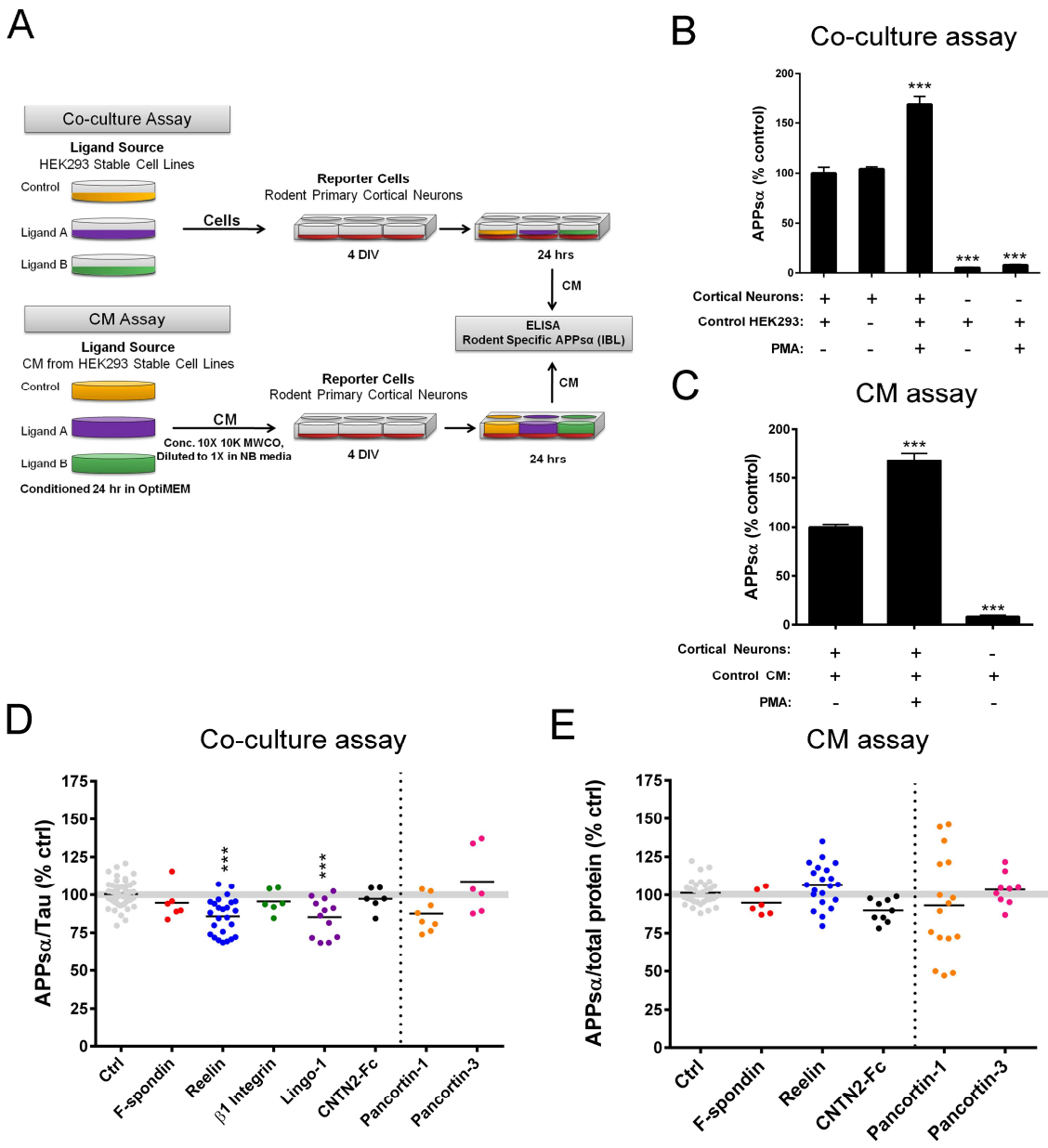

Figure 3.7 Effects of candidate ligands on APPsα levels in primary cortical cultures

(A) Schematic of methods used for co-culture and CM assays. **(B-C)** Positive controls (PMA treatment) and negative controls (neurons and HEK293 cells alone) for the co-culture **(B)** and CM **(C)** assays. **(D)** ELISA quantification of APPsα (endogenous, rodent) secreted from cortical neurons co-cultured with HEK293 cells stably expressing ligand of interest. **(E)** ELISA quantification of APPsα (endogenous, rodent) secreted from cortical neurons treated with CM from HEK293 cells expressing ligand of interest. Error bars represent s.e.m.; * p<.05

Reelin and Lingo-1 (which showed the most consistent effects in reducing APPsα in the HEK293 cell assays) significantly reduced neuronal APPsα in the co-culture assay (Fig 3.7D-E). Reelin reduced APPsα by 14.3 ± 2.4% ($p<0.001$), and Lingo-1 reduced APPsα by 14.7 ± 3.6% ($p<0.001$). F-spondin, β1 Integrin, and CNTN2-Fc did not significantly modulate APPsα levels in the neuronal co-culture assay (Fig 3.7D). Only those proteins that are secreted could be tested in the CM assay. As in the co-culture assay, treatment of neurons with F-spondin and CNTN2-Fc CM had no effect on APPsα levels (Fig 3.7E). In contrast to the neuronal co-culture assay and the two HEK293 assays, Reelin CM had no effect on neuronal APPsα levels (Fig 3.7E). For comparison, we performed experiments with Pancortin-1 and Pancortin-3 in both of these assays. We had previously reported a decrease in endogenous APPsβ but not APPsα levels by expressing Pancortin-1 in HEK293 cells. Here, we were only able to perform a rodent-specific ELISA for APPsα, since rodent-specific antibodies for APPsβ are not available, and we confirmed that there was no significant effect of either Pancortin isoform on APPsα secretion in neurons (Fig 3.7D,E).

Western blots from representative experiments are shown for both the co-culture (Fig 3.8A) and CM (Fig 3.8B) assays in rodent cortical neuronal cultures, demonstrating the expression levels of the candidate ligands and endogenous rat APP. Expression of endogenous holoAPP in the neuronal lysates was not affected by the candidate ligands in either assay (Fig 3.8A,B). Expression of Tau, which we used as a neuronal-specific protein for normalization, was relatively consistent across conditions (Fig 3.8A).

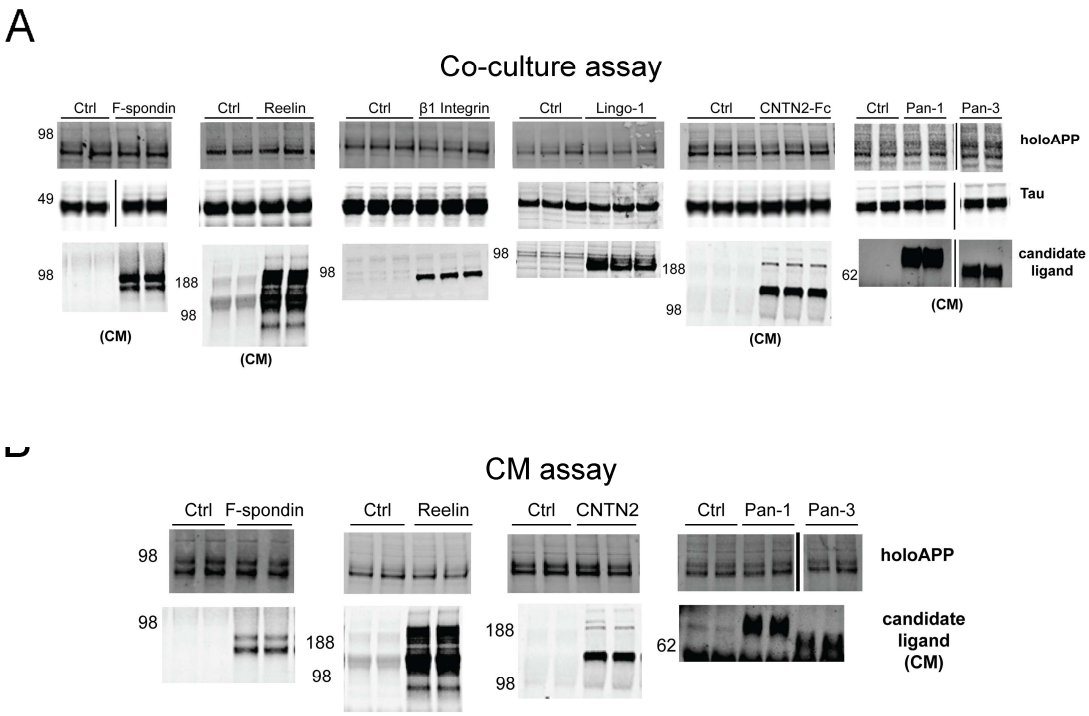

Figure 3.8 Representative Western blots of APP shedding assays with rat primary cortical cultures

(A) Western blot of lysates (and CM where noted) showing expression levels of holoAPP, Tau, and candidate ligands in a representative experiment with co-culture of neurons with HEK293 cells expressing putative ligands. **(B)** Western blot of lysates (and CM where noted) showing expression levels of holoAPP and candidate ligands from a representative experiment with neurons treated with CM from HEK293 cells expressing putative ligands.

Figure 3.9 Summary of candidate ligands tested in multiple APP shedding assays.

			F-spondin		Reelin		β1 Integrin		Lingo-1		CNTN2-Fc		Pancortin-1		Pancortin-3	
cell type	ligand source	APP	APPsα	APPsβ	APPsα	APPsβ	APPsα	APPsβ	APPsα	APPsβ	APPsα	APPsβ	APPsα	APPsβ	APPsα	APPsβ
HEK293	transient transfection	transient transfection	=	=	↓↓↓	↓↓	=	↑↑	↓↓	↓	=	=	–	–	–	–
HEK293	transient transfection	endogenous	↓	↓	↓	↓	↑	=	↓	↓↓	=	=	=	↓↓↓	=	=
primary rat cortical neurons	coculture with HEK293 stables	endogenous	=	–	↓	–	=	–	↓	–	=	–	=	–	=	–
primary rat cortical neurons	CM from HEK293 stables	endogenous	=	–	=	–	–	–	–	–	=	–	=	–	=	–

Figure 3.9 Summary of candidate ligands tested in multiple APP shedding assays. (continued)

The magnitude of statistically significant changes ($p < .05$) in APPsα or APPsβ are represented by arrows. ↑ or ↓ < 25% change relative to control; ↑↑ or ↓↓ = 25-50% change; ↑↑↑ or ↓↓↓ > 50% change. An equals sign (=) represents no significance difference. Gray boxes represent conditions not determined.

Addressing discrepancies in the effects of Reelin and Lingo-1 on APP cleavage

After testing these candidate ligands in assays on both overexpressed and endogenous APP and in both neuronal and non-neuronal cells, Reelin, Lingo-1 and Pancortin-1 emerged as the candidate APP ligands with the most consistent and quantitatively significant effects on the α- and/or β-secretase cleavages of APP (Fig. 3.9). However, the effects of Lingo-1 and Reelin in our assays were not identical to previous reports. We have already characterized in detail the interaction of the Pancortins with APP in a recent publication (Rice et al, 2012). Here, we attempt to reconcile experimentally the discrepancy between our data and previous reports for Reelin and Lingo-1.

For Lingo-1 in our HEK293 assay with overexpressed APP, the variability in the magnitude of reduction of APPsα and APPsβ (normalized to holoAPP) across experiments appears to be due to the expression levels of Lingo-1. The degree of reduction in APPsα and APPsβ was directly and significantly correlated with protein levels of Lingo-1 (APPsα: R^2 = .69, p<.001; APPsβ: R^2 = .76, p<.001) (Fig. 3.10A-B). The reduction of APPsβ by Lingo-1 was in contrast to a previous study (Bai et al, 2008) in which Lingo-1 enhanced β-secretase cleavage of APP. This discrepancy could be due to differences in the processing of wild-type APP, which we studied, and APP with the Swedish AD mutation that Bai et al (Bai et al, 2008) studied. Therefore, we tested the effects of Lingo-1 in HEK293 cells transfected with APP695 bearing the Swedish mutation (APPswe). Co-transfection of Lingo-1 with APPswe significantly reduced APPsα but, unlike with wild-type APP, had variable effects on APPsβ. Lingo-1 caused enhanced APPsβ in some experiments and reduced APPsβ levels in others and overall had no significant

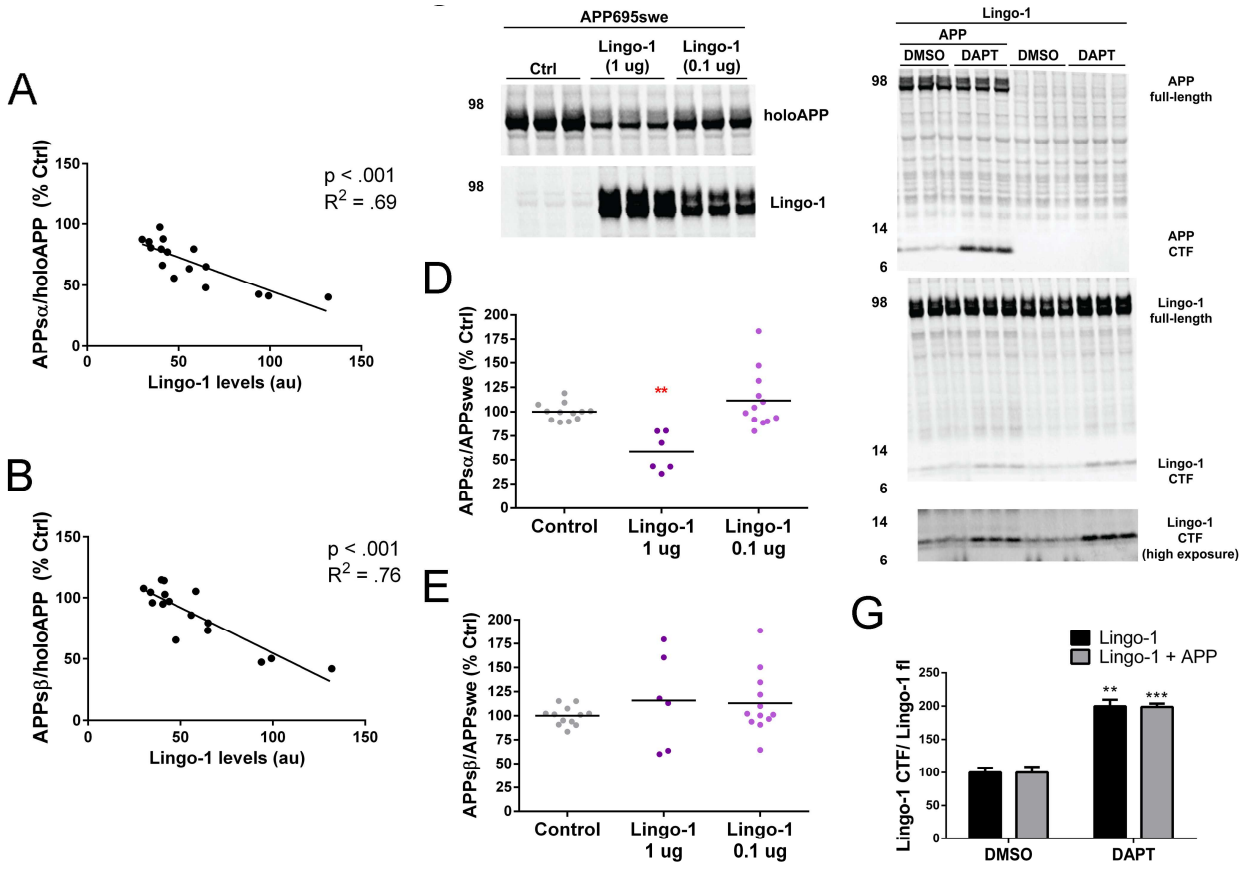

Figure 3.10 Biochemical analysis of the interaction of Lingo-1 with APP.

Figure 3.10 Biochemical analysis of the interaction of Lingo-1 with APP. (continued)

(A-B) For co-transfection of Lingo-1 and APP751 (human, wild-type) into HEK293 cells, the percent change in APPsα/holoAPP **(A)** or APPsβ/holoAPP **(B)** was graphed as a function of Lingo-1 expression. A regression correlation was performed, and p values represent statistical significance of the slope deviating from 0. **(C-E)** HEK293 cells were transfected with APP695-swedish (human) and either vector only (control) or Lingo-1 (with both 1.0 µg and 0 .1 µg of DNA). **(C)** Western blot of lysates showing expression levels of holoAPP and Lingo-1. Quantification of APPsα **(D)** APPsβ **(E)** for each replicate of each experiment shown with scatterplots. **(F-G)** HEK293were transfected with Lingo-1 or Lingo-1 plus APP751 (human, wild-type) and treated for 24 hrs with DAPT or DMSO (as control). **(F)** Western blot of lysates showing expression levels of holoAPP, APP CTF, Lingo-1 (apparent full-length and CTF). **(G)** Quantification of Lingo-1 CTF/full-length Lingo-1 with and without expression of APP. **p<.01, ***p<.001

effect on APPsβ (Fig 3.10C-D). However, we noticed that co-transfection of the standard 1 µg of Lingo-1 cDNA with APPswe cDNA reduced APPswe expression. Therefore, we tested 0.1 µg of Lingo-1 cDNA in which APPswe expression was less affected, but Lingo-1 still had variable effects on APPsα and APPsβ, with no overall significant effect on either (Fig 3.10C, E). In our studies of Lingo-1, we also uncovered evidence of the γ-secretase-dependent intramembrane cleavage of Lingo-1. Upon transfection of Lingo-1 into HEK293 cells, we detected a ~10 kDa fragment of Lingo-1 with a C-terminal Lingo-1 antibody, and the cellular levels of this CTF were enhanced 2-fold when the cells were treated with a γ-secretase inhibitor (DAPT) (Fig 3.10F-G). These data strongly suggest that Lingo-1 is processed by γ-secretase via the regulated intramembranous proteolysis mechanism, something which was not previously known. Overexpression of APP did not alter the production of the Lingo-1 CTF (Fig 3.10F-G).

Reelin was previously reported to enhance APPsα and CTF and reduce Aβ levels (Hoe et al, 2009; Hoe et al, 2006), whereas we found a reduction of APPsα and APPsβ levels by Reelin. First, we examined CTF and Aβ levels. Upon co-transfection of APP with Reelin in HEK293 cells, APP CTFs and Aβ40 and Aβ42 could be readily detected. Expression of Reelin not only decreased APPsα and APPsβ as documented above, but it also substantially reduced levels of the APP CTF, Aβ40, and Aβ42 (Figs. 3.4 and 3.11A). Next, we investigated whether the reduction in APPsα and APPsβ by Reelin expression was dose-dependent, or if differences in expression levels of Reelin might explain the conflicting results. Increasing concentrations of Reelin cDNA were transfected, leading to rising expression of Reelin secreted into the CM (Fig 3.11B) accompanied by a dose-dependent decrease in both APPsα and APPsβ (Fig 3.11C), consistent with our earlier Reelin results (Fig. 3.1A and B). Finally, the effect of Reelin on APPsα

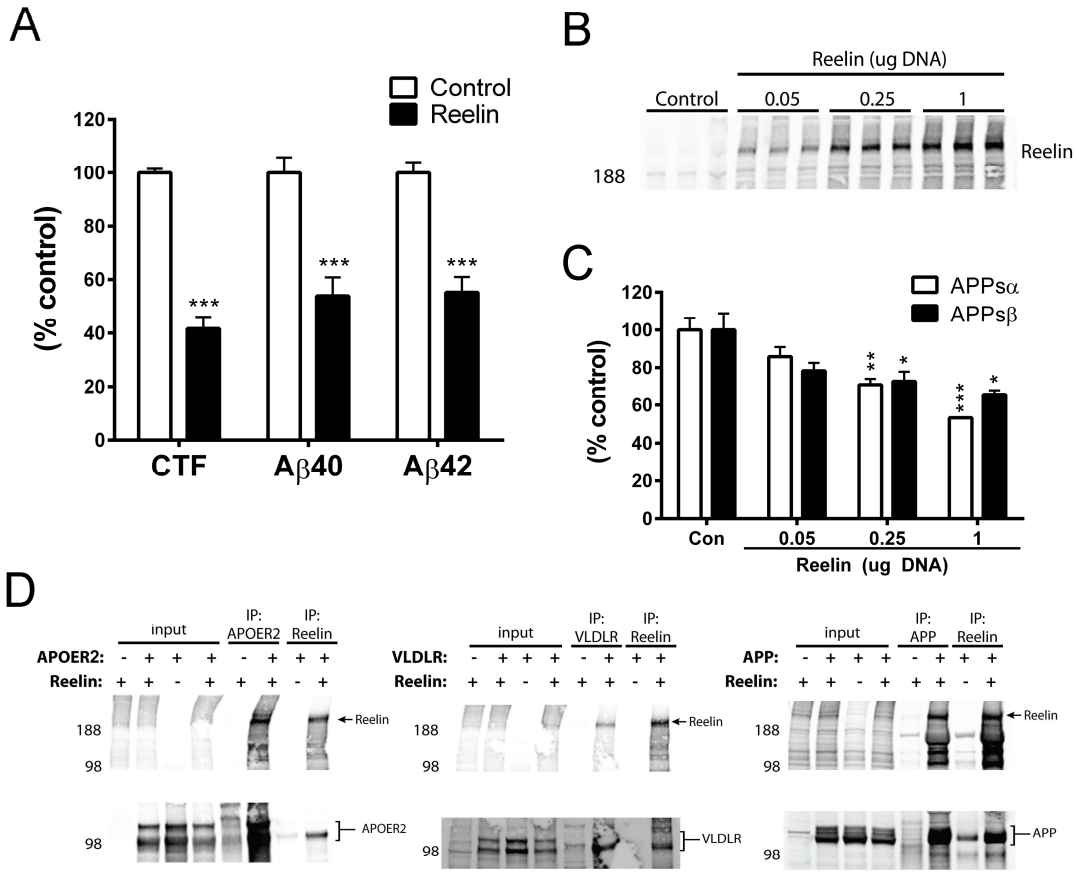

Figure 3.11 Biochemical analysis of the interaction of Reelin with APP.

(A) Quantification of Aβ40, and Aβ42 (by ELISA) and CTF (by WB) in HEK293 assay with over-expression of APP751 (human, wild-type). **(B)** Reelin expression in CM of HEK293 cells co-transfected with APP751 (human, wild-type) and increased concentrations of Reelin cDNA. **(C)** Quantification of APPsα and APPsβ levels in response to increasing Reelin expression. **(D)** HEK293 cells were transfected with listed combinations of Reelin, APP, APOER2, and VLDLR, and co-IPs were performed for Reelin or else APP, APOER2, or VLDLR. Error bars represent s.e.m.; * p<.05, **p<.01, ***p<.001

was investigated according to the methods in which Reelin was previously reported to enhance APPsα levels (Hoe et al, 2009; Hoe et al, 2006). Here, Reelin CM was applied to COS7 cells transfected with APP751. In contrast to this prior study, we found no effect of Reelin when utilizing this method (Fig 3.12).

Biochemical analysis of the interaction of Reelin with APP

Next, we sought to confirm whether Reelin and APP could physically interact. Reelin and APP were co-transfected into HEK293 cells, and lysates were immunoprecipitated (IP) for either Reelin or APP. Indeed, Reelin co-IPed with APP, and in the reverse direction, APP co-IPed with Reelin (Fig. 3.11D, right panel). As a negative control, IP with the APP antibody (C9) failed to co-IP Reelin in the absence of APP overexpression. IP with the Reelin antibody (G10) did IP detectable levels of APP in the absence of Reelin overexpression; however, overexpressing Reelin greatly enhanced the co-IP of APP with Reelin above this background endogenous level (Fig 3.11D). Importantly, we found that the co-IP of Reelin and APP was quantitatively comparable to the co-IP of Reelin with its canonical receptors, APOER2 and VLDLR (D'Arcangelo et al, 1999; Hiesberger et al, 1999; Trommsdorff et al, 1999) (Fig 3.11D).

Reelin undergoes proteolytic cleavages in primary neurons at both its C-terminal and N-terminal ends to generate five fragments (Fig 3.13A) (Jossin et al, 2007; Jossin et al, 2004; Lambert de Rouvroit et al, 1999). To determine which physiological fragments of Reelin may be sufficient for the inhibition of α-secretase cleavage of APP, HEK293 cells were co-transfected with APP751 and cDNAs for full-length Reelin or else each of the 5 known Reelin fragments. Reelin antibodies with epitopes towards the different regions of Reelin (G10, R4B, E5) (Fig

3.13A) were used to detect all of the Reelin fragments by Western blot (Fig 3.13B). Each fragment of Reelin significantly reduced α-secretase cleavage of APP compared to control (Fig 3.13C). However, expression of the fragments containing the N-terminal region of Reelin (N-R6 and N-R2) resulted in the greatest reduction in APPsα, and this lowering was not significantly different than that seen from full-length Reelin (Fig 3.13C). Conversely, expression of Reelin fragments containing the C-terminal region but lacking the N-terminal region (R3-8 and R7-8) led to relatively higher levels of APPsα, compared to the effect of full-length Reelin (Fig 3.13C). These differential effects due not appear to be due to differential expression levels. When the levels of each transfected Reelin fragment detected with single antibodies were compared to full-length Reelin, their expression levels were relatively similar to one another, with only R7-8 having higher expression levels but still less effect on APP shedding (Fig 3.13B). Thus, while each physiological proteolytic fragment of Reelin can inhibit α-secretase cleavage of APP to some extent, the N-terminal region of Reelin is the most active.

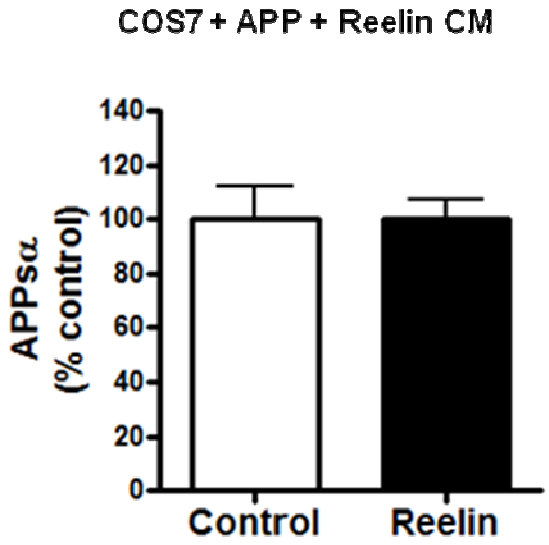

Figure 3.12 Effect of Reelin CM treatment on COS7 cells overexpressing APP751

COS7 cells transfected with APP were treated with CM from either control or Reelin stable cell lines, and APPsα levels were quantified by ELISA.

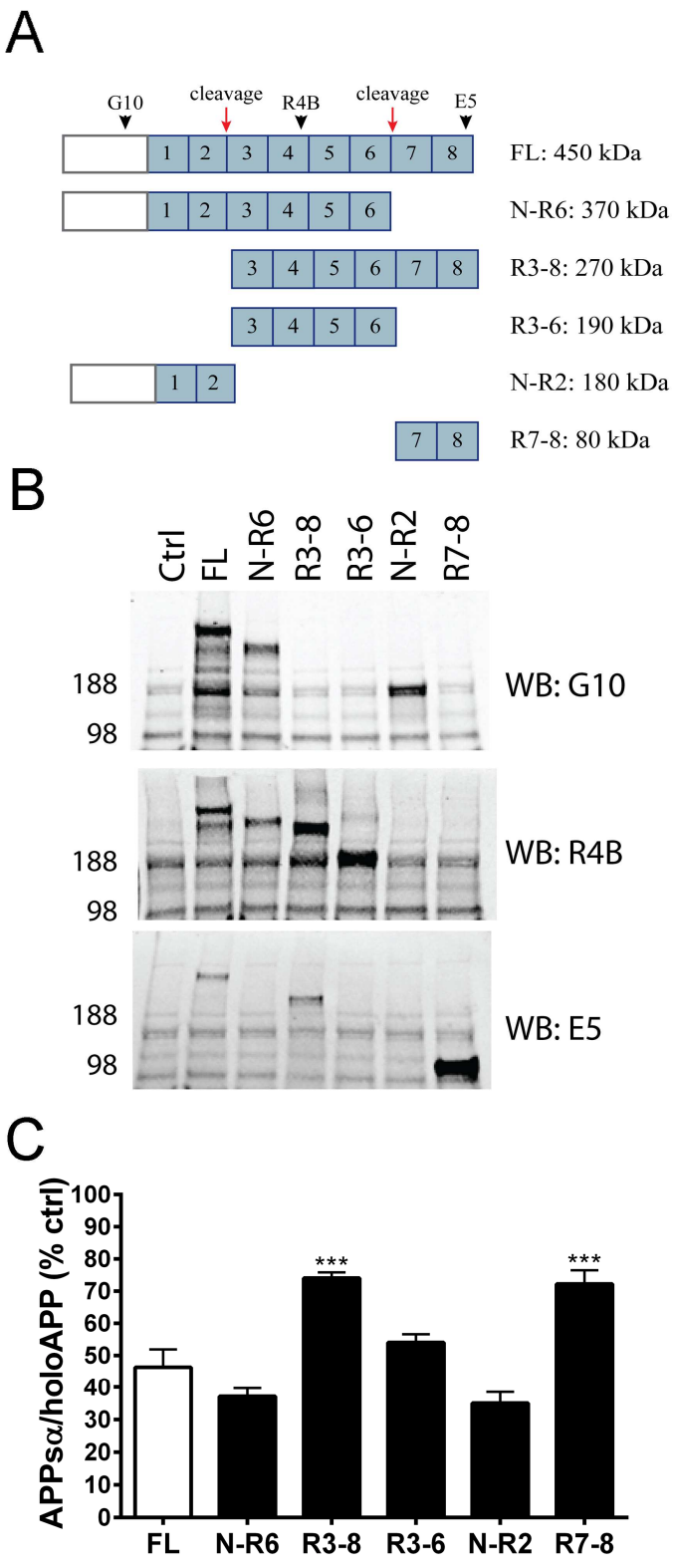

Figure 3.13 Effects of Reelin fragments on APPsα in HEK293 cells.

Figure 3.13 Effects of Reelin fragments on APPsα in HEK293 cells. (continued)

(A) Schematic of Reelin fragments generated from proteolytic processing. Reelin repeat domains are numbered in blue. Red arrows represent cleavage sites. Black arrowheads represent antibody epitopes. **(B)** Western blots of cell lysates showing expression of Reelin fragments transfected into HEK293 cells. **(C)** ELISA quantification of APPsα levels in HEK293 cells co-transfected with APP751 (human, wild-type) and either full-length Reelin or individual Reelin fragments. Error bars represent s.e.m.; ***p<.001, relative to full-length Reelin (FL)

Discussion

Novel and systematic approaches to analyze the effects of candidate ligands on APP processing

Several extracellular and membrane-bound proteins have been proposed as candidate ligands that may modulate proteolytic processing of the ubiquitously expressed APP polypeptide. However, these candidates have not been validated by multiple laboratories and have often been examined solely with overexpressed APP and with one or two assay systems. In an effort to clarify a role for one or more of the reported ligands in regulating the processing of APP, we systematically and rigorously investigated the ability of these candidates to modulate α- and β- secretase cleavage of APP. In contrast to virtually all prior studies, we used multiplex ELISA-based assays to obtain quantitative measures of both APPsα and APPsβ, as opposed to solely relying on Western blotting. Further, many of the previous studies show data from a single "representative" experiment. We chose to show our data by scatter-plot analysis of all experiments, and we found that for most putative ligands, a single experiment could not adequately represent the complete data set of the range of effects on APP cleavage and would thus be misleading. Instead, we report a comprehensive quantification of data points across all experiments to capture the inherent biological variability of the effects of each ligand, as well as the technical variability for different assay types. Furthermore, the quantification of secreted APPsα/β we used provides a direct measure of the α- and β-secretase cleavages, as opposed to measuring only CTFα/β, the levels of which can be further complicated by the degree of γ-secretase activity.

Another important aspect to consider when performing assays to accurately measure APPsα/β generation in the CM is the appropriate normalization. Changes in cellular holoAPP levels can change APPsα and APPsβ levels independent of any effects of a ligand on α- and β-secretase cleavage *per se*. Because co-transfection of APP concurrent with the candidate ligands could lead to differences in APP levels due to technical rather than biological reasons, we normalized data in which APP is overexpressed to holoAPP levels in the lysates of the same cultures. However, because normalizing to holoAPP, which as an end-point measurement in lysates may not fully correct for variations in the levels of APPs that accumulate in the media, we also checked for correlations between the holoAPP cellular level and the APPsα/holoAPP ratio (Fig 3.2). For assays measuring cleavage of endogenous APP, we observed no detectable differences in holoAPP in the lysates by Western blot and therefore normalized to the more quantitative measure of total intracellular protein concentration in the lysate. For the co-cultures of neurons with HEK293 cells, we normalized to a neuron-specific marker (Tau) in the lysate, in order to normalize only to the neuronal reporter cells but not the HEK293 ligand source.

As a result of attention to these various technical factors and controls, a side-by-side comparison of candidate ligands across multiple assays is presented here for the first time. We initially used an assay similar to the original reports for each of these ligands, i.e., with non-neuronal immortalized mammalian cells overexpressing APP, to enable direct comparisons to those previous reports. We found that co-transfection of APP with certain candidate ligands can lead to the most dramatic effects on APPsα/β levels, perhaps due to a wider dynamic range inherent to the overexpression assay or to artifacts from supraphysiological levels of APP or

non-biologically relevant changes in APP levels. For example, we found evidence that despite normalization to holoAPP, the effects of β1 Integrin in the overexpression assay were due to variations in APP expression levels (Fig 3.2). Furthermore, we found that APPsα/APPsβ ratios were more than 10-fold higher with overexpressed APP (~75) than with endogenous APP (~6), suggesting a fundamental alteration in the processing of overexpressed APP (Fig 3.3). A likely explanation is that β-secreatse (BACE1) is not highly expressed endogenously in these non-neuronal cells, and overexpressing APP leads to much greater processing in the α-secretase pathway. For these reasons and because the goal is to determine the *in vivo* neurobiological relevance of these ligands, it is critical to confirm any findings from APP-overexpressing systems in endogenous and, preferably, neuronal systems. In this context, we proceeded to develop novel assays to compare the candidate ligands in non-neuronal and neuronal cell lines relying on endogenous APP. In particular, we believe the co-culture assay using primary rat cortical neurons has advantages over other systems: 1) APP is endogenously expressed by the neuronal reporters; 2) necessary but unknown co-receptors/co-ligands also should be endogenously expressed in the neuronal reporters; 3) ligands are continuously produced by the co-cultured HEK cells (rather than requiring artificial pulse administration); 4) ligands that require expression on the plasma membrane for activity will be expressed in their natural state; and 5) effects on APP processing that could be relevant to AD are best studied in neurons.

F-spondin

While F-spondin was the first reported candidate APP ligand with perhaps the most evidence across laboratories for effects on APP cleavage (Hafez et al, 2012; Ho & Sudhof, 2004;

Hoe et al, 2005), we observed little evidence of these effects in our assays. We found no significant changes in APPsα or APPsβ levels in HEK293 cells co-transfected with APP and F-spondin (Fig 3.1A) or in primary neurons co-cultured with F-spondin stable cells lines (Fig 3.7D) or treated with F-spondin-containing CM (Fig 3.7F). However, we did observe a subtle decrease of endogenous APPsα and APPsβ in plain HEK293 cells transfected with F-Spondin (Fig 3.1D). A potential underlying difference between our results and previous results is that in order to maintain a less artificial system, we did not overexpress BACE1 (as in (Ho & Sudhof, 2004)) or APOER2 (as in (Hoe et al, 2005)). Perhaps the most direct contrast between our studies and previous studies was in the treatment of primary neurons with F-Spondin-containing CM. Previously, F-spondin CM was reported to enhance CTFα levels in primary neurons (Hoe et al, 2005), but we failed to observe an effect on APPsα with a similar assay.

Integrin β1

Expression of Integrin β1 was previously reported in one study to enhance APPsα and APP CTF (Hoe et al, 2009). Here, we found only minor evidence for a subtle overall enhancement of APPsα and APPsβ in HEK293 cells. However, this effect was not confirmed in primary neurons. Further, in contrast to the relative consistency of the rest of the candidate ligands, transfection of Integrin β1 in HEK293 cells overexpressing APP resulted in very high variability in APPs secretion. The effects ranged from very dramatic increases in APPsα and APPsβ to only subtle or no changes in APPsα/β levels or even reductions in APPsα/β levels in some experiments (Fig 3.1B-C). We found that this variability in APPsα was significantly correlated with the expression of holoAPP upon co-transfection of APP751 with β1 Integrin,

even after normalization to holoAPP levels (Fig 3.2). The changes in holoAPP levels do not appear to represent a biologically relevant effect of β1 Integrin on APP expression, as β1 Integrin did not change expression of endogenous APP. Thus, changes in APPsα upon co-transfection of β1 Integrin with APP appear to be an artifact due to differences in APP co-transfection efficiency.

Contactin-2

CNTN2 has been reported to modulate APP processing by increasing AICD, CTFα and CTFβ levels in both over expressed and endogenous assays (Ma et al, 2008). However, our data did not confirm these findings. We found no effects of a soluble (Fc-tagged) form of CNTN2 on APPsα or APPsβ both in our endogenous and overexpressed assays.

Lingo-1

Knockdown of Lingo-1 has been reported to enhance CTFα and reduce CTFβ levels, while overexpression of Lingo-1 was reported to enhance CTFβ levels in HEK293 cells overexpressing the APPswe mutation (Bai et al, 2008). As predicted from Bai et al. (Bai et al, 2008), we found that Lingo-1 reduced APPsα levels in each of our assays (Figs 3.1 & 3.7), including primary neuronal cultures (Fig 3.7). However, instead of an enhancement in β-secretase cleavage of APP by Lingo-1 (Bai et al, 2008), we found that Lingo-1 reduced β-secretase cleavage. The discrepancy between these effects on β-secretase cleavage of APP may be due to differences in the processing of wild-type APP and APPswe. The Swedish mutation of APP markedly enhances β-secretase cleavage of APP (Citron et al, 1992) and modifies the principal subcellular loci for β-secretase cleavage (Haass et al, 1995). β-secretase cleavage of

wild-type APP occurs in large part upon internalization and endosomal recycling of cell-surface APP, whereas the Swedish mutation causes APP to be cleaved in considerable part by β-secretase within the secretory pathway (Haass et al, 1995). In contrast to our results with wild-type APP, we found that Lingo-1 produced quite variable effects on β-secretase cleavage of APPswe (Fig 3.10E). Lingo-1 enhanced APPsβ-swe in some experiments (similar to (Bai et al, 2008)) but reduced APPsβ-swe in other experiments (similar to our data with wild-type APP, Fig 3.1C). Thus, the separate mechanisms of β-secretase cleavage of the two APP variants could explain the apparent differences in Lingo-1 effects on β-secretase cleavage of APP in these studies.

Reelin

The effects of Reelin on APP shedding was confirmed across our multiple assays, including with endogenous APP in neurons. However, in contrast to previous studies in which Reelin increased α-secretase cleavage of APP (Hoe et al, 2009; Hoe et al, 2006), we observed that Reelin decreased α-secretase cleavage of APP (Figs. 3.1 & 3.7). We also found that Reelin reduced β-secretase cleavage of APP (Fig 3.1), which corroborates a previous study in which a reduction of Reelin enhanced Aβ and CTFβ levels in APP transgenic mouse brain (Kocherhans et al, 2010). We solidified this evidence by showing that the effect of Reelin on APPsα is dose-dependent and that Reelin also decreases CTF, Aβ40, and Aβ42. Moreover, we confirmed reports of a physical interaction between Reelin and APP and showed a similar level of Reelin-APP co-IP as is seen with its canonical receptors, ApoER2 and VLDLR.

In an attempt to reconcile the opposing effects of Reelin on APPsα, we replicated as closely as we could the methods described previously that resulted in an increase in APPsα (Hoe et al, 2009; Hoe et al, 2006). However, using this method we found no significant effect of Reelin on APPsα levels (Fig 3.12). These conflicting effects on APPsα do not appear to be due to differences in the concentrations of Reelin, as a range of Reelin concentrations resulted in a decrease of APPsα in our hands (Fig 3.11C). Because Reelin is cleaved to generate several fragments, it is possible that different cell types secrete alternate Reelin products. However, we found that expression of cDNAs encoding each physiological Reelin fragment reduced APPsα to some extent in our assay (Fig 3.13).

Pancortins

Pancortin-1 produced the most robust and consistent effects on cleavage of endogenous APP of any of the candidate ligands tested (Fig 3.1D-F). Pancortin-1 also was the only candidate ligand which specifically reduced β-secretase processing while having no effects on α-secretase processing of APP. With Pancortins being expressed not only in embryonic but also adult cortex (Danielson et al, 1994; Nagano et al, 2000), regulation of β-secretase cleavage by Pancortin-1 could turn out to have important implications for the pathogenesis or treatment of Alzheimer's disease. Recently, Pancortin was shown to interact with members of the Lingo-1 signaling pathway and regulate axonal growth (Nakaya et al, 2012). As Pancortin and Lingo-1 were top APP ligands in our assays, future studies to determine how the Pancortin and Lingo-1 signaling pathways may intersect to regulate APP processing will be important.

A classic ligand for APP?

Since its cloning 25 years ago, APP has been intensively studied as regards its processing via regulated intramembrane proteolysis and the role of its Aß fragment in AD pathogenesis, but studies of its physiological function and processing have received less attention and led to an array of complex, sometimes conflicting findings. For example, analogous to the sizeable number of proteins purported to be candidate ligands for APP, a number of genes had been reported to be transcriptionally activated by the APP intracellular domain (AICD) (Baek et al, 2002; Kim et al, 2003; Pardossi-Piquard et al, 2005; von Rotz et al, 2004). Like the candidate APP ligands, potential target genes had usually been reported by single labs, and attempts to confirm them had been largely unsuccessful (Hass & Yankner, 2005; Hebert et al, 2006). One particularly clarifying study in this field published by De Strooper and colleagues systematically compared these target genes in the same assay system and found that each was at best indirectly and weakly influenced by APP processing or not at all (Hebert et al, 2006). A central goal of our study was to provide similar clarity for most of the reported candidate ligands of APP.

Our study raises the central question of whether a classic ligand for APP that positively triggers processing by α- or β- secretase exists. While we did find effects of Reelin, Lingo-1 and Pancortin-1 on APP processing to be consistent across the multiple assays we used, the effects of Reelin and Lingo-1 were subtle in endogenous systems and not identical to previous reports (Bai et al, 2008; Hoe et al, 2009; Hoe et al, 2006). Further, each ligand we tested turned out to inhibit cleavage rather than stimulate α- or β-secretase processing. Whereas a larger portion of

APP processing appears to be constitutive than regulated, in contrast to the ligand-regulated cleavage of Notch (Mumm et al, 2000; Schroeter et al, 1998), the ability of PMA to robustly stimulate α-secretase cleavage of APP (Fig 2 B-C and (Buxbaum et al, 1998; Hung et al, 1993; Lammich et al, 1999)) suggests that there is a cellular capacity for α-secretease cleavage of APP to be enhanced. On the other hand, it is possible that cognate ligand(s) for APP regulate neuronal functions of APP without significantly modulating its proteolytic processing. It is also possible that instead of a single protein ligand, several proteins and non-protein factors may have coordinated effects to regulate APP cleavage. Thus, each ectodomain-binding ligand may individually result in only subtle effects, particularly in the more biologically relevant context of endogenous, wild-type APP in neurons that we explored. Furthermore, it may be that apparent ligand effects are more indirect through competition of common binding partners (Hoe & Rebeck, 2008; Hoe et al, 2006; Hoe et al, 2005). The cellular context of APP may affect ligand binding and cleavage of APP, for example homo- or hetero- dimerization of APP (Libeu et al, 2012) or the subcellullar localization and trafficking of APP (Ehehalt et al, 2003; Haass et al, 1995a). Such further research is needed to better define the basic functions of this conserved and ubiquitously expressed protein and to better understand the consequences of chronically altering its proteolytic processing in older humans with AD-type cognitive syndromes.

References

Araki W, Kitaguchi N, Tokushima Y, Ishii K, Aratake H, Shimohama S, Nakamura S, Kimura J (1991) Trophic effect of β-amyloid precursor ptotein on cerebral cortical neurons in culture. *Biochem Biophys Res Commun* **181:** 265-271

Baek SH, Ohgi KA, Rose DW, Koo EH, Glass CK, Rosenfeld MG (2002) Exchange of N-CoR corepressor and Tip60 coactivator complexes links gene expression by NF-kappaB and beta-amyloid precursor protein. *Cell* **110:** 55-67

Bai Y, Markham K, Chen F, Weerasekera R, Watts J, Horne P, Wakutani Y, Bagshaw R, Mathews PM, Fraser PE, Westaway D, St George-Hyslop P, Schmitt-Ulms G (2008) The in vivo brain interactome of the amyloid precursor protein. *Mol Cell Proteomics* **7:** 15-34

Benhayon D, Magdaleno S, Curran T (2003) Binding of purified Reelin to ApoER2 and VLDLR mediates tyrosine phosphorylation of Disabled-1. *Brain Res Mol Brain Res* **112:** 33-45

Buxbaum J, Liu K, Luo Y, Slack J, Stocking K, Peschon J, Johnson R, Castner B, Cerretti D, Black R (1998) Evidence that tumor necrosis factor alpha converting enzyme is involved in regulated alpha-secretase cleavage of the Alzheimer amyloid protein precursor. *J Biol Chem* **273:** 27765-27767

Citron M, Oltersdorf T, Haass C, McConlogue L, Hung AY, Seubert P, Vigo-Pelfrey C, Lieberburg I, Selkoe DJ (1992) Mutation of the β-amyloid precursor protein in familial Alzheimer's disease increases β-protein production. *Nature* **360:** 672-674

D'Arcangelo G, Homayouni R, Keshvara L, Rice DS, Sheldon M, Curran T (1999) Reelin is a ligand for lipoprotein receptors. *Neuron* **24:** 471-479

D'Arcangelo G, Nakajima K, Miyata T, Ogawa M, Mikoshiba K, Curran T (1997) Reelin is a secreted glycoprotein recognized by the CR-50 monoclonal antibody. *J Neurosci* **17:** 23-31

Danielson PE, Forss-Petter S, Battenberg EL, deLecea L, Bloom FE, Sutcliffe JG (1994) Four structurally distinct neuron-specific olfactomedin-related glycoproteins produced by differential promoter utilization and alternative mRNA splicing from a single gene. *J Neurosci Res* **38:** 468-478

Ehehalt R, Keller P, Haass C, Thiele C, Simons K (2003) Amyloidogenic processing of the Alzheimer beta-amyloid precursor protein depends on lipid rafts. *J Cell Biol* **160:** 113-123

Förster E, Bock H, Herz J, Chai X, Frotscher M, Zhao S (2010) Emerging topics in Reelin function. *Eur J Neurosci* **31:** 1511-1519

Ghiso J, Rostagno A, Gardella JE, Liem L, Gorevic PD, Frangione B (1992) A 109-amino-acid C-terminal fragment of Alzheimer's-disease amyloid precursor protein contains a sequence, -RHDS-, that promotes cell adhesion. *Biochem J* **288:** 1053-1059

Haass C, Kaether C, Thinakaran G, Sisodia S (2012) Trafficking and Proteolytic Processing of APP. *Cold Spring Harbor Perspectives in Medicine* **2**

Haass C, Koo EH, Capell A, Teplow DB, Selkoe DJ (1995a) Polarized sorting of β-amyloid precursor protein and its proteolytic products in MDCK cells is regulated by two independent signals. *J Cell Biol* **128:** 537-547

Haass C, Lemere CA, Capell A, Citron M, Seubert P, Schenk D, Lannfelt L, Selkoe DJ (1995) The Swedish mutation causes early-onset Alzheimer's disease by β-secretase cleavage within the secretory pathway. *Nature Med* **1:** 1291-1296

Hafez D, Huang J, Richardson J, Masliah E, Peterson D, Marr R (2012) F-spondin gene transfer improves memory performance and reduces amyloid-β levels in mice. *Neuroscience* **223:** 465-472

Hass M, Yankner B (2005) A {gamma}-secretase-independent mechanism of signal transduction by the amyloid precursor protein. *J Biol Chem* **280:** 36895-37799

Hebert SS, Serneels L, Tolia A, Craessaerts K, Derks C, Filippov MA, Muller U, De Strooper B (2006) Regulated intramembrane proteolysis of amyloid precursor protein and regulation of expression of putative target genes. *EMBO Rep* **7:** 739-745

Hiesberger T, Trommsdorff M, Howell B, Goffinet A, Mumby M, Cooper J, Herz J (1999) Direct binding of Reelin to VLDL receptor and ApoE receptor 2 induces tyrosine phosphorylation of disabled-1 and modulates tau phosphorylation. *Neuron* **24:** 481-489

Ho A, Sudhof TC (2004) Binding of F-spondin to amyloid-beta precursor protein: a candidate amyloid-beta precursor protein ligand that modulates amyloid-beta precursor protein cleavage. *Proc Natl Acad Sci* **101:** 2548-2553

Hoe H-S, Lee K, Carney R, Lee J, Markova A, Lee J-Y, Howell B, Hyman B, Pak D, Bu G, Rebeck G (2009) Interaction of reelin with amyloid precursor protein promotes neurite outgrowth. *J Neurosci* **29:** 7459-7532

Hoe H-S, Rebeck G (2008) Functional interactions of APP with the apoE receptor family. *J Neurochem* **106:** 2263-2271

Hoe HS, Tran TS, Matsuoka Y, Howell BW, Rebeck GW (2006) DAB1 and Reelin effects on amyloid precursor protein and ApoE receptor 2 trafficking and processing. *J Biol Chem* **281:** 35176-35185

Hoe HS, Wessner D, Beffert U, Becker AG, Matsuoka Y, Rebeck GW (2005) F-spondin interaction with the apolipoprotein E receptor ApoEr2 affects processing of amyloid precursor protein. *Mol Cell Biol* **25:** 9259-9268

Honda T, Kobayashi K, Mikoshiba K, Nakajima K (2011) Regulation of cortical neuron migration by the Reelin signaling pathway. *Neurochem Res* **36:** 1270-1279

Hung AY, Haass C, Nitsch RM, Qiu WQ, Citron M, Wurtman RJ, Growdon JH, Selkoe DJ (1993) Activation of protein kinase C inhibits cellular production of the amyloid β-protein. *J Biol Chem* **268:** 22959-22962

Jossin Y, Gui L, Goffinet A (2007) Processing of Reelin by embryonic neurons is important for function in tissue but not in dissociated cultured neurons. *J Neurosci* **27:** 4243-4295

Jossin Y, Ignatova N, Hiesberger T, Herz J, Lambert de Rouvroit C, Goffinet A (2004) The central fragment of Reelin, generated by proteolytic processing in vivo, is critical to its function during cortical plate development. *J Neurosci* **24:** 514-521

Kang J, Lemaire H-G, Unterbeck A, Salbaum JM, Masters CL, Grzeschik K-H, Multhaup G, Beyreuther K, Muller-Hill B (1987) The precursor of Alzheimer's disease amyloid A4 protein resembles a cell-surface receptor. *Nature* **325:** 733-736

Kim HS, Kim EM, Lee JP, Park CH, Kim S, Seo JH, Chang KA, Yu E, Jeong SJ, Chong YH, Suh YH (2003) C-terminal fragments of amyloid precursor protein exert neurotoxicity by inducing glycogen synthase kinase-3beta expression. *Faseb J* **17:** 1951-1953

Kocherhans S, Madhusudan A, Doehner J, Breu K, Nitsch R, Fritschy J-M, Knuesel I (2010) Reduced Reelin expression accelerates amyloid-beta plaque formation and tau pathology in transgenic Alzheimer's disease mice. *J Neurosci* **30:** 9228-9268

Lambert de Rouvroit C, de Bergeyck V, Cortvrindt C, Bar I, Eeckhout Y, Goffinet A (1999) Reelin, the extracellular matrix protein deficient in reeler mutant mice, is processed by a metalloproteinase. *Exp Neurol* **156:** 214-217

Lammich S, Kojro E, Postina R, Gilbert S, Pfeiffer R, Jasionowski M, Haass C, Fahrenholz F (1999) Constitutive and regulated alpha-secretase cleavage of Alzheimer's amyloid precursor protein by a disintegrin metalloprotease. *PNAS* **96:** 3922-3927

Libeu C, Descamps O, Zhang Q, John V, Bredesen D (2012) Altering APP proteolysis: increasing sAPPalpha production by targeting dimerization of the APP ectodomain. *PloS one* **7**

Ma QH, Futagawa T, Yang WL, Jiang XD, Zeng L, Takeda Y, Xu RX, Bagnard D, Schachner M, Furley AJ, Karagogeos D, Watanabe K, Dawe GS, Xiao ZC (2008) A TAG1-APP signalling pathway through Fe65 negatively modulates neurogenesis. *Nat Cell Biol* **10:** 283-294

Mi S, Sandrock A, Miller R (2008) LINGO-1 and its role in CNS repair. *Int J Biochem Cell Biol* **40:** 1971-1978

Mumm J, Schroeter E, Saxena M, Griesemer A, Tian X, Pan D, Ray W, Kopan R (2000) A ligand-induced extracellular cleavage regulates gamma-secretase-like proteolytic activation of Notch1. *Molecular Cell* **5:** 197-206

Nagano T, Nakamura A, Konno D, Kurata M, Yagi H, Sato M (2000) A2-Pancortins (Pancortin-3 and Pancortin-4) are the dominant Pancortins during neocortical development. *J Neurochem* **75**

Nakaya N, Sultana A, Lee H-S, Tomarev S (2012) Olfactomedin 1 interacts with the nogo a receptor complex to regulate axon growth. *J Biol Chem* **287:** 37171-37184

Osterfield M, Egelund R, Young LM, Flanagan JG (2008) Interaction of amyloid precursor protein with contactins and NgCAM in the retinotectal system. *Development* **135:** 1189-1199

Pardossi-Piquard R, Petit A, Kawarai T, Sunyach C, Alves da Costa C, Vincent B, Ring S, D'Adamio L, Shen J, Muller U, St George Hyslop P, Checler F (2005) Presenilin-dependent transcriptional control of the Abeta-degrading enzyme neprilysin by intracellular domains of betaAPP and APLP. *Neuron* **46:** 541-554

Perez RG, Zheng H, Van der Ploeg LH, Koo EH (1997) The beta-amyloid precursor protein of Alzheimer's disease enhances neuron viability and modulates neuronal polarity. *J Neurosci* **17:** 9407-9414

Pramatarova A, Chen K, Howell BW (2008) A genetic interaction between the APP and Dab1 genes influences brain development. *Mol Cell Neurosci* **37:** 178-186

Priller C, Bauer T, Mitteregger G, Krebs B, Kretzschmar HA, Herms J (2006) Synapse formation and function is modulated by the amyloid precursor protein. *J Neurosci* **26:** 7212-7221

Rama N, Goldschneider D, Corset V, Lambert J, Pays L, Mehlen P (2012) Amyloid Precursor Protein Regulates Netrin-1-mediated Commissural Axon Outgrowth. *J Biol Chem* **287:** 30014-30023

Rice H, Townsend M, Bai J, Suth S, Cavanaugh W, Selkoe D, Young-Pearse T (2012) Pancortins interact with amyloid precursor protein and modulate cortical cell migration. *Development* **139:** 3986-3996

Schroeter E, Kisslinger J, Kopan R (1998) Notch-1 signalling requires ligand-induced proteolytic release of intracellular domain. *Nature* **393:** 382-386

Shimoda Y (2009) Contactins: Emerging key roles in the development and function of the nervous system. *Cell Adh Migr* **3:** 64-70

Soba P, Eggert S, Wagner K, Zentgraf H, Siehl K, Kreger S, Lower A, Langer A, Merdes G, Paro R, Masters CL, Muller U, Kins S, Beyreuther K (2005) Homo- and heterodimerization of APP family members promotes intercellular adhesion. *EMBO J* **24:** 3624-3634

Stein T, Walmsley A (2012) The leucine-rich repeats of LINGO-1 are not required for self-interaction or interaction with the amyloid precursor protein. *Neuroscience Letters* **509:** 9-12

Trommsdorff M, Gotthardt M, Hiesberger T, Shelton J, Stockinger W, Nimpf J, Hammer R, Richardson J, Herz J (1999) Reeler/Disabled-like disruption of neuronal migration in knockout mice lacking the VLDL receptor and ApoE receptor 2. *Cell* **97:** 689-701

von Rotz RC, Kohli BM, Bosset J, Meier M, Suzuki T, Nitsch RM, Konietzko U (2004) The APP intracellular domain forms nuclear multiprotein complexes and regulates the transcription of its own precursor. *J Cell Sci* **117:** 4435-4448

Wang Z, Wang B, Yang L, Guo Q, Aithmitti N, Songyang Z, Zheng H (2009) Presynaptic and postsynaptic interaction of the amyloid precursor protein promotes peripheral and central synaptogenesis. *J Neurosci* **29:** 10788-10801

Young-Pearse TL, Bai J, Chang R, Zheng JB, Loturco JJ, Selkoe DJ (2007) A Critical Function for beta-Amyloid Precursor Protein in Neuronal Migration Revealed by In Utero RNA Interference. *J Neurosci* **27:** 14459-14469

Young-Pearse TL, Chen A, Chang R, Marquez C, Selkoe DJ (2008) Secreted APP regulates the function of full-length APP in neurite outgrowth through interaction with integrin beta1. *Neural Development* **3**

Chapter 4:

Discussion and Future Directions

A classic ligand for APP?

Introduction

Since its initial cloning over 25 years ago, APP has been predicted to be a cell-surface receptor with a cognate ligand. However, much of the current evidence implicating a receptor-ligand interaction in the regulation of APP function and processing has been weak (i.e. comparison to Notch), controversial (i.e. AICD as a transcriptional regulator), or not widely validated (i.e. APP ligands). A number of secreted or cell-surface proteins have been reported to physically interact with the APP ectodomain and modulate its shedding, yet there remains to be a validated ligand for APP. Nearly all initial reports of such candidate ligands utilize primarily APP overexpression systems, report data as a representative Western blot lacking precise quantification and controls, and have not been followed up by multiple groups. Since there is currently not a well-established ligand for APP, I undertook both an unbiased approach in an attempt to identify novel potential ligands (Chapter 2) and a candidate-based approach in an attempt to confirm one or more of the previously reported ligands (Chapter 3).

In the unbiased approach to reveal novel ligands (Chapter 2), Pancortin was identified by a mass spectrometry-based screen for factors that bind to the APP ectodomain in rodent brain. Each of the Pancortin isoforms was confirmed to interact with APP. However, only specific Pancortin isoforms reduced β-secretase but not α-secretase cleavage of endogenous APP. Using in utero electroporation to overexpress or knockdown Pancortin isoforms in rodent cortex, a previously unidentified role for Pancortin in cortical cell migration with evidence for a functional interaction with APP was discovered.

In the candidate based approach to confirm one or more published APP ligands (Chapter 3), I developed new assays to compare each of these candidates side-by-side in biologically relevant culture systems. A comprehensive quantification by ELISA of APPsα and APPsβ, the immediate products of secretase processing, in both non-neuronal cell lines and primary neuronal cultures expressing endogenous APP, yielded no evidence that any of these published candidate ligands *stimulate* ectodomain shedding. Rather, Reelin, Lingo-1 and Pancortin emerged as the most consistent ligands for significantly *inhibiting* ectodomain shedding.

These findings prompt several key questions including 1) What are the precise mechanisms responsible for these effects of Reelin, Lingo-1, and Pancortin on APP processing and function? 2) Would any of the candidates found to inhibit shedding in my assays be viable drug targets to treat AD? 3) Is there a 'classic' ligand for APP? Here, I will discuss possible predictions based on my initial studies (reported in Chapters 2 and 3) as well as recent preliminary studies that are aimed at addressing these questions (reported in Appendix 2-5). Since these questions remain largely unanswered by current studies, I will also discuss several sets of experiments that could help shed further insight into these issues.

Potential mechanisms of the APP/Pancortin interaction in cortical cell migration

Previously, knockdown of APP in subset of neuronal precursor cells by in utero electroporation resulted in an arrest of electroporated cells immediately below the cortical plate (Young-Pearse et al, 2007). Both the ectodomain and intracellular domain of APP were required to be expressed as a holoprotein in order to mediate proper neuronal precursor cell migration(Young-Pearse et al, 2007), and the cytoplasmic factors disabled 1 (DAB1) and disrupted in schizophrenia 1 (DISC1) biochemically and functionally interact with APP in this

function (Young-Pearse et al, 2010; Young-Pearse et al, 2007). On the basis of these findings, we hypothesize that specific extracellular factors bind the ectodomain of holoAPP on the cell surface and transmit a signal to intracellular signaling cascades during development. Data presented in Chapter 2 suggest Pancortin may be such an extracellular factor that regulates APP-dependent cell entry into the cortical plate. Our in utero electroporation studies in Chapter 2 reveal a previously unidentified role of Pancortin in the migration of neuronal precursor cells into the cortical plate, with specific Pancortin isoforms having opposing roles. The AMY isoform inhibits cortical plate entry and BMZ promotes cortical plate entry, and rescue experiments suggest that BMZ can compete with AMY and act atleast in part through APP-dependent mechanisms (Fig 4.1A).

Model of APP-dependent Pancortin mechanisms

Similar to knockdown of APP, knockdown of the BMZ isoform of Pancortin resulted in a failure of cells to enter the cortical plate (Fig 4.1B). Interestingly, overexpression of APP does not rescue the loss of BMZ (Fig 4.1C), indicating that the migration-promoting effect of APP is dependent upon expression of BMZ. Overexpression of AMY (similar to loss of BMZ) blocked cortical plate entry (Fig 4.1D). Thus, AMY and BMZ have opposing roles. Previously, BMZ has been shown to negatively regulate AMY in neurogenesis in lower vertebrates (Moreno & Bronner-Fraser, 2005), and our data supports a similar type of regulation in cortical plate entry. Overexpression of BMZ rescued the defect of AMY overexpression (Fig 4.1E). In HEK293 cells, BMZ can reduce the physical interaction between APP and AMY, suggesting a mechanism whereby BMZ can negatively regulate AMY through competition with AMY for binding to APP (Fig 4.1E). Further supporting this hypothesis, APP overexpression can rescue the migration

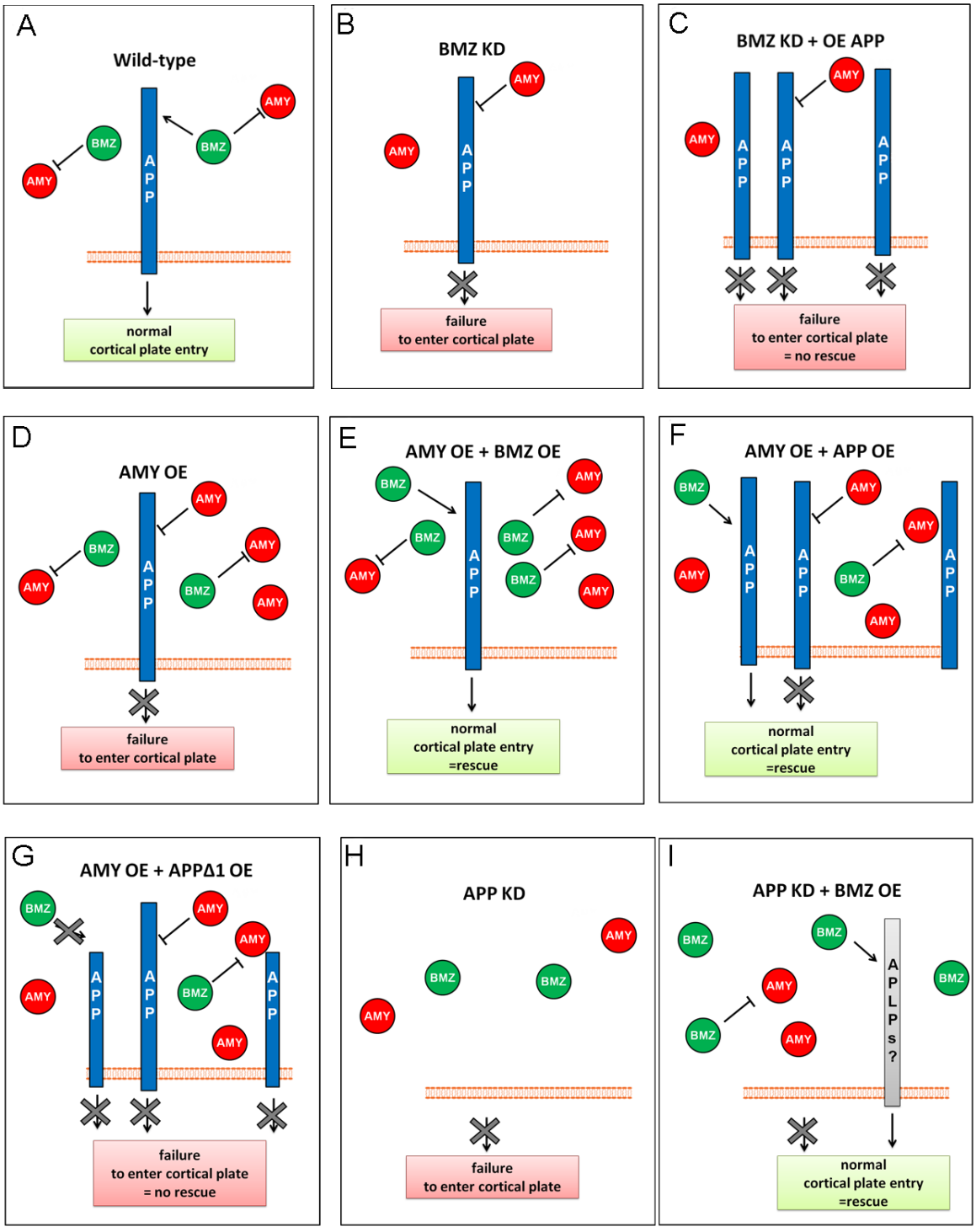

Figure 4.1: Model of mechanisms responsible for migration phenotypes

Schematic diagrams illustrating predicted molecular mechanisms leading to migration phenotypes of in utero electroporation experiments with APP and Pancortin. OE = overexpression, KD = knockdown

defect of AMY overexpression (Fig 4.1F), but blockade of the interaction through deletion of the AMY/BMZ binding site within APP prevents rescue (Fig 4.1G). I propose that with APP overexpression there is more APP remaining that is not being inhibited by the overexpressed AMY, and overexpression of APP with deletion of the BMZ binding site fails to rescue since BMZ is required for the migration promoting effects of the additional APP (Fig 4.1G). Taken together, these data support a model in which Pancortin is an important extracellular regulatory factor for the migration-promoting function of APP at the cell surface. The BMZ isoform of Pancortin is required for the migration-promoting effects of APP. BMZ also negatively regulates the AMY isoform of Pancortin, which would otherwise inhibit the migration-promoting effects of APP. Thus, the timing and localization of AMY and BMZ expression may provide an important mechanism for regulating APP-dependent cell migration in the cortex.

Model of APP-independent Pancortin mechanisms

Pancortin may also signal in part independently of APP. Overexpression of BMZ rescues the defect of APP knockdown indicating that BMZ functions in the absence of APP perhaps through other cell-surface proteins (Fig 4.1 H,I). Thus, it would be of interest to investigate the interaction of Pancortin with APLPs, as they are known to compensate for loss of APP. Interestingly, a recent study showed that knockdown of APLP2 by in utero electroporation produces a cell migration phenotype, which the author's attributed to an effect of APLP2 on neuronal differentiation and thus timing of migration(Shariati et al, 2013). Opposing roles for BMZ and AMY in neuronal differentiation have been well described in Xenopus (Moreno & Bronner-Fraser, 2005) and would match the opposing effects on cortical migration. Thus, future

experiments should be aimed at determining if effects on neuronal differentiation contribute to the cell migration phenotype of Pancortin isoforms and also explore the biochemical interactions of Pancortin isoforms with the APLPs and downstream effects on APLP proteolysis and cortical phenotypes.

Cell non-autonomous effects of Pancortins?

My model proposed here requires cell non-autonomous effects of Pancortin. While this has not been directly addressed, the immunostaining patterns of overexpressed Pancortin isoforms is diffuse and is not localized to just the cells expressing them, thus providing the potential for cell non-autonomous effects. To test this directly, in utero electroporations of embryonic rat cortices could be performed in succession, first to overexpress Pancortin isoforms and then to expression GFP with or without APP shRNA on a subsequent day to target two separate sets of cells. The cell non-autonomous effects of the Pancortins on the GFP electroporated cells could then be assayed.

Relationship between APP processing and function?

BMZ inhibits β-secretase cleavage of APP, however, whether this activity is mechanistically involved in regulating migration has yet to be determined. In fact, whether regulated cleavage is mechanistically involved in APP function in general is not well-established. Previous studies have used rescue of APP knock-down by different APP fragments to explore this question. For example, neither APP CTF nor APPsα can rescue the migration phenotype of APP knockdown, suggesting a requirement for full-length APP (Young-Pearse et al, 2007). However, this does not fully exclude the involvement of *regulated* APP cleavage, rather than artificial APPsα overexpression, in APP function. A more elegant experiment would be to

generate a non-cleavable APP construct to use for rescue of APP knockdown. This strategy has been utilized in at least one study in *Drosophila* (Luo et al, 1992) and would give much insight into the relationship between APP processing and function in the mammalian brain.

Potential mechanisms for the effects of candidate ligands on APP processing

Coupling of α- and β- secretase cleavage?

None of the candidate ligands examined stimulated α-secretase cleavage of APP in my assays, as might be predicted of a 'classic' ligand for APP. Instead, Reelin and Lingo-1 reduce both α- and β- secretase cleavage of APP and the BMZ and BMY isoforms of Pancortin reduce β-secretase cleavage of APP while sparing α-secretase cleavage. It had long been assumed that α- and β- cleavage are inversely coupled, and thus it is unexpected that reducing either α- or β-cleavage would not result in an enhancement of the other. However, a recent study using more physiological assays demonstrated that the activities of α- and β- secretases are uncoupled in mammalian cell lines similar to the HEK293 cells utilized for my studies (Colombo et al, 2012). Thus, this study may help to explain the reduction of both α- and β- secretase cleavage of APP by Reelin and Lingo-1 in my studies.

Direct binding?

A 'classic' ligand for APP would be predicted to bind directly to the APP ectodomain in trans to facilitate effects on APP processing. The confirmation of Lingo-1 and Reelin in the neuronal co-culture assay (designed to test this specifically) is evidence that these candidates do act on APP in trans. The biochemical interactions of Reelin, Lingo-1 and Pancortin with APP in cell culture and intact brain, suggest a physical interaction of these candidates with APP.

However, a *direct* interaction cannot be assumed by these co-IP studies alone. Performing classic in vitro ligand-receptor binding assays will be important to confirm the impact of ligand binding on APP shedding in future studies. For example, the technique of surface plasmon resonance could be use to compare relative binding constants for each of the candidates, and would be a valuable analysis to perform in the future.

Indirect interactions through common binding partners?

Rather than through direct binding, it may be that apparent ligand effects are more indirect, perhaps competition of common cell-surface binding partners. For example, APP has been shown to interact with a number of factors within the canonical Reelin signaling pathway, including its canonical receptors APOER2 and VLDLR as well as the adapter protein, Dab1 (Hoe & Rebeck, 2008; Hoe et al, 2006; Hoe et al, 2005). We have intriguing preliminary data that APP signaling intersects with the Reelin pathway at multiple levels. Transfections of APOER2 and VLDLR in HEK293 cells each increased APPsα secretion but had no effect on APPsβ, suggesting a specific effect on α- but not β- secretase cleavage of APP. Coexpressing Reelin cancelled the effects of the over-expressed APOER2 and VLDLR on APPsα but did not reduce APPsβ (Appendix 3). These data encourages further analyses of the involvement of Reelin and its canonical receptors on APP shedding. In addition to a DAB1-APP functional interaction, APOER2 and VLDLR expression seems necessary for the effects of APP loss in migration: our recent *in utero* electroporation experiments suggest that APP shRNA is less active if APOER2 and/or VLDLR are knocked down (unpublished result). Further experiments are clearly warranted to see whether and how APP and the Reelin signaling pathways intersect.

Involvement of HSPGs?

Heparan sulfate proteoglycans (HSPGs) often provide sites of interaction between ligands and their receptors, thereby serving as co-receptors in protein-mediated cell signaling (reviewed in (Lindahl, 2007)). Both APP and several of the candidate ligands we have assessed (e.g., F-spondin, Reelin) have heparin-binding domains (Small et al; Tan et al, 2008). Thus, the reported ability of the APP ectodomain to bind certain glycosaminoglycans and proteoglycans (Clarris et al, 1997; Mok et al, 1997; Narindrasorasak et al, 1991) may contribute to a multifactorial ligand regulation of APP secretory processing, and this should now be explored in the context of the ligands that most consistently affect the shedding of APP.

In preliminary studies, I have taken advantage of cell lines that have specific genetic deficiencies of proteoglycan formation. The CHO-745 line is defective in xylosyltransferase activity, the first sugar transfer in glycosaminoglycan (GAG) synthesis, and is thus deficient in GAG formation, including both heparan sulfate and chondroitin sulfate (Esko et al, 1985). The CHO-677 line lacks both the N-acetylglucosaminyl-transferase and glucuronyltransferase activities required for synthesis of heparan sulfate and thus are deficient in heparan sulfate but not chondroitin sulfate formation (Lidholt et al).

First, to determine if HSPGs are required for effects of Reelin on reducing APPsα levels, Reelin was transfected into control and HSPG deficient cell lines (Appendix 4). However, Reelin reduced APPsα whether in the presence or absence of HSPGs suggesting HSPGs are not required for the interactions of Reelin with APP. Next these mutant cell lines were used to determine if HSPGs more broadly regulate APP ectodomain shedding (Appendix 4). In initial experiments, HSPG deficient cell lines had reduced APPsα and CTF levels compared to wild-type cells. However, when additional wild-type cell lines were assayed, I noticed there were

significant differences between the multiple wild-type cell lines and no significant differences of the HSPG deficient cell lines when compared to *some* of the wild-type lines. Thus, effects potentially attributable to clonal variability were a concern. To determine the specificity of the apparent effects on APPsα generation, Exostosin-1 (the mutated gene in CHO-677 cells) was transfected into CHO-677 cell lines. However, Ext-1 failed to rescue the effect on APPsα levels in this experiment, despite confirmed expression of Ext-1 and partial rescue of HSPGs by Western blot. Thus far, these experiments are inconclusive for the effects that HSPGs may confer on APP processing in general but suggests HSPGs are not required for effects of Reelin. As an alternative or supplementary approach to using these GAG-deficient CHO-based cells, enzymatic heparinase treatment (which enzymatically digests heparan sulfate) antibody HS neutralization, or transfection of Extosin-1 shRNA in neurons could be used to compliment studies in mutant CHO cells.

Common signaling pathways for Lingo-1 and Pancortin?

Recently, a study reported that Pancortin competes with Lingo-1 for binding to Nogo A receptor (NgR1), and that Pancortin regulates the function of the NgR1 in growth cone collapse(Nakaya et al, 2012). Given that Lingo-1 and Pancortin emerged as top APP ligands in my assays, future studies to determine how the Pancortin and Lingo-1 signaling pathways may intersect to regulate APP processing will be important. Current studies are underway to determine if NgR1 is necessary for the effects of Lingo-1 or Pancortin on APP processing. Since APP also functions in neurite outgrowth, it will be of interest to determine potential functional interactions of Lingo-1, Pancortin, and APP at the growth cone.

Ligand regulation of a large multi-secretase complex?

In collaboration with Christina Muratore , Tracy Young-Pearse and others, I studied APP ectodomain shedding in neurons derived from induced pluripotent stem cells of control individuals and those carrying a familial 'London' AD mutation in APP (Appendix 1). The 'London' V717I mutation resides within the transmembrane domain of APP near the γ-secretase cleavage site and leads to increased Aβ42/40 ratio, which was confirmed in these neurons. Unexpectedly, I found that this mutation near the γ-secretase cleavage site of APP led to increased β-secretase cleavage, which was abolished by inhibiting γ-secretase. I also confirmed these effects in HEK293 cells with overexpression of either wild-type APP or APP with the London mutation. These findings represent a novel phenotype of the London mutation and suggest that β-secretase and γ-secretase activities are functionally linked. This data supports other recent findings in the Selkoe lab in which Allen Chen et al (unpublished) propose a model of a large multi-protease complexes containing both α- and γ-secretases or β- and γ- secretases that sequentially cleave APP. Upon identification of a cognate ligand for APP, studies should be directed at understanding how ligand binding might facilitate formation of these large complexes, trigger cleavage once complexes have formed, or direct APP towards one complex or the other.

Towards more physiological systems and drug targets

A major goal of my studies in Chapter 3 was to develop new assays that were more physiolgoical than previous studies to test the effects of candidate ligands. Indeed, I developed assay which utilized endogenous APP rather than overexpressed APP and examined neuronal cultures with the ligand presented in trans. However, one technical limitation of the neuronal co-culture assay was the unavailability of an APPsβ rodent-specific ELISA that was able to

reliably measure endogenous APPsβ from these neuronal cultures. Because Pancortin only affected APPsβ, but not APPsα, it was not possible to confirm these effects in the neuronal assays. In addition, while APP was endogenous, our assays utilized overexpression of the candidate ligands. To address these limitations, I have now begun to establish new assays to study ectodomain shedding by putative ligands in neuronal precursor cells and more mature neurons derived from human induced pluripotent stem cells. In these human neurons, I am able to measure both APPsα and APPsβ reliably. Candidate ligands are currently being studied by AMAXA nucleofection and co-culture with Chinese Hamster Ovary (CHO) using cell culture separation chambers. Our next studies are aimed at knocking-down the endogenous expression of these candidates, rather than artificial overexpression. A large scale Nanostring analysis of mRNA levels revealed that many of our genes are interest are expressed highly in these cells, particularly the Pancortin isoforms. Next, we will be using a large shRNA library to conduct a higher throughput 96-well plate based screen of our top candidate ligands as well as other interesting factors potentially involved in mediating these effects (i.e. APOER2, VLDLR, Dab1, Extosin-1, and NgR1, as discussed above). Thus, the goal is to not only confirm previous results in cultured human neurons (or understand any differences from previous findings) but also further investigate the mechanisms and other molecular players involved in mediating these effects.

Ultimately, a cognate ligand for APP should be confirmed *in vivo*. With this goal, I have begun preliminary experiments with Reelin knockout (Reeler) mice to investigate the in vivo effects of Reelin on APP processing. In initial preliminary experiments, I measured endogenous APPsα from cultures neurons of either wild-type, heterozygous, or homozygous knockout

embryos. However, the APPsα levels from cultured cells were too variable between embryos of even wild-type mice to be able to determine the effect the loss of Reelin expression might have in this system, particularly for small effects (Appendix 5). The next step will be to measure APPsα, Aβ, and full-length APP from brain homogenates of these mice. Another feasible approach is to dynamically measure Aβ in behaving wild-type and Reeler mice using the technique of in vivo brain microdialysis.

Lastly, the ultimate goal of these studies would be to develop drug targets based upon a putative APP ligand that under normal physiological conditions is a robust regulator of the initial cleavage event in APP processing. Of the candidates I studied, Pancortin appears to be the most promising in this regards. Pancortin specifically reduced β-secretase but not α-secretase cleavage and effects were much stronger than any of the other candidates. The first step would be to examine the effect of Pancortin on Aβ production and pathology in AD mouse models. Pancortin could be introduced to mouse brain by injection, transplantation of Pancortin expressing cells, or lentiviral transduction. Acute effects of Pancortin on Aβ production could be measured by in vivo brain microdialysis while more chronic effects could be determined by immunohistochemistry of brain slices.

Conclusions: A classic ligand for APP?

My studies raise the central question of whether a classic ligand that triggers α-secretase cleavage of APP exists. While I did find effects of Reelin, Lingo-1 and Pancortin on APP processing to be consistent across the multiple assays I used, the effects of Reelin and Lingo-1 were subtle in endogenous systems and not identical to previous reports (Bai et al, 2008; Hoe

et al, 2009; Hoe et al, 2006). Further, each ligand tested turned out to inhibit cleavage rather than stimulate α- or β-secretase processing. Thus, while Reelin, Lingo-1, and Pancortin may have important implications for APP processing and function, I do not find solid evidence that a 'classic' ligand for APP has been identified by the field. While the candidates I chose to study in my assays were prioritized based on those with the strongest data reported by the most groups, there remain other published candidates to be validated. In addition, future studies should continue to focus on identifying novel candidate ligands with much more emphasis on confirming direct interactions using in vitro binding assays and confirming effects on APP processing and function in more physiological systems with more careful quantification and controls. These studies and those outlined throughout Chapter 4 are needed to better define the mechanisms regulating the processing and the basic functions of this conserved and ubiquitously expressed protein and to better understand the consequences of chronically altering its proteolytic processing in older humans with AD-type cognitive syndromes.

References

Bai Y, Markham K, Chen F, Weerasekera R, Watts J, Horne P, Wakutani Y, Bagshaw R, Mathews PM, Fraser PE, Westaway D, St George-Hyslop P, Schmitt-Ulms G (2008) The in vivo brain interactome of the amyloid precursor protein. *Mol Cell Proteomics* **7:** 15-34

Clarris HJ, Cappai R, Heffernan D, Beyreuther K, Masters CL, Small DH (1997) Identification of heparin-binding domains in the amyloid precursor protein of Alzheimer's disease by deletion mutagenesis and peptide mapping. *J Neurochem* **68:** 1164-1172

Colombo A, Wang H, Kuhn P-H, Page R, Kremmer E, Dempsey P, Crawford H, Lichtenthaler S (2012) Constitutive α- and β-secretase cleavages of the amyloid precursor protein are partially coupled in neurons, but not in frequently used cell lines. *Neurobiology of disease* **49C:** 137-147

Esko J, Stewart T, Taylor W (1985) Animal cell mutants defective in glycosaminoglycan biosynthesis. *Proceedings of the National Academy of Sciences of the United States of America* **82:** 3197-3398

Hoe H-S, Lee K, Carney R, Lee J, Markova A, Lee J-Y, Howell B, Hyman B, Pak D, Bu G, Rebeck G (2009) Interaction of reelin with amyloid precursor protein promotes neurite outgrowth. *J Neurosci* **29:** 7459-7532

Hoe H-S, Rebeck G (2008) Functional interactions of APP with the apoE receptor family. *J Neurochem* **106:** 2263-2271

Hoe HS, Tran TS, Matsuoka Y, Howell BW, Rebeck GW (2006) DAB1 and Reelin effects on amyloid precursor protein and ApoE receptor 2 trafficking and processing. *J Biol Chem* **281:** 35176-35185

Hoe HS, Wessner D, Beffert U, Becker AG, Matsuoka Y, Rebeck GW (2005) F-spondin interaction with the apolipoprotein E receptor ApoEr2 affects processing of amyloid precursor protein. *Mol Cell Biol* **25:** 9259-9268

Lidholt K, Weinke J, Kiser C A single mutation affects both N-acetylglucosaminyltransferase and glucuronosyltransferase activities in a Chinese hamster ovary cell mutant defective in heparan. *Proceedings of the*

Lindahl U (2007) Heparan sulfate-protein interactions--a concept for drug design? *Thrombosis and haemostasis* **98:** 109-124

Luo L, Tully T, White K (1992) Human amyloid precursor protein ameliorates behavioral deficit of flies deleted for Appl gene. *Neuron* **9:** 595-605.

Mok S, Sberna G, Heffernan D, Cappai R, Galatis D, Clarris H, Sawyer W, Beyreuther K, Masters C, Small D (1997) Expression and analysis of heparin-binding regions of the amyloid precursor protein of Alzheimer's disease. *FEBS Lett* **415:** 303-310

Moreno T, Bronner-Fraser M (2005) Noelins modulate the timing of neuronal differentiation during development. *Developmental biology* **288:** 434-481

Nakaya N, Sultana A, Lee H-S, Tomarev S (2012) Olfactomedin 1 interacts with the nogo a receptor complex to regulate axon growth. *J Biol Chem* **287:** 37171-37184

Narindrasorasak S, Lowery D, Gonzalez-DeWhitt P, Poorman R, Greenberg B, Kisilevsky R (1991) High affinity interactions between the Alzheimer's beta-amyloid precursor proteins and the basement membrane form of heparan sulfate proteoglycan. *J Biol Chem* **266:** 12878-12961

Shariati S, Lau P, Hassan B, Müller U, Dotti C, De Strooper B, Gärtner A (2013) APLP2 regulates neuronal stem cell differentiation during cortical development. *Journal of Cell Science*

Small D, Nurcombe V, Reed G A heparin-binding domain in the amyloid protein precursor of Alzheimer's disease is involved in the regulation of neurite outgrowth. *The Journal of*

Tan K, Duquette M, Liu J-h, Lawler J, Wang J-h (2008) The crystal structure of the heparin-binding reelin-N domain of f-spondin. *Journal of molecular biology* **381:** 1213-1236

Young-Pearse T, Suth S, Luth E, Sawa A, Selkoe D (2010) Biochemical and functional interaction of disrupted-in-schizophrenia 1 and amyloid precursor protein regulates neuronal migration during mammalian cortical development. *The Journal of neuroscience : the official journal of the Society for Neuroscience* **30:** 10431-10471

Young-Pearse TL, Bai J, Chang R, Zheng JB, Loturco JJ, Selkoe DJ (2007) A Critical Function for beta-Amyloid Precursor Protein in Neuronal Migration Revealed by In Utero RNA Interference. *J Neurosci* **27:** 14459-14469

Appendix 1

In utero Electroporation followed by Primary Neuronal Culture for Studying Gene Function in Subset of Cortical Neurons

Heather C. Rice, Seiyam Suth, William Cavanaugh, Jilin Bai,

and Tracy L. Young-Pearse

Video Article

In utero Electroporation followed by Primary Neuronal Culture for Studying Gene Function in Subset of Cortical Neurons

Heather Rice[1], Seiyam Suth[1], William Cavanaugh[1], Jilin Bai[2], Tracy L. Young-Pearse[1]

[1]Center for Neurologic Diseases, Brigham and Woman's Hospital and Harvard Medical School
[2]Department of Physiology and Neurobiology, University of Connecticut

Correspondence to: Tracy L. Young-Pearse at tyoung@rics.bwh.harvard.edu

URL: http://www.jove.com/details.php?id=2103
DOI: 10.3791/2103

Keywords: Neuroscience, Issue 44, In utero electroporation, cortical neurons, neurite outgrowth, migration, neuroscience, development, brain,

Date Published: 8/10/2010

Citation: Rice, H., Suth, S., Cavanaugh, W., Bai, J., Young-Pearse, T.L. In utero Electroporation followed by Primary Neuronal Culture for Studying Gene Function in Subset of Cortical Neurons. J. Vis. Exp. (44), e2103, DOI : 10.3791/2103 (2010).

Abstract

In vitro study of primary neuronal cultures allows for quantitative analyses of neurite outgrowth. In order to study how genetic alterations affect neuronal process outgrowth, shRNA or cDNA constructs can be introduced into primary neurons via chemical transfection or viral transduction. However, with primary cortical cells, a heterogeneous pool of cell types (glutamatergic neurons from different layers, inhibitory neurons, glial cells) are transfected using these methods. The use of *in utero* electroporation to introduce DNA constructs in the embryonic rodent cortex allows for certain subsets of cells to be targeted: while electroporation of early embryonic cortex targets deep layers of the cortex, electroporation at late embryonic timepoints targets more superficial layers. Further, differential placement of electrodes across the heads of individual embryos results in the targeting of dorsal-medial versus ventral-lateral regions of the cortex. Following electroporation, transfected cells can be dissected out, dissociated, and plated *in vitro* for quantitative analysis of neurite outgrowth. Here, we provide a step-by-step method to quantitatively measure neuronal process outgrowth in subsets of cortical cells.

The basic protocol for *in utero* electroporation has been described in detail in two other JoVE articles from the Kriegstein lab [1, 2]. We will provide an overview of our protocol for *in utero* electroporation, focusing on the most important details, followed by a description of our protocol that applies *in utero* electroporation to the study of gene function in neuronal process outgrowth.

Video Link

The video component of this article can be found at http://www.jove.com/details.php?id=2103

Protocol

The basic protocol for *in utero* electroporation has been described in detail in another JoVE article from the Kriegstein lab [1, 2]. This technique was originally described in the Osumi lab [3] and our protocol is based upon one developed in the LoTurco lab [4]. We will provide an overview of the our protocol for *in utero* electroporation of rat embryos, focusing on the most important details, followed by a description of our protocol that applies *in utero* electroporation to the study of gene function in neuronal process outgrowth.

1. *In utero* Electroporation

1. **Preparing DNA and loading needles**
   The first step for *in utero* electroporations is to design your experiment to determine what DNA constructs you want to inject. This method is useful for both misexpressing or knocking down genes of interest. If you are planning on misexpressing or overexpressing a gene, be sure to use a promoter that is active in neuronal precursor cells. We recommend the CAGGS promoter, which consists of the chicken beta-actin promoter and the CMV enhancer [5]. Since only a small subset of cells are transfected using *in utero* electroporation, it is critical to include a plasmid encoding a fluorescent protein such as GFP so that you can follow those cells that were successfully electroporated. For the plasmid encoding GFP, we recommend preparing the DNA at a concentration of 0.5 µg per microliter. For shRNA constructs, we have found that 0.5-1.0 µG per µL results in efficient knock down of your gene of interest. For overexpression or misexpression, we use between 1.0 and 3.0 µG per microliter, depending upon the size of the gene and the level of expression that the experiment calls for. DNAs are prepared using a Qiagen endotoxin-free prep kit, and diluted in 1 x PBS. We inject approximately 0.5-1.0 µL per embryonic brain, so, for a litter of animals we prepare 10 µL of DNA mixture for injection. We add 1 µL of Fast Green to the DNA so that we can follow the injected DNA.
   Pulling needles to the correct shape is a critical step. Walantus *et al.* uses a different system for delivering the DNA and so their needle prep is also slighly different then ours[1,2]. The settings that you use to pull your needles will depend upon the brand of needle puller that you have. We use Model 750 from David Kopf. The settings we use are : Heat 1: 9.0, Heat 2: 0, Soleniod: 0, Filament size 3.0 mm, Heater Proximity: 3 mm, Time: 10 sec. Once pulled, we cut our needles with a razor blade at a ~45 degree angle such that the distance from the largest part of the opening to the tip is 11 mm. We then load the DNA from the back end of the needle. We then fill the remaining space in the needle with corn oil. For DNA injection, we use a Picospritzer III. Depending upon the exact bevel that is cut for each needle, we set the Picospritzer from 4.0 to 6.0. We use a foot pedal to deliver the pressurized air that expels the DNA from the needle.
2. **Preparing animals for surgery**
   We use pathogen-free Sprague Dawley rats exclusively for these surgeries. Several other labs use mice of varying genotypes as well. Here, we describe show our protocol for electroporation of E15 rat embryos, but *in utero* electroporation is routinely performed in rats between the

ages of E13 and E18. While early stage electroporation targets deep layers of the cortex, later stage electroporations target more superficial layers.
Animals are given a pre-operative dose of buprenorphine (0.05-0.1 mg/kg) before the surgery starts. There are multiple options for anesthetizing the animal. Walantus *et al.* utilizes isofuorane inhalation, while we routinely use intraperitoneal injection of ketamine (40-80 mg/kg) and xylazine (5-10 mg/kg)[1,2]. A toe pinch should always be performed to ensure that animals are fully anesthetized and unresponsive. Animals are kept on a heated pad throughout the surgical procedure.
The animal's fur is shaved in the region of incision, and washed three times with ethanol followed by three times with iodine. An incision is made in the skin just lateral to the midline, followed by an incision in the muscle. The uterine horns are exposed very carefully. They are gently teased out of the body cavity using your fingertips. Keep embryos hydrated with sterile PBS while they are outside of the body cavity.

3. **Injecting DNA and electroporation**
When you first start performing these surgeries, the hardest part is becoming familiar with where you need to inject the DNA so that you fill the lateral ventricles, and getting used to how deep you inject your needle in order to hit the correct region. Embryos are gently manipulated with your fingertips so that you can identify where the head is, and if you look closely you will be able to see the midline suture. This serves as a general landmark that you can use to determine where the lateral ventricle is located. We inject the DNA through the uterine wall and into the lateral ventricle. We use a footpedal to control the injection of the DNA - multiple pulses of DNA are performed until the lateral ventricle is filled with the DNA/dye mixture. We then place paddle electrodes on either side of the head of the embryo and use another footpedal to deliver the pulse across the head of the embryo. The placement of the electrodes is critical in determining which region of the cortex is electroporated. Since DNA is negatively charged, the DNA will travel toward the positive electrode when a charge is dispelled across the paddles. Depending on the exact placement of the electrodes, different subsets of cells will be targeted. We routinely place the positive electrode near the dorsal-medial positions across the cerebrum. However, the LoTurco lab beautifully showed that if you place the electrodes in more ventral lateral regions of the cerebrum you can target the cells of the cortical-striatal boundary and hit cells of the lateral cortical stream [6]. Each embryo can be electroporated, and different combinations of DNA constructs can be used in each embryo.
4. **Suturing and post-operative care**
Following electroporation of all embryos, the uterine horns are carefully returned to the body cavity, and both the muscle layer and the skin are sutured. The technique for this is outlined in Walantus *et al*[1,2]. Animals are monitored continuously until they recover from anesthesia, and the analgesic buprenorphine (0.05-0.1 mg/kg) is administered every 8-12 hours.

2. Culturing Electroporated Cortical Neurons

1. **Harvesting electroporated brains and dissecting electroporated region**
For *in vivo* analyses following *in utero* electroporation, animals can be harvested at any time point from 24 hours following electroporation to early after birth to adulthood. However, when culturing primary neurons we harvest 24 hours following electroporation at E16. At this time, the electroporated embryos are expressing detectable levels of GFP.
Animals are euthanized using carbon dioxide inhalation and rapid decapitation. Embryos are dissected out of the uterus and placed in HBSS with divalent cations, keeping track of which embryos were electroporated with which DNA plasmids. It is critical to use filtered HBSS, sterile tubes and plates, and autoclaved tools for dissection. The cortices are dissected out and the meninges removed using a microscope in a hood. These cortices are then observed under a dissecting microscope with the capacity to visualize GFP. GFP positive regions of the cortex are identified, and we ue a pair of vanna scissors to cut out the GFP positive regions from the cortex. These pieces are placed in HBSS without divalent cations in a 15 ml conical tube.
2. **Dissociating and plating neurons**
Once all GFP positive regions are dissected, HBSS is replaced with 0.25% trypsin, and incubated at 37 degrees for 5 minutes. Trypsin is removed, replaced with plating media (DMEM + 5% FBS + Penn/strep + glutamine), and triturated 5-7 times to dissociate the cells. Volumes used depend upon the amount of tissue present. Dissociated cells are then plated on CC2 coated chamber slides. For two chamber slides, we plate 200,000-350,000 cells per chamber in a volume of 1.5 mL of plating media. After 4 hours, plating media is aspirated and replaced with 1.5 mL Neuronal culture media (Neurobasal media + B27 supplement + glutamax + gentamycin) per chamber.

3. Analyzing Neuronal Process Outgrowth

1. **Fixing and immunostaining cultures**
In order to measure short term effecs of genetic manipulation of these cells, we harvest the primary neurons after three days *in vitro*. If primary neurons are to be cultured longer for additional analyses, half of the media should be replaced every three days. For fixing cultures, we aspirate the media from the chambers, and fix the neurons in 4% paraformaldhyde for 15 minutes. Following fixation, cells are washed two times in PBS and then put in blocking solution (2% donkey serum with 0.1% Triton X-100 in PBS) for one hour. Cells are then incubated in primary antibody for 1 hour. For analyses of neuronal process outgrowth, we use anti-beta tubululin antibody to identify neurons - beta II tubulin immunostaining labels the neruonal cell body, dendrites and axons. Cells are then washed three times in PBS for five minutes, and then incubated in Cy3-anti mouse for 1 hour, followed by three more PBS washes, counterstaining nuclei with DAPI and mounting.
2. **Measuring neurite length**
Images of GFP positive, beta-III tubulin positive neurons are acquired on a Zeiss Axioskop with a MC100 camera system. Several variables can be examined in these GFP positive cells including length of all neurites, length of the longest neurite, branching of neurites, size of cell soma, etc. We have used this method to analyze neuronal process outgrowth upon knock down or overexpression of genes relating to neurodevelopment and neurodegeneration, with a focus on neuronal process length. In order to measure neuronal processes outgrowth, we use Axiovision LE 4.4 software (from Zeiss). Within this software, there is an option to select the "outline" tool. Using this tool, you can use your computer's mouse to trace the length of each neuronal process. It is critical to define the objective that you are using in order to get an accurate measure of your neurites. For these analyses, we usually use a 20x objective.

4. Representative Results

We have found that Sprague Dawley litter size ranges between 6 and 14 embryos. We usually electroporate all of the embryos. Each embryo can be electroporated with a different combination of DNAs. However, we usually electroporate at least four brains with the same condition and pool these brains before dissociating and plating.

We have found that with this technique approximately 75% of electroporated brains are targeted to the desired region of the cortex, whether that be dorsal medial or ventral lateral cortex (Figure 1). In addition, we have found early electroporations at E13-14 target deep layer neurons such as Tbr1 positive layer VI neurons, while later electroporations target CTIP2 positive, TBR1 negative layer V cells, and still later electroporations

target Brn2 positive layer II/III cells. An excellent description of different markers and explanation of neuronal subtype specification in the cortex in found an article by Moleneaux et al [7]. Figure 2 shows coronal sections of brains electroporated at either embryonic day 15.5 or 17.5 and harvested at postnatal day 5. Shown in red is immunostaining for Oct6. You can immunostain for markers in culture to confirm what cell layer populations you have targeted. We have found that you can expect to target the same cell layer population of cells in every embryo of the same litter (in other words, the targeting depends upon the embryonic timepoint rather then on other technical variations).

In culture, the percent of cells that are GFP positive can range widely depending on how conservative you are when dissecting out the GFP positive region (Figure 3). However, even when we are very conservative and dissect out only the GFP positive patch of cells, the highest percentage that we observe is 5-10% - although you are dissecting the region of the cortex that was electroporated, cells in only one layer will be targeted. This low transfection effciency is helpful in identifying which processes belong to the electoporated cell that you are analyzing. Plating cells at this higher density contributes to having heathier cultures, however, it is difficult to discern which process belongs to which cell body in the GFP negative cells (Figure 3).

If you have trouble seeing all of the fine processes of the electroporated cells, you can either increase the concentration of GFP DNA that you are electroporating to increase expression of GFP, or you can immunostain the dissociated cells using an anti-GFP antibody (from Invitrogen) along with a Cy2 secondary antibody.

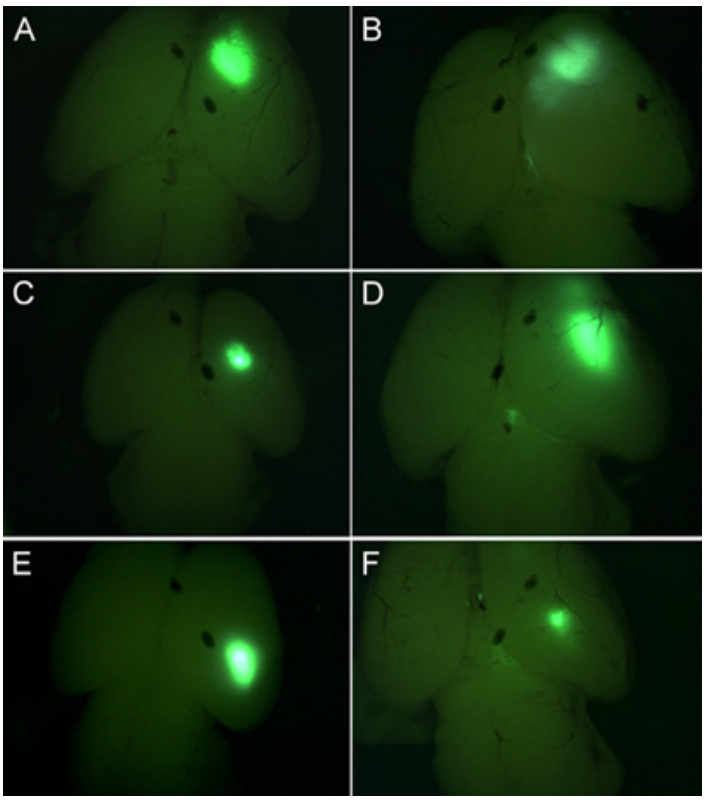

Figure 1. E15.5 Sprague-Dawley rats were electroporated with GFP plasmid and harvested three days later. Based upon the placement of the electrodes, different regions of the cortex will be targeted. A-F show GFP fluorescence in whole brains.

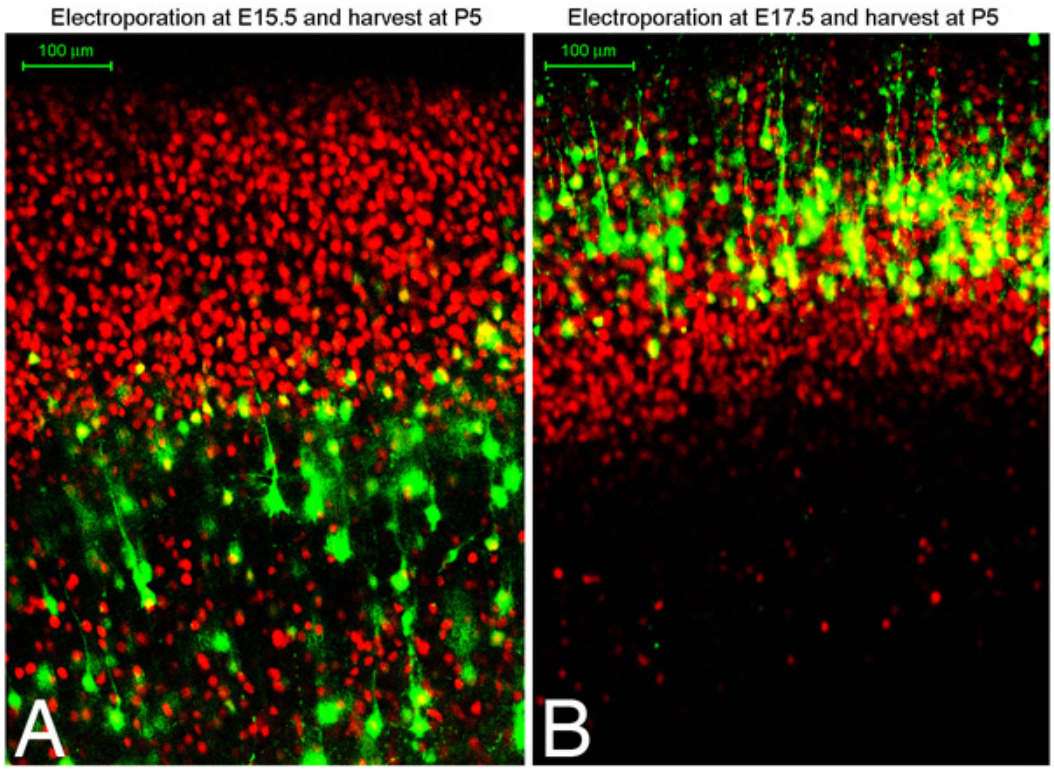

Figure 2. E15.5 (A) or E17.5 (B) Sprague-Dawley rats were electroporated with GFP plasmid and harvest at postnatal day 5. Brains were fixed, sectioned coronally using a vibratome (100 micron sections), and immunostained for Oct6 (red). A and B show confocal images of immunostained sections.

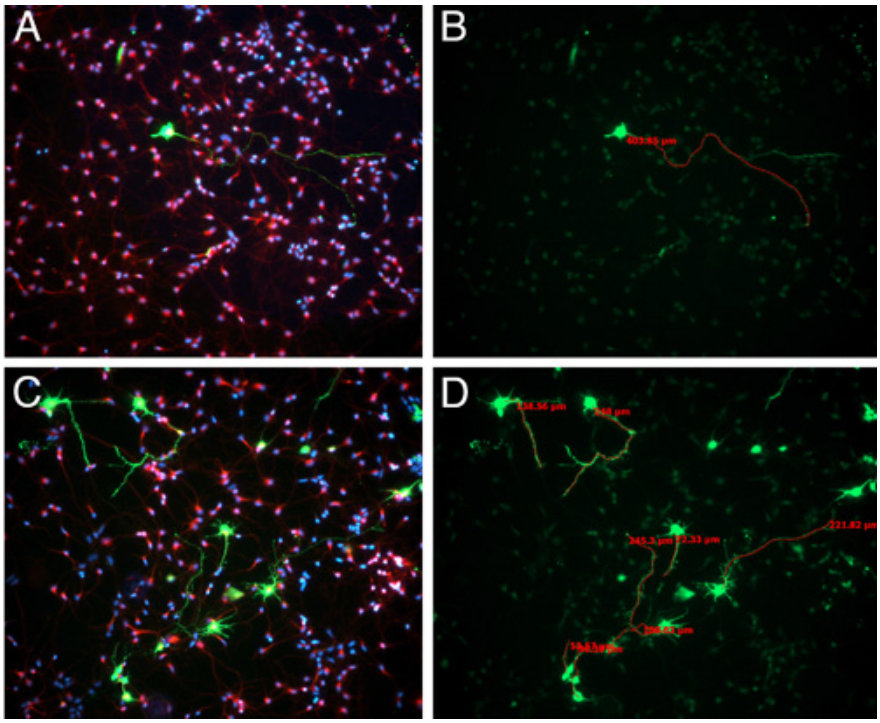

Figure 3. E15.5 Sprague-Dawley rats were electroporated with GFP plasmid. 24 hours following electroporation, brains were harvested and GFP-positive, electroporated regions were dissected and dissociated, as described in the video. After 3 days in vitro, cells were fixed and immunostained for bIII-tubulin (red) and staining nuclei with DAPI (blue) (A,C). The length of the longest neurite was measured using Axiovision software (B,D).

Discussion

In vitro study of primary neuronal cultures allow for quantitative analyses of neurite outgrowth. In order to study how genetic alterations affect neuronal process outgrowth, shRNA or misexpression constructs can be introduced into primary neurons via chemical transfection or viral transduction. However, with primary cortical cells, a heterogeneous pool of cell types (glutamatergic neurons from different layers, inhibitory neurons, glial cells) are transfected using these methods. The use of *in utero* electroporation to introduce DNA constructs in the embryonic rodent cortex allows for certain subsets of cells to be targeted: while electroporation of early embryonic cortex targets deep layers of the cortex,

electroporation at late embryonic timepoints targets more superficial layers. Further, differential placement of electrodes across the heads of individual embryos results in the targeting of dorsal-medial versus ventral-lateral regions of the cortex.

Targetting of specific layers:

When you inject DNA into the lateral ventricle and electroporate, only the cells immediately lining the lateral venrtricle are targeted: these cells are the radial glial progenitor cells of the neocortex, as well as cells that have just undergone their terminal mitosis. Interestingly, when examined in the days following electroporation, the cells targeted match the pattern of birthdated cells. In other words, cells that are born , that is to say those that undergo their terminal mitosis on the day of electropoartion, are the cells that are targeted. Since radial glial cells also are present at the ventricular surface, one might hypothesize that these cells would be targeted, and that all of the progeny from these cells would also be targeted. However, this is not the case, later generations of cells do not express GFP. It may be that multiple rounds of division in the radial glial cells dilutes out the plasmid.

Applications:

This method is an excellent way to examine the effects of gene knock down via electroporation of shRNA contructs, as well as by misexpression of cDNA constructs. We are applying this techniqe to the study of genes involved in neurodegeneration and psychiatric disease. Through this technique, we introduce both wild type and mutant forms of genes critical in these diseases, and examine the effects on neuronal morphology. In addition, we can examine the effects of mutation or alternative splice variant expression in the absence of the endogenous gene product by co-electroporating the cDNA and the shRNA contruct. Co-electorporation also can be utilized to look at genetic interactions between two gene products: by knocking down multiple genes and by attempting to rescue effects of knock down of one gene product with other gene products [8, 9].

Disclosures

No conflicts of interest declared.

Acknowledgements

The authors would like to thank Joseph LoTurco and Dennis Selkoe for helpful discussions on this technique. The authors thank the donors of the American Health Assistance Foundation, for support of this research.

References

1. Walantus, W., Castaneda, D., Elias, L., & Kriegstein, A. *In utero* intraventricular injection and electroporation of E15 mouse embryos. *J Vis Exp* (6): 239 (2007).
2. Walantus, W., Elias, L., & Kriegstein, A. *In utero* intraventricular injection and electroporation of E16 rat embryos. *J Vis Exp*, (6): 236 (2007).
3. Takahashi, M., Sato, K., Nomura, T., & Osumi, N. Manipulating gene expressions by electroporation in the developing brain of mammalian embryos. *Differentiation* 70(4-5): 155-62 (2002).
4. Bai, J., Ramos, R.L., Ackman, J.B., Thomas, A.M., Lee, R.V., & LoTurco, J.J. RNAi reveals doublecortin is required for radial migration in rat neocortex, in Nat Neurosci. 1277-83 (2003).
5. Okada, A., Lansford, R., Weimann, J.M., Fraser, S.E., & McConnell, S.K. Imaging cells in the developing nervous system with retrovirus expressing modified green fluorescent protein. Exp Neurol. 156(2): 394-406 (1999).
6. Bai, J., Ramos, R.L., Paramasivam, M., Siddiqi, F., Ackman, J.B., & LoTurco, J.J. The role of DCX and LIS1 in migration through the lateral cortical stream of developing forebrain, in Dev Neurosci 144-56 (2008).
7. Molyneaux, B.J., Arlotta, P., Menezes, J.R., & Macklis, J.D. Neuronal subtype specification in the cerebral cortex. *Nat Rev Neurosci* 427-37 (2007).
8. Young-Pearse, T.L., Bai, J., Chang, R., Zheng, J.B., Loturco, J.J., & Selkoe, D.J. A Critical Function for -Amyloid Precursor Protein in Neuronal Migration Revealed by In Utero RNA Interference. J Neurosci 27(52): 14459-14469 (2007).
9. Young-Pearse, T.L., Chen, A.C., Chang, R., Marquez, C., & Selkoe, D.J. Secreted APP regulates the function of full-length APP in neurite outgrowth through interaction with integrin beta1. Neural Develop 3: 15 (2008).

Appendix 2

Human iPSC-derived neurons reveal novel effects of a familial Alzheimer's disease (fAD) APP mutation and show cell fate-specific AD relevant phenotypes

Christina Muratore, Heather C. Rice, Priya Srikanth, Lawrence Benjamin,

Dennis J. Selkoe and Tracy L. Young-Pearse

Abstract

Alzheimer's disease (AD) is a complex neurodegenerative disorder characterized by extracellular plaques containing amyloid β-protein (Aβ) and intracellular tangles containing hyperphosphorylated Tau protein. Distinct brain regions are differentially susceptible to neurodegeneration in AD, with the cortex and hippocampus being primarily affected and the cerebellum and spinal cord being relatively spared. While familial AD (fAD) comprises <1% of cases, analyses of these patients have advanced understanding of molecular mechanisms and therapeutic approaches for all AD cases. Here, we describe the first generation of inducible pluripotent stem cells (iPSCs) from humans harboring the London fAD APP mutation (V717I), and examine AD-relevant phenotypes following directed differentiation of these cells to rostral forebrain neuronal fates vulnerable in AD, as well as more caudal fates, which are relatively spared in AD. In all fates examined, the APP V717I mutation led to elevated production of Aβ42 and Aβ38. Unexpectedly, this mutation, which lies near the γ-secretase cleavage site in the transmembrane domain of APP, also led to increased β-secretase cleavage of APP. This increase was abolished by inhibiting γ-secretase, suggesting that the two protease activities are functionally linked. Interestingly, directing cells to different neuronal fates resulted in altered cleavage patterns of APP. From both control and fAD lines, Aβ generated from neurons directed to forebrain cortical fates showed a higher Aβ42 to Aβ40 ratio relative to neurons directed to more caudal fates of the hindbrain and spinal cord. Moreover, consistent with fate-specific biochemical effects on Aβ, the APP V717I mutation led to increased Tau expression in forebrain cultures but not in more caudally directed neurons. These studies identify previously unappreciated effects of an fAD APP mutation in human neurons and demonstrate that human iPSC technology provides a powerful system for analyzing the effects of both genetic alterations and cell types on processes directly relevant to human brain diseases.

Introduction

Alzheimer's disease (AD) is a common and devastating dementia that is pathologically defined by the accumulation of extracellular Aβ-containing amyloid plaques and intraneuronal hyperphosphorylated Tau protein aggregates associated with neuronal loss in the cerebral cortex. Over 200 known missense mutations in APP or the Presenilin-1 and -2 genes (PSEN1/2) can cause dominantly inherited, early-onset forms of AD, termed familial AD (fAD) (reviewed in [1]). The catalytic site of γ-secretase activity resides within PSEN[2], and APP is cleaved within its transmembrane domain by the PSEN/γ-secretase complex to generate Aβ species primarily of 42, 40, or 38 amino acid lengths[3]. The fAD mutations in APP or PSEN have been shown to either increase Aβ production generally or to increase the ratio of Aβ42 to Aβ40 peptides (reviewed in[1,4]). These genotype-to-phenotype relationships provide strong evidence that Aβ42 plays a causal role in at least some cases of AD.

APP V717I was the first mutation linked to fAD[5] and is the most common fAD APP mutation[6]. Residue 717 resides in the transmembrane domain of APP, near the γ-secretase cleavage site. Previous studies have shown that transfection of APP cDNA with the V717I mutation results in an increase in the ratio of Aβ42/40 generated in cell lines[7] and mouse primary neurons[8]. Brain lysates from transgenic mice expressing human APP V717I also showed an increased Aβ42/40 ratio[9,10]. In most studies, the increased ratio of Aβ42/40 is mainly attributable to an increase in

Aβ42 with no effect or a slight decrease of Aβ40. Importantly, both plasma and lysates of brains of patients carrying APP V717I have shown elevated Aβ42 levels relative to total Aβ, confirming the effect of this mutation on Aβ42 levels in the subjects of interest[11,12].

Rapid advancements in stem cell biology in recent years have provided neuroscientists with a unique opportunity to examine the effects of genetic alterations in disease-relevant human cell types. Previously, analyses of risk genes for neurological diseases were primarily limited to research on postmortem brains, mouse models, and heterologous cell lines. With the advent of induced pluripotent stem cell (iPSC) technology[13–17] it is now possible to study genetic risk factors in neurons derived from primary cells of affected subjects[18]. Two recent studies showed that neurons derived from iPSCs generated from subjects with APP duplication or triplication (including from a Down's syndrome line) secreted higher levels of Aβ and developed increased levels of Tau phosphorylated at Thr231[19,20]. In another study, iPSC lines were derived from two fAD subjects, one harboring a mutation in PSEN1 and another in PSEN2[13]. This study showed that each mutation increased secretion of Aβ42 and that γ-secretase inhibitors and modulators effectively decreased Aβ generation[13]. Additionally, another study using direct conversion of PSEN1 and PSEN2 fibroblasts into neurons showed an increase in total Aβ as well as an increase in the Aβ42 to 40 ratio, with γ-secretase inhibitors decreasing production of Aβ[21]. These first studies utilizing iPSCs to study AD provided an important proof-of-principle regarding the utility of such cells to model biochemical processes relevant to AD.

Here, we establish an independent cell model of AD using iPSCs from subjects harboring a dominant point mutation in APP (V717I) that causes fAD. Further, we take advantage of the unique property of stem cells to generate multiple neuronal types in order to address, for the first time, key questions regarding how developmental cell state and cell fate affects cleavage of APP by the α-, β-, and γ-secretases to generate APPsα, APPsβ and Aβ. In neurons of forebrain fate derived from human iPSCs, we confirm the previous finding that the V717I mutation leads to increased Aβ42 levels, and identify additional effects of this mutation on Aβ38 and APPs-β generation. In addition, we show that APP cleavage is altered in neurons directed to a rostral, cortical fate relative to neurons directed to more caudal neuronal fates of the hindbrain and spinal cord. APP V717I neurons express higher levels of Tau protein relative to wild type neurons when directed to rostral neuronal fates, but not when directed to a caudal neuronal fate. Interestingly, cortical and hippocampal cells are the most affected neuronal fates in Alzheimer's disease, and the data presented here may provide insights into the mechanisms of the differential susceptibility observed in the disease.

Results

Generation and differentiation of iPS cell lines with the London (V717I) APP mutation

Skin biopsies were obtained from a father and daughter each harboring a mutation in APP (V717I) (Fig.1A). The father was 57 years old and was diagnosed with Alzheimer's disease while the daughter remained asymptomatic at age 33 (Fig.1A). Fibroblasts from the biopsy were reprogrammed using lentiviruses encoding Oct4, SOX2, cMYC and KLF4, and three iPSC clones from each subject were established and characterized by the Harvard Stem Cell Institute (HSCI) iPSC core facility (Supp. Fig. S1). All clones maintained stem cell morphology,

expressed the pluripotency-associated genes OCT4, NANOG, SSEA3, SSEA4, TRA-1-60, and Alkaline Phosphatase, repressed retroviral transgenes, and could be differentiated into cells of ectodermal, mesodermal, and endodermal lineages *in vitro* (Supp. Fig. S1A, B, C). All clones from the daughter (fAD2) displayed a normal euploid karyotype (Supp. Fig. S1D), while all clones from the father (fAD1) displayed a normal chromosome number, but a balanced (t(1;12)(q42.1;q15)) translocation in all cells from four clonal lines (Supp. Fig. S1E). The fibroblasts obtained from this subject displayed the same abnormal karyotype, suggesting that this was a preexisting abnormality that did not arise during the reprogramming process.

Because variability exists in the differentiation efficiency among pluripotent stem cell lines, we first compared the capacity of each line to differentiate to neuronal fates. In order to direct the differentiation of these cells to forebrain neuronal fates, we utilized an embryoid body-based protocol[22] (with modifications described in Methods). Using this method, cultures highly enriched in cells expressing neuronal markers were generated, with over 90% of the cells expressing MAP2 in each well (Fig. 1C). Initial characterizations of each clone for differentiation capacity informed the selection of two clones from each subject to be further analyzed. In parallel, differentiation experiments were performed with iPSC lines generated from healthy donors, which were obtained from the HSCI iPSC Core and from the UCONN Stem Cell Core (Fig. 1A). No significant differences were observed in differentiation capacity between the control and fAD cell lines, as assayed by immunostaining for the general neuronal markers MAP2, Tau and TUJ1, synaptic markers synapsin, PSD95 and VGLUT1, and markers of upper (Cux1) and lower (Tbr1) layer cortical neurons (Fig. 1C). To provide a more quantitative analysis of differentiation capacity over multiple clones and rounds of differentiation, NanoString analyses were performed with a custom designed probe set measuring 150 genes. Quantitative comparison of control and fAD lines showed no significant differences in expression of general neuronal markers (Fig. 1D) or markers of cell fate (Fig. 1E).

Cleavage of APP by α-, β- and γ-secretases in fAD and control stem cell-derived neurons

Multiple studies in non-neuronal cell lines and transgenic mice overexpressing the APP V717I mutation report that this mutation alters γ-secretase cleavage of APP to generate higher levels of Aβ42[1,3,5,7,8,11,12,23] . Here, we aimed to examine the effects of this mutation expressed from the endogenous APP gene in human neuronal cells. Human iPSC lines were differentiated to neuronal phenotypes using the protocol described above. At 40-50 days of differentiation, conditioned media were collected 48 hours after application for analysis of secreted APP cleavage products, and cells remaining in the well were lysed to collect RNA for expression analyses. NanoString analyses showed no significant differences in RNA expression between control and fAD lines for APP splice variants and APP family members (APLP1 and APLP2) (Supp. Fig. S2A). Furthermore, no significant changes were observed in expression of genes encoding α-secretases, β-secretases, or components of γ-secretase (Supp. Fig. S2B). However, Western blot analyses suggested that APP and Tau protein levels were higher in lysates of fAD APP V717I neurons relative to wild type neurons (Supp. Fig. S2C, D).

Conditioned media from days 40-50 of differentiation from control and APP V717I lines were analyzed to examine Aβ38, 40 and 42 levels using a multiplex ELISA. In agreement with data from previous studies using other experimental paradigms, neurons derived from each clonal line harboring this APP fAD mutation secreted Aβ with a higher ratio of 42 to 40 than

neurons from control lines (control 0.25 SD+/-0.05; fAD 0.39 +/- 0.10; Fig. 2B). Notably, the ratios observed here appear to be physiologically relevant, as published results examining Aβ in TBS-extracted human brain lysates showed a highly similar range of Aβ 42/40 ratio (0.25-0.42)[24]. Furthermore, the increase in ratio with the V717I mutation (1.6-fold) is highly similar to the previously reported ratio increase observed in the plasma of human subjects with the same mutation (1.7-fold)[12]. Here, data from each Aβ species show that this ratio change was primarily due to a 2-fold increase in production of Aβ42 (Fig. 2C-D, F-G, Supp. Fig. S3A-B). Interestingly, human neurons harboring the APP V717I mutation also secreted higher levels of Aβ38 (Fig. 2E,H, Supp. Fig. S3C). Accordingly, the calculated Aβ38 to 40 ratio was also significantly higher with the fAD mutation (data not shown). Thus, the precise site of γ-secretase cleavage is altered with V717I mutation in neuronal cells. Of note, the intra- and inter-clonal variability in Aβ secretion was quite low between wells and between experiments in both fAD and control cell lines (Fig. 2A). The variability observed was due in part to slight technical differences between rounds of differentiation, with differences between ELISA plates also contributing to the modest variability observed (Supp. Fig. 3D,E).

Prior to cleavage by γ-secretase, APP must first be cleaved by α- or β-secretase to release the large N-terminal fragment of APP, termed APPsα or APPsβ[25] (Fig. 1B). Cleavage by β-secretase prior to γ-secretase generates Aβ, while α-cleavage precludes Aβ generation. Because of the importance of these initial cleavage events in determining Aβ generation, we next examined whether the V717I APP fAD mutation affects α- and/or β-secretase cleavage of APP in a neuronal context. Surprisingly, fAD neurons secreted a lower ratio of APPsα to APPsβ relative to control neurons (Fig. 3A), and this decrease was due to a 1.4-fold increase in the production of APPsβ (Fig. 3B,C). This effect was not due to increased expression of β-secretase, as both NanoString and Western blot analyses showed no differences in RNA or protein levels of the genes encoding β-secretase activity (BACE 1 and 2) (Supp. Fig. S2A-C). In order to test whether γ-secretase activity is necessary for the enhancement of β-secretase cleavage of APP by V717I, differentiated neuronal cells from control and fAD mutant lines were treated with a low dose (5 μM) of a potent γ-secretase inhibitor (DAPT) for 48 hours. As expected, this treatment efficiently inhibited the production of Aβ38, 40, and 42 in both control and fAD neurons (Fig. 2F-H). Interestingly, inhibition of γ-secretase potently blocked the effect of V717I in increasing β-secretase cleavage of APP (Fig. 3E,F). Further, γ-secretase inhibition increased APPsα generation relative to APPsβ generation in control neurons (Fig. 3D-F). The effect on this ratio was dramatically greater in neurons harboring the APP V717I mutation. Taken together, these results suggest that β- and γ-secretase cleavages of APP are tightly linked processes, and that a single point mutation of APP near the γ-secretase cleavage site may alter both cleavage events. Of note, the effects of the APP V717I mutation, including increased β-secretase cleavage of APP and elevated Aβ38 and 42 generation, were confirmed in HEK cells following transient transfection with cDNAs encoding wild type or V717I human APP (Supp. Fig. S4).

Changes in APP processing across differentiation from stem cell to neuron

We next addressed whether the effects observed on APP cleavage varied as a function of cell fate. RNA and conditioned media were collected from control and fAD iPSCs at multiple time points during differentiation from stem cell to neuron, in order to assess whether and how progressive differentiation alters the secretion of APPsα, APPsβ and Aβ. As expected, over differentiation time, cells changed morphologically and lost expression of pluripotency markers (OCT4) while first turning on neuronal precursor markers (CyclinD1 and Nestin, not shown) and then markers of mature neurons (MAP2, TAU, VGLUT1, GAD1) (Fig. 4A-B). Over differentiation time from d0 to d100, Aβ secretion increased markedly in both control and fAD lines, and the fAD-dependent increase in Aβ38 and 42, caused by the V717I mutation, was observed consistently and significantly after day 40 (Fig. 4C-E). Accordingly, we observed higher Aβ42/40 ratios in fAD versus control lines, over the differentiation time-course, with statistical significance obtained beginning around day 24 (Fig. 4F). Furthermore, as cells became more neuronal in their RNA and protein expression profiles, there was a consistent and steady decrease in the ratio of APPsα to APPsβ secreted by these cells (Fig. 4I). While both APPsα and APPsβ increase over differentiation (in part due to an increase in APP expression (Fig. 4J)), there is a greater increase in APPsβ due to a robust increase in expression of BACE with neuronal differentiation (Fig. 4G, H, J). The effect of the APP V717I mutation in significantly elevating the β-secretase cleavage of APP was observed at all time points examined (Fig. 4H).

APP is differentially processed in human iPSCs directed to caudal versus rostral neuronal fates

Human iPSCs were directed to neuronal fates using the same general protocol described above. In order to direct the differentiation of these cells to caudal neuronal fates, retinoic acid (RA) and Sonic Hedgehog (Shh) were added to cultures at the neural progenitor stage between days 10-24 and 15-24 of differentiation, respectively (Fig. 5A). At day 40 of differentiation, conditioned media were collected and RNA or protein was harvested from the remaining cells in order to analyze gene expression (Fig. 5C-E, Supp. Fig. 5). Alternatively, remaining cells were fixed and immunostained for cell fate markers (Fig. 5B). Markers of general neuronal fate were unchanged when differentiation proceeded in the absence or presence of RA/Shh (Fig. 5B, C, Supp. Fig. S5A). However, markers of neuronal fates of the forebrain (cortical) were downregulated (Fig. 5B, left panel, 5D, Supp.Fig. S5B), while markers of more caudal (hindbrain/spinal cord) fates were upregulated (Fig. 5B middle, right panels, 5E, Supp. Fig. S5C,D). The gene showing the most significant upregulation with RA/Shh was HOXB4 (Fig. 5B,E). In the nervous system, HOXB4 is expressed in the spinal cord and hindbrain with no expression in the mid- and forebrain reported[26]. HB9, EN-1, and Irx3 also were upregulated, consistent with the presence of spinal cord interneurons and motor neurons in caudally directed cultures[27,28].

Neurons directed to caudal neuronal fates secreted more Aβ40 (Fig. 5F) relative to forebrain neuronal fates, which led to a decrease in the Aβ42/40 ratio in both control and fAD lines (Fig. 5G). Further, neurons with caudal fates secreted more APPsα and APPsβ relative to those of more rostral fates (Fig. 5I,J). However, in fAD lines this increase is more pronounced for APPsβ, resulting in a net decrease in the ratio of α- to β-cleavage of APP (Fig. 5H).

To determine whether iPSC-derived human neurons can reflect putative downstream

effects of the APP V717I mutation observed in AD patients, we quantified the levels and phosphorylation state of Tau. Neurons directed to forebrain neuronal fates and expressing the APP V717I mutation exhibited higher levels of Tau mRNA (Fig. 6A) and a 1.7 fold increase in protein levels (Fig. 6B, D, Supp. Fig. S2C,D) at both d40 and d100 of differentiation. At d100, APP V717I neurons exhibited higher levels of phospho-Tau at two different amino acids (S202 and S262). In the case of pS202, this increase was proportional to an increase in total Tau (Fig. 6B). However, when normalized to total Tau, pS262 was significantly elevated beyond the increase of total Tau expression observed (Fig. 6B, D, E). Importantly, the increases in total and phospho-Tau levels caused by the fAD mutation in forebrain neurons were no longer observed when neurons were directed to more caudal fates (Fig. 6D,E). Consistent with the data observed at day 40 (Supp.Fig. 2C, D), APP protein levels also were elevated in d100 cultures directed to a cortical fate (Fig. 6B, C). Similar to effects on Tau expression, neurons directed to a caudal fate did not show a significant increase in APP expression (Fig 6B-E).

Discussion

Aβ homeostasis plays a central role in the pathogenesis of AD[29]. Aβ is generated physiologically by sequential cleavages of APP by β- and γ-secretase. Cleavage by γ-secretase is imprecise and results in the generation of a variety of Aβ species varying in length between 36 and 43 residues. Aβ40 is the most abundant, followed by Aβ42 and 38[25,29]. Although Aβ42 is a minor form, the two extra amino acids (isoleucine and alanine) make this peptide more hydrophobic and prone to self-aggregation. It has been previously shown that fAD mutations in APP, PSEN1 or PSEN2 each act to either increase total Aβ levels or (more commonly) to increase the amount of Aβ42 relative to Aβ40 generated (reviewed in [3]). Here, we demonstrate that human neurons derived from iPSC lines established from subjects harboring one such mutation (V717I) generate significantly more Aβ42. The fold-increase in Aβ42/40 ratio reported here (1.6-fold) is highly similar to that observed in plasma from subjects with the V717I mutation (1.7-fold)[12]. We extend these findings to show that Aβ38 also is elevated, in accordance with the helical model of γ-secretase processivity within the transmembrane domain[30]. This model of APP cleavage describes stepwise cleavages of APP by γ-secretase, beginning with epsilon cleavage near the transmembrane-cytoplasmic interface to release Aβ of 48 or 49 residues[31]. These longer Aβ-like species are then cleaved every 3-4 amino acids along the transmembrane domain to generate smaller species, such that Aβ49 is cleaved to generate Aβ peptides of 46, 43 and 40 amino acids, whereas Aβ48 is similarly cleaved to generate Aβ peptides of 45, 42, and 38 amino acids[25,32]. In agreement with this processivity model, we observed an increase in both Aβ42 and 38 caused by the APP V717I mutation, suggesting that this mutation may primarily act to alter the initial epsilon site of cleavage within APP.

In addition to effects on the sites of γ-secretase cleavage within APP, we also describe an unexpected effect of this fAD mutation on β-secretase cleavage of APP. β-secretase activity is encoded by the genes BACE1 and BACE2[33–35],and expression of these genes is high in the CNS[35–37]. Human pluripotent cells provide a model system to examine the activity of these enzymes during simulated, *in vivo* human neuronal development. Here, we show a dramatic increase in β-secretase cleavage of APP as cells differentiate to neuronal fates. Moreover,

although the V717I mutation occurs at the site of the γ-secretase cleavages in the transmembrane domain of APP, a significant effect of this mutation on β-secretase cleavage of APP was observed at all differentiation time points examined. The increase was not due to indirect effects on BACE expression, as both RNA and protein levels of BACE were unchanged in the fAD neurons. One possible explanation is that the V717I mutation affects the position of APP within the membrane, which in turn affects both the site of epsilon cleavage of APP and the position of APP relative to the active site of BACE, which is a membrane-anchored protease that cleaves its substrates just outside of their transmembrane domains. α- or β-cleavage must occur prior to γ-secretase cleavage, as APP holoprotein cannot access the active site of γ-secretase. To examine whether γ-secretase activity was necessary for the effect of V717I mutation on β-secretase activity, we asked whether γ-secretase inhibition could rescue the effect of the APP V717I mutation on β-cleavage. Indeed, γ-secretase inhibition by DAPT prevented the effect of the V717I mutation in elevating β-secretase processing of APP. This was observed in both iPSC-derived human neurons and HEK cells confirming the novel observation and suggesting that these enzymatic activities are functionally interdependent. This result is in agreement with very recent evidence that these proteases may exist in a previously unrecognized complex and affect the activities of each other (Chen, Shepardson, Patel, Guo, Lehm, Rice, LaVoie and DJS, in preparation). Further studies are therefore warranted to examine whether other fAD mutations affect β-secretase cleavage of APP, in addition to their known effects on γ-secretase processivity.

The accumulation of Aβ in all AD brains, as well as the dominant effects of APP, PSEN1 and PSEN2 mutations in causing an accelerated but otherwise typical AD phenotype, point to Aβ being critical to pathogenesis. Accumulation of intraneuronal hyperphosphorylated Tau is a key feature observed in the AD brain. Multiple lines of evidence suggest that this pathological hallmark of AD can arise as a downstream result of accumulation of extracellular Aβ [20,38–40]. Here, we observed a significant increase in Tau protein levels in neurons of forebrain fate derived from APP V717I iPSCs. This indicates that increased Tau levels can result from the effects of an APP fAD mutation in a relatively simple neuronal cell culture system, thus connecting the two major abnormalities of AD pathogenesis. Notably, cultures of both wild type and fAD neurons of rostral or caudal fates remain healthy at d100 of differentiation, with no obvious cell death observed (data not shown). However, in contrast to other studies, which have shown an increase in death of primary rodent neurons in response to exogenously added Aβ, in this study the extracellular Aβ is cleared from the cultures every 2-3 days with full media changes. The use of this system provides the opportunity to further probe the initiating events in AD pathogenesis, namely, the generation of pathological Aβ and the accumulation of phosphorylated Tau, in the absence of frank cell loss, which is not observed until late stages of Alzheimer's disease.

The effects of the APP V717I mutation on the β- and γ-secretase processing of APP were observed in human iPSC-derived neurons from both fAD subjects as well as in HEK cells transfected with APP V717I cDNA, supporting the validity of using each of these models to study mechanisms relevant to AD. A powerful advantage of using human iPSCs, however, is the potential to direct the fates of these cells to any cell type. Therefore, iPSCs provide a unique opportunity to compare functional effects of endogenous genetic alterations between multiple

neural cell types derived from the same human donor. Importantly, distinct brain regions are differentially susceptible to neurodegeneration in AD, but the mechanistic basis for this is poorly understood. AD progression varies somewhat among subjects but often begins stereotypically with gradual loss of episodic declarative memory that correlates with synapse loss and neuritic/neuronal degeneration in the hippocampus and certain connected regions of the association neocortex (reviewed in [3]). Although APP, β-secretase and γ-secretase are each expressed in all neurons, some regions of the CNS outside of the limbic and cerebral cortices, such as cerebellum, thalamus, midbrain and spinal cord are relatively spared of amyloid plaque accumulation and local synapse/neuron loss[41]. Here, we exploited the pluripotent nature of stem cells to show that APP processing differs significantly in neurons having distinct cell fates both in wild-type and APP V717I lines. Our data suggest that neurons of a forebrain (cortical) fate, which are more affected in AD, secrete Aβ that has a higher level of the pathogenically critical Aβ42/40 ratio, than neurons with more caudal fates of the hindbrain and spinal cord. Interestingly, the increase in total Tau levels observed with the fAD mutation in cortically-directed cultures is not observed in neurons directed to a caudal fate. The observed ratio changes in our cell cultures and differences in cleavage products support the hypothesis that alterations in cleavage of APP in different neuronal subtypes may, in part, underlie the differential susceptibility observed in AD.

Taken together, the findings presented here provide several unexpected insights into the effects of APP fAD mutations on processing by the β- and γ-secretases. Furthermore, we provide evidence that APP is differentially cleaved in neurons of alternate fates and that different neuronal subtypes may respond differentially to an APP fAD mutation. Our work demonstrates the utility of iPSCs from human donors to model the differential neuronal susceptibility and downstream biochemical effects observed in AD, with related therapeutic implications.

Figure Legends

Figure 1. Characterization of the neuronal differentiation capacity of familial AD iPSC lines harboring the APP V717I mutation.
Human iPSC lines were derived from a father and daughter with an fAD mutation (APP V717I). A) Table summarizing human iPS lines used in this study. B) Schematic outlining α-, β-, and γ-secretase cleavage sites in APP. Residue in red is V717, those in blue encode wild type Aβ. C) Control and fAD lines were differentiated to neuronal fates using an embryoid aggregate protocol. After 40 days of differentiation, cells were fixed and immunostained for general neuronal markers such as MAP2, Tau and TUJ1, a marker of lower layer cortical neurons (TBR1), a marker of upper layer cortical neurons (CUX1), and/or synaptic markers (PSD95, synapsin, VGLUT1). Data shown are representative images from control and fAD lines. Scale bars = 50 μm. Magnified views of dotted boxes are shown as insets or adjacent to each image. D, E) After 40 days, cells were lysed, RNA extracted, and expression of 150 genes analyzed using the NanoString platform. Expression of general neuronal markers are shown in D, cell fate specific markers are shown in E. Error bars = SEM.

Figure 2. FAD mutation (APP V717I) in forebrain neuronal cells leads to increased Aβ42 and Aβ38 production.
Control and fAD iPSC lines were differentiated for 40-60 days to neuronal fates. Media conditioned on the cells for the final 48 hr were collected, and Aβ 38, 40, and 42 were detected in a single well using a multiplex ELISA (MesoScale Discoveries). Following collection of media, cells were lysed and RNA collected for parallel analyses of markers of differentiation. A, B) Aβ 42/40 ratio. Data are shown for individual clones (A) or pooled as control and APP V717I (fAD) (B-H). For B-H, Aβ data were generated from the two control and four fAD lines shown in A and averaged over 13 rounds of differentiation (YZ1 n=45, YK26 n=24, 1a n=33, 1b n=16, 2a n=29, 2b n=41). One way ANOVA performed with Tukey's multiple comparisons test, ** $p<0.01$, *** $p<0.001$. In A, black asterisks show significance vs. YZ1 and green asterisks show significance vs. YK26. In F-H, day 40 cells were treated with vehicle or DAPT (5 μM) for the final 48 hr of differentiation (n = 4-5 for each condition). Two-tailed t-tests were performed, ** $p<0.01$, *** $p<0.001$. Error bars = SEM.

Figure 3. APP V717I mutation in forebrain neuronal cells leads to increased cleavage of APP at the β-secretase site.
Control and fAD iPSC lines were differentiated for 40-60 days to neuronal fates. Media conditioned for the final 48 hr were collected, and APPsα and APPsβ detected in a single well using a multiplex ELISA (MesoScale Discovery). Following collection of media, cells were lysed and RNA collected for parallel analyses of markers of differentiation. A) Ratio of APPs α/β in each line analyzed. Green asterisks represent significance relative to YZ1, red asterisks relative to YK26. (B) APPsα or (C) APPsβ levels normalized to total RNA from control and fAD neurons are shown, summary data. Data in A is combined from 6 differentiation rounds, for YZ1 n=19,

YK26 n=11, 1A n=8, 1B n=, 2a n=26, and 2b n=28; for B and C n=20 for controls and n=38 for fAD. One way ANOVA performed with Tukey's multiple comparisons test, * p<0.05; ** p<0.01, *** p<0.001. (D-F) Cells differentiated to neuronal fates for 50 days were treated with 5 μM DAPT or vehicle (DMSO) for the last 48 hr of culture prior to lysis. Media were collected and APPsα and APPsβ measured using multiplex ELISA. In D, "pre" conditions show data from the media collected from the same wells 48 hr prior to treatments. Green asterisks in (D) show significance relative to control cells treated with DMSO, and the purple asterisk in (F) shows significance relative to fAD DMSO. Representative data from a single round of differentiation are shown, n=3-5. Error bars represent SEM, ** p<0.01, *** p<0.001.

Figure 4. Examination of APP cleavage products generated during differentiation to mature neuronal fates.

Control and APP V717I (fAD) iPSC lines were differentiated over 100 days to neuronal fates. (A) At multiple time points, cells were fixed and immunostained for a pluripotency marker (OCT4) and a neuronal marker (MAP2). (B) Alternatively, cells were lysed following collection of media and RNA purified for qPCR analysis. Media were analyzed by ELISA to measure levels of Aβ (C-F) and/or APPsα and APPsβ (G-I). (J) qPCR analysis of APP and BACE mRNAs across the differentiation time course. For data in B-J, error bars = SEM. For each comparison, a two-tailed t-test was performed, * p<0.05; ** p<0.01, *** p<0.001. For d9, d17, d24, n=2-4, for d40 n=70-100, for d60, d80, d100 n = 5-10.

Figure 5. Directed differentiation to alternate neuronal fates significantly affects β- and γ-secretase processing of APP.

A) Schematic of differentiation to neuronal fates showing window of morphogen treatment. B) Immunostaining of day 40 iPSCs differentiated to neuronal fates with and without retinoic acid (RA) and Sonic hedgehog (Shh) treatment. Scale bars = 100 μm. C-E) NanoString analysis of expression of a subset of 150 genes analyzed in control lines differentiated for 40 days with (+) and without (-) RA and Shh treatment. With RA/Shh treatment, general markers of neuronal fate were unchanged (C), markers of more rostral fates were downregulated (D), and markers of more caudal fates were upregulated (E). Data in (C-E) are derived from two lines over six rounds of differentiation. -RA/Shh n=25, +RA/Shh n=8. Error bars represent SEM. For each gene, a two-tailed t-test was done, * p<0.05; ** p<0.01, *** p<0.001. F-G) Conditioned media from day 40 differentiations with and without RA/Shh in control and APP V717I (fAD) lines were analyzed by Aβ triplex ELISA to measure 38, 40, and 42 levels. Aβ levels normalized to total RNA (F) and the Aβ 42/40 ratio (G) are shown separately for each line. APPsα and APPsβ were measured in the same samples using a duplex ELISA (MesoScale Discovery), and ratios of α/β are shown (H), as well as APPsα normalized to total RNA (I) and APPs-β normalized to total RNA (J). Data in H-J are combined from five differentiation rounds, two control lines, two fAD #1 lines and two fAD #2 lines. n=35, 19, 32, 22 for ctl (-), ctl (+), fAD (-), and fAD (+), respectively. For each comparison in H-L, a two-tailed t-test was performed, * p<0.05; ** p<0.01, *** p<0.001. Error bars = SEM.

Figure 6. Tau proteins levels are increased in fAD neurons directed to a forebrain fate.

A) NanoString analysis of Tau mRNA expression (normalized to the geometric mean of 7

housekeeping genes) in control and fAD lines at days 40 and 100 (n = 25, 9, 3, 3 for ctl d40, fAD d40, ctl d100, fAD d100). B-E) Western blot for total and phospho-Tau of lysates from control and fAD iPSCs differentiated to day 100 with and without RA/Shh (B), and quantification by densitometry (D,E). C) Quantification by densitometry of APP normalized to GAPDH. * p<0.05; ** p<0.01, *** p<0.001. Error bars = SEM.

Supplementary Figure S1. Characterization of human iPSC lines generated in this manuscript.
A) Representative images showing fAD 2 iPSCs stained for Alkaline Phosphatase or else immunostained for OCT4, NANOG, SSEA3, SSEA4, or TRA-1-60. B) RNA templates purified from iPSC lines were first reversed-transcribed to cDNA (+) or without reverse transcription (-), followed by PCR for markers listed. A representative example for fAD line 2 is shown. C) To test for pluripotency, each line was differentiated using an embryoid body protocol, and RT-PCR was utilized to test for the ability to generate all three germ layers. A representative example for fAD line 2 is shown. Karyotyping results from fAD 2 clone b (D) and fAD 1 clone a (E) performed by Cell Line Genetics.

Supplementary Figure S2. Human neurons derived from APP V717I carriers do not have altered gene expression profiles of cell fate markers or secretase components.
Control and fAD APP V717I lines were differentiated to neuronal fates. A,B) After 40 days, cells were lysed, RNA extracted, and expression of 150 genes analyzed using the NanoString platform. Expression of APP family members are shown in A and components of α-, β- and γ-secretases in B. Each bar represents data from 9 independent wells collected from three rounds of differentiation. Data from four different iPSC lines are represented. Error bars represent SD. C) Representative Western blot analysis of selected genes following 40 days of differentiation. For the final 48 hours of differentiation, wells were treated with vehicle or DAPT (a γ-secretase inhibitor, 5uM). D) Quantification by densitometry of APP and Tau normalized to GAPDH. Individual samples are shown. Two-tailed t-tests for each comparison were performed ***p<0.001.

Supplementary Figure S3. FAD mutation (APP V717I) in forebrain neuronal cells leads to increased Aβ42 and Aβ38 production, shown relative to total protein and shown by differentiation round.
Control and fAD iPSC lines were differentiated for 40-60 days to neuronal fates. Media conditioned on the cells for the final 48 hours was collected, and Aβ40 (A), Aβ42 (B), and Aβ38 (C) were detected in a single well using a multiplex ELISA (MesoScale Discoveries) and normalized to total protein. Error bars represent SEM, control n=4, APP V717I (fAD) n=19 *p<0.05. Aβ ELISA data shown in Figure 3 is broken down by round of differentiation (D) and by ELISA plate (E). Each point represents data form a single well.

Supplementary Figure S4. APP V717I mutation increases Aβ42 and Aβ38 generation as well as increases APPsβ generation in HEK cells.
HEK cells were transiently transfected with APP V717I or wild type APP. 24 hours later, cells

were treated with DAPT (5 μM) or vehicle for 24 hours, followed by collection of media and lysis of cells. A-G) In the media, Aβ40 (A,C), Aβ42 (A,B), and Aβ38 (D) were detected using a multiplex ELISA, and APPsα (E,F) and APPsβ (E,G) were detected using a duplex ELISA. H) Western blots were performed on the lysates and conditioned media to confirm equal levels of expression of APP. Error bars represent SEM, Two-tailed t-tests for each comparison were performed * p<0.05; ** p<0.01, *** p<0.001. ND=not detectable.

Supplementary Figure S5. Control and APP V717I mutation lines differentiate similarly in the presence of RA and Shh.

Control and APP V717I iPS lines were differentiated with and without RA/Shh as in Figure 5. Quantitative RT-PCR was performed for a general neuronal marker (A, MAP2), a marker of rostral forebrain fate (B, Tbr1), a marker of more caudal hindbrain (C, HoxB6) and a lower motor neuron (D, HB9) marker. Data shown are from four differentiation rounds, two control lines and three fAD lines. n=10-20 for each condition. For each comparison, a two-tailed t-test was performed, * p<0.05; ** p<0.01, *** p<0.001. Error bars = SEM.

Methods

Patients and fibroblast derivation and iPSC generation

iPSCs were generated in collaboration with the Harvard Stem Cell Institute. Skin punch biopsies were taken from a father and daughter pair, each with the APP (V717I) mutation, after informed consent and in accordance with Institutional Review Board approval. iPSCS were reprogrammed as described[18]. cDNAs for Oct4, Sox2, Klf4 and Myc were cloned into pMIG vectors and packaged into VSVG-pseudotyped retroviruses. Fibroblasts (~1×10^5) were transduced with retroviruses. Valproic acid (50uM) was added for 7 days, beginning on day 2 after transfection. iPSC colonies appeared after ~3 weeks and were picked based on morphology and GFP silencing. Colonies were transferred to 6-well plates containing irradiated mouse embryonic fibroblasts (MEFs). ROCK inhibitor (Y27632) (Millipore) was used at 10uM to increase cell survival. Each picked colony was one line. For passaging, cells were dissociated with collagenase (Stemcell Technologies). For a 10cm culture plate, between 5-50 colonies emerged.

Karyotype Analysis and Characterization

iPS clones were karyotyped by Cell Line Genetics. For pluripotency assays, iPSCs were dissociated from the plate with collagenase and then resuspended in ultra low-attachment plates and fed with iPSC media. Cells were re-plated onto gelatin after 1 week with DMEM 10% FBS. Cells were harvested for RNA extraction after 1 week of plating. Karyotyping was routinely performed using the NanoString **nCounter CNV CodeSets,** in order to ensure a normal chromosome number across passages.

iPS Cell Culture: iPSCs were cultured in medium consisting of 400 mL Dulbecco's Modified Eagle's Medium: Nutrient Mixture F12 (DMEM/F12, Gibco), 100 mL Knockout Serum Replacement (Gibco), 5 mL MEM-NEAA (Invitrogen), 5 mL of Penicillin/Streptomycin/Glutamine (Invitrogen) and 500 μL 2-Mercaptoethanol (100x) (Invitrogen). bFGF (Millipore) was added fresh daily at 10 μg/ml (1000x). Cells were maintained at 37°C/5% CO_2 and were split as necessary based on colony growth (5-6 days). Differentiating colonies were removed from the

plate prior to splitting. iPSCs were maintained on a mouse embryonic fibroblast (MEF) feeder layer at 1.7-2.0 x10^5 cells/well (Globalstem). For passaging, cells were dissociated with collagenase (Stemcell Technologies).

Neuronal Differentiation: For the induction of forebrain neurons, iPSCs were differentiated using an embryoid body-based protocol[22] that was further optimized (Muratore and Young-Pearse, unpub.). iPSC colonies were dissociated from MEFs at day 1 and cultured as aggregates 4 days in suspension with iPSC media. Aggregates were plated on matrigel-coated (BD Biosciences) culture dishes at day 7, forming primitive neuroepithelial (NE) structures over 10 days with Neural Induction media (N2). By day 17 definitive NE structures were present, and cells were dissociated and further cultured in suspension using Neural Induction media (N2/B27 with cAMP (Sigma) and IGF-1 (Peprotech). Neural rosettes were either selected manually or with STEMDiff Neural Rosette Selection reagent (Stemcell Technologies). The second culture in suspension aimed to purify neuronal progenitors, by clearing improperly differentiating cells. Cells were dissociated to single cells with accutase (Innovative Cell Technologies) and plated on matrigel for final differentiation at day 24 in Neural Differentiation media (N2/B27, Invitrogen) with ROCK inhibitor (Millipore, 10uM). Matrigel was used per the manufacturer's instructions. *Neural Induction Medium* consisted of 490 mL DMEM/F12, 5 mL N2 supplement (Invitrogen), 10 mL B27 supplement (Invitrogen), 5 mL MEM-NEAA and 2 μg/ml Heparin (Sigma-Aldrich). *Neural Differentiation Medium* consisted of 490 mL of Neurobasal medium (Gibco), 5 mL of N2 supplement, 5 mL of MEM-NEAA, and 10 mL of B27 supplement (Invitrogen) with the addition of fresh cAMP (1 μM) (Sigma), BDNF, GDNF, and IGF1 (PeproTech, 10 ng/mL) to the medium. A full media change was performed every 2-3 days for the duration of the experiment. For the induction of more caudal neurons, iPSCs were differentiated using the protocol described above. The aforementioned differentiation medias were used, with the addition of retinoic acid (100mM) (Sigma) and Sonic Hedgehog (100μg/mL) (R+D) from days 10-24 and 15-24 (as per [22]).

Primers

Actin: Forward, ggacttcgagcaagagatgg; Reverse, agcactgtgttggcgtacag
Dnmt3b: Forward, ataagtcgaaggtgcgtcgt; Reverse, ggcaacatctgaagccattt
hTERT: Forward, tgtgcaccaacatctacaag; Reverse, gcgttcttggctttcaggat
Nanog: Forward, tccaacatcctgaacctcag; Reverse, gactggatgttctgggtctg
Oct4: Forward (transgene), gtggaggaagctgacaacaa; Reverse (endogenous), caggttttctttccctagct
Rexl: Forward, tggacacgtctgtgctcttc; Reverse, gtcttggcgtcttctcgaac
Sox2: Forward, ttgtcggagacggagaagcg; Reverse, tgaccaccgaacccatggag
β-Tubulin: Forward, cagatgttcgatgccaagaa; Reverse, tgctgttcttgctctggatg
NCAM: Forward, atggaaactctattaaagtgaacctg; Reverse, tagacctcatactcagcattccagt
Pax6: Forward, tctaatcgaagggccaaatg; Reverse, tgtgagggctgtgtctgttc
AFP: Forward, agcttggtggtggatgaaac; Reverse, ccctcttcagcaaagcagac
GATA4: Forward, ctagaccgtgggttttgcat; Reverse, tgggttaagtgcccctgtag
Flk1: Forward, agtgatcggaaatgacactgga; Reverse, gcacaaagtgacacgttgagat
GATA2: Forward, gcaacccctactatgccaacc; Reverse, cagtggcgtcttggagaag
PECAM: Forward, cccagcccaggatttcttat; Reverse, accgcaggatcatttgagtt
VECAD: Forward, cagcccaaagtgtgtgagaa; Reverse, tgtgatgttggccgtgttat

qPCR

qpcr was performed using Fast SYBR Green Master Mix (Applied Biosystems) and run on a ViiA 7 System (Applied Biosystems). Samples were assayed in 2 technical replicates. Data was

analyzed using the $\Delta\Delta C_T$ method and expression was normalized to GAPDH expression[42]. RNA was purified from individual samples and processed through a PureLink RNA Mini Kit (Ambion), followed by reverse transcription using SuperScript II (Invitrogen). Primer efficiency was calculated for each pair of primers and the slope of the dilution line was found to be within the appropriate range. Dissociation curves also showed single peak traces, indicating template-specific products.

Immunocytochemistry and microscopy

Cultures were fixed with 4% paraformaldehyde, followed by membrane permeabilization with 0.1% TritonX-100 and then staining with primary and secondary antibodies (see Antibodies). Imaging was performed using a Zeiss LSM710 confocal microscope and images were acquired using ZEN black software. Software was used to pseudo-color images and add scale bars.

Western Blots and antibodies

Lysates and conditioned media were electrophoresed on 4-12% Bis-Tris gels (Invitrogen) and transferred to nitrocellulose. Lysates were prepared with standard buffer containing 1% NP40, 0.5M EDTA, 5M NaCl, 1M Tris and cOmplete protease inhibitors and phosSTOP (Roche). Western blotting and immunostaining were performed with the following antibodies: MAP2 (1:5000), Oct4 (1:1000), Tbr1 (1:200), Cux1 (1:100), SYP (1:250), PSD95 (1:250) VGLUT1 (1:500), Nanog (1:50), abcam; SSEA3 (1:200), SSEA4 (1:200), TRA-1-60 (1:200), GAPDH (1:2000), BACE (1:500), Millipore; Tau (1:200, Dako), TuJ1 (1:1000, Sigma), Hoxb4 (1:50, Developmental Studies Hybridoma Bank), APP (C9) (1:1000, Selkoe Lab, Brigham and Women's Hospital), APPs (4F2) (1:1000, Selkoe Lab, Brigham and Women's Hospital), pS262 (12E8) (1:2000, Malinow Lab, UCSD), pS202 (AT8) (1:200, Pierce). Secondaries were from Jackson ImmunoResearch: anti-chicken cy2/cy3/cy5, anti-rabbit cy2/cy3, anti-mouse cy2/cy3, anti-rat cy2/cy3 (1:1000). TOPRO3, DAPI 1:1000 Invitrogen.

Aβ and sAPPα/β measurements

Neural cells were plated in 96-well plates at various time-points up to 100 days. ELISA assays was carried out using the reagents, protocols, and imager manufactured by Meso Scale Diagnostics, LLC. Media were collected after 48-hours and analyzed using the 6E10 Abeta Triplex or sAPPα/sAPPβ ELISA assays (specific to human). Data were normalized to either total RNA or intracellular protein values, as noted.

Inhibitor treatments

Neural cells were plated at day 24 and allowed to differentiate until day 40-50. Conditioned media were collected 48-hours prior to treatment and saved for ELISA assays. Cultures were then treated with either 5μM DAPT or DMSO (Sigma) for 48-hours, followed by media collection and harvesting for either RNA or protein. RNA was purified from individual wells and processed through a PureLink RNA Mini Kit (Ambion). For protein, cells were lysed with standard buffer containing 1% NP40, 0.5M EDTA, 5M NaCl, 1M Tris and cOmplete protease inhibitors and phosSTOP (Roche).

Nanostring analysis

To analyze gene expression for a large number of genes from an individual sample, we utilized a custom probe set designed by NanoString Technologies (nCounter Gene Expression Assay). The assays were performed using the NanoString protocols, 12 samples per run. The first step hybridization reactions were carried out with 100-200 ng RNA. Post-hybridization samples were

processed with the nCounter Prep-station. Following run completion, the cartridge was scanned using the nCounter Digital Analyzer, at max resolution (~1000 images/sample). Data were analyzed using the nSolver Analysis Software and normalized to a set of 7 house-keeping genes or to the total gene set, as noted.

Transfections

HEK293 cells were transiently transfected with cDNA encoding either wild type human APP695 or with the V717I mutation, using Fugene HD (Promega). 24-hours after transfection, media were changed and cells were treated with either DMSO or 5μM DAPT. 48-hours after transfection, conditioned media were collected and cells lysed in 1% NP40 STEN buffer.

Statistics

Data was analyzed using GraphPad PRISM 5 software. Values are expressed as either ±s.d or ±s.e.m, as indicated by figure legend text. Statistical significance was tested by either an unpaired Student's *t* test (two-tailed) or by One-way ANOVA with a Tukey's post-test. Statistically significant differences were determined by *P* values less than 0.05.

References

1. Bertram, L., Lill, C. M. & Tanzi, R. E. The genetics of Alzheimer disease: back to the future. *Neuron* **68**, 270–281 (2010).
2. Wolfe, M. S. *et al.* Two transmembrane aspartates in presenilin-1 required for presenilin endoproteolysis and gamma-secretase activity. *Nature* **398**, 513–517 (1999).
3. Selkoe, D. J. & Podlisny, M. B. Deciphering the genetic basis of Alzheimer's disease. *Annu Rev Genomics Hum Genet* **3**, 67–99 (2002).
4. Bertram, L. & Tanzi, R. E. The genetics of Alzheimer's disease. *Prog Mol Biol Transl Sci* **107**, 79–100 (2012).
5. Goate, A. *et al.* Segregation of a missense mutation in the amyloid precursor protein gene with familial Alzheimer's disease. **349**, 704–706 (1991).
6. Cruts, M., Theuns, J. & Van Broeckhoven, C. Locus-specific mutation databases for neurodegenerative brain diseases. *Hum. Mutat.* **33**, 1340–1344 (2012).
7. Suzuki, N. *et al.* An increased percentage of long amyloid beta protein secreted by familial amyloid beta protein precursor (beta APP717) mutants. *Science* **264**, 1336–1340 (1994).
8. De Jonghe, C. *et al.* Pathogenic APP mutations near the gamma-secretase cleavage site differentially affect Abeta secretion and APP C-terminal fragment stability. *Hum. Mol. Genet.* **10**, 1665–1671 (2001).
9. Moechars, D. *et al.* Early phenotypic changes in transgenic mice that overexpress different mutants of amyloid precursor protein in brain. *J. Biol. Chem.* **274**, 6483–6492 (1999).
10. Dewachter, I. *et al.* Modeling Alzheimer's disease in transgenic mice: effect of age and of presenilin1 on amyloid biochemistry and pathology in APP/London mice. *Exp. Gerontol.* **35**, 831–841 (2000).
11. Tamaoka, A. *et al.* APP717 missense mutation affects the ratio of amyloid beta protein species (A beta 1-42/43 and a beta 1-40) in familial Alzheimer's disease brain. *J. Biol. Chem.* **269**, 32721–32724 (1994).

12. Scheuner, D. *et al.* Secreted amyloid β–protein similar to that in the senile plaques of Alzheimer's disease is increased in vivo by the presenilin 1 and 2 and APP mutations linked to familial Alzheimer's disease. *Nature Medicine* **2**, 864–870 (1996).
13. Yagi, T. *et al.* Modeling familial Alzheimer's disease with induced pluripotent stem cells. *Hum. Mol. Genet.* **20**, 4530–4539 (2011).
14. Ooi, L. *et al.* Induced pluripotent stem cells as tools for disease modelling and drug discovery in Alzheimer's disease. *J Neural Transm* **120**, 103–111 (2013).
15. Malgrange, B. *et al.* Using human pluripotent stem cells to untangle neurodegenerative disease mechanisms. *Cell. Mol. Life Sci* **68**, 635–649 (2011).
16. Takahashi, K. *et al.* Induction of Pluripotent Stem Cells from Adult Human Fibroblasts by Defined Factors. *Cell* **131**, 861–872 (2007).
17. Park, I.-H. & Daley, G. Q. Human iPS cell derivation/reprogramming. *Curr Protoc Stem Cell Biol* **Chapter 4**, Unit 4A.1 (2009).
18. Park, I.-H. *et al.* Disease-Specific Induced Pluripotent Stem Cells. *Cell* **134**, 877–886 (2008).
19. Shi, Y. *et al.* A human stem cell model of early Alzheimer's disease pathology in Down syndrome. *Sci Transl Med* **4**, 124ra29 (2012).
20. Israel, M. A. *et al.* Probing sporadic and familial Alzheimer's disease using induced pluripotent stem cells. *Nature* **482**, 216–220 (2012).
21. Qiang, L. *et al.* Directed conversion of Alzheimer's disease patient skin fibroblasts into functional neurons. *Cell* **146**, 359–371 (2011).
22. Zeng, H. *et al.* Specification of Region-Specific Neurons Including Forebrain Glutamatergic Neurons from Human Induced Pluripotent Stem Cells. *PLoS ONE* **5**, e11853 (2010).
23. Theuns, J. *et al.* Alzheimer dementia caused by a novel mutation located in the APP C-terminal intracytosolic fragment. *Human Mutation* **27**, 888–896 (2006).
24. Moore, B. D. *et al.* Overlapping profiles of Aβ peptides in the Alzheimer's disease and pathological aging brains. *Alzheimer's Research & Therapy* **4**, 18 (2012).
25. Haass, C., Kaether, C., Thinakaran, G. & Sisodia, S. Trafficking and Proteolytic Processing of APP. *Cold Spring Harb Perspect Med* **2**, a006270 (2012).
26. Graham, A. *et al.* Characterization of a murine homeo box gene, Hox-2.6, related to the Drosophila Deformed gene. *Genes Dev.* **2**, 1424–1438 (1988).
27. Chen, J.-A. *et al.* Mir-17-3p controls spinal neural progenitor patterning by regulating Olig2/Irx3 cross-repressive loop. *Neuron* **69**, 721–735 (2011).
28. Tanabe, Y. & Jessell, T. M. Diversity and pattern in the developing spinal cord. *Science* **274**, 1115–1123 (1996).
29. Suh, Y.-H. & Checler, F. Amyloid precursor protein, presenilins, and alpha-synuclein: molecular pathogenesis and pharmacological applications in Alzheimer's disease. *Pharmacol. Rev.* **54**, 469–525 (2002).
30. Lichtenthaler, S. F. *et al.* Mechanism of the cleavage specificity of Alzheimer's disease γ-secretase identified by phenylalanine-scanning mutagenesis of the transmembrane domain of the amyloid precursor protein. *PNAS* **96**, 3053–3058 (1999).
31. Qi-Takahara, Y. *et al.* Longer forms of amyloid beta protein: implications for the mechanism of intramembrane cleavage by gamma-secretase. *J. Neurosci.* **25**, 436–445 (2005).

32. De Strooper, B. Proteases and proteolysis in Alzheimer disease: a multifactorial view on the disease process. *Physiol. Rev.* **90**, 465–494 (2010).
33. Ahmed, R. R. *et al.* BACE1 and BACE2 enzymatic activities in Alzheimer's disease. *Journal of Neurochemistry* **112**, 1045–1053 (2010).
34. Cai, H. *et al.* BACE1 is the major β-secretase for generation of Aβ peptides by neurons. *Nature Neuroscience* **4**, 233–234 (2001).
35. Vassar, R. *et al.* Beta-secretase cleavage of Alzheimer's amyloid precursor protein by the transmembrane aspartic protease BACE. *Science* **286**, 735–741 (1999).
36. Marcinkiewicz, M. & Seidah, N. G. Coordinated expression of beta-amyloid precursor protein and the putative beta-secretase BACE and alpha-secretase ADAM10 in mouse and human brain. *J. Neurochem.* **75**, 2133–2143 (2000).
37. Bennett, B. D. *et al.* Expression Analysis of BACE2 in Brain and Peripheral Tissues. *J. Biol. Chem.* **275**, 20647–20651 (2000).
38. Roberson, E. D. *et al.* Reducing endogenous tau ameliorates amyloid beta-induced deficits in an Alzheimer's disease mouse model. *Science* **316**, 750–754 (2007).
39. Jin, M. *et al.* Soluble amyloid {beta}-protein dimers isolated from Alzheimer cortex directly induce Tau hyperphosphorylation and neuritic degeneration. *Proc Natl Acad Sci U S A* (2011).doi:10.1073/pnas.1017033108
40. Lewis, J. *et al.* Enhanced neurofibrillary degeneration in transgenic mice expressing mutant tau and APP. *Science* **293**, 1487–1491 (2001).
41. Morrison, J. H. & Hof, P. R. Life and death of neurons in the aging cerebral cortex. *Int. Rev. Neurobiol* **81**, 41–57 (2007).
42. Livak, K. J. & Schmittgen, T. D. Analysis of relative gene expression data using real-time quantitative PCR and the 2(-Delta Delta C(T)) Method. *Methods* **25**, 402–408 (2001).

Figure-1 (Young-Pearse)

A

Lines	sex	age at tissue collection	Neurological diagnosis at time of tissue collection	APP/APOE genotype	provider/origin
hFib2-iPS4	F	fetal	Normal	ε3/ε3	Daley Lab
HDFa-YK-26	F	adult	Normal	ε3/ε3	Uconn Stem Cell Core
YZ1	F	fetal	Normal	ε3/ε3	Uconn Stem Cell Core
hFAD-1 clone a	M	57	Alzheimer's disease	APP V717I, ε3/ε3	HSCI iPS core/Young-Pearse Lab
hFAD-1 clone b	M	57	Alzheimer's disease	APP V717I, ε3/ε3	HSCI iPS core/Young-Pearse Lab
hFAD-2 clone a	F	33	Normal	APP V717I, ε3/ε3	HSCI iPS core/Young-Pearse Lab
hFAD-2 clone b	F	33	Normal	APP V717I, ε3/ε3	HSCI iPS core/Young-Pearse Lab

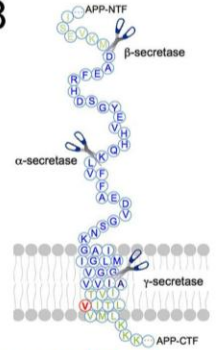

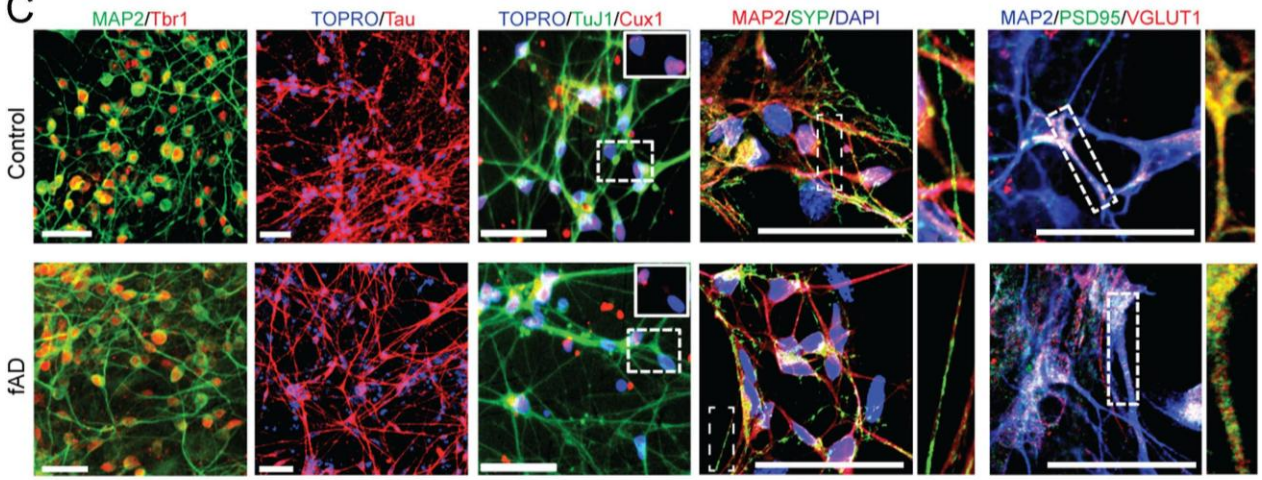

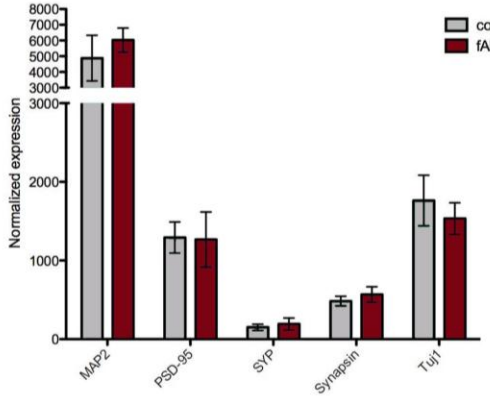

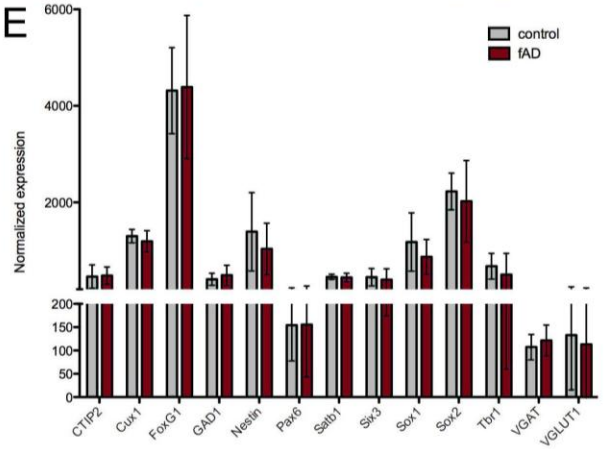

Figure-2 (Young-Pearse)

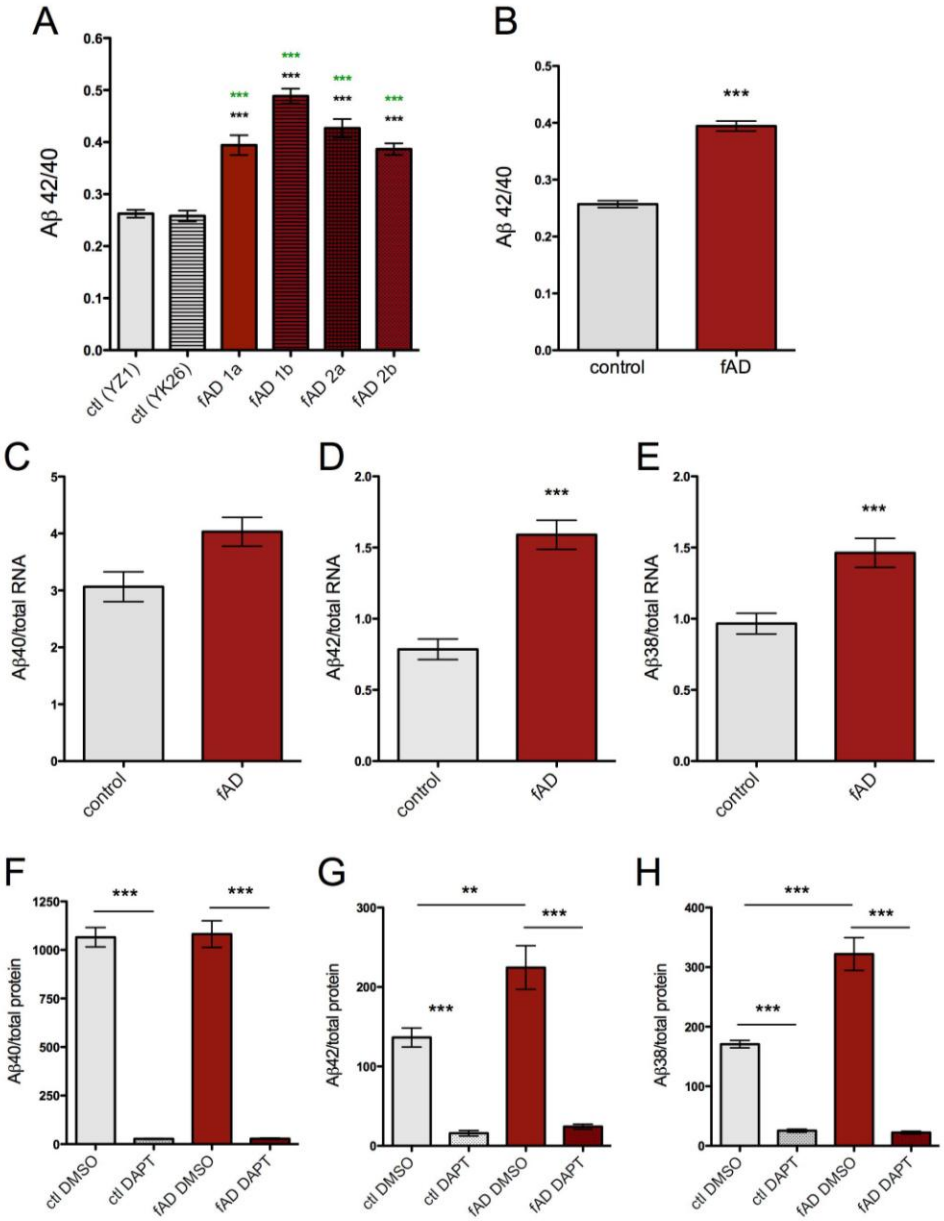

Figure-3 (Young-Pearse)

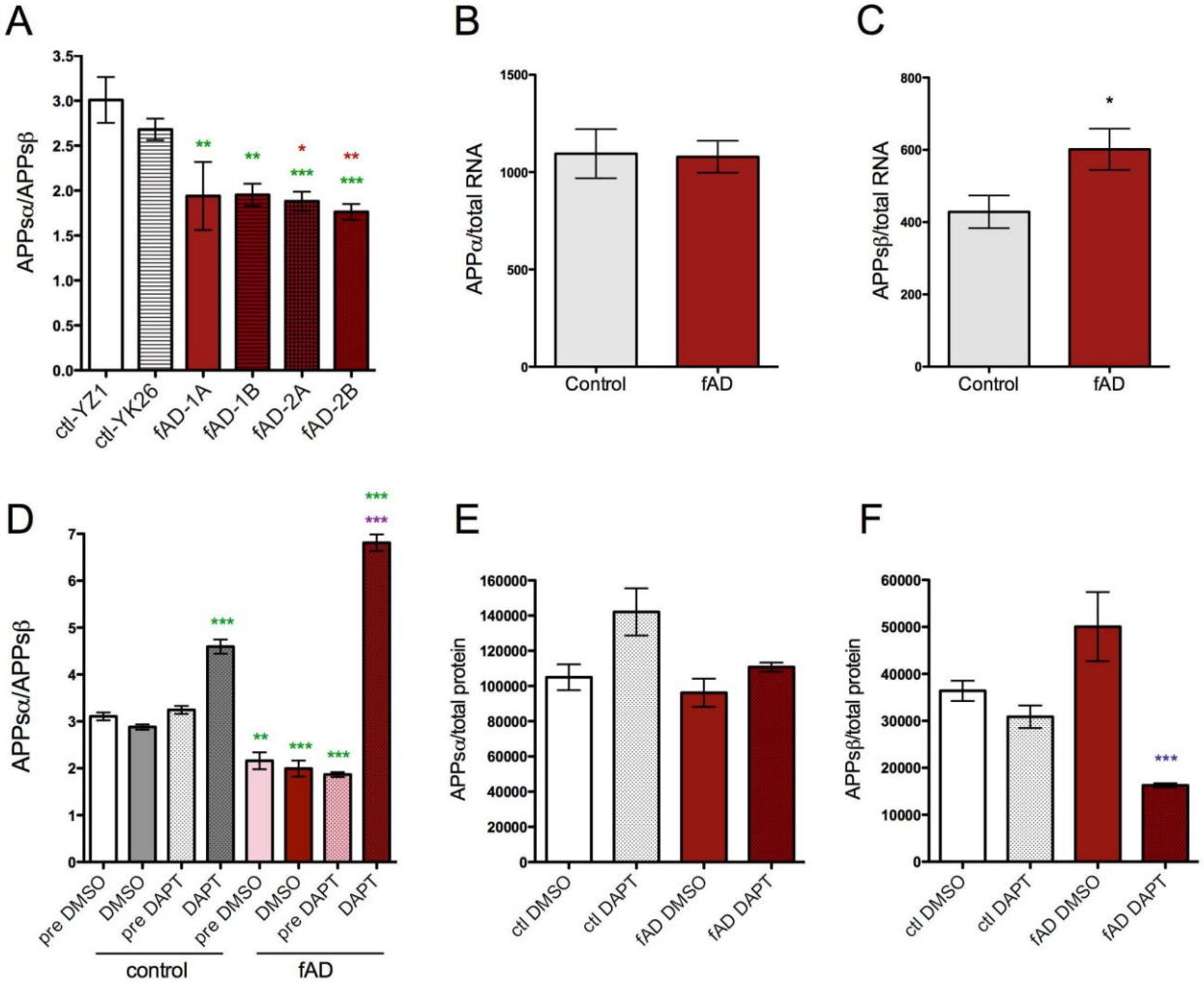

Figure-4 (Young-Pearse)

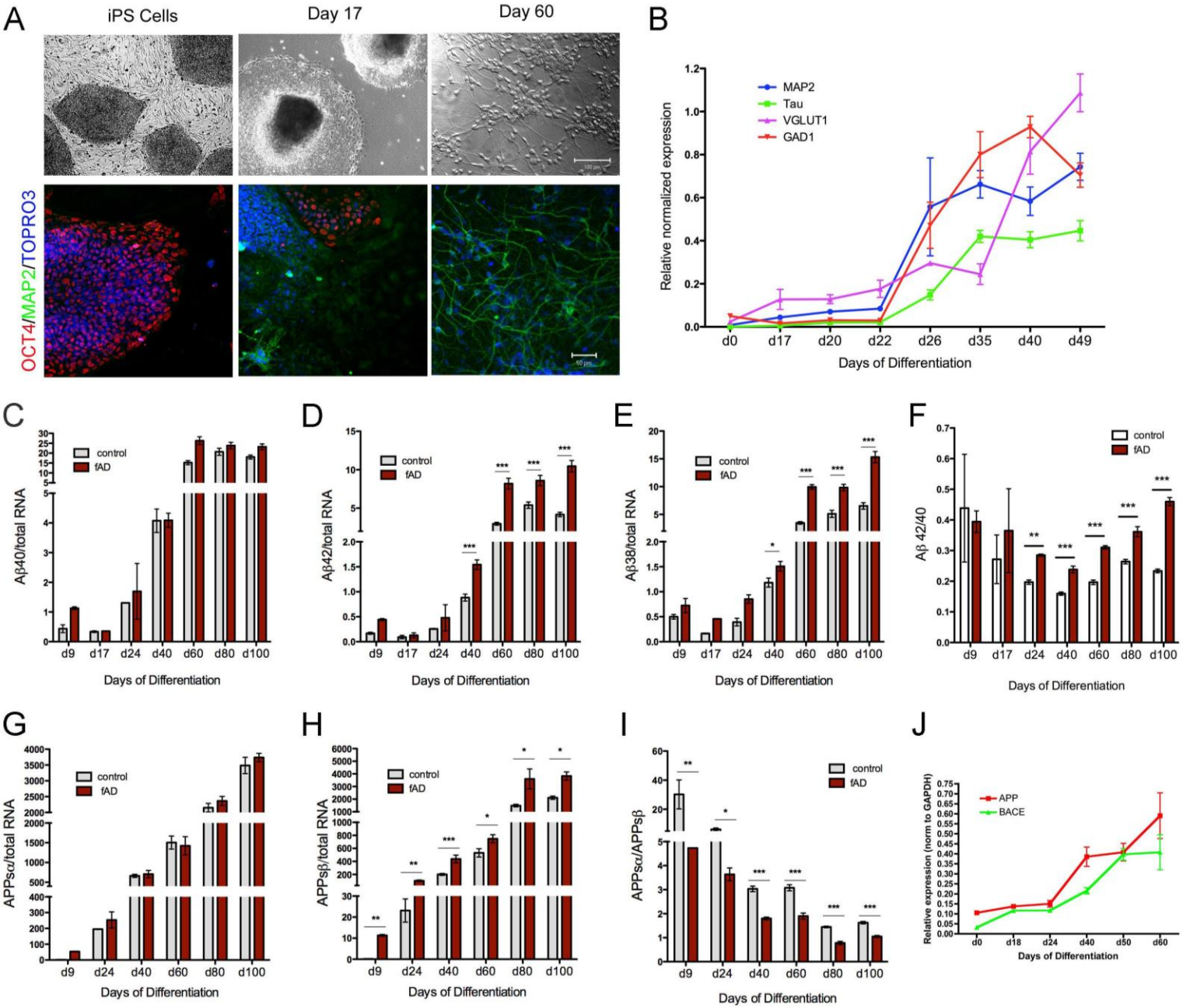

Figure-5 (Young-Pearse)

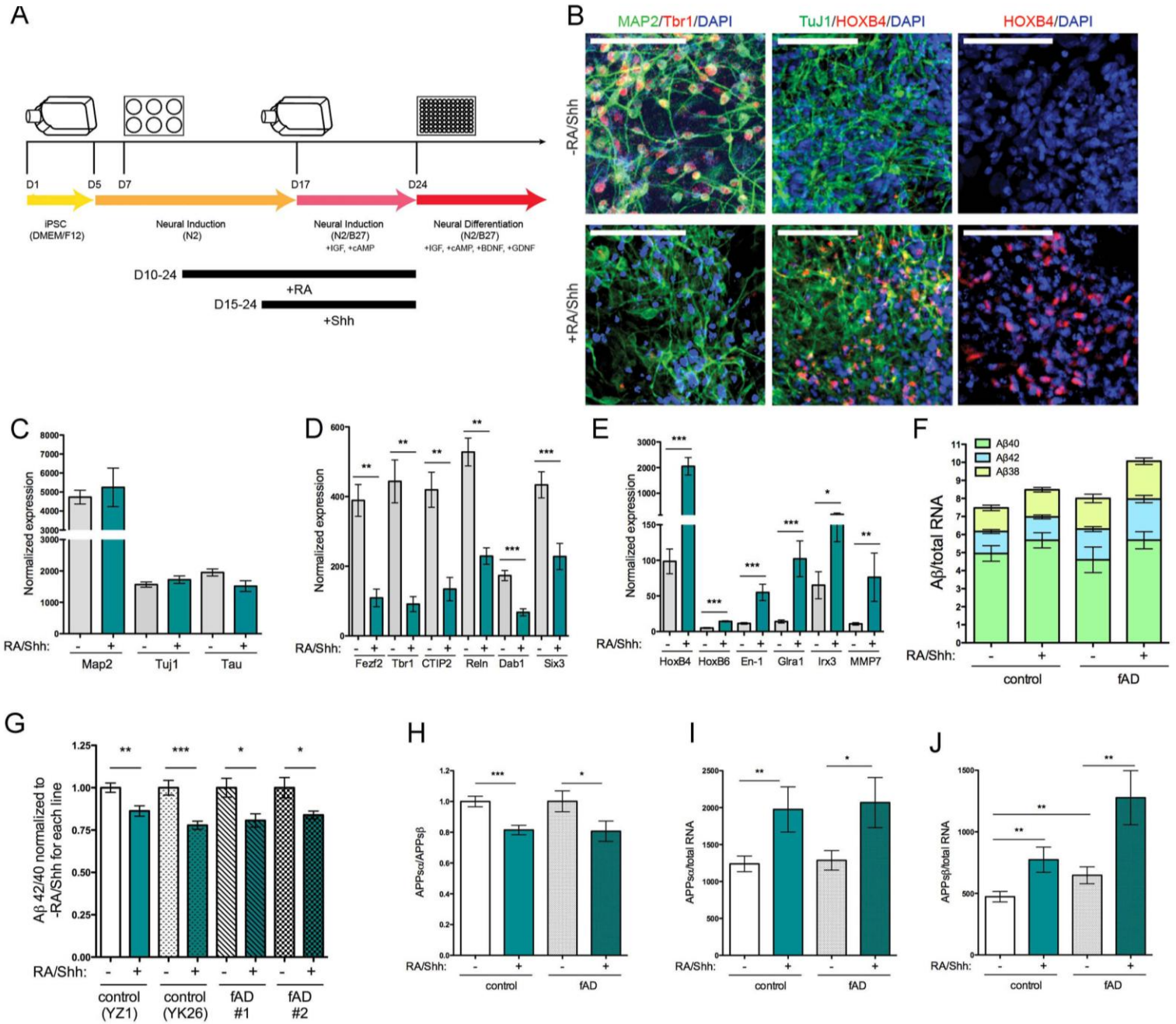

Figure-6 (Young-Pearse)

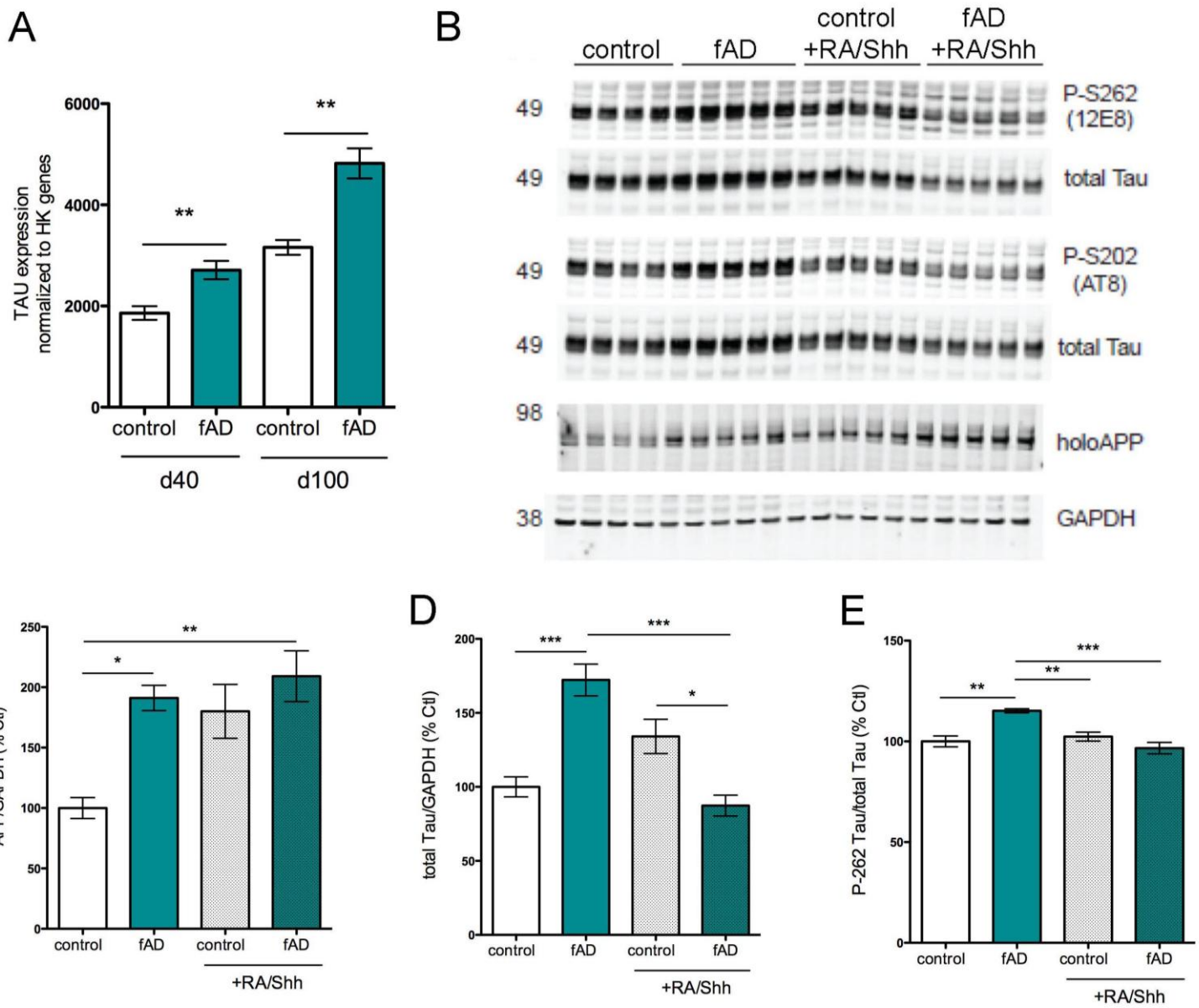

Supplementary Figure-1 (Young-Pearse)

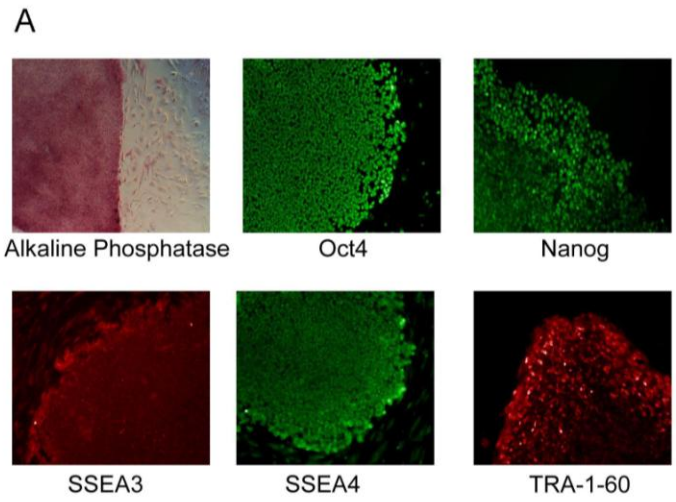

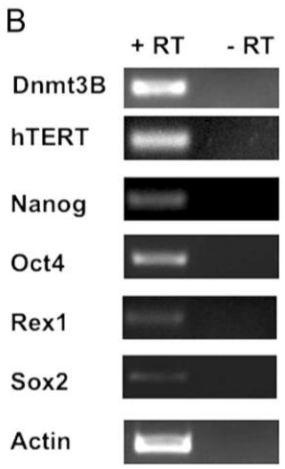

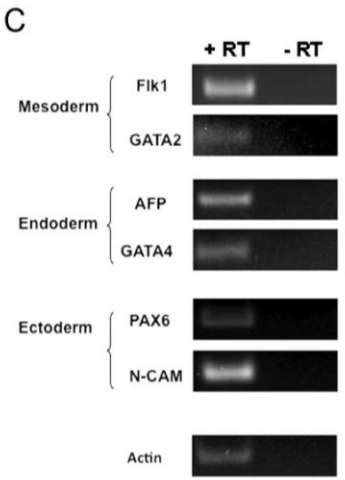

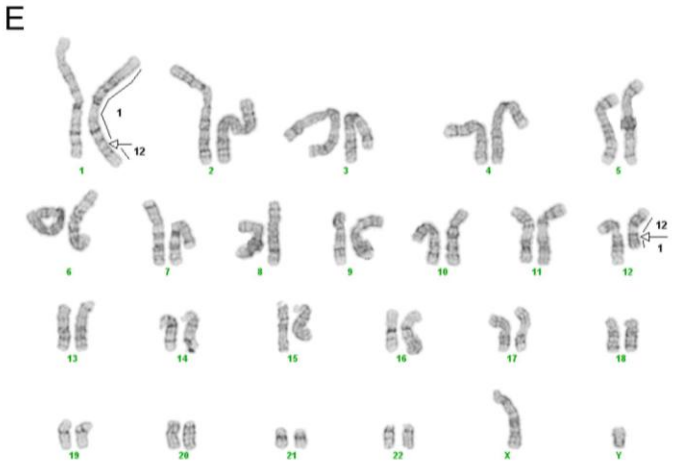

Supplementary Figure-S2 (Young-Pearse)

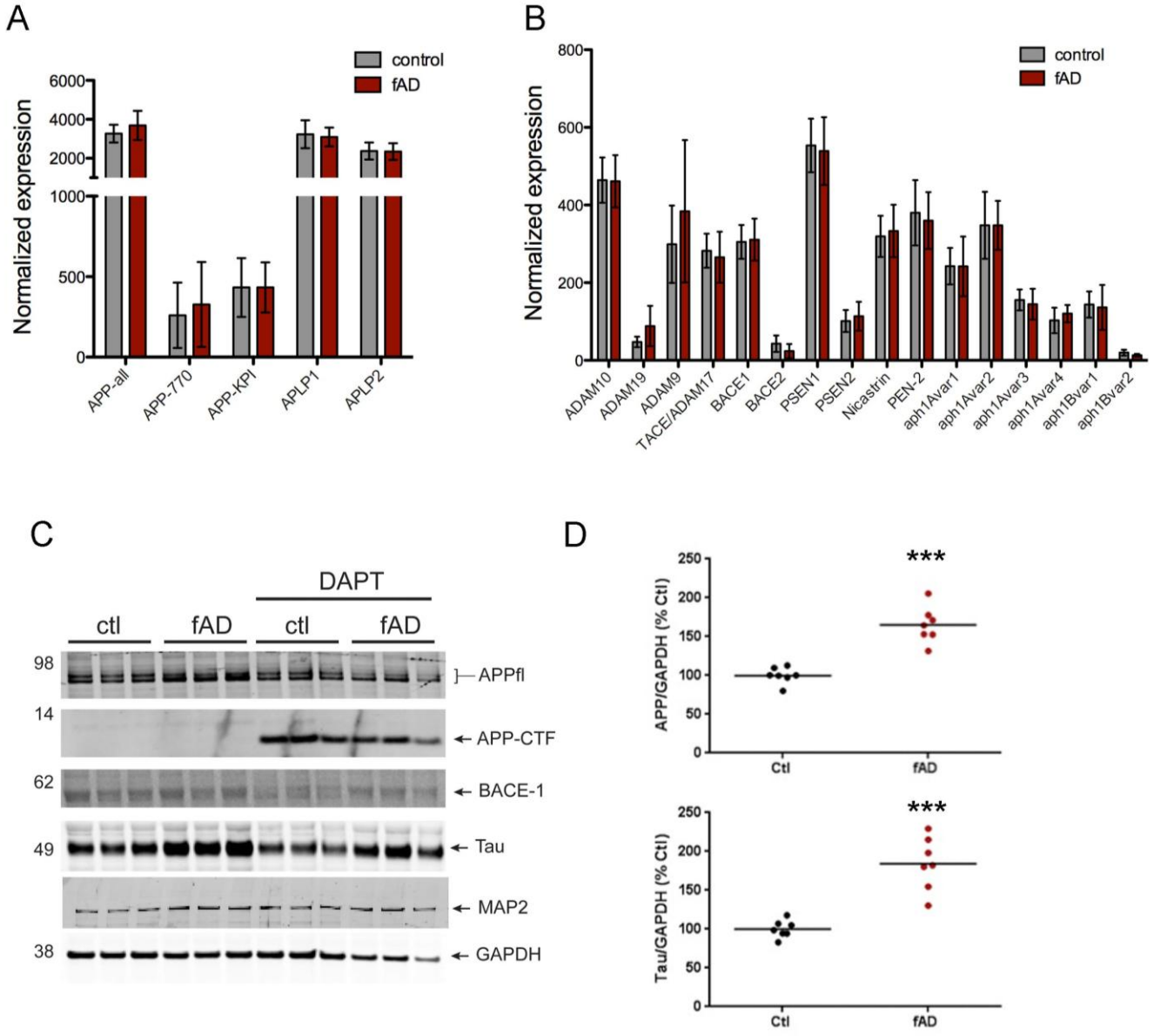

Supplementary Figure-S3 (Young-Pearse)

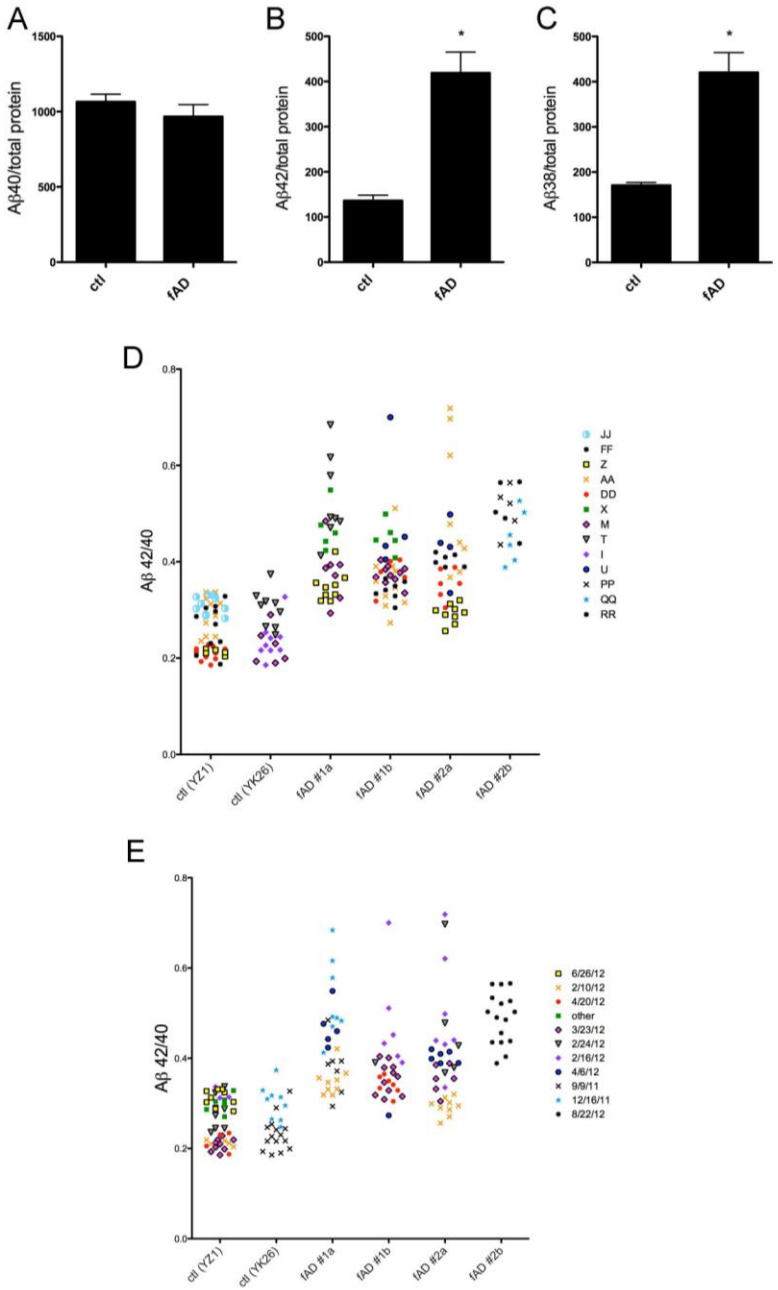

Supplementary Figure-S4 (Young-Pearse)

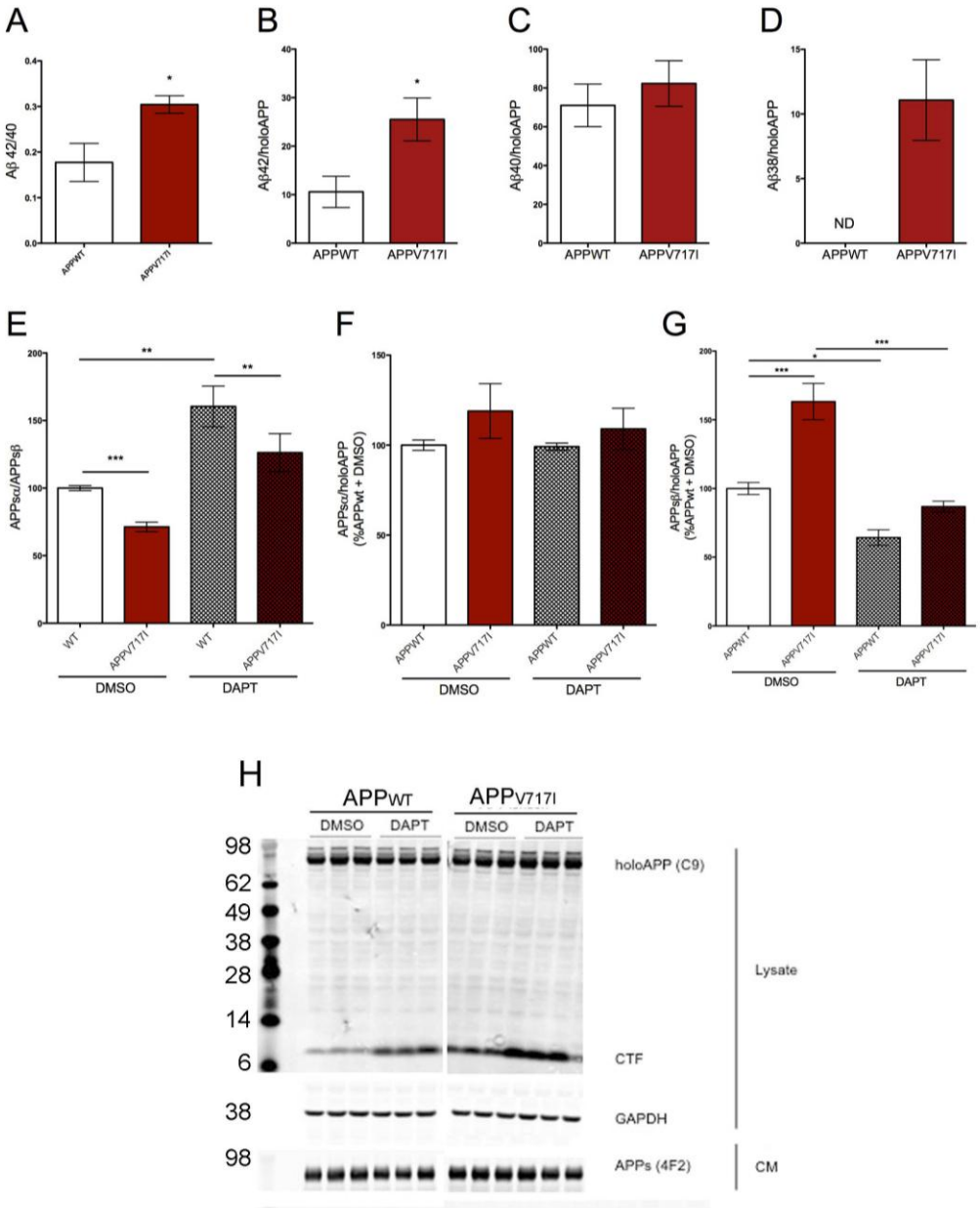

Supplementary Figure-S5 (Young-Pearse)

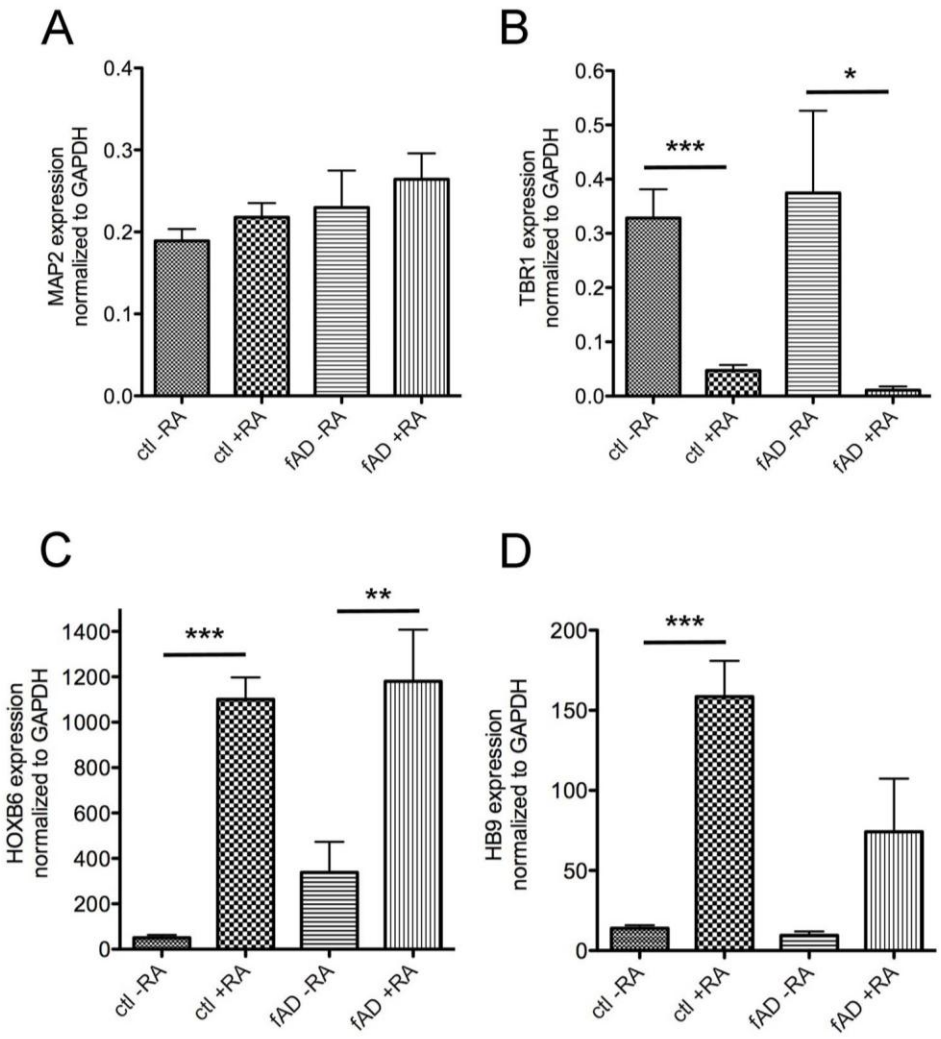

Supplementary Figure-1 (Young-Pearse)

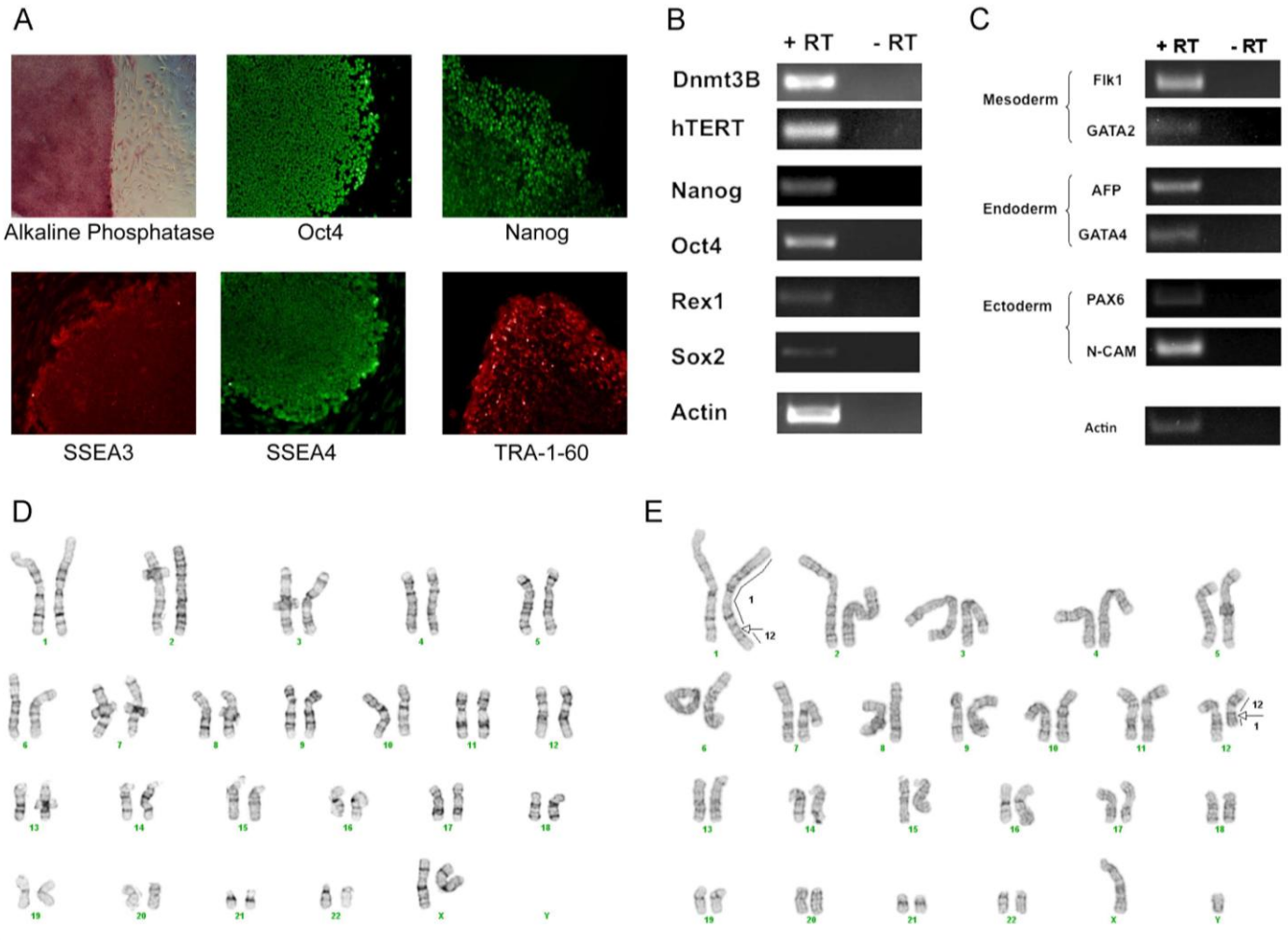

Supplementary Figure-S2 (Young-Pearse)

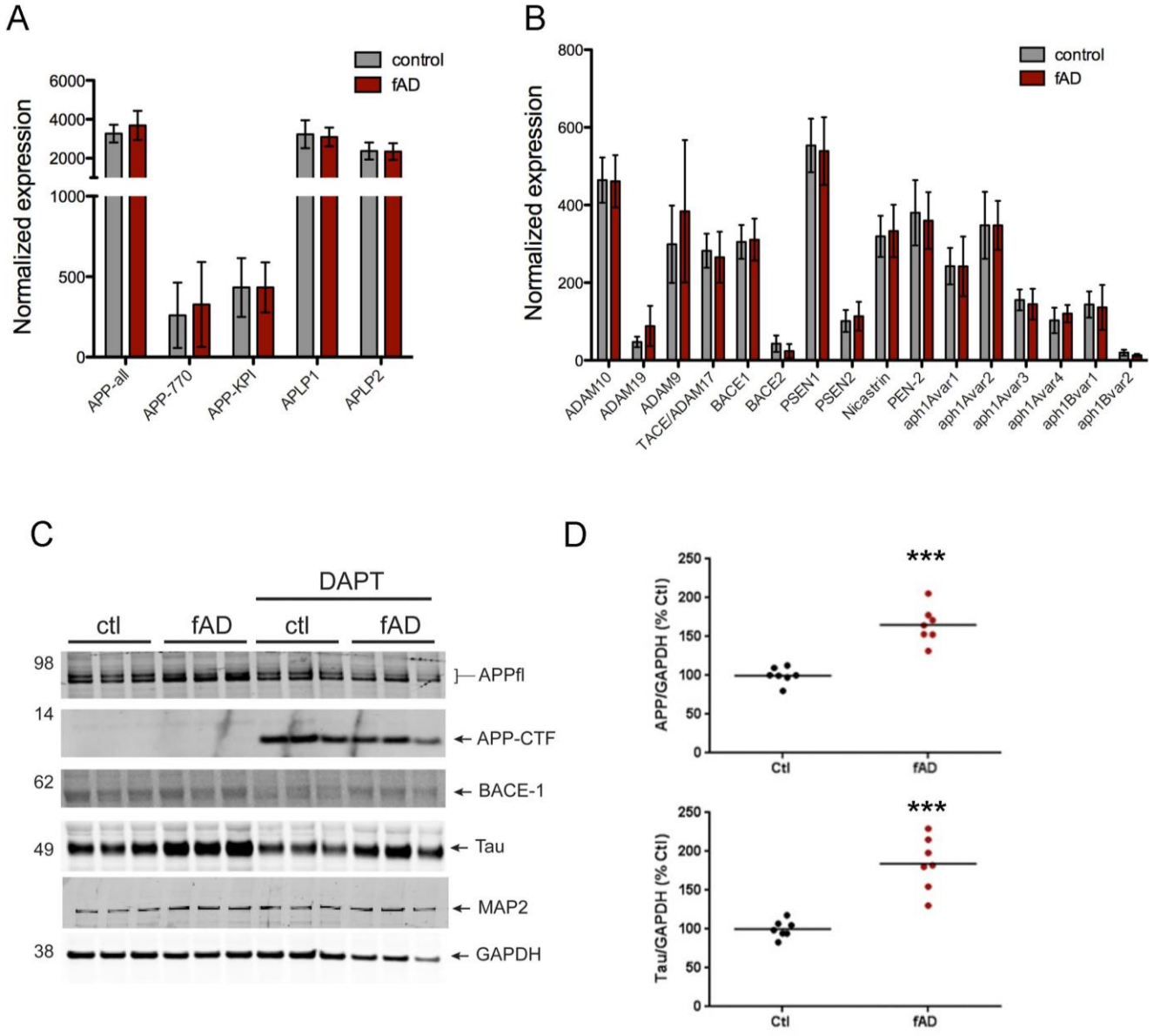

Supplementary Figure-S3 (Young-Pearse)

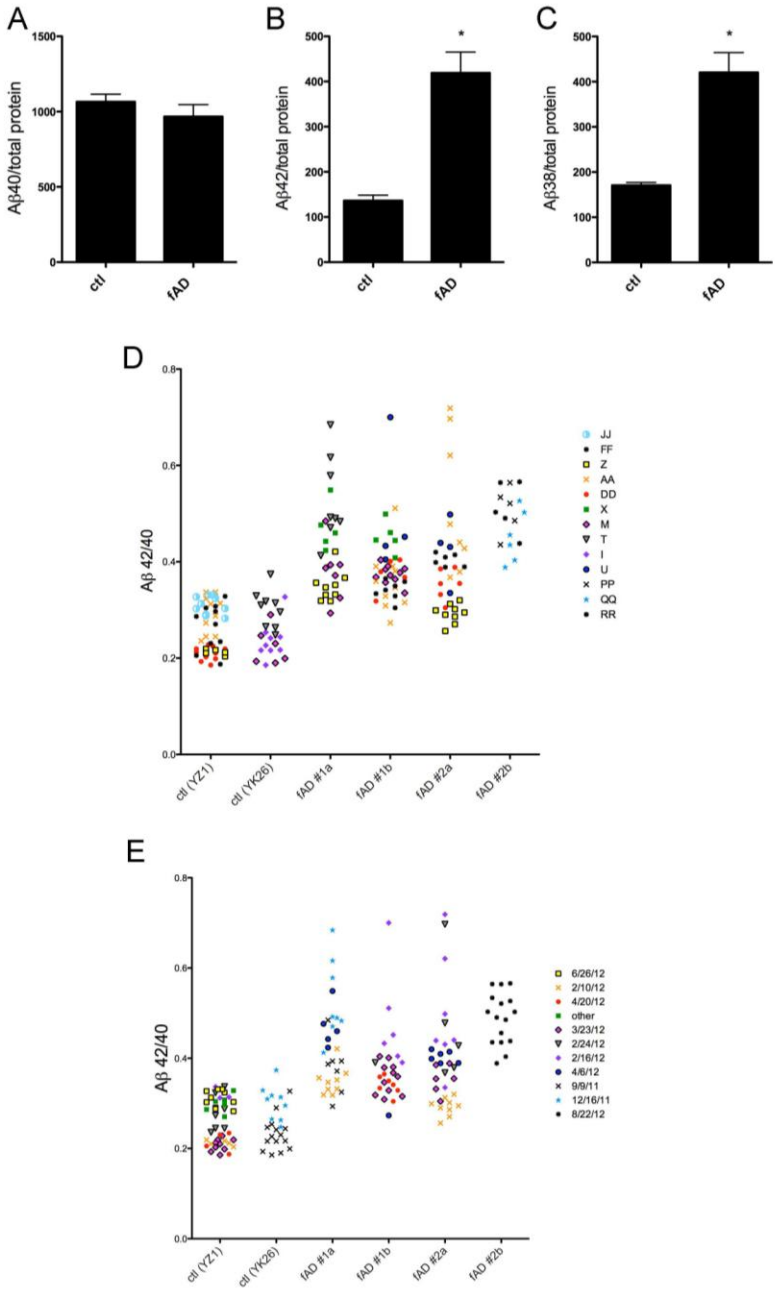

Supplementary Figure-S4 (Young-Pearse)

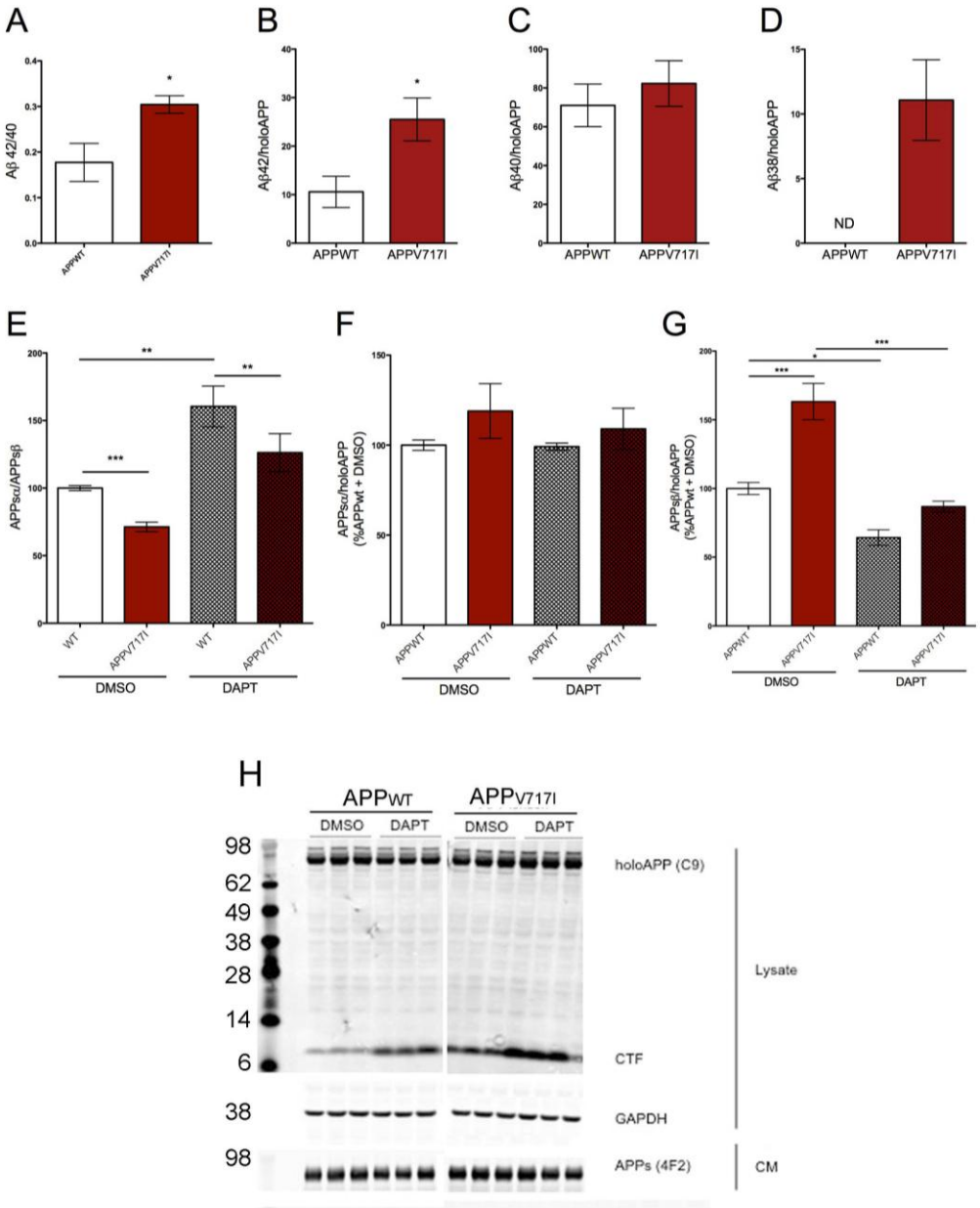

Supplementary Figure-S5 (Young-Pearse)

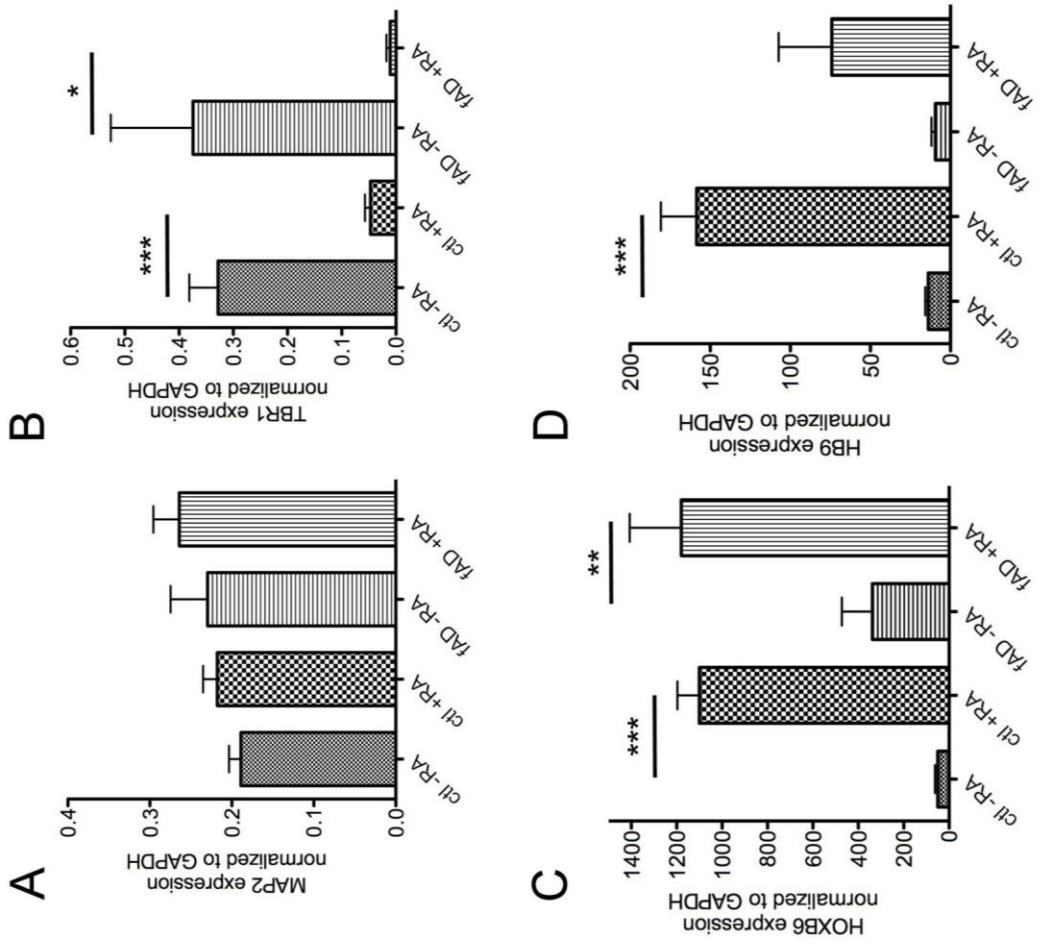

Appendix 3

Effects of APOER2/VLDLR on ectodomain shedding of APP

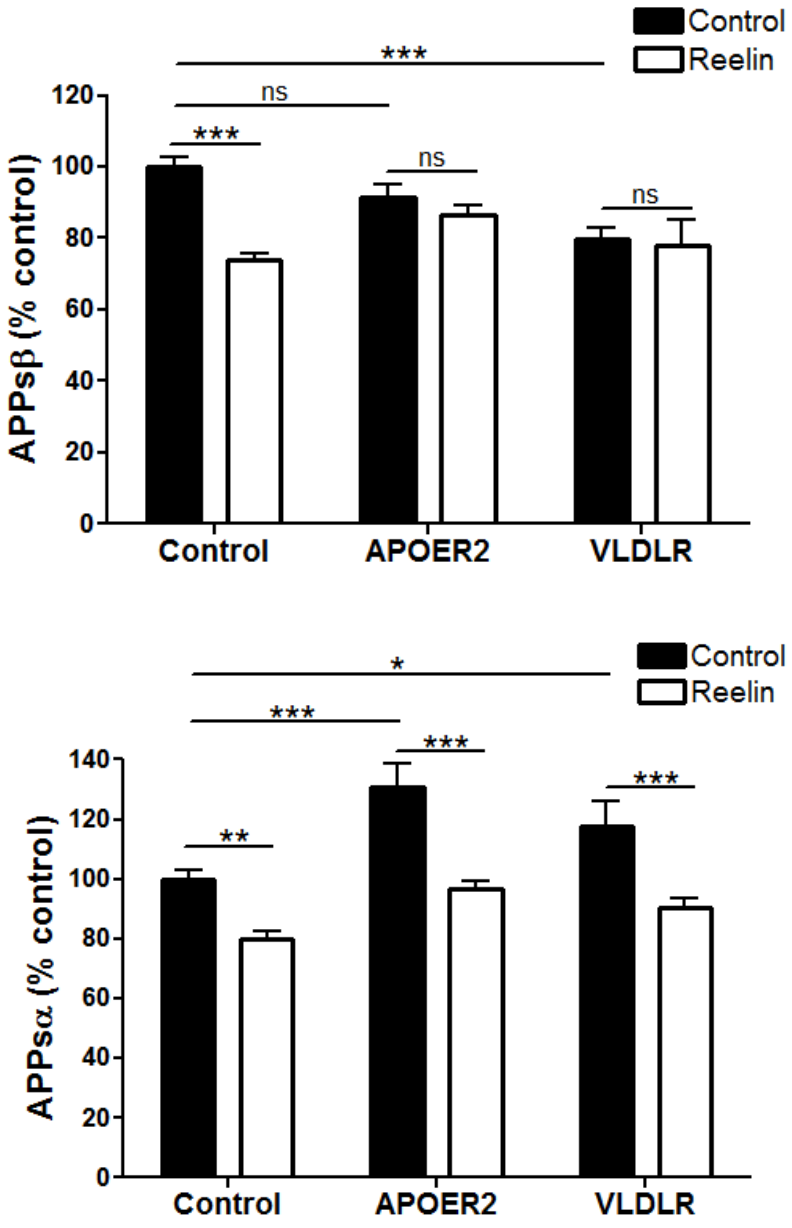

Figure A3.1: Effects of APOER2/VLDLR on ectodomain shedding of APP

HEK293 cells were co-transfected with combinations of Reelin, APOER2, and VLDLR cDNA . Endogenous APPsα and APPsβ levels were quantified by ELISA and shown as a percentage of control.

Appendix 4

Effects of HSPGs on ectodomain shedding of APP

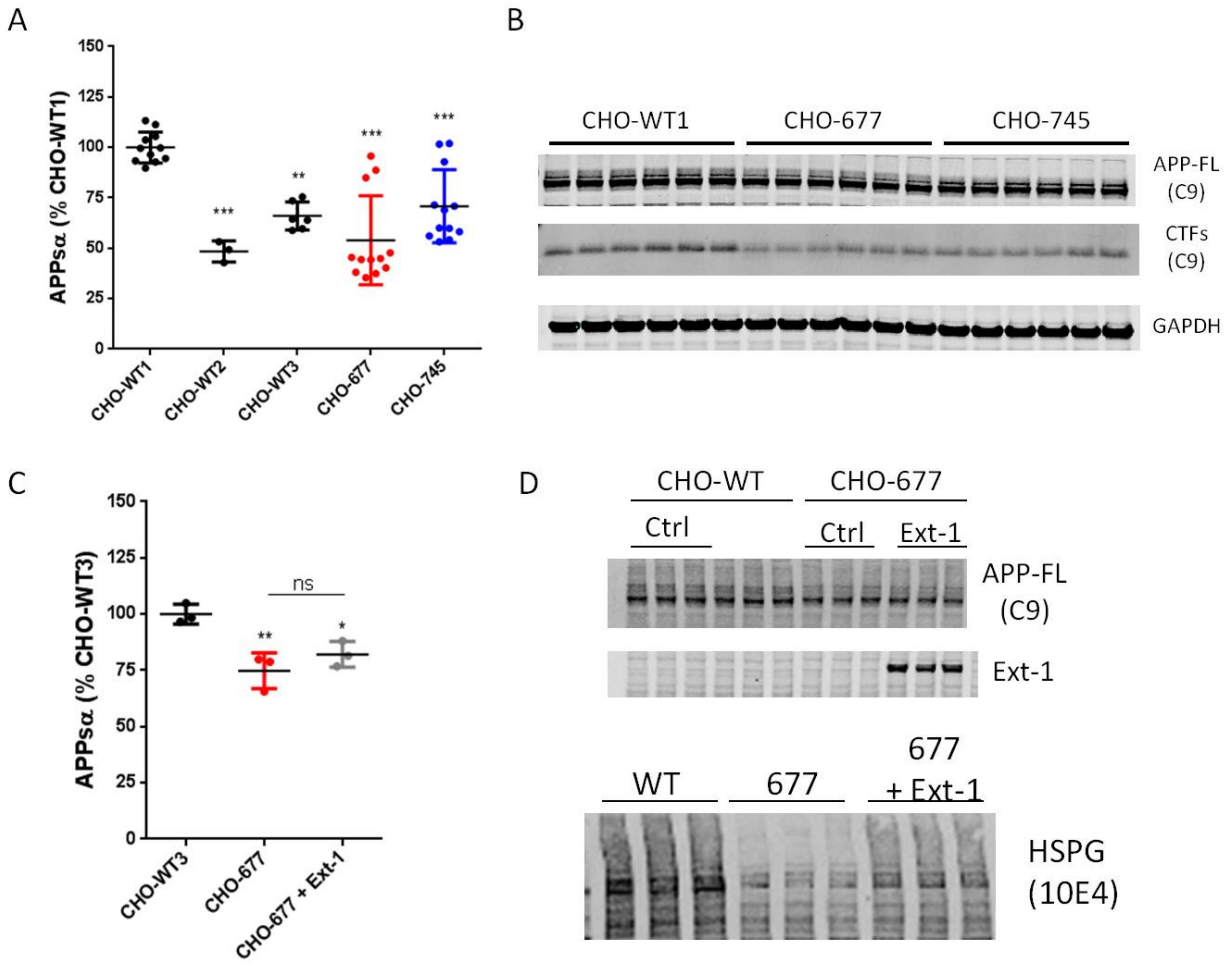

Figure A4.1 Effects of HSPGs on ectodomain shedding of APP A, B) Endogenous APPsα levels were measured by ELISA from several wild-type CHO lines (CHO-WT1 , 2 or 3) or CHO cells deficient in HSPGs (CHO-677) or HSPGs + chondroitin sulfate (CHO-745) for 24 hr. Blots show the corresponding FL- and CTF levels in some of the cells. C, D) Ext-1 (the mutated gene in CHO-677 cells) was transfected into CHO-677 cell lines in an attempt to rescue the effects on APPsα.

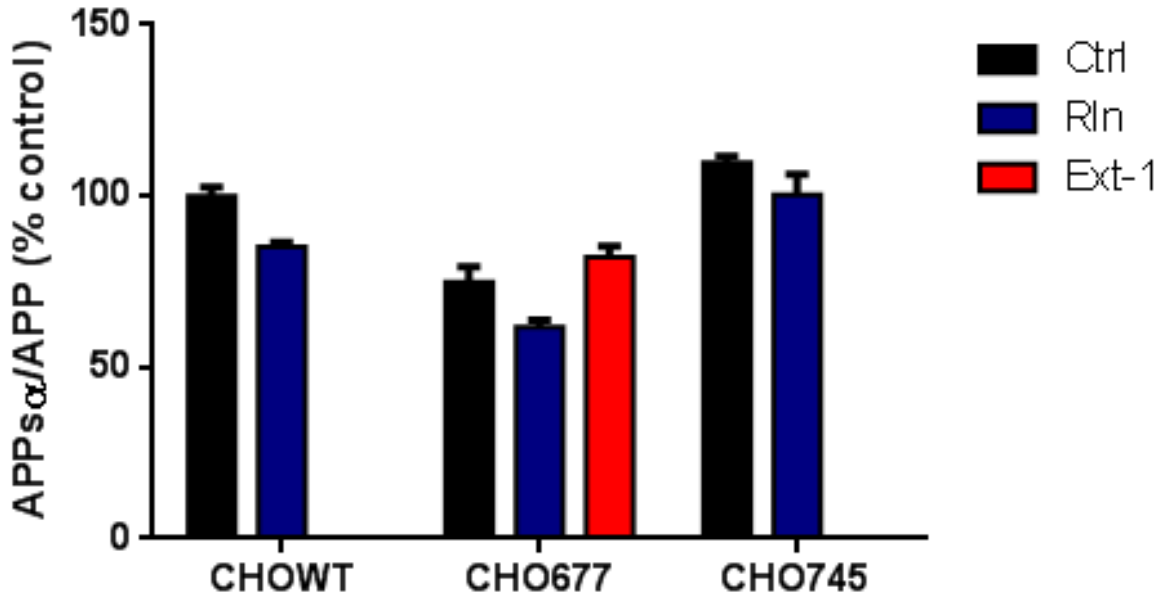

Figure A4.2 HSPG-independent effects of Reelin on APP ectodomain shedding

Ext-1 and Reelin were transfected into CHO-WT, CHO-677, CHO-745 cell lines.

Endogenous APPsα levels were measured by ELISA .

Appendix 5

APP ectodomain shedding in Reeler primary neuronal cultures

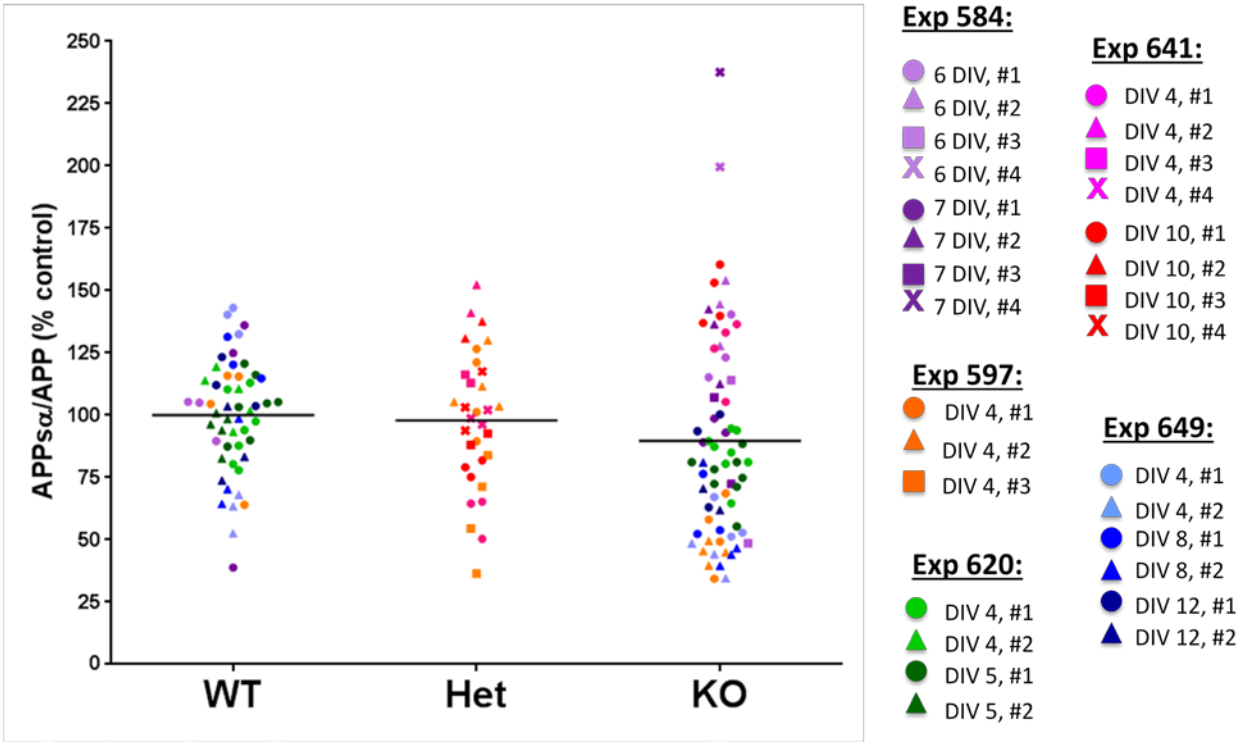

Figure A5 APP ectodomain shedding in Reeler primary neuronal cultures

Cortical neurons from WT, Het, or Reelin KO E18 mouse embryos were cultured over multiple days in vitro (DIV). Media was collected and APPsα was measured by ELISA.